**Universidade do Minho**
Escola de Engenharia

José Ricardo Loureiro Cruz

**Multi-scale investigation on durability and long-term behaviour of concrete elements strengthened with CFRP laminates according to the EBR and NSM techniques**

Multi-scale investigation on durability and long-term behaviour of concrete elements strengthened with CFRP laminates according to the EBR and NSM techniques

José Ricardo Loureiro Cruz

UMinho | 2023

August 2023

# Universidade do Minho
## Escola de Engenharia

José Ricardo Loureiro Cruz

# Multi-scale investigation on durability and long-term behaviour of concrete elements strengthened with CFRP laminates according to the EBR and NSM techniques

Doctoral Thesis

Doctoral Program in Civil Engineering

Work developed under the supervision of
**Professor Doctor José Manuel de Sena Cruz**
**Doctor Luís Luciano Gouveia Correia**
**Doctor Susana Bravo Cabral-Fonseca**

August 2023

# DECLARATION

**Name**: José Ricardo Loureiro Cruz

**Email:** a51314@alunos.uminho.pt     **Phone number:** +351 913927087

**Citizen Card Number:** 13563672

**Title of the Doctoral Thesis:** Multi-scale investigation on durability and long-term behaviour of concrete elements strengthened with CFRP laminates according to the EBR and NSM techniques

**Supervisors:**

Professor Doctor José Manuel de Sena Cruz

Doctor Luís Luciano Gouveia Correia

Doctor Susana Bravo Cabral-Fonseca

**Year of Conclusion**: 2023

Doctoral Program in Civil Engineering

THE ENTIRE REPRODUCTION OF THIS DOCTORAL THESIS IS AUTHORIZED ONLY FOR RESEARCH PURPOSES, UPON WRITTEN DECLARATION BY THE INTERESTED PERSON, WHICH IS COMMITTED TO.

University of Minho, 01/08/2023

Signature:

# ACKNOWLEDGEMENTS

First of all, I really want to express my gratitude to Professor José Sena Cruz for the challenge, encouragement, support and, of course, technical contributions to this work. His guidance and motivation were of paramount importance for me and for the development of this work. To Doctor Luís Correia, I really want to acknowledge the technical discussions, their support especially in the long working journeys both in the laboratory and during the trips throughout Portugal. To Doctor Susana Cabral Fonseca, I really want to acknowledge her committed support, encouragement, and technical enhancements. A special thanks to Doctor Pedro Fernandes for his dedicated help with contributions especially during the preliminary work.

I want also to thank the staff of the Department of Civil Engineering of the University of Minho, particularly, the staff of the Structural Laboratory (LEST) for their commitment and help in carrying out this work. A special thanks to Marco Peixoto, António Matos and other all the technicians for their availability and professionalism. I would like also to acknowledge the ISISE – Institute for Sustainability and Innovation in Structural Engineering for the facilities and resources indispensable to perform this work.

# ABSTRACT

In recent decades, the strengthening of existing reinforced concrete (RC) structures has become an option widely adopted, entailing a sustainable way of preserving and extending the service life of such structures. Carbon Fibre Reinforced Polymer (CFRP) laminates have been increasingly used as strengthening material mainly by using the passive techniques such as Externally Bonded Reinforcement (EBR) and Near Surface Mounted (NSM). Furthermore, EBR technique can be improved with the use of active external prestressing by means of the Mechanical Anchorage (MA) and Gradient Anchorage (GA). Typically, structural epoxy adhesives are used to ensure the bond between CFRP laminates and the concrete surface.

The present work intends to contribute for the existing knowledge on the durability and long-term behaviour of RC structures strengthened with CFRP laminates under natural ageing since the available literature in this area is scarce.

The study carried out comprises an extensive multi-scale experimental program involving three types of specimens at meso- and full-scale, namely: (i) specimens of the involved materials, (ii) specimens to study the bond between CFRP laminates and concrete, and (iii) RC slabs strengthened in flexure with CFRP laminates under sustained load. Four natural environments were selected to induce ageing mainly by carbonation, freeze-thaw cycles, elevated temperatures, and airborne chlorides from seawater. Additionally, a control and a water immersion environment were considered. The evolution of the durability was evaluated mainly throughout mechanical characterization of the materials and bond specimens up to 2 years. The RC slabs under sustained load were continuously monitored for 3 years. The experimental program was complemented with attempts of correlations between accelerated and natural ageing, and with proposals for improving the existing design guidelines.

**KEYWORDS:** durability and long-term behaviour; multi-scale investigation; natural ageing; strengthening of RC structures with CFRP laminates.

# RESUMO

Nas últimas décadas, o reforço de estruturas de betão armado (BA) existentes tornou-se uma opção largamente adotada, consistindo numa forma sustentável de preservar e prolongar a vida útil dessas estruturas. Os laminados de Polímeros Reforçados com Fibra de Carbono (CFRP) têm vindo a ser cada vez mais utilizados como material de reforço, principalmente utilizando técnicas passivas tais como a colagem externa de laminados (*Externally Bounded Reinforcement*, EBR) e a inserção de laminados no betão de recobrimento (*Near Surface Mounted*, NSM). Além disso, a técnica EBR pode ser tornada mais eficiente através da aplicação de pré-esforço externo ativo e utilizando o método da Ancoragem Mecânica (MA) ou do Gradiente de Ancoragem (GA). Tipicamente, são utilizados adesivos epóxi para garantir a ligação entre os laminados de CFRP e o betão.

O presente trabalho pretende contribuir para o conhecimento existente sobre durabilidade e comportamento a longo prazo de estruturas de BA reforçadas com laminados de CFRP em ambientes de envelhecimento natural uma vez que a literatura nesta área é escassa.

O estudo realizado comtemplou um extenso programa experimental multi-escala incluindo três tipos de provetes à mesoescala e escala real, nomeadamente: (i) provetes dos materiais envolvidos, (ii) provetes para estudo da ligação entre laminados de CFRP e betão e (iii) lajes de BA reforçadas à flexão com laminados de CFRP sob carregamento constante. Foram considerados quatro ambientes naturais para indução de envelhecimento sobretudo por carbonatação, ciclos gelo-degelo, temperaturas elevadas e ação dos cloretos transportados pelo ar da água do mar. Adicionalmente, foi considerado um ambiente de controlo e um ambiente de imersão continua em água. A evolução da durabilidade foi avaliada sobretudo pela caracterização mecânica dos provetes dos materiais e da ligação durante 2 anos. As lajes de BA reforçadas com laminados de CFRP sob carregamento constante foram monitorizadas continuamente durante 3 anos. O programa experimental foi complementado com tentativas de comparações entre envelhecimento acelerado e natural, e ainda com propostas para melhorar as normas de projeto existentes.

**PALAVRAS-CHAVE:** durabilidade e comportamento a longo prazo; investigação multi-escala; envelhecimento natural; reforço de estruturas de BA com laminados de CFRP.

# TABLE OF CONTENTS

# LIST OF FIGURES

# LIST OF TABLES

# LIST OF ABBREVIATIONS AND SYMBOLS

## Abbreviations

| | |
|---|---|
| ACI | American Concrete Institute |
| ADH1 | Adhesive 1 |
| ADH2 | Adhesive 2 |
| APDL | Administração dos Portos do Douro, Leixões e Viana do Castelo |
| CEN | European Committee for Standardization |
| CFRP | Carbon Fibre Reinforced Polymer |
| CNR | Advisory Committee on Technical Recommendations for Construction |
| $CO_2$ | Carbon Dioxide |
| CoV | Coefficient of Variation |
| E1 | Environment 1 |
| E2 | Environment 2 |
| E3 | Environment 3 |
| E4 | Environment 4 |
| E5 | Environment 5 |
| E6 | Environment 6 |
| EBR | Externally Bonded Reinforcement |
| EMPA | Swiss Federal Laboratories for Materials Science and Technology |
| Env. | Environment |
| FCT | Portuguese Foundation for Science and Technology |
| FIB | Fédération Internationale du Béton/International Federation for Structural Concrete |
| FIEC | European Construction Industry Federation |
| FM | Failure Mode |
| FRP | Fibre Reinforced Polymer |
| GA | Gradient Anchorage |
| GFRP | Glass Fibre Reinforced Polymer |
| IPQ | Portuguese Quality Institute |
| ISI | International Scientific Indexing |
| L10 | Laminate with 10 mm width |

| | |
|---|---|
| L50 | Laminate with 50 mm width |
| LNEC | National Laboratory of Civil Engineering |
| MA | Mechanical Anchorage |
| N/A | Not Accessed |
| NSM | Near Surface Mounted |
| RC | Reinforced Concrete |
| REF | Reference specimens |
| RH | Relative Humidity |
| R1 | Roll number 1 |
| R2 | Roll number 2 |
| R3 | Roll number 3 |
| RTFE | Real-time Field Exposure |
| SDG | Sustainable Development Goals |
| StDev | Standard Deviation |
| T0 | Time 0 of evaluation (initial characterization) |
| T1 | Time 1 of evaluation (after one year of exposure) |
| T2 | Time 2 of evaluation (after two years of exposure) |
| $T_g$ | Glass transition temperature |
| UM | University of Minho |
| UN | United Nations |
| UV | Ultraviolet radiation |

## Symbols

| | |
|---|---|
| $E_a$ | Elastic modulus of the adhesive |
| $\varepsilon_a$ | Ultimate strain of the adhesive |
| $E_{cm}$ | Elastic modulus of the concrete |
| $E_f$ | Elastic modulus of the CFRP laminate |
| $\varepsilon_f$ | Ultimate strain of the CFRP laminate |
| $f_a$ | Tensile strength of the adhesive |
| $f_{cm}$ | Compressive strength of the concrete |
| $f_{ctm}$ | Tensile strength of the concrete |

xii

| | |
|---|---|
| $f_f$ | Tensile strength of the CFRP laminate |
| $F_{max}$ | Maximum pullout force |
| $K$ | Initial stiffness |
| $s_{lmax}$ | Loaded end slip |

# LIST OF CUMULATIVE PAPERS OF THE THESIS

1. Cruz, R., Correia, L., Cabral-Fonseca, S., and Sena-Cruz, J. 2021. Effects of the preparation, curing and hygrothermal conditions on the viscoelastic response of a structural epoxy adhesive. *International Journal of Adhesion and Adhesives*, 110, 102961. https://doi.org/10.1016/j.ijadhadh.2021.102961. **[NC=3]** (Scopus at 31-10-2022)
Impact Factor: **3.848** (2021)

2. Cruz, R., Correia, L., Dushimimana, A., Cabral-Fonseca, S., and Sena-Cruz, J. 2021. Durability of Epoxy Adhesives and Carbon Fibre Reinforced Polymer Laminates Used in Strengthening Systems: Accelerated Ageing versus Natural Ageing. *Materials*, 14(6), 1533. https://doi.org/10.3390/ma14061533. **[NC=12]** (Scopus at 31-10-2022)
Impact Factor: **3.748** (2021)

3. Cruz, R., Correia, L., Cabral-Fonseca, S., and Sena-Cruz, J. 2022. Durability of bond between NSM CFRP strips and concrete under real-time field and laboratory accelerated conditioning. *Journal of Composites for Construction*, 26(6), 04022074. https://doi.org/10.1061/(ASCE)CC.1943-5614.0001262. **[NC=0]** (Scopus at 31-10-2022)
Impact Factor: **3.925** (2021)

4. Cruz, R., Correia, L., Cabral-Fonseca, S., and Sena-Cruz, J. 2022. Durability of bond of EBR CFRP laminates to concrete under real-time field exposure and laboratory accelerated ageing. Submitted to *Construction and Building Materials* on 05-10-2022.
Impact Factor: **7.693** (2021)

5. Cruz, R., Correia, L., Dushimimana, A., Cabral-Fonseca, S., and Sena-Cruz, J. 2022. Long-term flexural behaviour of slabs strengthened with CFRP laminate systems under different accelerated and natural environmental conditions. Paper to be submitted.

# CHAPTER 1

## INTRODUCTION

*This chapter presents an overview of the topic addressed in this PhD thesis, particularly regarding its contextualization for civil engineering applications. It includes the motivation for this work, highlighting (i) the reasons for strengthening of reinforced concrete structures and (ii) durability and long-term behaviour of the strengthening systems addressed. At the end, the research objectives and the structure of the thesis are presented.*

### 1.1. Motivation

Reinforced Concrete (RC) structures are part of our everyday lives in different ways, such as in form of buildings and infrastructures. It is expected that during their service life, the behaviour of RC structures follows the design purposes established in terms of safety, functionality, and durability, e.g. (CEN 2000; IPQ 2010; FIB 2013). However, in several cases, the maintenance and conservation of these structures have been neglected, mainly due to the lack of knowledge and planning, which has led to their premature degradation. In this situation, structural rehabilitation may be the option. Furthermore, several factors may underlie the need for intervention, namely (ACI 2007): (i) exposure to aggressive environmental conditions; (ii) structural problems resulting from excessive loads that have acted on the structure; (iii) design and construction poor practices; and (iv) actions with a very low probability of occurrence, such as an earthquake or an explosion, among others. On the other hand, the urban rehabilitation has led (v) to a change in the use of various buildings, which may imply the need for strengthening in case of higher loading capacity requirements with the new use. Additionally, (vi) the update and change of the design codes may also imply the upgrade of buildings designed according to the previous standards, that, therefore, are not conform with the current standards and need to be strengthened (ACI 2007). It should be highlighted that from the socio-economical point of view, solutions based on demolition followed by reconstruction are usually more expensive and cause also higher economic, environmental and social impacts than the solutions based on rehabilitation, which increases the global relevance of rehabilitation (ACI 2007).

The construction industry in Europe has recovered and currently surpasses the levels of 2010 (Deloite 2018). Regarding the Southern Europe, although the construction sector has been recovering, this sector has not yet reached the levels of 2010, with production volumes of ~95% in Spain, ~90% in France and ~68% in Italy, ~53% in Portugal and ~52% in Greece (Deloite 2018). The rehabilitation and maintenance sector, which includes the repair and strengthening of RC structures, have been growing, especially in developed countries. According to FIEC, the rehabilitation and maintenance sectors represented a total of 28% of the construction market in Europe (FIEC 2020). Moreover, a significant expansion of the rehabilitation subsector is estimated for the next years. As it is known, developed economies have in general more capital for investing in infrastructures, facing the challenge of maintaining, modernizing, and upgrading the transport, energy, water supply, and telecommunications networks.

Several strengthening techniques, usually classified as "traditional" or "innovative", can be used to repair or strengthen existing RC structures. The traditional techniques include, among others: (i) reinforced concrete overlays, (ii) application of steel plates fixed with a structural adhesive and/or bolts, (iii) external prestressing and (iv) reduction of spans by adopting new structural supports. More recently, the techniques using FRP (Fibre Reinforced Polymers) have immerged as viable alternatives, usually named as innovative techniques. The most used FRP materials in the context of Civil Engineering are the GFRP (Glass Fibre Reinforced Polymers) and the CFRP (Carbon Fibre Reinforced Polymers). As more frequently used for strengthening (Sen 2015), the CFRP material has become the main target of researchers and applications on RC structures. These innovative techniques/materials present several advantages when compared with the traditional techniques such as, lightness, corrosion resistance, ease of application (Al-Tamimi Adil et al. 2015), good fatigue behaviour (Sena-Cruz et al. 2012; Fernandes et al. 2015), high strength/weight ratio and, a wide variety of solutions and shapes available on the market. However, these techniques/materials/solutions also present some disadvantages, namely, the high initial cost, lower resistance to fire and the need for skilled labour to their application.

The strengthening of RC structures with CFRP laminates can be applied either using passive (non-prestressed) or active (prestressed) systems. The passive systems include the EBR (Externally Bonded Reinforcement) technique, which consists of the externally bond of CFRP laminates or sheets on the surface of the RC elements to be strengthened. However, this technique does not present high efficiency at the ultimate level since the tensile capacity of the CFRP laminate, typically, is not achieved,

as it is commonly observed the early detachment of the CFRP from the concrete substrate (Sena-Cruz et al. 2012). Another passive strengthening technique is the NSM (Near Surface Mounted) which consists in the application of the CFRP laminates into the concrete cover of the RC element to be strengthened. The CFRP laminate is introduced in grooves previously cut in the surface of the concrete, which allows the minimization of some problems faced by the EBR technique, leading to (De Lorenzis and Teng 2007; Coelho et al. 2015): (i) higher efficiency in the use of the FRP materials, due to the reduced probability of premature debonding from the higher bonded contact (the FRP failure is achieved in many cases); (ii) easier extending of the strengthening material for anchoring into adjacent elements; (iii) better protection of the FRP to the exterior aggressive factors and acts of vandalism; (iv) slighter visual impact. However, the field of application of the EBR technique is larger than the one of the NSM technique as the EBR can be used for flexural, shear and confinement strengthening, whereas the NSM is very efficient only for flexural and shear strengthening applications (FIB 2022).

In some cases, the use of external prestressing in the EBR-CFRP system may be advantageous or even necessary. The prestressing has several advantages since these systems combine the benefits of the passive EBR technique with the benefits provided by the active systems, such as (Correia et al. 2017), increase of ultimate capacity and reduction of the existing deflections and crack width. With the prestressed EBR-CFRP systems, the CFRP laminate is normally fixed at the ends, which can be performed using mechanical systems or through the accelerated curing of the structural adhesive that bonds the CFRP to the concrete. In the former, the prestressed CFRP is fixed at the ends by using mechanical anchorage plates (commonly denominated as MA – mechanical anchorage system), whereas in the latter, the CFRP strip is fixed at the ends by the accelerated curing of the adhesive (commonly denominated as GA – gradient anchorage system)(Correia et al. 2015).

As previously mentioned, the FRP materials can be a viable alternative to conventional materials (e.g., steel, concrete), both technically and economically, as indicated by different published literature, e.g., (CNR 2013; Sen 2015; Pellegrino and Sena-Cruz 2016; ACI 2017; FIB 2019). Nevertheless, there are several open issues regarding the durability and long-term behaviour of these systems, which limits their wider application, at least from a theoretical point of view. In this context, the long-term behaviour of RC structures strengthened with CFRP laminates and their durability have been appointed as key aspects for the widespread of these techniques. Consequently, research works can be found addressing

these aspects, e.g., (Al Chami et al. 2009; Fernandes 2016; Correia et al. 2017; Cabral-Fonseca et al. 2018; Correia 2018; Fernandes et al. 2018; Sousa et al. 2018; Tatar and Milev 2021).

According to CERF (CERF 2001), the durability of a material, component or structure is stated as its capacity to resist to cracking, oxidation, chemical degradation, delamination, wear, and/or the effects of damage caused by a foreign object for a specified period of time, under the appropriate load conditions, under specified environmental conditions. Several degradation factors can act on a structure leading to its damage, namely (i) environmental (e.g., moisture, temperature, UV radiation and chemicals) and (ii) mechanical factors (such as excessive or accidental impact loads).

The moisture can damage composite materials as can affect the three components of the system: fibre, matrix, and the interface fibre-matrix. The matrix is the most affected component, with a possible change of the structure of the polymer (Helbling and Karbhari 2007). Moisture can also reduce the fibre-matrix bond, leading to the deterioration of the fibre-matrix interface and damage of the fibre. The absorption of water in polymers and adhesives can cause physical ageing, partially recoverable after drying. Two physical ageing mechanisms should be mentioned: (i) plasticization, characterized by the decrease of the elastic modulus and strength and a possible increase of the ductility (Cabral-Fonseca et al. 2018) and (ii) swelling, characterized by the volumetric change of the material as a result of the moisture content only, regardless of the thermal expansion. The absorption of water may also lead to the decrease of the glass transition temperature ($T_g$) of the epoxy adhesive or polymer resin. The $T_g$ is defined as the temperature that, if surpassed, there is a significant decrease in stiffness and strength (Sen 2015; Cabral-Fonseca et al. 2018; FIB 2019). Since the mechanical properties of resins depend on the temperature, the presence of elevated temperatures near the $T_g$ can cause the softening of the resin matrix, leading to an increase in the viscous behaviour on it, which culminates in a viscous response of the composite, accompanied with decrease of stiffness and strength. Nevertheless, the elevated temperatures can be responsible by the positive post-cure phenomenon, as the post-cure of the material can increase the $T_g$ (FIB 2019) as well as the tensile properties of the material (strength and elastic modulus), as demonstrated by Cromwell et al. (2011) for CFRP strips. In general, the thermal cycles cause small effects on the mechanical properties of the FRP materials, except if the temperature range is extremely high. Nevertheless, the performance of the resin and of the interface between fibre and resin decrease when the FRP faces freeze-thaw or thermal cycles, which results from the difference on the coefficients of thermal expansion of the resin and fibre. The UV radiation, in

general, almost does not affect the mechanical properties of the carbon fibre composite material (Cabral-Fonseca et al. 2011; FIB 2019). Only the top few microns of the surface of composites are predominantly affected by the UV radiation and, therefore, mainly the aesthetic properties are affected (Cabral-Fonseca et al. 2011; Cabral-Fonseca et al. 2018). Finally, the chemical ageing may take place from a long exposure to moisture, being mainly an irreversible process affecting all the components of the system (fibre, resin and interface fibre-resin) (Helbling and Karbhari 2007).

The durability and long-term behaviour of these type of strengthened structures can be studied using accelerated ageing tests in the laboratory or through exposure to real environmental conditions (also known as natural outdoor exposure and as real-time field conditioning). The accelerated ageing protocols are sometimes much more aggressive than the real environmental conditions, which can lead to the underestimation of the real durability of the system, if similar periods of exposure are adopted (Tatar and Hamilton 2016). On the other hand, although more time-consuming, only studies in a real environment allow gaining knowledge regarding what really happens in terms of the degradation phenomena that act on CFRP strengthened RC structures (Fernandes et al. 2018). Additionally, it should be highlighted that it is a challenge to establish the relationship between the effects resulting from accelerated ageing conditions and the results of the real ageing tests, remaining not completely understood (Tatar and Hamilton 2016).

In both types of exposure, it is typically used prototype specimens at a multi-scale level, namely: (i) samples of the constitutive materials of the strengthening system (e.g., (Fernandes et al. 2018; Sousa et al. 2018)), (ii) specimens to study the bond behaviour between the strengthening material and concrete (e.g., (Kabir et al. 2016; Fernandes et al. 2018)) and (iii) full-scale specimens (e.g., (Subhani et al. 2016; Correia et al. 2017; Correia 2018)). These studies usually involve a set of reference specimens (under controlled exposure conditions) and exposed specimens (submitted to the environmental conditions to be studied).

It is clear the higher number of investigations performed under accelerated ageing when compared with natural ageing in the literature. This finding can be related with the higher complexity of developing natural ageing when compared with laboratory accelerated tests. It should be stated that natural exposure comprises several environmental degradation factors acting simultaneously (e.g., moisture, thermal effects and/or UV exposure), which are difficult to simulate simultaneously in the laboratory

conditions. Therefore, the real behaviour (under natural ageing) of this type of structures remains a gap in the existing knowledge.

## 1.2. Research Objectives

Considering all the aspects addressed in the previous section, this PhD thesis aims to give new insights regarding the durability and long-term behaviour of RC structures strengthened with CFRP laminate strips, applied according to the EBR and NSM techniques, by passive and active systems, under real environmental exposure. Therefore, it was intended, at the end, to assess the influence of the long-term behaviour on full-scale RC slabs strengthened with CFRP laminates, combined with moisture, carbonation of concrete, freeze-thaw cycles, elevated temperatures, and chlorides from seawater. To better understand and complement the full-scale study, tests at material and bond scales were also conducted. From the work developed, it was expected relevant contributions to the existing knowledge as well as the proposal of design recommendations. Additionally, to this global objective, several specific objectives were also established, namely:

(i) Explore the influence of the preparation methods and initial curing type on the tensile properties and tensile creep behaviour of epoxy adhesives;

(ii) Assessment of the level of degradation caused by the exposure to real environmental actions in the constitutive materials of the strengthening system, i.e., concrete, adhesive and CFRP;

(iii) Assessment of the level of degradation caused by the exposure to real environmental actions on the bond performance of the EBR and NSM systems (concrete-adhesive-CFRP);

(iv) Study of the long-term behaviour of RC structures strengthened with CFRP laminates when subjected to the synergistic actions that result from a state of permanent stress (using gravity loads) and exposed to different real environmental actions;

(v) Establishment of correlations between the accelerated ageing tests developed under laboratory conditions and studies carried out under real environments;

(vi) Contribution to the improvement of existing design standards of this type of strengthening system, particularly regarding the service life prediction.

To achieve these objectives, the work included three fundamental components: (i) an extensive multi-scale experimental program; (ii) the establishment of correlations between accelerated and real ageing; and (iii) elaboration of recommendations for improving existing design guidelines.

The experimental program is composed of different types of specimens, placed in different locations of Portugal, whose corresponding environmental characteristics are representative of the effects of each environmental ageing action targeted. Then, the results obtained in this work are compared with other experimental programs in the literature, that result from accelerated ageing tests and suggestions of improvements of existing guidelines are provided.

The United Nations (UN) established a total of 17 Sustainable Development Goals (SDG) to advance in health and education, reduce inequality, and promote the economic growth, while stopping the climate changes and preserving our oceans and forests. This work can be suited particularly in Goal 9 – "Build resilient infrastructure, promote inclusive and sustainable industrialization and foster innovation" and Goal 11 – "Make cities and human settlements inclusive, safe, resilient and sustainable".

Finally, it should be mentioned that this PhD thesis was developed under the work carried out in the FRPLongDur research project - Long-term structural and durability performances of reinforced concrete elements strengthened in flexure with CFRP laminates (POCI-01-0145-FEDER-016900 (FCT PTDC/ECM-EST/1282/2014)), supported by the Portuguese Foundation for Science and Technology (FCT). This project was a partnership between the University of Minho (UMinho), the National Laboratory of Civil Engineering (LNEC) and the Swiss Federal Laboratories for Materials Science and Technology (EMPA). Therefore, it should be mentioned that some results presented in this PhD thesis are also a part of the results of this research project.

## 1.3. Structure of the Thesis

This PhD thesis is presented as a collection of papers published, submitted to peer-review and to be submitted in SCI international journals, preceded by three introductory chapters and followed by one concluding chapter and annexes, as follows:

(i) Chapter 1: describes the scope of the thesis and motivation, explains the general and specific objectives, and presents the structure of this thesis;

(ii) Chapter 2: provides the global methodology adopted to achieve the objectives proposed;

(iii) Chapter 3: presents a summary and justification of the papers that compose this thesis;

(iv) Chapter 4: provides the concluding remarks and possible future works derived from the research line followed in this doctoral thesis;

(v) Annexes: composed by Annex I and Annex II, providing, respectively, the cumulative publications that resulted from the conducted investigation and the detailed experimental results, which complement those published in the papers.

# CHAPTER 2

## RESEARCH METHODOLOGY

*The main purpose of this research is to provide further knowledge of the long-term structural behaviour and durability performance of reinforced concrete (RC) elements strengthened in flexure with CFRP laminates under accelerated ageing and real environmental conditions. This work was developed in the scope of the FRPLongDur project. In the following sections, a general overview of the methodology adopted is presented.*

### 2.1. General Methodology

Figure 2.1 presents a flowchart of the main steps followed in this work. Multi-scale specimens were designed and produced, namely, meso-scale samples of the involved materials (concrete, epoxy adhesives and CFRP laminates), meso-scale bond specimens (EBR and NSM techniques) and full-scale RC slabs strengthened in flexure with CFRP laminates with the EBR (passive and active systems) and NSM (passive) techniques, under sustained loading.

These specimens were, therefore, exposed to six different environments. Given the significant amount and size of the specimens and to facilitate the monitoring and collection of the samples, an experimental station per environment was created (see Figure 2.2 and Figure 2.3).

The experimental station comprising the reference environment (E1) possesses controlled hygrothermal conditions (20 °C of temperature and 55% of relative humidity), while the environment E2, aimed at accelerating ageing, consisted in continuous immersion in tap water at a constant temperature (20 °C). Four outdoor environments were adopted. Despite the difficulties on isolating environmental effects, each outdoor environment aimed targeting a specific degradation factor, namely:
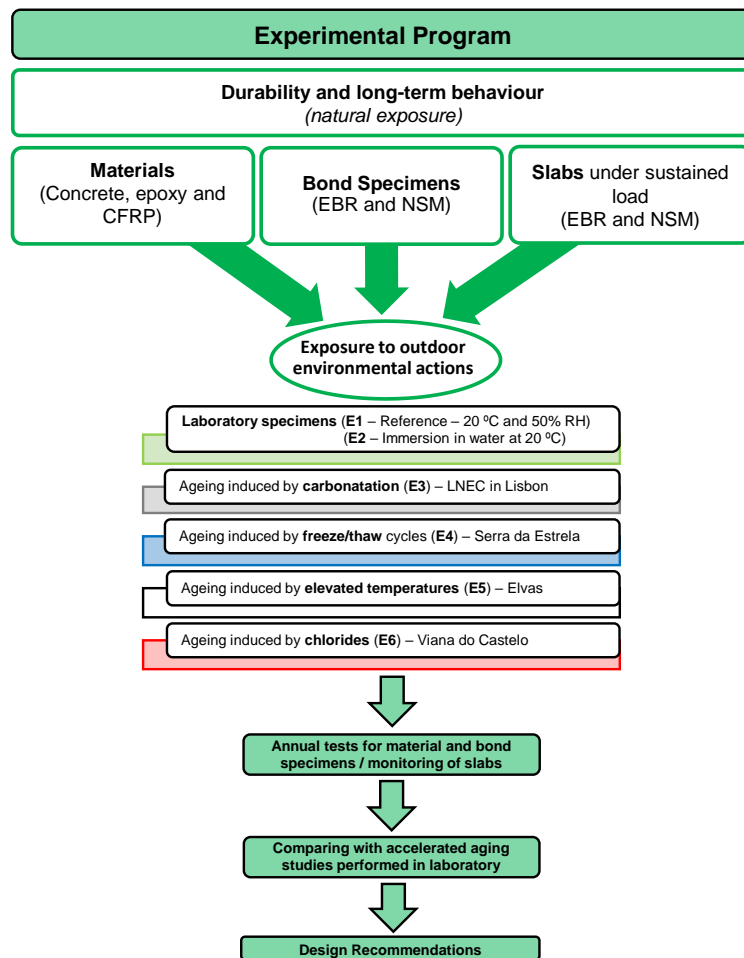
Figure 2.1 - Flowchart of the methodology adopted.
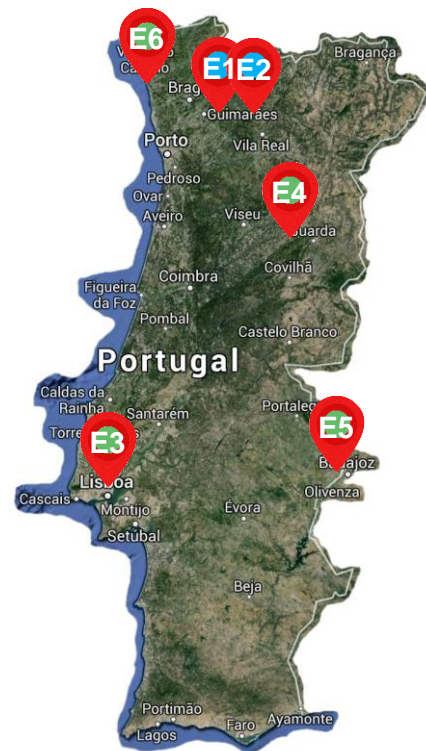


Figure 2.2 - Location of the experimental stations.

(i)     Environment E3 – located in Lisbon (near the International Airport of Portela and near to highway with heavy traffic load) to induce ageing mainly by carbonation of concrete due to the elevated levels of $CO_2$ from the anthropogenic pollution in this region; this environment is characterized by the "Mild subtropical Mediterranean climate" (short and mild winters and warm to hot summers);

(ii)    Environment E4 – located in 'Serra da Estrela' (the highest mountain in continental Portugal) to induce ageing mainly by freeze-thaw cycles due to the snow and low temperatures characteristic in this region during the wintertime; this environment is characterized by the "Mild subtropical Mediterranean climate" (low temperatures and snow during the wintertime and warm to hot summers);

(iii)   Environment E5 – located in 'Elvas' (located in 'Alentejo' typically know by the hot weather and cold winters) to induce ageing mainly by the elevated temperatures due to the high

temperatures faced in this region, especially during the summertime; this environment is characterized by the "Hot summer Mediterranean climate" (high temperatures and drought specially during the summer);

(iv)    Environment E6 – located in 'Viana do Castelo' (in the APDL port of sea) to induce ageing mainly by airborne chlorides from the seawater due to the proximity to the Atlantic Ocean; this environment is characterized by the "Hot summer Mediterranean climate" (high temperatures and drought specially during the summer).



Figure 2.3 - Experimental stations.

## 2.2. Production, Preparation, and Installation

The production and preparation of specimens is briefly presented in Figure 2.4 and Figure 2.5 and involved the main flowing steps:

(i)     preparation of the formwork for all the concrete specimens and steel reinforcement arrangements for the RC slabs as well as installation of all monitoring sensors;

(ii)    casting, including 90 prisms of 200 mm × 200 mm × 400 mm (for bond EBR specimens; also used for assess the tensile properties of concrete and its carbonation depth), 90 cubes of 200 mm × 200 mm × 200 mm (for bond NSM specimens), 30 RC slabs of 600 mm × 120 mm × 2600 mm, and 130 cylinders of 150/300 mm (diameter/height) for assessment of compressive properties;

(iii)   preparation of the concrete surface by sandblasting (EBR technique) and opening of the grooves (NSM technique);

(iv)    application of CFRP laminates according to the corresponding strengthening technique, to the slabs and bond specimens;

(v)     and finally, manufacturing of specimens to study the durability of the epoxy adhesives and prepare the CFRP laminate samples.

A ready-mix concrete batch of about 12 m³ was ordered to cast all the specimens, with the following characteristics: compressive characteristic strength (cylinder/cube) of 30/37 MPa (C30/37), exposure class XC4(P) (cyclic wet and dry), water/cement ratio (W/C) of 0.40, maximum aggregate size ($d_{max}$) of 12.5 mm, slump class S4 (slump of 160–210 mm) and produced with Portland cement type CEM II/A–L 42.5R (Eurocode 2 (IPQ 2010)/EN 206-1(CEN 2000)).

For the internal reinforcement of the RC slabs, steel rebars of class A400 NR SD (Eurocode 2 (IPQ 2010)) of 8 mm (∅8) and 6 mm (∅6) diameter were applied. Two batches of steel were used (batch 1 for EBR, MA and GA slabs; batch 2 for NSM slabs).

The commercial cold-curing epoxy adhesive S&P Resin 220 Epoxy Adhesive (also referred as ADH1 in this work) supplied by S&P® Clever Reinforcement Ibérica Lda. Company, was applied for strengthening all the specimens and for assessment of the durability of the material itself. According to the supplier datasheet (S&P 2015), the average flexural elastic modulus is higher than 7.1 GPa.

Additionally, the commercial cold-curing epoxy adhesive trademarked as Sikadur®-30 (also referred as ADH2 in this work), supplied by SIKA Schweiz AG was used to study the durability of the material itself. According to the datasheet provided by the supplier (Sika 2017), this adhesive presents a tensile strength of 26 MPa (with curing at +15 °C) and 29 MPa (with curing at +35 °C), after 7 days of curing. Additional details regarding both epoxy adhesives can be found in Cruz et al. (2021).



| (a) | (b) |
| (c) | (d) |
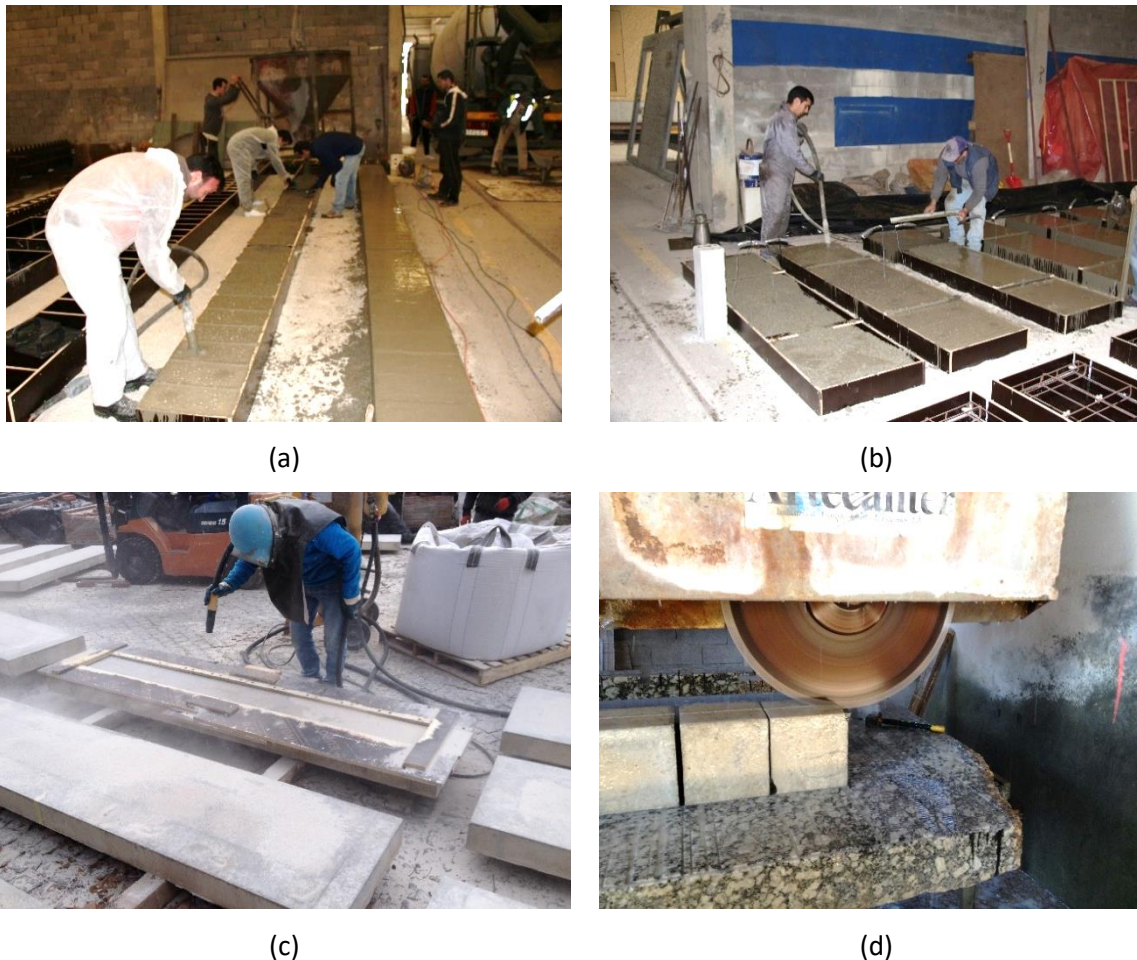
Figure 2.4 - Main steps on the production and preparation of the specimens (concrete): (a) casting of bond concrete substates; (b) casting of RC slabs; (c) sandblasting of the concrete surface for EBR specimens and, (d) grooves' opening for NSM specimens.

The CFRP laminate strips applied in this work are supplied by S&P® Clever Reinforcement Ibérica Lda. Company with the trademark CFK 150/2000. This CFRP is prefabricated by pultrusion and composed by unidirectional carbon fibres (fibre content higher than 68%) held together by a vinyl ester resin matrix. This CFRP laminate presents a black and smooth external surface. According to the technical datasheet presented by the supplier (S&P 2014), this CFRP laminate presents a characteristic elastic

modulus higher than 170 GPa and a characteristic tensile strength higher than 2000 MPa. Three distinct cross-section geometries were used: (i) 10 mm × 1.4 mm (also referred as L10 in this work) for the NSM technique, (ii) 50 mm × 1.2 mm (also referred as L50 in this work) for the EBR, MA and GA techniques and, (iii) 100 mm × 1.2 mm (also referred as L100 in this work) for the EBR technique.

The application of strengthening with EBR and NSM techniques followed several steps. After the sandblasting of the concrete surface (EBR) and opening of the groves (NSM), and before bonding the CFRP strip, the sandblasted surface and the grooves were cleaned with compressed air. To avoid the application of epoxy adhesive in non-desired zones, an insulation process was developed on concrete (see Figure 2.5). The preparation of the CFRP itself involved the following steps: (i) adoption of delimitators and spacers (fixed at the loaded and free ends on bond specimens and on the extremities of the CFRP in the slabs) to ensure the desired bond length, accurate epoxy thickness (in EBR ~1.5-2 mm), and correct positioning of the laminate along the bonded length; (ii) cleaning of the CFRP with acetone; (iii) application of epoxy adhesive in the prepared surface (EBR) and filling of the groove (NSM) in the bonding zones and corresponding bonding areas of the CFRP laminate (a thin layer of the epoxy adhesive); (iv) application of the CFRP to the prepared surface (EBR) and insertion into the groove (NSM) followed by a slight pressure to force the excess epoxy adhesive to flow out of the bonded zone; and finally, (v) removing of epoxy adhesive in excess and levelling of the surface.

The process of strengthening the prestressed slabs with me Mechanical Anchorage (MA) and Gradient Anchorage (GA) systems is more complex than non-prestressed systems previously described (see Figure 2.5(e) and Figure 2.5(f)). The MA system is based on the use of metallic plates at the ends of the CFRP strip while the GA system applies a non-metallic anchorage, materialized by the fast curing (accelerated) of the adhesive at high temperatures. Both systems are commercially available and have been used in various RC structures that needed to be strengthened (Correia et al. 2017).
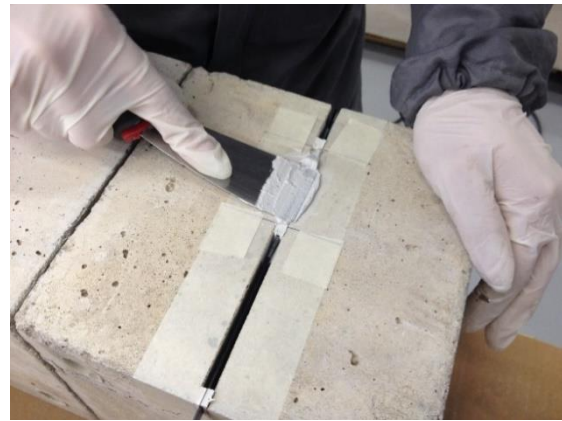
(a)                                                          (b)

(c)                                                          (d)
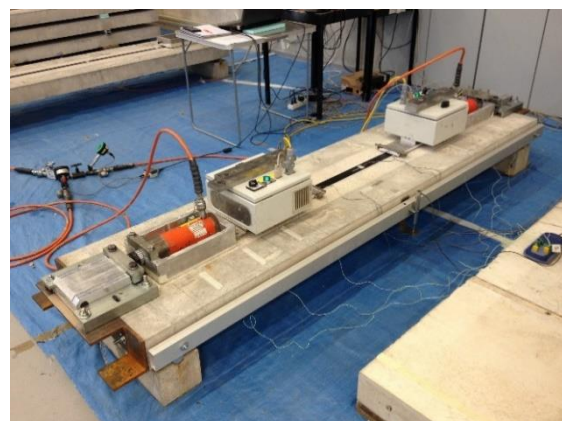
(e)                                                          (f)

Figure 2.5 - Application of the CFRP laminate strips: (a) bond EBR specimens; (b) bond NSM specimens; (c) non prestressed EBR slabs; (d) non prestressed NSM slabs; (e) prestressed MA slabs; and, (f) prestressed GA slabs.

Figure 2.6 presents the main procedures followed for the strengthening with Mechanical Anchorage (MA) and Gradient Anchorage (GA) systems. Both systems use common components (clamp units, guides, aluminium frames, hydraulic jack and hoses, and a manual hydraulic pump) and specific

components, namely: (i) with the MA system, a hard-aluminium rectangular anchor plate (200 mm × 270 mm × 10 mm) with six anchor bolts of 16 mm diameter (M16) and, (ii) with the GA system, a heating electronic device with several heating elements (100 mm × 100 mm, type 'Termofoil'), manometers and valves (S&P 2010; Michels et al. 2014). On the MA system, only one active anchorage was used while for GA system, both end sides were used as active anchorages.
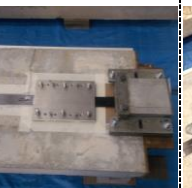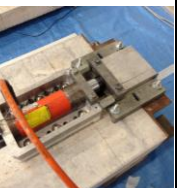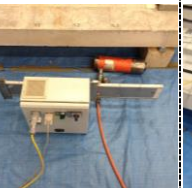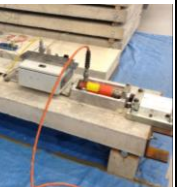
| | 1 | 2 | 3 | 4 | 5 | 6 |
|---|---|---|---|---|---|---|
| **MA** | | | | | Installation of the mechanical anchor plates | Prestressing of CFRP laminate and fixing the metallic anchor plate |
| **GA** | Sandblasting | Installation of prestress components | Application of adhesive in the CFRP laminate | Installation of CFRP laminate | Installation of the heating devices | Prestressing of CFRP laminate and fast curing of adhesive |

Figure 2.6 – Main strengthening procedures for the Mechanical Anchorage (MA) and Gradient Anchorage (GA) systems.

The strengthening with the MA and GA systems shares common application steps (see also Figure 2.6), namely:

(i) Step 1 – As previously mentioned, preparation of the concrete surface by sandblasting (similar to non-prestressed EBR system) the area of application of the CFRP laminate strip and cleaning with a compressed air, was performed;

(ii) Step 2 – Drilling of holes to accommodate permanent and temporary bolt anchors and cleaning with an airbrush after drilling; the MA system comprises six permanent bolt anchors used to fix each metallic anchorage plate while the GA system requires six temporary bolts only for prestressing purposes. A chemical bond agent (HIT-HY 200-A®) was applied to fix these bolts to concrete; installation of two metallic guides to guide and fix the clamps, which are then placed in between the guides at each extremity of the CFRP laminate;

(iii)        Step 3 – Preparation of the epoxy adhesive according to the datasheet provided by the supplier; application of the adhesive on the CFRP laminate (previously cut and cleaned) and on the respective concrete surface;

(iv)        Step 4 – Installation of the CFRP in the final position and slightly pressuring against the concrete surface; spacers were used to assure an epoxy thickness of ~1.5-2 mm; closing of the clamps to fix the CFRP laminate strip with a torque of 170 N.m in each screw;

(v)        Step 5 – Installation of the metallic anchor plates and heating devices in their respective positions of the MA and GA systems, respectively;

(vi)        Step 6 – Installation of the aluminium frames in their desired positions and fixed against the concrete substrate by the anchor bolts to accommodate the hydraulic jack; installation of the hydraulic jack on the aluminium frame and application of prestress on the CFRP laminate strip using a manual hydraulic pump; a pre-strain level of 0.4% was defined; the strain was controlled using a strain gauge installed at mid-span on the CFRP laminate.

Distinct processes were followed with the MA and GA systems after prestressing the CFRP laminate. Regarding the MA system, the anchor bolts were tightened applying a torque level of 150 N.m to improve the confinement offered by metallic anchor plate and reduce the probability of the slippage of the CFRP laminate at the ends. To avoid prestress losses during the curing of the epoxy, spacers were installed in between the aluminium frames and clamps. Nevertheless, in the similar work developed by Correia (2018) prestress losses of ~0.015% on the CFRP laminate were recorded. Finally, after approximately 24 h, the application of the strengthening was concluded and the prestressing equipment was removed, since after this period of curing, the curing level in the epoxy is at least about 90% of the maximum curing (Fernandes et al. 2015).

Concerning the specifications implemented for the GA system in this work, gradient anchorage zones of 600 mm length including three sectors (S1, S2 and S3) of 50 mm wide and 200 mm long were adopted. The applied force by the hydraulic jacks and the temperature in the different sectors that compose the heating devices were continuously acquired throughout the application of the gradient of temperature. Figure 2.7 presents the typical evolution of the temperature, force in the hydraulic jack and CFRP mid-span strain over time. Regarding the heating process, the first sector (S1) was heated to a plateau of 160 °C for 15 min, followed by an exponential decrease of temperature during 20 min (down to 120 °C), and finally by a cooling phase. In the following sectors (S2 and S3), the same

heating process was conducted, starting 10 min after the beginning of the cooling phase on the previous sector. Approximately 15 min after the start of the cooling phase in each sector, 1/3 of the total applied force was carefully released. This interval of time was adopted to assure that the temperatures on the epoxy adhesive had cooled down to lower than 50 °C. In general, short pre-strain losses of ~0.012% (Correia 2018) on the CFRP laminate are registered at the first release of force (see Figure 2.7(a)), probably related with the lower elastic modulus of the epoxy adhesive due to the curing process (Michels et al. 2013).



| (a) | (b) |
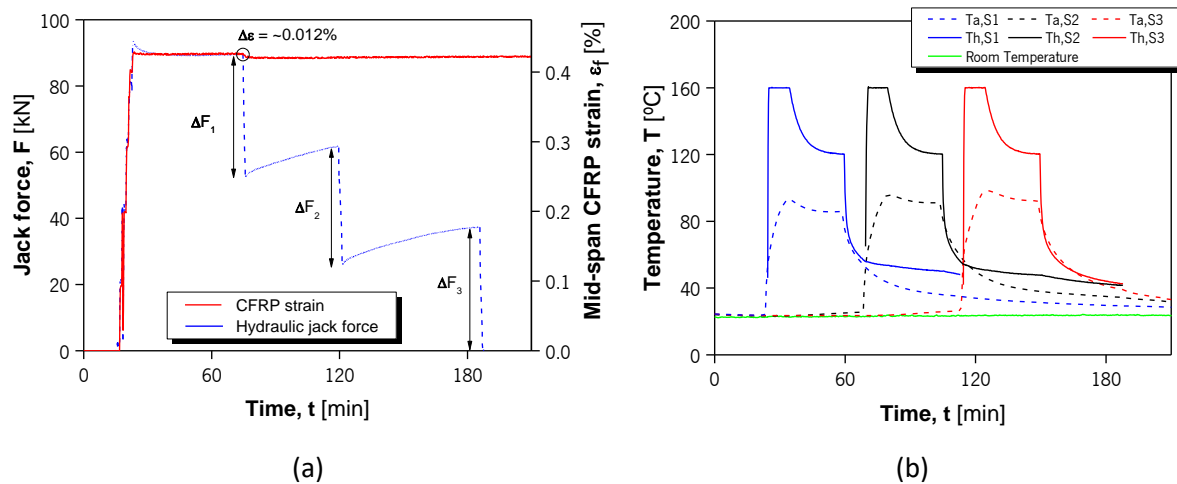
Figure 2.7 – Typical evolution of the temperature, jack force and CFRP mid-span strain with the GA system over time: (a) force of the hydraulic jack and mid-span CFRP strain and (b) temperature in the heating sectors (Th) and in the epoxy adhesive (Ta). Adapted from Correia (2018).

The installation of the laboratory experimental stations (E1 and E2) lasted around 5 days each while the installation of the experimental stations in the outdoor environments (E3 to E6) lasted 1 day each. However, it should be highlighted that the preparation of all specimens and auxiliary systems for each experimental station lasted several weeks.

## 2.3. Testing Plan

After the production of the specimens and prior to the installation, an experimental campaign of tests was carried out for the assessment of the initial mechanical properties of all types of specimens (time T0). This campaign included: (i) material characterization of concrete (elastic modulus, compressive strength, and pull-off strength), epoxy adhesives (elastic modulus and tensile strength) and CFRP laminate (elastic modulus and tensile strength); (ii) bond characterization with the EBR and NSM

techniques and, (iii) flexural tests on the RC slabs strengthened with CFRP laminate strips using the EBR, NSM, MA and GA techniques. An additional reference RC slab (REF, non-strengthened with CFRP) was also tested. These tests allow the comparison between aged and non-aged specimens. Finally, uniaxial tensile tests were also carried out to characterize the mechanical properties of the steel rebars used to produce the RC slabs.

This PhD thesis included an annual experimental testing campaign on the collected specimens of the materials and bond for testing at the laboratory, after 1 (T1) and 2 (T2) years of exposure to evaluate the physical and mechanical properties over the time. The strengthened RC slabs were continuously monitored over 3 years. Table 2.1 presents the set of annual tests performed for the assessment of the mechanical properties of the materials, bond specimens and the monitoring plan designed for the slabs under sustained loads. Figure 2.8 illustrates the timeline of the main tasks involved in the experimental work.
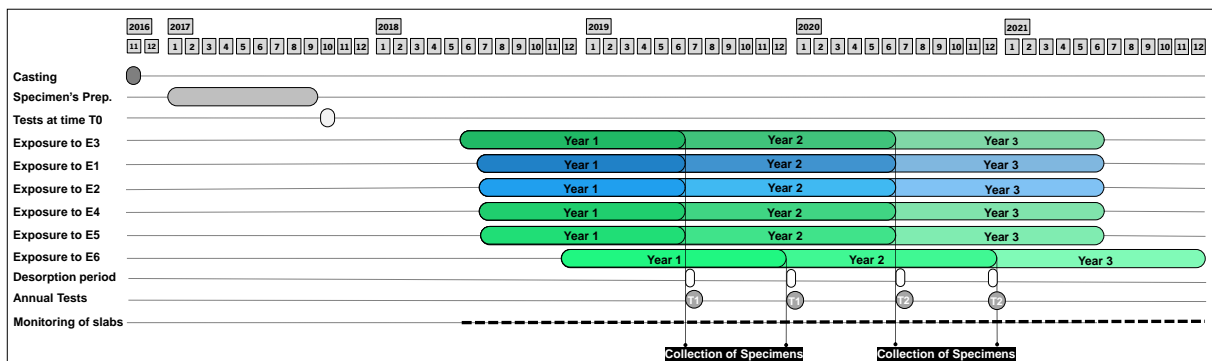


Figure 2.8 - Timeline of the experimental work.

Table 2.1 – Experimental campaigns carried out in the scope of this PhD thesis.

| *Epoxy adhesive: Effect of the different preparation, curing and hydrothermal conditions (meso-scale)* | | | | | |
|---|---|---|---|---|---|
| **Material** | **Property to evaluate** | **Type of specimen** | **Type of test** | **Testing variables** | **Nº of specimens by series** |
| **Adhesive** *S&P Resin 220* | • Mechanical proprieties: elastic modulus and tensile strength | "Dogbone" | Tensile test | Type of mixing, curing and hydrothermal conditions | 6 |
| | • Tensile creep behaviour | | Creep test | | 2 |

| *Durability under natural exposure: Materials constitutive of the strengthening system (meso-scale)* | | | | |
|---|---|---|---|---|
| **Material** | **Property to evaluate** | **Type of specimen** | **Times of testing** | **Nº of specimens by time of testing and environment** |
| **Concrete** | • Elastic modulus and compressive strength | Cylinders of 150/300 mm (diameter/height) | Initial characterization (T0) and annual tests (T1 and T2) | 3 |
| | • Tensile strength (superficial) | "Pull-off specimen" with 50 mm diameter | | 4 |
| | • Carbonation depth | Core with 50/100 mm (diameter/ height) | Annual tests (T1 and T2) | 2 |
| **Adhesive ADH1** *S&P Resin 220* | • Mechanical properties: elastic modulus and tensile strength <br> • Thermal properties: DMA <br> • Higrothermal properties: water absorption <br> • Chemical composition (FTIR) | "Dogbone" | Initial characterization (T0) and annual tests (T1 and T2) | 8 |
| **Adhesive ADH2** *Sikadur 30* | | | | 8 |
| **CFRP L10** *(width: 10 mm)* | • Mechanical properties: elastic modulus and tensile strength <br> • Higrothermal properties: water absorption | Laminate strip | | 6 |
| **CFRP L50** *(width: 50 mm)* | | | | 6 |

| *Durability under natural exposure: Bond specimens (meso-scale)* | | | | |
|---|---|---|---|---|
| **Strengthening system** | **Property to evaluate** | **Type of specimen** | **Times of testing** | **Nº of specimens by time of testing and environment** |
| **EBR** | • Maximum force ($F_{max}$) <br> • Loaded end slip at maximum force ($s_{max}$) <br> • Force *versus* loaded end slip relationships <br> • Bond strength ($\tau_{max}$) <br> • Visual inspection | Bond specimens with a prismatic substate | Initial characterization (T0) and annual tests (T1 and T2) | 4 |
| **NSM** | | Bond specimens with a cubic substate | Initial characterization (T0) and annual tests (T1 and T2) | 4 |

| *Durability and long-term behaviour under natural exposure: RC CFRP strengthened slabs (full-scale)* | | | | |
|---|---|---|---|---|
| **Strengthening system** | **Property to evaluate** | **Type of specimen** | **Times of testing/type of test** | **Nº of specimens by time of testing and environment** |
| **EBR** <br><br> **NSM** <br><br> **MA** <br><br> **GA** | *Short-term tests:* <br> • Load carrying capacity ($F_{max}$) <br> • Mid-span displacement <br> • Force *versus* mid-span displacement relationships <br> • Strain in the constitutive materials <br> *Long-term tests:* <br> • Mid-span displacement *versus* time relationships <br> • Evolution of the strain in concrete, steel and CFRP at mid-span <br> • Evolution of the crack width <br> • Creep coefficient <br> • Visual inspection | RC slab strengthened with CFRP | *Short-term tests:* <br> Initial characterization with flexural tests up to failure (T0) <br><br> *Long-term tests:* <br> Flexural creep tests with monitoring for measurements during three years (T1, T2 and T3) | 4 |

The experimental results of the specimens tested annually are compared with the results collected from the existing literature, mainly accelerated ageing test results from different environmental conditions. Attempts of establishing correlations between the effects of accelerated and natural ageing are also developed. Considering the information previously reported, the last task consisted of establishing proposals to contribute for improving the existing design guidelines on the topic, e.g., CNR DT 200 R1 (CNR 2013) and ACI 440.2R-17 (ACI 2017).

## 2.4. Preliminary Work

Prior to the execution of the main programme, a preliminary set of tests was carried out. This set of tests included: (i) an analysis of the specimen's geometries and test configurations suggested in the standards for the material characterization; (ii) the evaluation of the geometry for specimens for the characterization of the bond between CFRP and concrete with the EBR and NSM techniques, and (iii) the assessment of the RC slabs established in terms of geometry, strengthening configurations and test methods. The actions (ii) and (iii) were performed in collaboration with the development of a MSc thesis (Soares 2016). Therefore, the work performed in (ii) was published in an International Journal (Soares et al. 2019).

An experimental campaign was also developed to study the viscoelastic behaviour of a commercial cold-curing epoxy adhesive. This campaign included the study of the (i) preparation methods for the epoxy adhesive (with and without degassing during the manufacturing), (ii) temperature of the initial curing (room temperature of 20 °C for 7 days and accelerated curing at 90 °C for 30 minutes followed by curing at 20 °C and 55% RH for 7 days) and (iii) tensile creep behaviour of the specimens prepared with distinct methods, under different hygrothermal conditions and distinct tensile stress levels, up to 2400 hours. The main obtained achievements were, therefore, published in a journal paper, being this work included in the present list of publications (Cruz et al. 2021).

# CHAPTER 3

## SUMMARY OF THE PAPERS

*This chapter presents a summary of the cumulative publications that is the result of the work performed in this PhD thesis. Therefore, a general overview and the interconnection between the papers is explained. Finally, the key points addressed in each paper is also given.*

### 3.1. Introduction

Figure 3.1 presents in a schematic way, the main topics addressed in each paper and corresponding scale of the study, namely material, bond and full-scale levels.
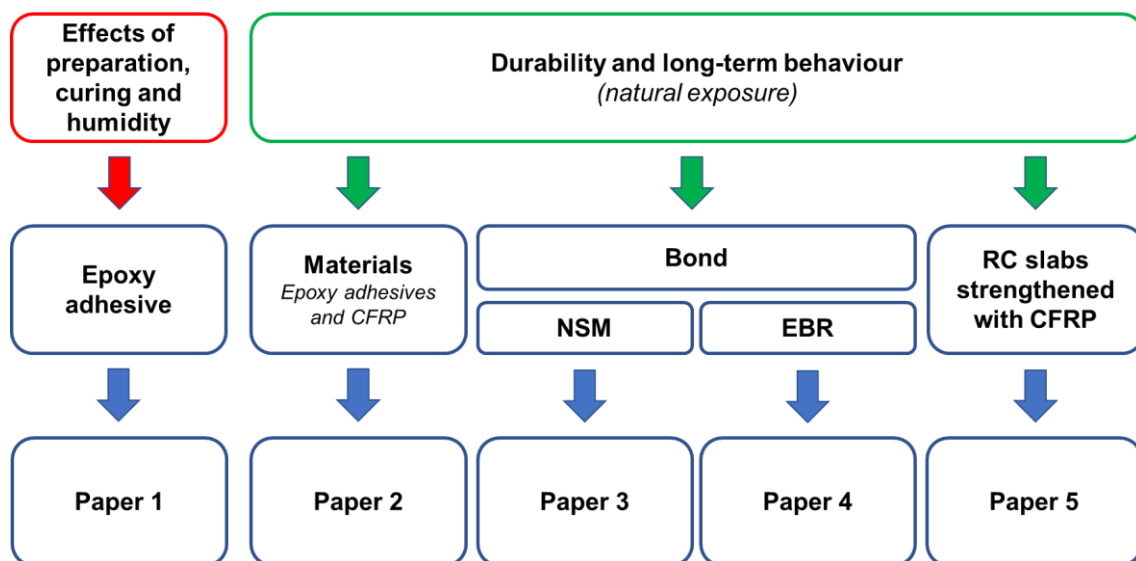


Figure 3.1 - Rationale of the papers developed in the scope of this PhD thesis.

As previously explained, this PhD thesis was developed within the scope of the FRPLongDur research project. Therefore, one of the first research questions investigated was about the effects of the epoxy preparation and curing conditions on its performance at short and long-term. In fact, this is a relevant matter for this work, particularly in the case of the RC slabs strengthened with prestressed CFRP laminates with the Gradient Anchorage (GA) method. In fact, previous investigations at Swiss Federal Laboratories for Materials Science and Technology revealed mechanical degradation of the epoxy

adhesive when it is cured fast at elevated temperatures (Michels et al. 2013). Furthermore, some attempts to improve the mechanical properties of epoxy cured fast at elevated temperatures, e.g., degassing, have been proposed by Michels et al. (Michels et al. 2013). Therefore, Paper 1 gives new insights in terms of the effects of the preparation, curing and hygrothermal conditions on the viscoelastic response of a structural epoxy adhesive used in the present research.

Once designed and produced, the specimens were installed in the six abovementioned environments. After one and two years of exposure, a group of predefined samples of the involved materials and bond specimens were collected and then tested, while the RC slabs were periodically monitored up to three years. Moreover, initial characterization tests were also performed for the involved materials and bond specimens, as well as the RC slabs. While Paper 2 addresses the studies of the durability of epoxy adhesives and CFRP laminates, Papers 3 and 4 provide the outputs of the bond durability of CFRP to concrete systems when the strengthening techniques NSM and EBR are used, respectively. Furthermore, attempts of correlating the results obtained at material (Paper 1) and bond levels (Papers 3 and 4) are done in the scope of the latter papers.

Finally, Paper 5 describes the work on the full-scale tests with the RC slabs strengthened with CFRP laminates systems, assessed under the same environments adopted for the other studies (Papers 2 to 4). This part of the work comprises (i) short-term flexural tests and (ii) long-term flexural creep tests. Similarly, in Paper 5, attempts to correlate the results of Papers 2 to 4 with the ones obtained in the RC slabs strengthened with CFRP laminates systems are also performed.

## 3.2. Paper 1

*Cruz, R., Correia, L., Cabral-Fonseca, S., and Sena-Cruz, J. 2021. Effects of the preparation, curing and hygrothermal conditions on the viscoelastic response of a structural epoxy adhesive. International Journal of Adhesion and Adhesives, 110, 102961. https://doi.org/10.1016/j.ijadhadh.2021.102961.*

The main purpose of this paper was to investigate the viscoelastic behaviour of the commercial cold-curing epoxy adhesive used as bonding agent between the CFRP laminate and concrete. In total, three experimental campaigns were performed addressing the influence of the (i) use of degassing during the preparation, (ii) temperature of the initial curing, including room temperature (20 °C) for 7 days and

accelerated curing at 90 °C for 30 minutes followed by 20 °C for 7 days and (iii) different hygrothermal conditions and distinct tensile stress levels on the epoxy's tensile creep behaviour, up to 2400 hours.

The tensile tests for mechanical characterization were performed after 7 days of curing. Tensile creep tests were developed with (i) the creep loads of 30% and 40% of the adhesives' tensile strength at 20 °C and 55% RH and (ii) creep load of 40% of the adhesives' tensile strength and hygrothermal conditions of 20 °C and 98% RH. In order to better understand the creep behaviour of the tested specimens, an analytical analysis was also developed using (i) the Burgers model and (ii) the modified Burgers model.

## 3.3. Paper 2

*Cruz, R., Correia, L., Dushimimana, A., Cabral-Fonseca, S., and Sena-Cruz, J. 2021. Durability of Epoxy Adhesives and Carbon Fibre Reinforced Polymer Laminates Used in Strengthening Systems: Accelerated Ageing versus Natural Ageing. Materials, 14(6), 1533. https://doi.org/10.3390/ma14061533.*

This paper presents the part of the experimental work performed on the material's durability regarding the epoxy adhesives and CFRP laminates, under natural ageing. Therefore, an experimental campaign for environmental exposure, including the four natural outdoor environments, a laboratory environment of water immersion under controlled temperature and a control (reference) environment with constant hygrothermal conditions was implemented.

The material's characterization was performed for two years by assessment of the physical, chemical, and mechanical properties. The investigation also includes a comparison between the results of exposure to natural ageing of this work and results of accelerated ageing tests from the literature. Moreover, suggestions for the environmental conversion factors for the epoxy adhesives and CFRP laminates are also provided.

## 3.4. Paper 3

*Cruz, R., Correia, L., Cabral-Fonseca, S., and Sena-Cruz, J. 2022. Durability of bond between NSM CFRP strips and concrete under real-time field and laboratory accelerated conditioning. Journal of*

This paper includes the work on the durability of the bond between CFRP laminate strips and concrete with the NSM technique, under natural outdoor ageing (real-time field conditioning) and accelerated ageing (laboratory accelerated conditioning). The study lasts up to two years, mainly by testing the mechanical properties of the (i) bond specimens (NSM technique) and (ii) constitutive materials (concrete, epoxy adhesive and, CFRP strips). The evolution of the mechanical properties was assessed after submission of the specimens under the environments of this work, including: (i) a control environment (20 °C and 55% RH), (ii) a water immersion environment under controlled temperature (20 °C) and (iii) the four natural outdoor environments to induce ageing mainly by carbonation, freeze-thaw cycles, elevated temperatures, and airborne chlorides from seawater.

Finally, this paper also includes the comparison between results from real-time field conditioning (of this work) and laboratory accelerated conditioning (from the existing literature). It became clear that the environmental design conversion factors provided by the existing guidelines require improvements to consider the bond durability aspects of the NSM system.

## 3.5. Paper 4

*Cruz, R., Correia, L., Cabral-Fonseca, S., and Sena-Cruz, J. 2022. Durability of bond of EBR CFRP laminates to concrete under real-time field exposure and laboratory accelerated aging. Submitted to Construction and Building Materials in 05-10-2022.*

This paper addresses the part of the experimental work related with the durability of the bond between CFRP laminates and concrete using the EBR technique. This investigation was also developed under natural exposure, here designed by real-time field exposure (RTFE) and laboratory accelerated ageing. The experimental program included, again, the exposure to the four different outdoor environments to induce especially ageing from carbonation, freeze-thaw attack, elevated temperatures, and airborne chlorides from the ocean. Additionally, it was also considered an environment with controlled conditions (20 °C and 55% RH) used as reference and an environment based on water immersion under controlled temperature (20 °C) was also considered. This study comprises the assessment of the bond

between EBR-CFRP laminates and concrete by means of single-lap shear tests during two years of ageing. For comparison purposes between the results of the durability of the constitutive materials and bond durability, the results of the involved materials (CFRP laminates, epoxy adhesive, and concrete) are recalled. The results regarding the involved materials were already published in Paper 3, being again presented to help on interpreting the results obtained for the bond of EBR-CFRP to concrete system. Nevertheless, it should be highlighted that the way of presenting such results is very different from Paper 3.

A comparison between the results from RTFE (from this work) and laboratory accelerated ageing (from the literature) was also developed. This paper also includes attempting suggestions to enhance the existing guidelines on the predictions for service life design of the EBR-CFRP to the concrete.

## 3.6. Paper 5

*Cruz, R., Correia, L., Dushimimana, A., Cabral-Fonseca, S., and Sena-Cruz, J. 2022. Long-term flexural behaviour of slabs strengthened with CFRP laminate systems under different accelerated and natural environmental conditions. Paper to be submitted.*

The Paper 5, the last paper of this PhD thesis, provides results from the full-scale tests. Therefore, this paper addresses the durability and long-term flexural behaviour of full-scale RC slabs strengthened with CFRP laminate systems, investigated under laboratory and natural environments. These slabs were strengthened using the EBR and NSM systems (non-prestressed), and the MA and GA systems (prestressed). The exposure conditions chosen were similar to the adopted in Papers 2 to 4, including laboratory exposure with a reference (control) environment and a water immersion environment (under controlled conditions) and, natural exposure with four distinct characteristic environments for inducing ageing mainly by carbonation, freeze-thaw attack, elevated temperatures, and airborne chlorides from the ocean seawater. The experimental program included two components: (i) short-term flexural tests after finishing the production of the slabs to determine the respective load-carrying capacity and, (ii) long-term flexural creep tests performed under the different environmental conditions studied/loaded conditions for up to 3 years. These latter tests were developed to study the time-dependent behaviour due to the synergistic effects of a continuous stress state imposed by a gravity sustained load and a typical environmental exposure type.

This paper also includes a comparison between the long-term creep coefficients obtained with the other ones suggested in literature approaches and existing guidelines.

# CHAPTER 4

## CONCLUSIONS AND FUTURE WORK

*The durability and long-term behaviour of reinforced concrete elements strengthened with CFRP laminates under natural exposure conditions was investigated in this PhD thesis. Three main parts composed this work: (i) a wide experimental program at a multi-scale level, (ii) attempts of establishing relationships between laboratory accelerated and natural ageing, and (iii) proposals for enhancing the existing design guidelines. A compilation of five papers comprises all the work developed, and, therefore, in the next paragraphs the main conclusions achieved are briefly presented, as well as suggestions for future work.*

## 4.1. Conclusions

### *Effects of preparation methods and curing conditions on the creep behaviour of a structural epoxy adhesive*

The preparation method used for the production of the epoxy adhesive influences significantly its tensile properties. The degassing during manufacturing provides higher elastic modulus (+45% on average) and tensile strength (+38% on average), especially when the initial accelerated curing is used. The creep behaviour of the adhesive is greatly influenced by the hygrothermal conditions, within the 2400 h of testing: (i) similar behaviour was observed with both tensile creep loads of 30% and 40% of the epoxy adhesive tensile strength at 20 °C and 55% RH, whereas (ii) tertiary creep stage (failure) was observed in the majority of the specimens exposed to 20 °C and 98% RH.

The degassing and initial accelerated curing allowed an improvement of creep behaviour, with a short tendency of better results with only degassing. As the use of vacuum is a challenge in real applications, which becomes even more difficult with application of accelerated curing, the adoption of these processes should be carefully evaluated. Moreover, as the hygrothermal conditions present a great influence on the creep behaviour, under environments with high humidity levels, it is suggested to implement strategies to avoid moisture absorption by the epoxy.

## *Durability of epoxy adhesives and CFRP laminate strips*

Regardless the type of outdoor environment, the epoxy adhesives revealed an increase in the glass transition temperature over the time while the tensile properties decreased. After one year of exposure, a distinct evolution on the tensile properties of both adhesives was obtained, with a negligible variation in ADH1 and a significant increase (up to 48%) in ADH2, for all the environments (except E2). Furthermore, after two years of exposure, a reduction of the tensile properties (up to 25%) was verified on both adhesives, with all the environments (except E2). The environment E2 was extremely detrimental for the tensile properties of both adhesives, independently of the exposure time, yielding a significant decrease (up to 75%). A complexity and simultaneity of post-curing processes and degradation factors must occurred to justify such behaviour. The mechanical properties of the CFRP laminates were only slightly affected by the environmental conditions. Regardless of the significant dispersion of the accelerated ageing tests results found in literature, this type of testing protocol yielded higher mechanical degradation than natural ageing.

## *Durability of bond between CFRP laminates and concrete with EBR and NSM techniques*

The durability of bond EBR specimens was not significantly influenced by outdoor exposure; furthermore, a bond improvement was even observed in some tests. On outdoor specimens, the maximum pull-out force varied in between a marginal degradation of 4.3% and an increase up to 16.2%, both after two years of exposure, while water-immersed accelerated ageing led to a maximum pullout force decrease of ~8%. All tested specimens faced cohesive failure in concrete, that, only in some tests, appeared together with debonding at the laminate-adhesive interface. This additional component of debonding at the laminate-adhesive interface was common at the early ages of characterization.

The durability of bond with NSM technique was only slightly affected. The maximum pull-out force on outdoor specimens varied between -8.2% and +5.9%. Additionally, accelerated ageing of water-immersion was the most deleterious environment with a maximum average bond strength decrease of approximately 12%. The failure modes were affected by the type of environment and time of exposure. Debonding failure at laminate-adhesive interface was observed in almost all tests. The exposure to outdoor environments caused the increase of the complexity of the failure modes, mainly by appearing a component of concrete cracking or splitting.

## *EBR versus NSM on the bond between CFRP laminates and concrete*

During the whole ageing period, variations in between -8.2% and +5.9% were found in the maximum force of the bond NSM-CFRP to concrete systems, excluded for specimens immersed in water. These findings mean that, in general, this system was not significantly affected by the natural ageing, at least, up to two years of exposure. On the other hand, the maximum force attained on the bond EBR-CFRP to concrete varied in between -4.3% and +16.2%, which means that this system faces marginal degradation or improvements. The improvements are not linked with better mechanical properties in the involved materials, but a better interaction among them promoting less stress concentrations along the bond line. Furthermore, while in the case of NSM-CFRP to concrete systems the average CFRP tensile stress versus tensile strength ratio was 76%, in the EBR counterpart was 19%. This also indicates that the former is less sensitive to ageing regardless of the CFRP stress level mobilized.

## *Long-term flexural creep tests on the full-scale RC slabs*

On the long-term flexural creep tests of the full-scale slabs, the lowest increase on the mid-span deflection overtime was verified on the laboratory slabs whereas the slabs exposed to the outdoor environments faced higher increase in the mid-span deflection. Regardless the type of environment, similar magnitude of creep displacements was observed in all outdoor environments, for each type of strengthening technique. It was undoubtable, the higher creep coefficients on outdoor slabs than on laboratory slabs. Additionally, higher creep coefficient values were verified in the slabs strengthened with the EBR system than in the ones strengthened with the NSM technique. The prestressed solutions (MA and GA) also showed higher creep coefficients than non-prestressed ones (EBR and NSM). Furthermore, lower creep behaviour was observed with MA system than with GA system, which indicates a better performance of the MA system than GA system.

## *Laboratory accelerated versus natural outdoor ageing*

In general, comparisons of the levels of degradation between the results of accelerated ageing and natural ageing are difficult to be developed mainly due to (i) the significant dispersion of the results of accelerated ageing tests and (ii) the scarcity of the results of natural ageing tests. Nevertheless, considering the work performed and similar times of exposure at material level (both epoxy adhesives and CFRP laminates), a tendency of having higher or similar degradation with accelerated ageing was verified. Regarding NSM-CFRP to concrete systems, similar levels of bond strength were obtained with natural and laboratory exposure, whereas on the bond between EBR-CFRP and concrete, the laboratory

accelerated aging seems more detrimental than natural exposure. Finally, the creep displacements on the RC CFRP strengthened slabs are undoubtedly higher in the slabs exposed to the outdoor environments when compared with the slabs exposed to the laboratory environments, both room (E1) and water immersion environment (E2), which makes the temperature as key aspect governing this phenomenon.

***Proposals for conversion factors and long-term creep coefficients***

Finally, conversion factors based on the meso-scale tests (materials and bond) were suggested. Based on the studies carried out, for outdoor applications, the following conversion factors were proposed: (i) adhesives – 0.55; (ii) CFRP laminates – 0.85; (iii) bond of NSM-CFRP and concrete – 0.85; and (iv) bond of EBR-CFRP and concrete – 0.75. The long-term creep coefficients found for strengthened slabs (in between 0.64 and 2.93) were compared with the existing literature approaches and design guidelines for predicting the long-term behaviour of this systems. In general, conservative estimations were obtained for non-prestressed slabs; nevertheless, the estimations are not suitable for various prestressed slab cases, mainly of prestressed GA system under outdoor exposure.

## 4.2. Suggestions for Future Work

In retrospect, the objectives established for this work were successfully achieved. The experimental work developed contributed to enhance the knowledge on the durability and long-term behaviour of the RC structures strengthened with CFRP laminates using the EBR and NSM techniques. The comparisons between results of accelerated and natural ageing allowed to better understand the effects of each type of exposure. The conversion factors suggested for the adhesives, CFRP laminates and bond with EBR/NSM systems will undoubtedly contribute to enhance the existing guidelines, particularly in regard the prediction of the long-term behaviour. However, further research is needed in this field.

The effects of the preparation, curing and hygrothermal conditions on the viscoelastic response of a structural epoxy adhesive should be further investigated by using shear tests, to simulate appropriately the shear stresses faced by the epoxy adhesive in the EBR and NSM techniques and develop attempts of correlating shear test results with tensile test results, since the latter are easier to perform. It is also suggested to establish relations between effects of the processes of accelerated curing used in this work and effects of accelerated curing with GA system used for the slabs.

In this work, 2 years of the time of exposure was used in meso-scale specimens and 3 years in the cases of full-scale specimens, which is a relatively short period for obtaining a consistent trend of evolution of mechanical properties. Therefore, it is suggested to adopt higher exposure times in future research.

Several challenges were faced in the attempts to establish relationships between accelerated and natural ageing. Therefore, more test results should be drawn, and longer times of exposure are needed to obtain more consistent relationships. Additionally, regarding the conversion factors established to the bond with EBR and NSM techniques, a methodology of transforming the conversion factors suggested for the bond strength into design approaches for the existing guidelines should be performed. Furthermore, since the existing guidelines only provide conversion factors for reducing the mechanical properties of the FRP, it is also suggested to improve them by extending the durability effects to the bond level.

Finally, the significant amount of experimental work developed in this work did not leave room for the development of analytical and numerical studies. Therefore, analytical and numerical studies should be carried out to contribute for the better understanding of the observed phenomena.

# REFERENCES

ACI (American Concrete Institute). 2007. *Guide for Evaluation of Concrete Structures before Rehabilitation*, 364.1R-07. American Concrete Institute (ACI). Farmington Hills (MI).

ACI (American Concrete Institute). 2017. *Guide for the design and construction of externally bonded FRP systems for strengthening concrete structures*, ACI 440.2R-17. American Concrete Institute. Farmington Hills (MI).

Al-Tamimi Adil, K., Hawileh Rami, A., Abdalla Jamal, A., Rasheed Hayder, A., and Al-Mahaidi, R. 2015. "Durability of the Bond between CFRP Plates and Concrete Exposed to Harsh Environments." *Journal of Materials in Civil Engineering*, 27(9), 04014252.

Al Chami, G., Thériault, M., and Neale, K. W. 2009. "Creep behaviour of CFRP-strengthened reinforced concrete beams." *Construction and Building Materials*, 23(4), 1640-1652.

Cabral-Fonseca, S., Correia, J. R., Custódio, J., Silva, H. M., Machado, A. M., and Sousa, J. 2018. "Durability of FRP - concrete bonded joints in structural rehabilitation: A review." *International Journal of Adhesion and Adhesives*, 83, 153-167.

Cabral-Fonseca, S., Nunes, J. P., Rodrigues, M. P., and Eusébio, M. I. 2011. "Durability of carbon fibre reinforced polymer laminates used to reinforced concrete structures." *Science and Engineering of Composite Materials*, 18(4), 201-207.

CEN (European Committee for Standardization). 2000. *EN 206-1. Concrete — Part 1: Specification, performance, production and conformity*, European Committee for Standardization (CEN). 2000.

CERF (ASCE Civil Engineering Research Foundation). 2001. *Gap Analysis for Durability of Fiber Reinforced Polymer Composites in Civil Infrastructure*, Civil Engineering Research Foundation, American Society of Civil Engineers (ASCE), Reston, VA.

CNR (Advisory Committee on Technical Recommendations for Construction). 2013. *CNR-DT 200 R1/2013. Guide for the design and construction of externally bonded FRP systems for strengthening existing structures.*

Coelho, M. R. F., Sena-Cruz, J. M., and Neves, L. A. C. 2015. "A review on the bond behavior of FRP NSM systems in concrete." *Construction and Building Materials*, 93, 1157-1169.

Correia, L. 2018. *Durability and long-term behaviour of RC slabs strengthened in flexure with prestressed CFRP laminate strips*, PhD Thesis. University of Minho, Portugal. 2018.

Correia, L., Sena-Cruz, J., Michels, J., França, P., Pereira, E., and Escusa, G. 2017. "Durability of RC slabs strengthened with prestressed CFRP laminate strips under different environmental and loading conditions." *Composites Part B: Engineering*, 125, 71-88.

Correia, L., Teixeira, T., Michels, J., Almeida, J. A. P. P., and Sena-Cruz, J. 2015. "Flexural behaviour of RC slabs strengthened with prestressed CFRP strips using different anchorage systems." *Composites Part B: Engineering*, 81, 158-170.

Cromwell, J. R., Harries, K. A., and Shahrooz, B. M. 2011. "Environmental durability of externally bonded FRP materials intended for repair of concrete structures." *Construction and Building Materials*, 25(5), 2528-2539.

Cruz, R., Correia, L., Cabral-Fonseca, S., and Sena-Cruz, J. 2021. "Effects of the preparation, curing and hygrothermal conditions on the viscoelastic response of a structural epoxy adhesive." *International Journal of Adhesion and Adhesives*, 110, 102961.

Cruz, R., Correia, L., Dushimimana, A., Cabral-Fonseca, S., and Sena-Cruz, J. 2021. "Durability of Epoxy Adhesives and Carbon Fibre Reinforced Polymer Laminates Used in Strengthening Systems: Accelerated Ageing versus Natural Ageing." *Materials*, 14(6), 1533.

De Lorenzis, L., and Teng, J. G. 2007. "Near-surface mounted FRP reinforcement: An emerging technique for strengthening structures." *Composites Part B: Engineering*, 38, 119-143.

Deloite. 2018. "European Construction Monitor 2017–2018: A looming new construction crisis?".

Fernandes, P. 2016. *Bond behaviour of NSM CFRP-concrete systems: durability and quality control*, PhD Thesis. University of Minho, Portugal. 2016.

Fernandes, P., Granja, J. L., Benedetti, A., Sena-Cruz, J., and Azenha, M. 2015. "Quality control and monitoring of NSM CFRP systems: E-modulus evolution of epoxy adhesive and its relation to the pull-out force." *Composites Part B: Engineering*, 75, 95-103.

Fernandes, P., Sena-Cruz, J., Xavier, J., Silva, P., Pereira, E., and Cruz, J. 2018. "Durability of bond in NSM CFRP-concrete systems under different environmental conditions." *Composites Part B: Engineering*, 138, 19-34.

Fernandes, P. M. G., Silva, P. M., and Sena-Cruz, J. 2015. "Bond and flexural behavior of concrete elements strengthened with NSM CFRP laminate strips under fatigue loading." *Engineering Structures*, 84, 350-361.

FIB (Fédération internationale du beton/International Federation for Structural Concrete (fib)). 2013. *Fib Model Code for Concrete Structures 2010*, Ernst & Sohn, a Wiley brand.

FIB (Fédération Internationale du Béton). 2019. *Fib Bulletin 90. Externally applied FRP reinforcement for concrete structures*, Fédération Internationale du Béton.

FIB (Fédération Internationale du Béton/International Federation for Structural Concrete (fib)). 2022. *fib Bulletin 103. Guide for Strengthening of Concrete Structures. Guide for good practice*.

FIEC. 2020. "Key Figures 2019. Construction Activity in Europe. Edition 2018." *European Construction Industry Federation*.

Helbling, C., and Karbhari, V. M. (2007). "3 - Durability of composites in aqueous environments." *Durability of Composites for Civil Structural Applications*, Vistasp M. Karbhari, ed., Woodhead Publishing, 31-71.

IPQ (Instituto Português da Qualidade). 2010. *NP EN EN 1992-1-1. Eurocode 2: design of concrete structures - Part 1-1: general rules and rules for buildings*, Instituto Português da Qualidade (IPQ). Caparica, Portugal. 2010.

Kabir, M. I., Shrestha, R., and Samali, B. 2016. "Effects of applied environmental conditions on the pull-out strengths of CFRP-concrete bond." *Construction and Building Materials*, 114, 817-830.

Michels, J., Sena-Cruz, J., Czaderski, C., and Motavalli, M. 2013. "Structural Strengthening with Prestressed CFRP Strips with Gradient Anchorage." *Journal of Composites for Construction*, 17(5), 651-661.

Michels, J., Zile, E., Czaderski, C., and Motavalli, M. 2014. "Debonding failure mechanisms in prestressed CFRP/epoxy/concrete connections." *Engineering Fracture Mechanics*, 132, 16-37.

Pellegrino, C., and Sena-Cruz, J. 2016. *Design Procedures for the Use of Composites in Strengthening of Reinforced Concrete Structures: State-of-the-Art Report of the RILEM Technical Committee 234-DUC*.

S&P. 2010. "Pre-stressed S&P laminates CFK. Manual for applicators." *Pre-stressed S&P Laminates CFK. Manual for Applicators*.

S&P. 2014. "S&P CFRP Laminates. Technical Datasheet."Seewen, Switzerland.

S&P. 2015. "S&P 220 Resin epoxy adhesive. Technical Data Sheet."Seewen, Switzerland.

Sen, R. 2015. "Developments in the durability of FRP-concrete bond." *Construction and Building Materials*, 78, 112-125.

Sena-Cruz, J. M., Barros, J. A. O., Coelho, M. R. F., and Silva, L. F. F. T. 2012. "Efficiency of different techniques in flexural strengthening of RC beams under monotonic and fatigue loading." *Construction and Building Materials*, 29, 175-182.

Sika. 2017. "Sikadur®-30. Product Data Sheet "SIKA: Dublin, Ireland, 2017.

Soares, S., Sena-Cruz, J., Cruz, J., and Fernandes, P. 2019. "Influence of Surface Preparation Method on the Bond Behavior of Externally Bonded CFRP Reinforcements in Concrete." *Materials*, 12, 414.

Soares, S. R. R. (2016). "Estruturas de betão armado reforçadas com laminados de CFRP: caracterização da aderência e do comportamento em flexão." Mestrado, Univesidade do Minho, Guimarães.

Sousa, J. M., Correia, J. R., and Cabral-Fonseca, S. 2018. "Durability of an epoxy adhesive used in civil structural applications." *Construction and Building Materials*, 161, 618-633.

Subhani, M., Al-Ameri, R., and Al-Tamimi, A. 2016. "Assessment of bond strength in CFRP retrofitted beams under marine environment." *Composite Structures*, 140, 463-472.

Tatar, J., and Hamilton, H. R. 2016. "Comparison of laboratory and field environmental conditioning on FRP-concrete bond durability." *Construction and Building Materials*, 122, 525-536.

Tatar, J., and Milev, S. 2021. "Durability of Externally Bonded Fiber-Reinforced Polymer Composites in Concrete Structures: A Critical Review." *Polymers*, 13(5), 765.

# Annex I - Cumulative Papers of the Thesis

## Paper 1

**Title:** Effects of the preparation, curing and hygrothermal conditions on the viscoelastic response of a structural epoxy adhesive

**Reference:**

Cruz, R., Correia, L., Cabral-Fonseca, S., and Sena-Cruz, J. 2021. Effects of the preparation, curing and hygrothermal conditions on the viscoelastic response of a structural epoxy adhesive. *International Journal of Adhesion and Adhesives*, 110, 102961. https://doi.org/10.1016/j.ijadhadh.2021.102961.
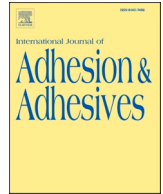
# Effects of the preparation, curing and hygrothermal conditions on the viscoelastic response of a structural epoxy adhesive

Ricardo Cruz [a], Luís Correia [a], Susana Cabral-Fonseca [b], José Sena-Cruz [a,*]

[a] University of Minho, ISISE, IB-S, Department of Civil Engineering, 4800-058, Guimarães, Portugal
[b] LNEC, National Laboratory of Civil Engineering, 1700-075, Lisboa, Portugal

## ABSTRACT

This paper addresses the viscoelastic behaviour of a commercially available cold-curing structural epoxy adhesive, under different preparation, curing and hygrothermal conditions. The main parameters studied were the preparation method (influence of the degassing and the temperature of the initial curing), the creep stress level, and the hygrothermal conditions. Tensile creep tests last up to 2400 h. Test results revealed that the preparation method has great influence on the tensile properties of the adhesive, particularly on the viscoelastic response where degassing and curing at 20 °C showed lower creep deformations. Specimens under 98% of relative humidity faced tertiary creep and then rupture. For the adopted levels of creep stress, the adhesive shows a linear creep behaviour, being parameterized using the Burgers and the modified Burgers equations.

## 1. Introduction

The use of fibre reinforced polymer (FRP) materials for strengthening existing reinforced concrete (RC) structures has been constantly increasing during the past few decades [1,2]. Typically, FRP materials are externally bonded (EBR – Externally Bonded Reinforcement strengthening technique) or inserted into grooves opened on the concrete cover (NSM – Near Surface Mounted strengthening technique) of the elements to be strengthened [3]. FRP materials can be also applied in the prestressed state throughout the EBR or the NSM techniques. Several advantages have been appointed to the use of prestress, mainly because it combines the benefits of passive EBR or NSM FRP systems with the advantages associated with external prestressing (deflection and crack width reduction, use of non-corrosive materials, more efficient use of the FRP materials, increase in the ultimate carrying capacity, among others) [4–6]. Epoxy adhesives, in particular cold-curing adhesives (able to cure under ambient temperature after the different components have been mixed), present a large variety of properties that make them suitable and very appealing for the bonding operation inherent to the EBR and NSM techniques, namely: (i) limited and low cure shrinkage; (ii) great compatibility with the concrete substrate and which allows good stress transfer between materials; (iii) good mechanical properties; (iv) wide range of operating temperature; (v) applicable in vertical surfaces, when presenting thixotropic characteristics; (vi) long open time; and (vii)

good wetting properties for a variety of substrates. Bonding with epoxy adhesives can serve as an alternative to mechanical fasteners, which can be incompatible with several FRP systems [7–11].

The physical and mechanical properties of a cured epoxy are highly influenced by the curing conditions, in particular by the temperature, humidity and duration. Low temperature or excessive humidity can compromise the curing of the epoxy adhesive and undermine its performance and durability. In fact, extremely low temperatures (0 °C) inhibited the curing from happening, whereas low temperatures (5 °C to 10 °C) may cause material vitrification and slowed down the curing process [11–13]. In contrast, elevated temperature accelerates the curing process of the epoxy adhesive. The adhesive's ability to cure fast at high temperatures has been used in the development of the gradient anchorage method, which is a non-mechanical anchorage used for pre-stressing EBR-FRP strips [4,8,14,15]. There are several advantages on using gradient anchorage method for FRP prestressing, namely the immunity to corrosion and the shorter duration for prestressing the FRP (finished after 3 h). When compared with the ideal curing conditions (typically it last 3–7 days at 20 to 25 °C, depending on the type of adhesive), accelerated curing with high temperature can lead to higher glass transition temperature [15]. Michels et al. [8] investigated the effect of different mixing and curing procedures on the mechanical performance of three different commercially available epoxy resins. The study included specimens subjected to accelerated curing (30 min at

---

\* Corresponding author.
*E-mail address:* jsena@civil.uminho.pt (J. Sena-Cruz).

90 °C) and to curing under room temperature (21 °C) for different periods of time (1–7 days). Specimens exposed to accelerated curing presented lower tensile properties (reduction up to 39% and 36% in strength and elastic modulus, respectively) and higher porosity when compared with specimens cured at room temperature. The porosity increased when the high temperature was applied, and it appears to be the cause for the apparent reduction on the tensile properties. The authors also used a degassing mixer to minimize gas inclusion on the final mixture of the epoxy and, with it, observed a strong reduction on the porosity on both type of specimens (with and without accelerated curing). Specimens prepared with the degassing mixer presented the highest tensile modulus of elasticity (increase of 88% and 38% for accelerated curing and room temperature curing, respectively) and tensile strength (increase of 119% and 43% for accelerated and room temperature curing, respectively). Moussa et al. [12] investigated the influence of curing a cold-curing epoxy adhesive at low temperatures and a significant increase in the curing time was observed with lower temperatures; at high temperatures, in between 35 °C to 60 °C, few hours (3.7–1.6 h) were necessary to attain the full curing, whereas at a low temperature of 5–10 °C, longer curing periods (3 days) were need. Moussa et al. [13] performed another investigation where an epoxy adhesive was cured at different isothermal temperatures (5–70 °C) during different curing periods. To evaluate the influence, the authors characterized the physical and mechanical properties of the adhesive. From the mechanical point of view, the development of tensile strength and stiffness *versus* time during isothermal curing rapidly increased at high curing temperatures, while a delay in the curing process was observed at low temperatures, mainly during the initial curing stage. Additionally, the authors concluded that the maximum stiffness was lower at 70 °C of curing temperature than at 25 °C. Savvilotidou et al. [16] studied the influence of curing level and exposure to humidity and alkalinity on the long-term physical and mechanical properties of an epoxy adhesive. The authors concluded that water uptake led to a reduction on the tensile E-modulus and tensile strength as a function of weight increase and immersion time. Additionally, the plasticization caused by the water uptake has changed the stress-strain curve of the specimens from initially almost linear to considerable non-linear. Moreover, there was a decrease in stiffness and strength, whereas the strain at failure increased.

In the context of FRP materials used in the EBR or NSM strengthening techniques, the knowledge on durability and long-term behaviour of the constituent materials is crucial. In particular, the creep behaviour of the bonding adhesive, which has been already recognized as one of the most relevant properties to guarantee proper stress transfer in a bonded joint over time [10]. When exposed to sustained stress, epoxy adhesives typically present relevant creep deformation, which are strongly affected by the loading age, stress level and exposure conditions (temperature and humidity) [7,10]. Costa and Barros [10] carried out a study on the tensile creep behaviour of a commercially available epoxy adhesive used for construction. Specimens were loaded with a constant stress of 20%, 40% and 60% of the adhesive's tensile strength, for a period of 1000 h, under controlled environment (20 °C and 60% of relative humidity). The epoxy adhesive presented a linear viscoelastic/viscoplastic behaviour up to the maximum stress level (60% of the tensile stress), parameterized using the modified Burgers model. It is noteworthy to mention that the specimens were loaded with 3 days of curing, for which the authors agreed to be enough time of curing to reach the adequate bond strength to concrete and to stabilize the tensile strength and elastic modulus.

In prestress applications with EBR-FRP strips, the epoxy adhesive might be subjected to sustained stress at early ages (after 24 h) [4,5]. In this context, it is essential to understand the creep behaviour of the adhesive at early stages, because excessive creep can compromise the effectiveness of the prestress application [10]. Silva et al. [7] performed an experimental tensile creep test with epoxy adhesive, since its early ages. Epoxy specimens were exposed to (i) two different creep load

levels (30% and 40% of the tensile strength) at (ii) four different loading ages (1, 2, 3, and 7 days). In agreement with Costa and Barros [10], Silva et al. [7] observed a significant development of the instantaneous tensile properties (modulus and strength) up to the 3 days of age, for which the rate of increase of stiffness slowed down and stabilized. The creep coefficient (ratio of the creep and instantaneous deformations/strain) decreased with the age of loading, being equal to 4.1, 2.1, 1.9 and 1.3 for specimens loaded at the ages of 1, 2, 3, and 7 days, respectively. The results showed that the curing of the adhesive, specifically the formation of cross-links of the polymer chains, continued to occur during the creep loading, which led to similar post-unloading phase between all specimens. Results also showed that the epoxy presented linear viscoelastic behaviour up to the maximum stress level (40% of the tensile stress). With an unsuccessful attempt to simulate the creep behaviour of epoxy adhesive in early ages with the modified Burgers model, the authors presented a new framework based on the generalized Kelvin model, with excellent fit to the experimental results since the early ages (1 day of curing), in both the loading and recovery phase of the creep tests.

The long-term behaviour of an adhesive can be compromised by the environmental conditions to which it is exposed. Therefore, research has been carried out to evaluate the durability of epoxy adhesives, namely the most severe environments, degradation mechanisms and the effect of such environments have been reported [9,11,17]. Cabral-Fonseca et al. [11] presented an exhaustive literature review on the durability of FRP-concrete bonded joints, with a great focus on the durability of the adhesive in several environments (water/moisture, temperature, freeze-thaw, chemical environments, UV radiation, and fire). According to their literature review, exposure to moisture can result in reversible degradation processes such as swelling and plasticization and, with time, to irreversible processes like chemical degradation, micro cracking and chain scission. Temperature can influence the propagation of moisture and potentiate the degradation process on epoxy resins. Therefore, the hygrothermal conditions have great influence on the long-term properties of epoxy adhesive and, consequently on FRP-concrete bonded joins. The experimental work and literature review carried out by Sousa et al. [9] and Silva et al. [17] on the durability of epoxy adhesives for construction sector subjected to different hygrothermal environments supports the former statement. In both studies, a generalized decrease on the on the glass transition temperature and on the tensile properties was detected. Both authors observed that a less severe degradation occurred for specimens immersed in saltwater, than in regular water. Additionally, Silva et al. [17] noted that specimens subjected to thermal cycles showed an increase on the tensile properties (up to 15% and 33% on the modulus and ultimate strength, respectively) due to a post-curing event motivated by the exposure to high temperatures.

In spite of these recent studies on epoxy resins typically used for RC strengthening with FRP materials, the existing knowledge about its durability is still scarce. Moreover, the effect of different mixing and curing conditions on the long-term behaviour of such adhesives is unknown. Epoxy adhesives commonly used in EBR-FRP prestress applications are continuously subjected to a stress state face environment where the effect of moisture and temperature is also unknown and can be relevant.

This study intends to extend the existing knowledge namely in the following topics: (i) creep behaviour of epoxy adhesives manufactured with degassing and accelerated curing; (ii) influence of the relative humidity on the creep behaviour of epoxy adhesives prepared with distinct processes; and (iii) suitability of existing models to simulate the creep behaviour of epoxy adhesives prepared using different processes. Therefore, this work aims at assessing the tensile creep behaviour of a commercially available epoxy-based structural adhesive (traded under the name "S&P Resin 220"), used for bonding Carbon FRP (CFRP) to concrete throughout the EBR and NSM techniques. This epoxy has been also used for EBR-FRP prestress applications, therefore specific focus was given to the preparation and curing conditions and to the effect of

the hygrothermal conditions under creep stress. The experimental work included the following variables: (i) three distinct preparation procedures; (ii) two creep stress levels; and (iii) two different hygrothermal conditions.

This paper presents the results of an experimental work on the tensile mechanical properties and the viscoelastic behaviour of a commercially available cold-curing structural epoxy adhesive. Three different preparation methods (application or not of degassing during mixing and of high temperatures during the curing) were considered during samples manufacturing. Tensile tests after 7 days were performed. Then, tensile creep tests were conducted, varying the creep stress level and the hygrothermal conditions up to 2400 h. The linear creep behaviour observed for the adopted levels of creep stress, was parameterized using the Burgers and the modified Burgers equations.

## 2. Experimental programme

### 2.1. The epoxy adhesive studied

The 'S&P Resin 220 epoxy adhesive' was studied in the present investigation. It is a commercially available epoxy adhesive widely used in retrofitting reinforced concrete structures with FRP laminate strips. This structural epoxy is a grey two-component mix, where the component A (Bisphenol A based resin, light grey colour) is mixed with the component B (hardener, black colour) with the ratio of 4:1 (Component A: Component B). This epoxy adhesive is solvent free, thixotropic and, after mixing the two components, presents the density of 1.70–1.80 [g/cm$^3$]. According to the supplier, after 3 days of curing at 20 °C, this epoxy adhesive should present the following mechanical properties [18]: (i) compressive strength >70 MPa (EN 12190:1999 [19]); (ii) flexural E-modulus >7.1 GPa (EN ISO 178:2002 [20]); (iii) shear strength >26 MPa (EN 12615:1999 [21]).

### 2.2. Specimens, test setup and methods

Specimens were prepared with Teflon moulds in which the mixed compound was filled in. Each specimen was produced according to "type 1A″ defined in EN ISO 527–2:2012 [22], with a total length of 170 mm and a thickness of 4 mm, in a dogbone shape (see Fig. 1a). In total, 60 specimens were prepared, 24 of them were used to assess the instantaneous mechanical tensile properties while the remaining 36 specimens were used to study the tensile creep behaviour. Three batches were used

for manufacturing of the epoxy specimens, each one planned for studying the effect of a specific set of hygrothermal conditions on the viscoelastic response of the adhesive. The preparation of the epoxy specimens was carried out using three different preparation methods and curing conditions:

i. REF method, in which the epoxy adhesive was prepared following the instructions of the supplier [18]: first, each component was separately stirred; then component A was mixed with the component B with the weight ratio of 4:1; the compound was thoroughly and slowly manually mixed until the colour was uniformly grey and free of any streaks; the mixing process lasted approximately 4 min. Afterwards, the uniform mixture was poured into the Teflon moulds. Then, an acetate sheet was placed on the top surface and pressed with a steel roller, thus ensuring the correct thickness. The specimens were demoulded after 24 h and kept in a climatic chamber at 20 (±2) °C of temperature and 55 (±2)% of relative humidity (20 °C/55% RH), for 7 days before testing;

ii. V20 method, in which the mix process involved degassing in order to minimize the gas inclusion in the final mixture (see Fig. 2). The mix process was identical to the adopted process for REF specimens, with the inclusion of degassing during the mixing. V20 specimens were also kept in a climatic chamber at 20 °C/55% RH, for 7 days before testing;

iii. V90 method, in which the initial step of mixing and degassing used in V20 specimens was also adopted. However, just after casting on the Teflon moulds, these specimens were subjected to an accelerated curing process, exposing them to a temperature of 90 (±2) °C during 30 min. Then, the specimens were kept for 7 days at 20 °C/55% RH, in a climatic chamber.

The tensile properties of the epoxy adhesive were assessed throughout the standard ISO 527–1:2012 [23]. The tensile tests were carried out in a universal testing machine under displacement control of 1 mm/min (see Fig. 3a). The applied load was measured using a load cell with 10 kN of maximum capacity (linearity error less than ± 0.05%) and the axial strain was measured using a clip gauge with a base length of 50 mm (precision of ±1 μm) placed at the middle specimen height. Prior performing the tensile tests, the thickness and width of all specimens was assessed using a digital calliper (0.01 mm of precision) in three different sections (one at middle height and two at 25 mm apart to the
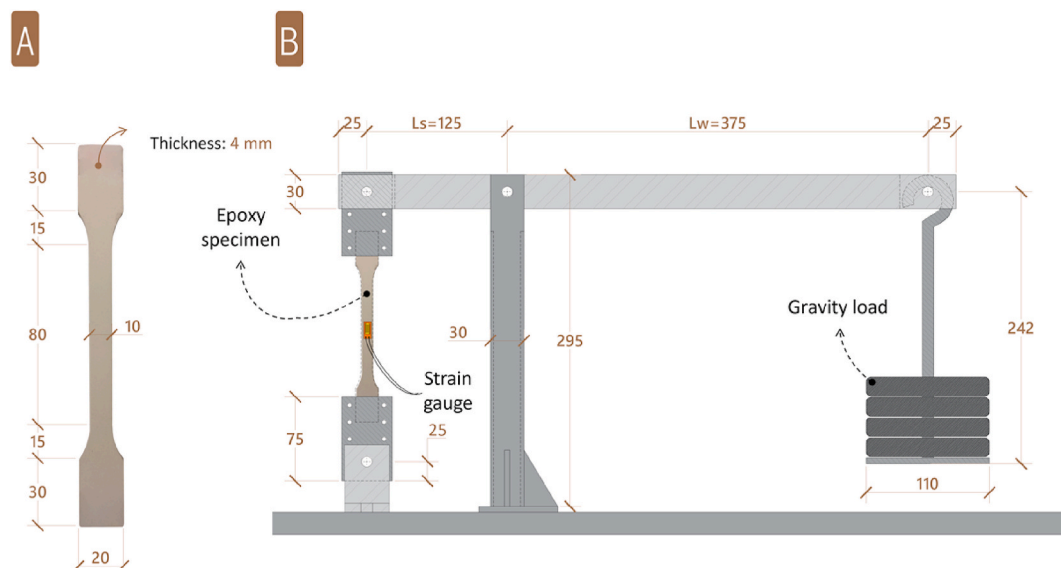


**Fig. 1.** (a) Tensile test specimen's geometry; (b) tensile creep test setup. All units in [mm].
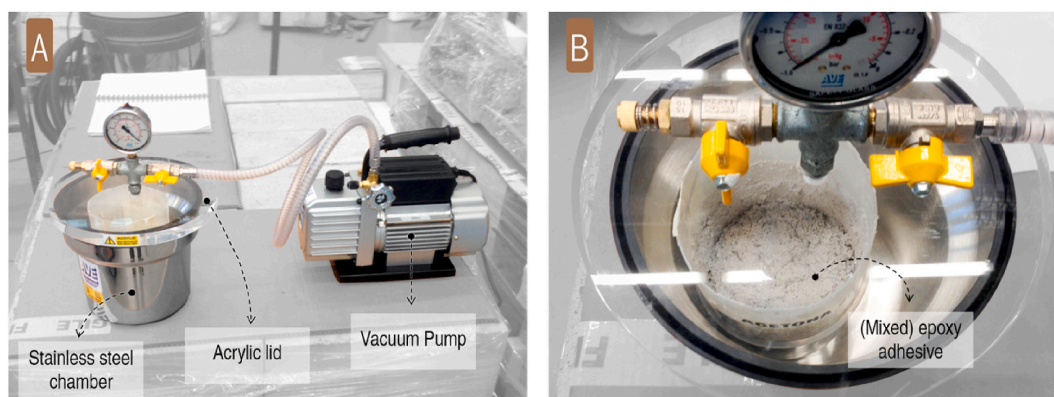
**Fig. 2.** (a) Vacuum system; (b) degassing of mixed epoxy adhesive components.
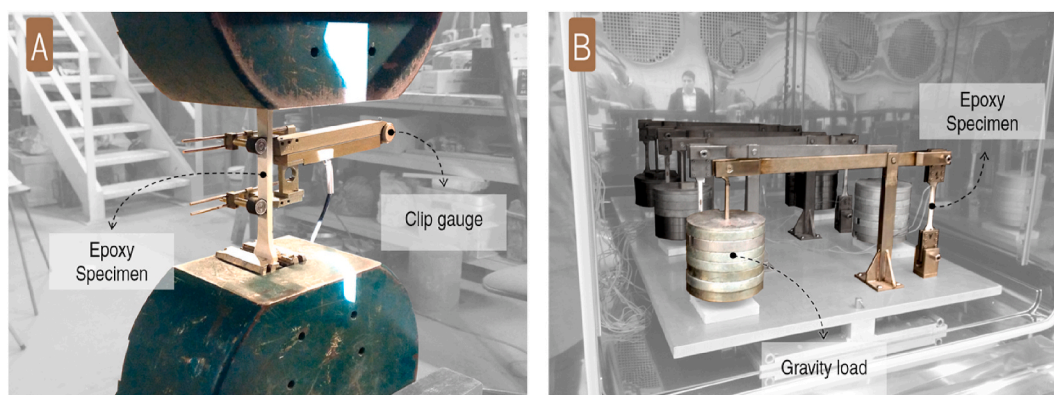


**Fig. 3.** Test setup for (a) tensile tests; (b) tensile creep tests in the climatic chamber.

former). In total, 24 specimens were tested, eight for each type of preparation method (see Table 1). The tensile creep properties were assessed using a mechanical system based on a lever structure [7,10], schematically represented in Fig. 1b, where each epoxy specimen was subjected to constant stress throughout application of a predefined gravity load (see Fig. 3b). A total of 18 specimens were submitted to a constant tensile stress for a minimum period of 100 days (2400 h). These specimens were grouped in the following three series:

i. EP1 series (composed of 6 specimens: 2 REF, 2 V20 and 2 V90), where specimens were subjected to a creep load equal to 40% of the adhesive's tensile strength, in a controlled environment characterized by 20 °C/55% RH;

ii. EP2 series (composed of 6 specimens: 2 REF, 2 V20 and 2 V90), where specimens were subjected to a load of 30% of the adhesive's tensile strength in the same environmental conditions as specimens from series EP1;

iii. EP3 series (composed of 6 specimens: 2 REF, 2 V20 and 2 V90), where specimens were subjected to a creep load equal to 30% of the adhesive's tensile strength, and to the hygrothermal conditions of 20 °C/98% RH.

To secure the referred environmental conditions, a climatic chamber FITOCLIMA 1500EC45 (temperature range: 45 °C to 180 °C; humidity range: 10%–98%) was used. In the creep test programme, the specimens were labelled according to the following mask X_Y_Z, where the variables are: X stands for the series (EP1, EP2, and EP3); Y corresponds to the preparation method (REF, V20, and V90); and Z is used to differentiate specimens from the same series and preparation method (1 and 2). The instrumentation included two strain gauges with a 5 mm measuring length (type BFLA-5-3-3L from TML) installed precisely at the

middle height of each face (see Fig. 1b). The data was acquired at frequency of 1 Hz during the first hour of loading, followed by 16,67 Hz (one record per minute) during 2 h, and finally 1,67 Hz (one record every 10 min) until the end of the test. Nine "dummy" specimens were also manufactured (3 for each series, where each specimen was prepared according to the preparation methods described above) and instrumented with one strain gauge to measure possible environmental effects on the material and on the strain gauge wires. Nine additionally specimens were used in EP3 series (three specimens for each preparation method) to measure the mass variation. The tensile tests and the creep loading were always conducted 7 days after the adhesive preparation.

## 3. Results and discussion

### 3.1. Tensile properties

The stress-strain curves obtained from the tensile tests are presented in Fig. 4a, while the tensile strength ($f_{ult}$), the elastic modulus ($E_{adh}$) and the ultimate strain ($\varepsilon_{ult}$) are graphically presented throughout boxplot diagrams in Fig. 4b. Table 1 presents the main parameters obtained from the tensile tests.

Results in Fig. 4a show that the preparation method has great influence in the mechanical properties of the epoxy adhesive, namely that the degassed specimens (V20 and V90) exhibited a clear increase on the tensile strength and elastic modulus and decrease on ultimate strain, when compared with REF specimens. The tensile properties, $E_{adh}$, $f_{ult}$, and $\varepsilon_{ult}$, obtained in REF specimens are equal to 7.81 GPa (CoV = 3.16%), 22.0 MPa (CoV = 6.02%), and 0.40% (CoV = 29.91%), respectively. Because this epoxy adhesive is commercially available, several authors have already characterized the tensile properties, e.g. Refs. [7,8,10,17,24], and their results are in agreement with the ones

**Table 1**
Results of tensile tests.

| Preparation Method | Series (1) | Specimen | $f_{ult}$ [MPa] | $E_{adh}$ [GPa] | $\varepsilon_{ult}$ [%] |
|---|---|---|---|---|---|
| **REF** | EP1 | REF_1 | 21.5 | 7.65 | 0.48 |
| *1. Manual* | | REF_2 | 20.4 | 7.39 | 0.39 |
| *mixing* | | REF_3 | 20.5 | 7.67 | 0.34 |
| *2. Curing at* | | REF_4 | 23.0 | 7.67 | 0.59 |
| *20 °C and 55%* | EP2 | REF_5 | 24.4 | 7.88 | 0.55 |
| *RH for 7 days* | | REF_6 | 23.2 | 8.11 | 0.32 |
| | | REF_7 | 21.8 | 7.98 | 0.27 |
| | | REF_8 | 21.2 | 8.16 | 0.25 |
| | | **Average** | **22.0** (6.02%) | **7.81** (3.16%) | **0.40** (29.91%) |
| **V20** | EP1 | V20_1 | 29.5 | 11.12 | 0.31 |
| *1. 1. Manual* | | V20_2 | 28.1 | 11.31 | 0.27 |
| *mixing +* | | V20_3 | 25.4 | 11.11 | 0.23 |
| *degassing* | | V20_4 | 29.0 | 11.24 | 0.29 |
| *2. Curing at* | EP2 | V20_5 | 30.0 | 11.15 | 0.26 |
| *20 °C and 55%* | | V20_6 | 30.3 | 10.86 | 0.30 |
| *RH for 7 days* | | V20_7 | 28.4 | 10.48 | 0.28 |
| | | V20_8 | 30.3 | 10.70 | 0.33 |
| | | **Average** | **28.9** (5.25%) | **11.00** (2.45%) | **0.28** (10.40%) |
| **V90** | EP1 | V90_1 | 31.5 | 12.96 | 0.25 |
| *1. Manual* | | V90_2 | 31.3 | 12.02 | 0.27 |
| *mixing +* | | V90_3 | 31.4 | 12.01 | 0.27 |
| *degassing* | | V90_4 | 32.6 | 11.54 | 0.30 |
| *2. Accelerated* | EP2 | V90_5 | 29.9 | 11.04 | 0.27 |
| *curing at 90 °C* | | V90_6 | 33.5 | 11.22 | 0.37 |
| *for 30 min* | | V90_7 | 33.6 | 11.30 | 0.35 |
| *3. Curing at* | | V90_8 | 31.5 | 10.96 | 0.31 |
| *20 °C and 55%* | | **Average** | **31.9** (3.58%) | **11.63** (5.39%) | **0.30** (13.27%) |
| *RH for 7 days* | | | | | |

**Notes:** (1) Tests were conducted 7 days after casting – specimens from EP1 and EP2 series were manufactured/tested in distinct dates (only one batch per series); the values between parentheses are the corresponding coefficient of variation.

obtained during this study (regarding the REF preparation procedure). When compared with the REF specimens, the V20 specimens presented an increase on the average tensile strength and elastic modulus of 31% and 41%, respectively, whereas the V90 specimens show an even higher growth on $f_{ult}$ and $E_{adh}$ of 45% and 49%, respectively. The increase on these two parameters was expected in degassed specimens, since the vacuum process drastically reduces the quantity of pores (created by the existence of air and volatiles). According to Michels et al. [8], the porosity values of ~2.5%–3.5% can be found in normal epoxy mixing by hand followed by curing at room temperature, while specimens that undergo degassing process have porosity values of ~0.5%. The same authors also realized that curing at higher temperatures (80 °C to 90 °C for 25 min), led to faster development of strength and stiffness and it might cause an increase on the porosity ratio. In the present study, results show an increase on the tensile strength and elastic modulus of specimens prepared with the V90 method, when compared with the V20 (see Table 1 and Fig. 4b). The boxplot diagrams presented in Fig. 4b shows the dispersion on the results of each method of preparation and supports the influence between the preparation method and the mechanical performance of the epoxy. Fig. 4b also presents the average value for each studied parameter. In average the ultimate strain on the REF specimens was greater than on V20 and V90 specimens. It is, however, noteworthy to mentioned that the ultimate strain observed on REF specimens exhibit the greatest dispersion of results. In all the three evaluated parameters ($E_{adh}$, $f_{ult}$, and $\varepsilon_{ult}$), the lowest dispersion of results was observed on degassed specimens cured at room temperature, followed by the specimens subjected to accelerated curing at 90 °C.

### 3.2. Tensile creep behaviour

As introduced before, the assessment of the tensile creep properties

of the epoxy adhesive was carried out throughout three series of tests, each one composed of 6 specimens. The main variables in the study were (i) the preparation procedure; (ii) the creep load; and the (iii) hygrothermal conditions. For each series, three "dummy" specimens (each one with a different preparation procedure) were instrumented with one strain gauge to measure the other effects, namely (i) epoxy curing effects due to hygrothermal conditions and (ii) thermal effect on the measuring system (sensors, wires, etc.). Fig. 5 shows the typical evolution of strain with the time observed on the "dummy" specimens – EP2_V20 ("Dummy") –, on the creep specimens – EP2_V20_1 (Original) –, and the result when the strain value from the "dummy" specimen is subtracted from the creep specimen – EP2_V20_1 (Final). As can be seen in Fig. 5, the strain variation overtime in the control specimen could not be neglected and, therefore, the strain measured in the test specimens was rectified based on the measurements from the control specimens manufactured with the same preparation procedure. In general, the "dummy" specimens showed a constant strain increase (expansion) of 0.002% of strain and 0.005% of strain every 100 days, for the environments with 50% RH and 98% RH, respectively. After 2400 h, the average 0.048% of strain measured on the "dummy" specimens subjected to 55% RH represented, approximately 14% and 16% of the total strain registered in the "original" specimens from EP1 series (load equal to 40% of the adhesive's tensile strength) and EP2 series (load equal to 30% of the adhesive's tensile strength), respectively. Although the strain increase on the "dummy" specimens from EP3 series (98% RH) was the highest, it represented, in average, 17% of the total strain registered in the "original" specimens at failure. It should be noted that in EP3 series, the failure typically occurred before 2400 h. Also, the strain was registered at the end of the test, with the full development of the primary, secondary and tertiary creep stages. Therefore, the abovementioned ratio between "dummy" strain and "original" strain cannot be directly compared between series. It should be also noted that within each series, the "dummy" strain observed on specimens prepared with the degassing procedure (V20 and V90) presented slightly lower values than the reference specimens (REF). This observation reveals that the degassing procedure might led to greater water uptake resistance. For the EP3 series, the kinetic of the "dummy" strains is similar to the mass variation depicted in Fig. 9, due to water uptake, being much higher in REF than in V20 and V90 series. Furthermore, swelling effects may justify such level of strains. Additional curing of specimens along the time can result in negative strains due to densification, but the swelling effect can lead to higher expansion, which can compensate the former effect.

Based on the abovementioned correction, the creep strain curves were plotted and are presented in Fig. 6. Per specimen, this figure presents (i) the envelope of the strain overtime measured in both monitored faces and (ii) the average strain. The largest difference between the strain gauges recorded from the opposite faces was registered on specimens EP2_REF_2 (smaller than 0.1% of strain). It is noteworthy that in the case of specimens EP2_REF_1, EP2_V20_2, EP3_REF_1, EP3_REF_2, EP3_V20_1, and EP3_V20_2 only one strain gauge was used since the other sensor faced technical issues and, thus, had to be disregarded. To facilitate the analysis of the tensile creep results, Fig. 7 presents the average strain *versus* time and average creep compliance *versus* time. Table 2 shows the main parameters extracted from the creep strain curves.

The modulus of elasticity, $E_{(t\,=\,0)}$, based on the instantaneous elastic strain observed at the moment of loading, $\varepsilon_{(t\,=\,0)}$, was computed for all creep specimens (see Table 2). REF, V20 and V90 specimens presented the average value of 8.59 GPa (CoV = 9.2%), 12.6 GPa (CoV = 6.2%), and 12.8 GPa (CoV = 3.5%), respectively. These values are slightly higher (~12%) than the modulus of elasticity, $E_{adh}$, obtained in the tensile tests according to ISO 527–1:2012 [23]. It is noteworthy that the latter values are computed throughout the secant modulus between strain 0.05% and 0.25% of the stress-strain curves, whereas the elastic strain, $\varepsilon_{(t\,=\,0)}$, was typically inferior to 0.1%.

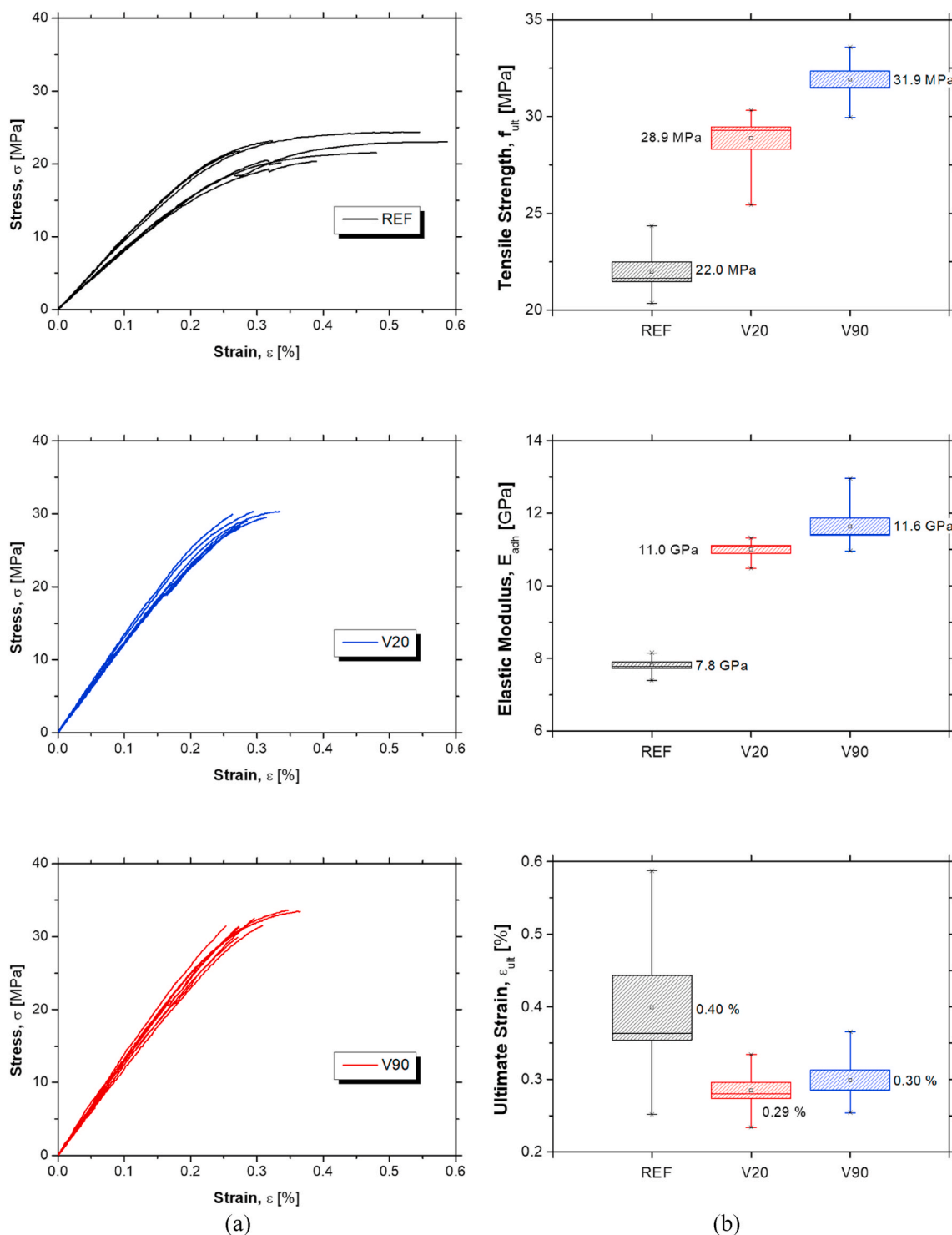Results clearly show that the hygrothermal conditions (EP2 *versus*

**Fig. 4.** (a) Experimental tensile stress *versus* strain curves; (b) boxplot representation of the tensile strength, elastic modulus and ultimate strain. Notes: the square point is the mean value, the bottom and top lines of the box plot are the 25th percentile and 75th percentile, the line inside the box is the median and the vertical line is whisker boundaries.

EP3 series) had major influence on the adhesive's creep behaviour (see Figs. 6 and 7). Similar behaviour between EP1 and EP2 series (kept at 20 °C and 55% of relative humidity) was observed, with the development of primary creep within the first 500 h, followed by a secondary creep stage until the end of the test. Specimens from EP3 series (kept at 20 °C and 98% of relative humidity) experienced the three stages of creep (primary, secondary and tertiary) followed by fracture. It should be noted that in EP3 series, significant differences were observed

between specimens manufactured with different methods (REF, V20 and V90): in EP3 series, specimens prepared with the REF method, exhibit the highest creep strain (at failure, equal to 0.57% and 0.56% for EP3_REF_1 and EP3_REF_2, respectively), with the primary creep being develop in the first 200 h, secondary creep stage in the following 600–800 h, and, lastly, the tertiary creep stage (rupture occurred after 2116 h and 1476 h of test for specimens EP3_REF_1 and EP3_REF_2, respectively); in contrast, the specimen EP3_V20_1, manufactured with
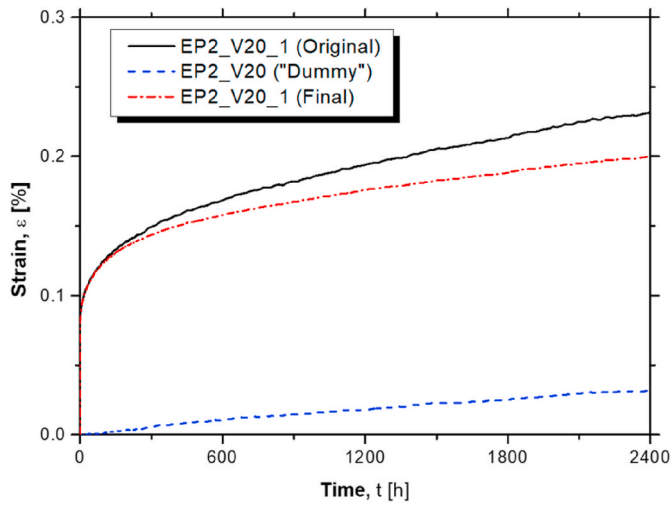
**Fig. 5.** Typical strains measured in tested and "dummy" specimen.

the V20 preparation method (EP3_V20_2 had to be disregarded due to malfunction of the strain gauges), presented the slowest creep development, with the failure occurring after 3628 h for a strain value of 0.45%, and with the complete development of the primary and secondary creep stages within the first 400 h and 1500 h, respectively; lastly, the V90 specimens exhibit the primary (within the first 300 h), secondary (duration of 700 h) and tertiary (until rupture at 1977 h and 2124 h, for specimens EP3_V90_1 and EP3_V90_2, respectively) stages, with the maximum strain of 0.43% registered in specimens EP3_V90_2. The creep coefficient, $\phi_{(t\,=\,2400)}$, was computed as the ratio between the increment of creep strain ($\varepsilon_{(t\,=\,0)}$- $\varepsilon_{(t\,=\,2400)}$) and the instantaneous strain ($\varepsilon_{(t\,=\,0)}$) at the onset of the creep loading, and the obtained values are presented in Fig. 8. The creep coefficient was computed after 2400 h of loading, with exception to EP3 series, where the maximum attained strain value was considered because failure was typically observed before the predefined time period. Again, EP1 and EP2 series presented similar creep coefficients. More specifically, specimens prepared according to the REF method, presented creep coefficient of 2.53 and 2.55 for EP1 and EP2 series, respectively. The $\phi_{(t\,=\,2400)}$ for the V20 and V90 specimens was in average equal to 2.23 and 2.13, respectively, for EP1 series and equal to 2.03 and 2.00, respectively, for EP2 series. These similarities between EP1 and EP2 series (see Figs. 7b and 8) revealed that this epoxy adhesive can be assumed as linear viscoelastic material, for creep stress levels used. Other authors [7,10] have also observed the same property for this epoxy adhesive. In contrast, EP3 series presents creep coefficients significantly higher, mainly because the hydrothermal conditions led to the development of tertiary creep stage and rupture, within the first 2400 h. The creep coefficient in these specimens was computed for the test period, using the last value of strain before the specimen's failure. The differences in the creep coefficients (were 88%, 111% and 93% higher than in EP1 and EP2 series, for the REF, V20 and V90 methods, respectively) are clearly shown in Fig. 8.

It is state-of-art [9,11,17] that moisture exposure leads to a significant reduction on the mechanical properties of epoxy resins, explicitly by reducing tensile strength and stiffness throughout the plasticization phenomenon. In order to measure the moisture absorption on specimens from EP3 series, 9 additional specimens (three specimens for each preparation method) were placed in the same hygrothermal condition during the creep test. The mass variation (mass increase divided by the initial mass) is depicted in Fig. 9. After 2400 h of exposure the mass variation on REF, V20 and V90 specimens was close to 0.93%, 0.66% and 0.65%, respectively. There is higher moisture absorption on the REF specimens, mainly because the degassing decreases the porosity of the adhesive. The hygrothermal condition of EP3 series can be assumed as an extreme environment and its consequent degradation effect
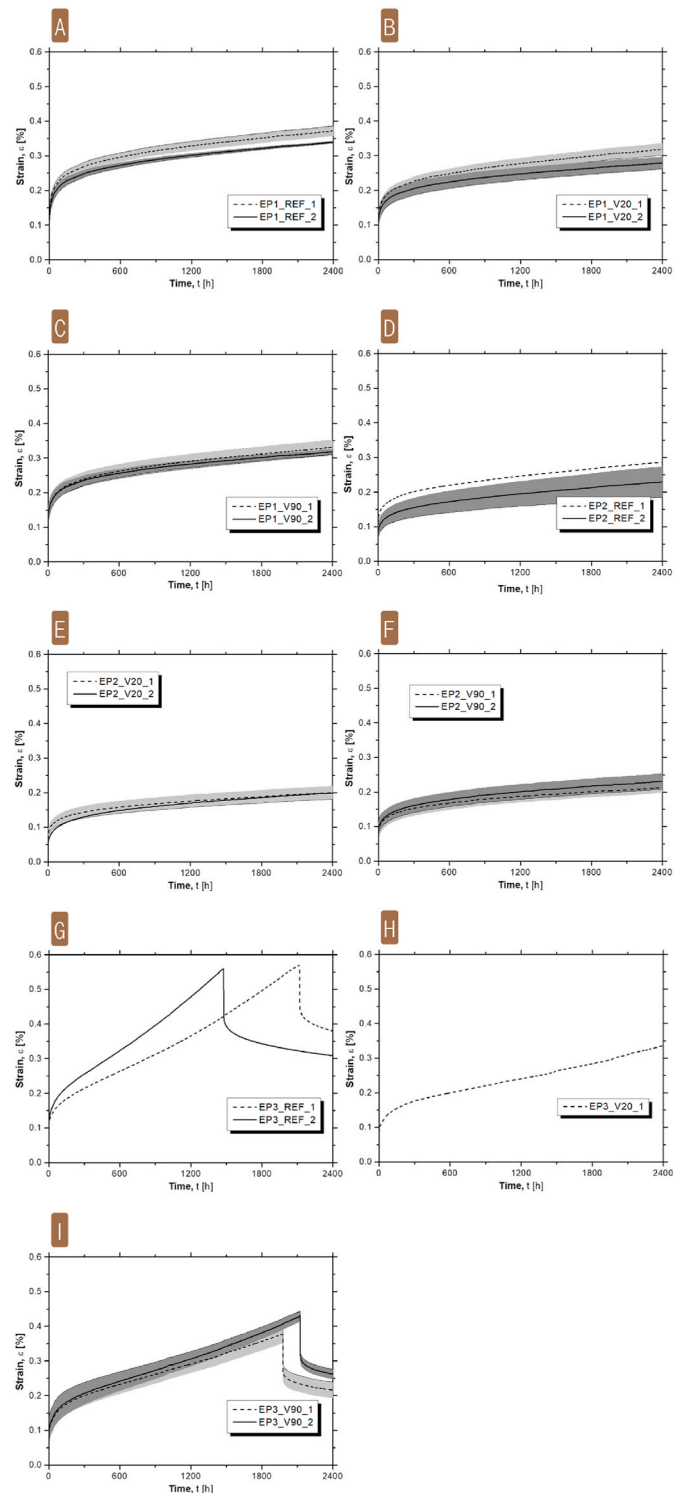


**Fig. 6.** Strain *versus* time for the tested series (envelopes): (a) to (c) EP1 series; (d) to (f) EP2 series; (g) to (i) EP3 series.

accelerated the creep development on the epoxy adhesive. Consequently, the influence of the preparation method became more evident in test series EP3, and specimens prepared with the degassing procedure (V20 and V90) showed higher modulus of elasticity and smaller creep coefficient.

Table 2 also presents the time for reaching the failure, $t_{rup}$, and the modulus of elasticity, $E_{rup}$, based on the instantaneous strain variation after rupture, $\Delta\varepsilon_{rup}$. The time for reaching the failure is higher in

**Fig. 7.** (a) Strain *versus* time and (b) creep compliance *versus* time all the tested specimens.
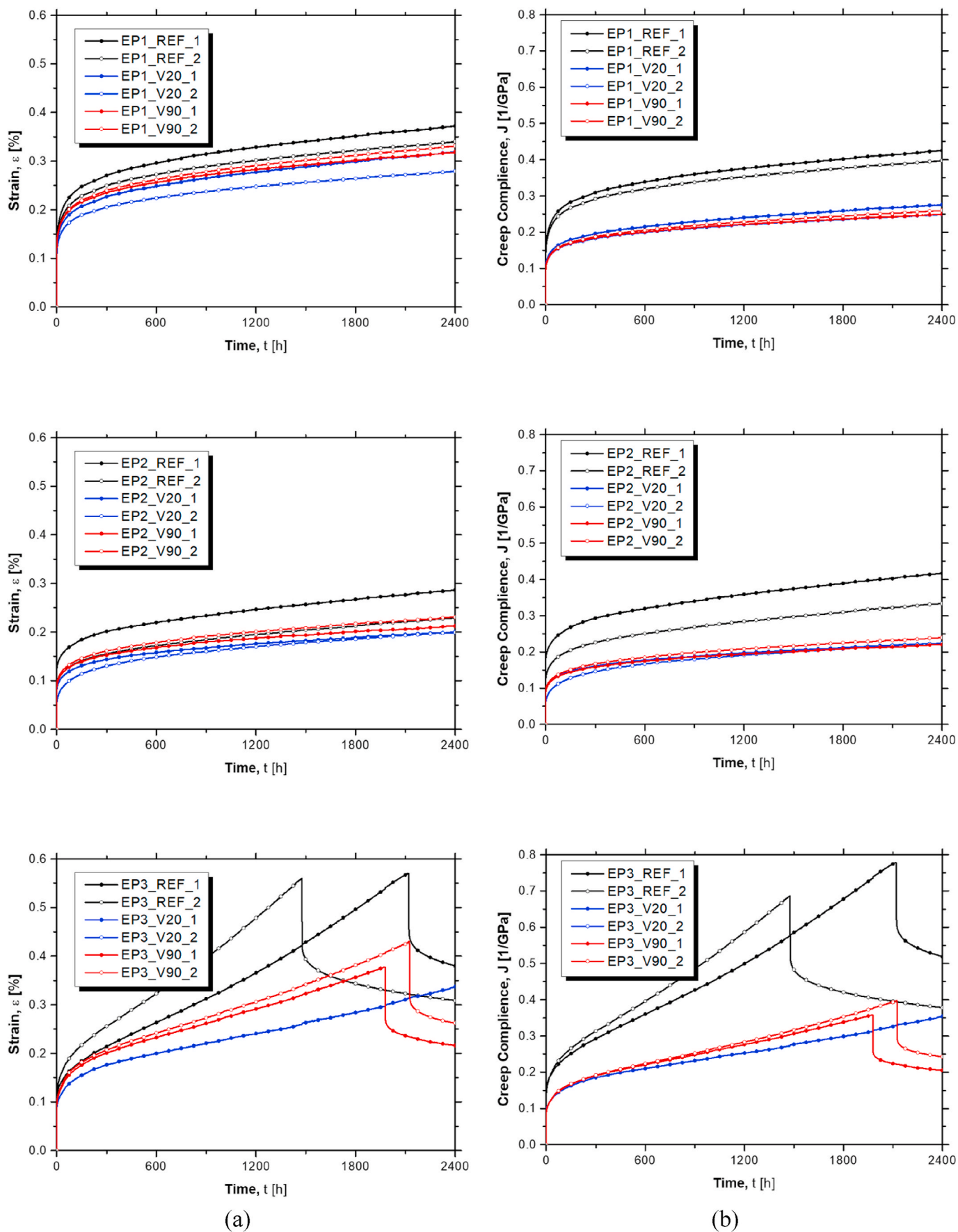
**Table 2**
Results of tensile creep tests and curve parameters.

| Series | Specimen | $\sigma_{creep}$ [MPa] | $\varepsilon_{t0}$ [%] | $E_{(t=0)}$ [GPa] | $\varepsilon_{t=2400}$ [%] | $J_{t=2400}$ [1/GPa] | $t_{rup}$ [h] | $\Delta\varepsilon_{rup}$ [%] | $E_{rup}$ [GPa] | $\phi_{t=2400}$ |
|---|---|---|---|---|---|---|---|---|---|---|
| ηEP1 | EP1_REF_1 | 8.74 | 0.10 | 8.78 | 0.37 | 0.43 | – | – | – | 2.72 |
|  | EP1_REF_2 | 8.55 | 0.10 | 8.37 | 0.34 | 0.40 | – | – | – | 2.33 |
|  | EP1_V20_1 | 11.6 | 0.09 | 12.4 | 0.32 | 0.28 | – | – | – | 2.43 |
|  | EP1_V20_2 | 11.2 | 0.09 | 12.2 | 0.28 | 0.25 | – | – | – | 2.03 |
|  | EP1_V90_1 | 12.8 | 0.11 | 12.0 | 0.32 | 0.25 | – | – | – | 1.98 |
|  | EP1_V90_2 | 12.8 | 0.10 | 12.6 | 0.33 | 0.26 | – | – | – | 2.28 |
| EP2 | EP2_REF_1 | 6.87 | 0.08 | 9.00 | 0.29 | 0.42 | – | – | – | 2.77 |
|  | EP2_REF_2 | 6.86 | 0.07 | 9.91 | 0.23 | 0.33 | – | – | – | 2.32 |
|  | EP2_V20_1 | 8.91 | 0.07 | 13.3 | 0.20 | 0.22 | – | – | – | 1.99 |
|  | EP2_V20_2 | 8.90 | 0.07 | 13.7 | 0.20 | 0.22 | – | – | – | 2.06 |
|  | EP2_V90_1 | 9.63 | 0.07 | 13.2 | 0.21 | 0.22 | – | – | – | 1.91 |
|  | EP2_V90_2 | 9.64 | 0.08 | 12.9 | 0.23 | 0.24 | – | – | – | 2.08 |
| EP3 | EP3_REF_1 | 7.32 | 0.10 | 7.36 | 0.57 [1] | 0.78 [1] | 2112.5 | −0.10 | 7.20 | 4.73 [1] |
|  | EP3_REF_2 | 5.60 | 0.10 | 8.14 | 0.56 [1] | 0.69 [1] | 1475.5 | −0.12 | 7.02 | 4.59 [1] |
|  | EP3_V20_1 | 4.55 | 0.08 | 11.5 | 0.46 [1] | 0.48 [1] | 3627.5 | −0.09 | 10.46 | 4.48 [1] |
|  | EP3_V20_2 | – | – | – | – | – | – | – | – | – |
|  | EP3_V90_1 | 3.78 | 0.08 | 13.2 | 0.38 [1] | 0.36 [1] | 1977.0 | −0.09 | 12.00 | 3.72 [1] |
|  | EP3_V90_2 | 4.30 | 0.08 | 13.2 | 0.43 [1] | 4.25 [1] | 2123.5 | −0.09 | 11.58 | 4.25 [1] |

$\sigma_{creep}$ – creep stress; $\varepsilon_{(t=0)}$ – instantaneous elastic strain at the instance of loading (t = 0 h); $E_{(t=0)}$ – Modulus of elasticity based on the instantaneous deformation; $\varepsilon_{(t=2400)}$ – strain registered after 2400 h of creep loading; $J_{(t=2400)}$ – creep compliance for 2400 h; $t_{rup}$ – time of failure; $\Delta\varepsilon_{rup}$ – instantaneous strain variation after rupture; $E_{rup}$ – Modulus of elasticity based on the instantaneous strain variation after rupture; $\varphi_{(t=2400)}$ – creep coefficient.
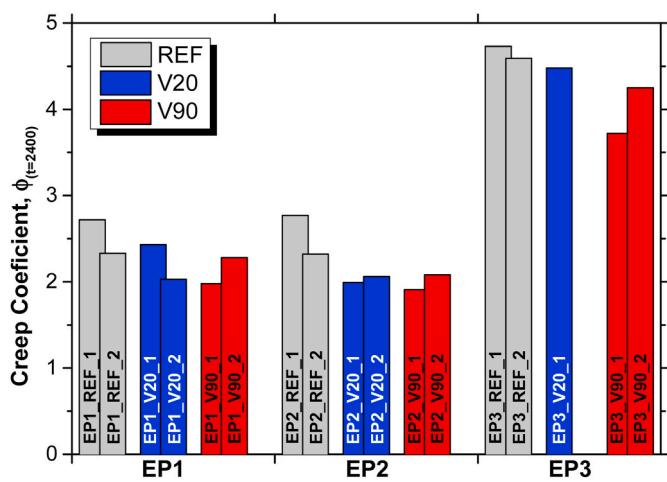**Note**: [1] Value obtained at rupture.



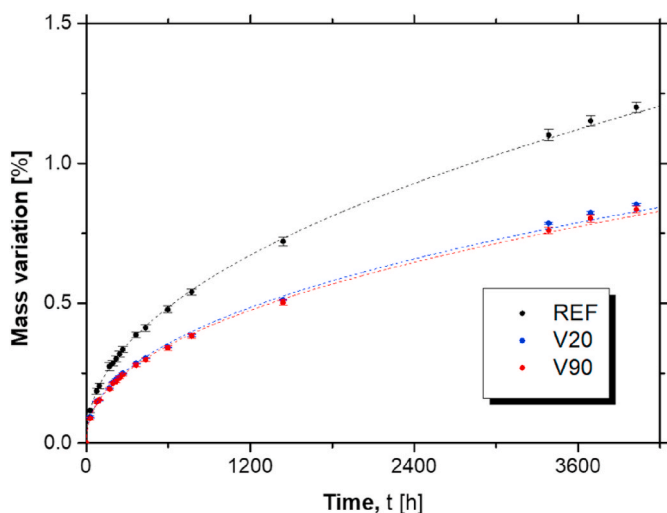**Fig. 8.** Creep coefficient for all tested specimens.



**Fig. 9.** Mass variation over time for EP3 series.

specimens with the degassing procedure (2142.6 h) than on the REF specimens (1794.0 h). At this final stage, V90 and V20 specimens present higher stiffness than the REF specimens, confirming, once again, that the preparation method has great influence on the mechanical behaviour of the epoxy adhesive. The $E_{rup}$ is lower than the $E_{(t=0)}$ (reduction of 8.3%, 8.6% and 10.6% for REF, V20 and V90, respectively), which could be an indicator of the degradation effect of this extreme environment. It should be noted that the strain at failure on the creep tests was 35%–59% higher than the ultimate strain obtained from the tensile tests. Similar behaviour was obtained by Costa and Barros [10], whom affirm that the adhesive is able to reorganize its internal structure during sustained loading.

### 3.3. Analytical modelling

To further understand the creep behaviour of all tested specimens, analytical modelling was carried out using, firstly, the Burgers model and, then, the modified Burgers model. The Burgers model is a rheological model widely used for the creep assessment of epoxy adhesives [7,10,25,26]. It is expressed by Equation (1):

$$\varepsilon_{creep}(t) = \sigma \cdot \left[ \frac{1}{E_M} + \frac{t}{\eta_M} + \frac{1}{E_K} \cdot \left( 1 - \exp\left( -\frac{E_K}{\eta_K} \cdot t \right) \right) \right] \qquad (1)$$

where, $\varepsilon_{creep}(t)$, is the strain at a certain time instant, $t$; $\sigma$, is the applied creep stress; $E_M$, is the Maxwell's modulus of elasticity; $\eta_M$, is the Maxwell's coefficient of dynamic viscosity; $E_K$, is the Kelvin's modulus of elasticity; $\eta_K$, is the Kelvin's coefficient of dynamic viscosity. Fig. 10 illustrates the typical response when the Burgers model is used. In the Burgers model, the Maxwell's modulus of elasticity is inversely proportional to the elastic strain observed at the instance of loading, $\varepsilon_M$, and it is given by Equation (2):

$$E_M = \frac{\sigma}{\varepsilon_M} \qquad (2)$$

The Maxwell's coefficient of dynamic viscosity is obtained from the steady-state branch of the creep curve. For the EP1 and EP2 series, the steady state branch was defined as the last third of the creep monitoring interval (from $t = 1600$ h to $t = 2400$ h), whereas for EP3 series, a shorter steady state interval was defined for each individual specimen. The steady-state branch is located at the secondary creep stage, when the
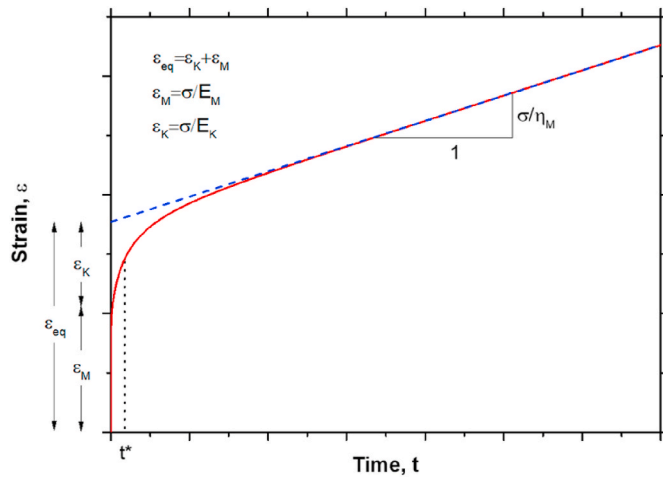
**Fig. 10.** Strain evolution with time according to Burgers model.

creep strain variation with the time, $\varepsilon'_M$, is constant. The parameter $\eta_K$ is obtained by Equation (3):

$$\eta_M = \frac{\sigma}{\varepsilon'_M} \tag{3}$$

The Kelvin's elastic modulus is obtained from the following Equation (4):

$$E_K = \frac{\sigma}{\varepsilon_{eq} - \varepsilon_M} = \frac{\sigma}{\varepsilon_K} \tag{4}$$

where the $\varepsilon_{eq}$ is the value of strain obtained with the interception of the steady state branch (blue dashed line in Fig. 10) with the vertical axis. The last parameter required in the definition of the Burgers model, $\eta_K$, is obtained from the multiplication of the Kelvin's modulus of elasticity and the retardation time, $t^*$, according to Equation (5):

$$\eta_K = E_K \cdot t^* \tag{5}$$

The retardation time is obtained from the exponential term from Equation (1) and it corresponds to the time required to reach 63.2% of the deformation accounted in the model by the Kevin-Voigt term, $\varepsilon_K$ (see Fig. 10). To calculate the retardation time, the procedure adopted by

Costa and Barros [5], was followed: (i) isolate the Kevin-Voigt term from Equation (1), as given in Equation (6), (ii) subtract the Maxwell terms $(\sigma/E_M + t \cdot \sigma/\eta_M)$ from the experimental creep curve and then iii) determine the time necessary to achieve 63.2% of $\varepsilon_K$ (see Equation (4)).

$$\varepsilon_K(t) = \varepsilon_{creep}(t) - \left(\frac{\sigma}{E_M} + \frac{\sigma}{\eta_M} \cdot t\right) \tag{6}$$

Table 3 presents the Burgers model parameters computed for each specimen, whereas in Fig. 11a the relationship between numerical and experimental strain is presented for each series. Results showed good correlations between the experimental and numerical results, with the maximum deviation close to 0.05% of strain on EP2_REF_1. The mean absolute percentage deviation, *MAPD*, was computed to evaluate the prediction accuracy of the Burgers model. The MAPD is calculated using the following expression:

$$MAPD = \frac{1}{N} \cdot \sum_{i=1}^{N} \left|\frac{\varepsilon_{exp,i} - \varepsilon_{num,i}}{\varepsilon_{exp,i}}\right| \tag{7}$$

where, *N*, is the number of sampling points (two points for each hour, for a minimum of 4800 points); $\varepsilon_{exp,i}$, is the experimental strain measured at a sampling point *i*; and, $\varepsilon_{num,i}$, is the analytical strain obtained for the sampling point *i*. The MAPD values are presented in Table 3.

For EP1 and EP2 series, an average MAPD value of 2.60% was obtained, whereas in EP3 series, the average MAPD was equal to 3.26%. It should be noted that the Burgers model is used for the prediction of the time-dependent strain within the first two (out of three) characteristic stages of creep. As referred before, specimens from EP3 series experienced a full development of the tertiary creep stage and failure during the creep loading. Therefore, the creep predictions using the Burgers model should deviate from the experimental results for the final part of the test. Nevertheless, results showed that the Burgers model can successfully predict the creep component of the epoxy adhesive, for each tested series. However, as referred by Costa and Barros [10], the prediction of the experimental strains can be improved with the introduction of a new parameter, *n*, in the exponential term from the Burgers model (Eq. (1)). In this modified Burgers model, the time-dependent strain is obtained with the given Equation (8):

$$\varepsilon_{creep}(t) = \sigma \cdot \left[\frac{1}{E_M} + \frac{t}{\eta_M} + \frac{1}{E_K} \cdot \left(1 - \exp\left(\left(-\frac{E_K}{\eta_K} \cdot t\right)^{1-n}\right)\right)\right] \tag{8}$$

**Table 3**
Parameters used for the Burgers equation.

| Series | Specimen | $\varepsilon_M$ [%] | $\varepsilon'_M$ [%/h] | $\varepsilon_{eq}$ [%] | $\varepsilon_K$ [%] | t* [h] | $E_M$ [GPa] | $\eta_M$ [GPa·h] | $E_K$ [GPa] | $\eta_K$ [GPa·h] | MAPD [%] |
|---|---|---|---|---|---|---|---|---|---|---|---|
| EP1 | EP1_REF_1 | 0.10 | 3.52e-05 | 0.29 | 0.19 | 56.25 | 8.78 | 24853 | 4.65 | 261.72 | 2.74 |
| | EP1_REF_2 | 0.10 | 3.05e-05 | 0.27 | 0.17 | 65.15 | 8.37 | 280523 | 5.19 | 338.10 | 2.75 |
| | EP1_V20_1 | 0.09 | 336e-05 | 0.24 | 0.15 | 56.67 | 12.4 | 34423 | 7.97 | 451.42 | 2.64 |
| | EP1_V20_2 | 0.09 | 2.53e-05 | 0.22 | 0.13 | 64.91 | 12.2 | 443189 | 8.85 | 574.74 | 2.57 |
| | EP1_V90_1 | 0.11 | 3.27e-05 | 0.25 | 0.15 | 61.28 | 12.0 | 39001 | 8.73 | 527.44 | 2.56 |
| | EP1_V90_2 | 0.10 | 2.87e-05 | 0.25 | 0.15 | 65.37 | 12.6 | 44396 | 8.61 | 570.67 | 2.44 |
| EP2 | EP2_REF_1 | 0.08 | 3.25e-05 | 0.21 | 0.13 | 40.98 | 9.00 | 21132 | 5.21 | 213.32 | 2.69 |
| | EP2_REF_2 | 0.07 | 2.78e-05 | 0.16 | 0.09 | 66.86 | 9.91 | 24718 | 7.37 | 492.89 | 2.57 |
| | EP2_V20_1 | 0.07 | 1.96e-05 | 0.15 | 0.09 | 79.19 | 13.3 | 45457 | 10.4 | 821.21 | 2.53 |
| | EP2_V20_2 | 0.07 | 2.29e-05 | 0.14 | 0.08 | 137.82 | 13.7 | 38880 | 11.3 | 1550.76 | 2.58 |
| | EP2_V90_1 | 0.07 | 2.05e-05 | 0.16 | 0.09 | 80.39 | 13.2 | 47089 | 10.7 | 856.93 | 2.56 |
| | EP2_V90_2 | 0.08 | 2.44e-05 | 0.17 | 0.10 | 82.25 | 12.9 | 39578 | 9.87 | 811.99 | 2.65 |
| EP3 | EP3_REF_1 | 0.10 | 1.63e-04 | 0.17 | 0.07 | 22.68 | 7.36 | 3716 | 14.0 | 248.69 | 3.24 |
| | EP3_REF_2 | 0.10 | 2.23e-04 | 0.19 | 0.09 | 19.27 | 8.14 | 3201 | 10.2 | 178.01 | 2.71 |
| | EP3_V20_1 | 0.08 | 0.67e-04 | 0.16 | 0.08 | 49.14 | 11.5 | 11471 | 13.9 | 608.54 | 4.14 |
| | EP3_V20_2 | – | – | – | – | – | – | – | – | – | – |
| | EP3_V90_1 | 0.08 | 0.98e-04 | 0.17 | 0.09 | 36.82 | 13.2 | 10239 | 11.3 | 415.56 | 1.36 |
| | EP3_V90_2 | 0.08 | 1.06e-04 | 0.18 | 0.10 | 35.18 | 13.2 | 9080 | 11.9 | 399.19 | 2.00 |

$\varepsilon_M$ – instantaneous elastic strain at the instance of loading; $\varepsilon'_M$ – strain variation at the steady-state branch; $\varepsilon_{eq}$ – strain obtained from the interception of the steady state branch with the vertical axis; $\varepsilon_K$ – maximum strain obtained from the Kevin-Voigt term; t* – time required to reach 63.2% of the $\varepsilon_K$; $E_M$ – Maxwell's modulus of elasticity; $\eta_M$ – Maxwell's coefficient of dynamic viscosity; $E_K$ – Kelvin's modulus of elasticity; $\eta_K$ – Kelvin's coefficient of dynamic viscosity; **MAPD** – mean absolute percentage deviation.
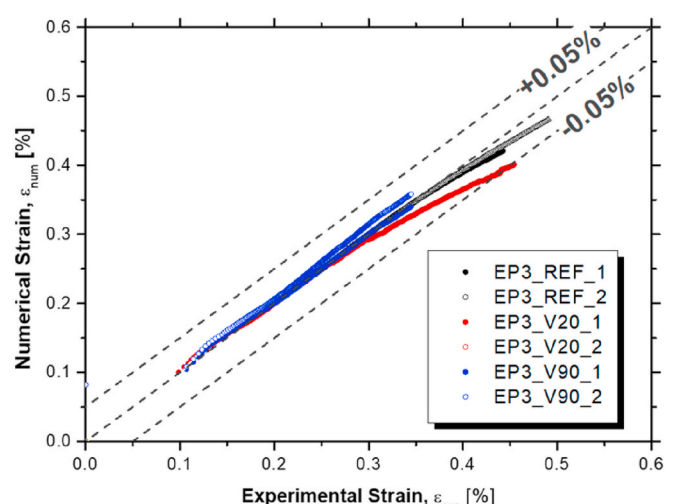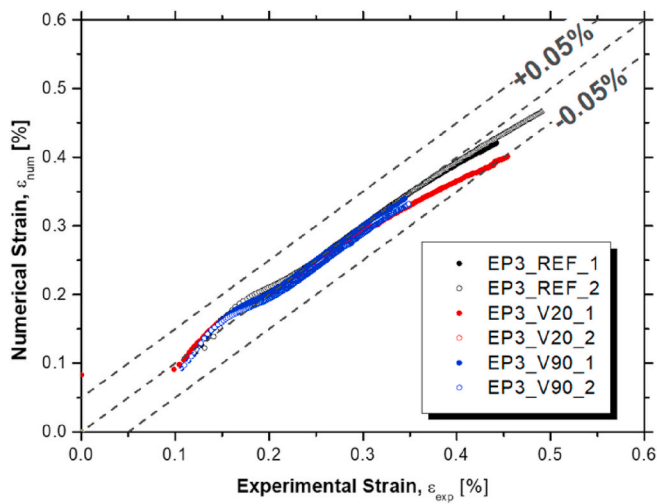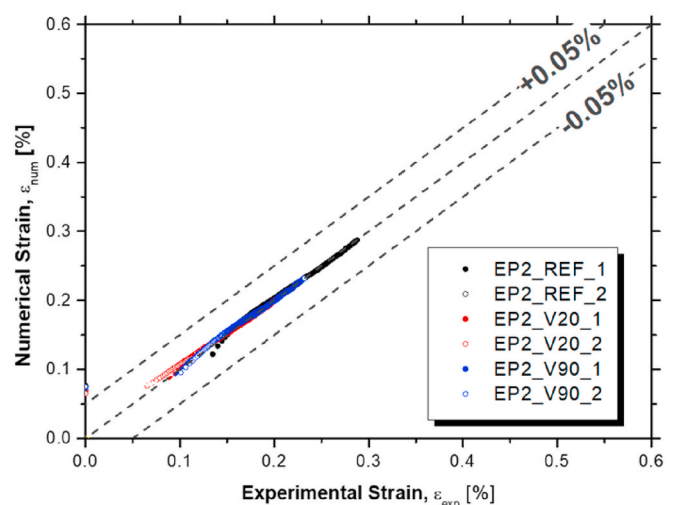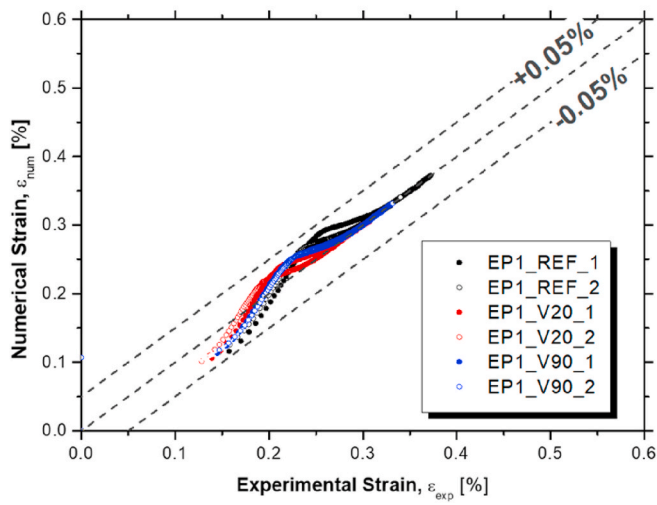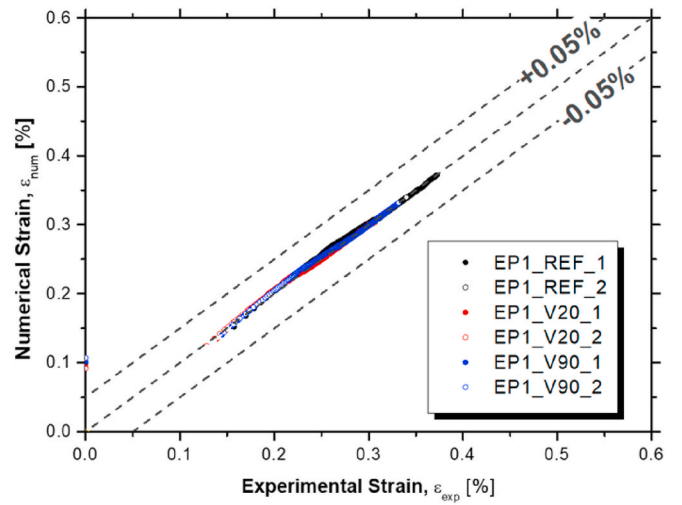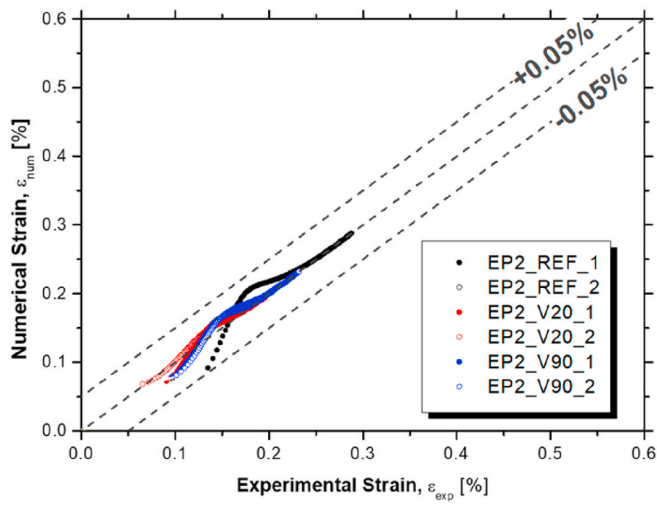
Fig. 11. (a) Relationship between Burgers model strain and experimental strain; (b) Relationship between modified Burgers model strain and experimental strain.

The parameter $n$ of the modified Burgers model was computed by forcing the slope between the numerical and experimental values, throughout the Generalized Reduced Gradient (GRG) nonlinear function from Microsoft Excel. Table 4 presents the obtained $n$ parameter of the modified Burgers model for each tested specimen, and the corresponding result from the MAPD analysis. The relationship between numerical and experimental strain is presented in Fig. 11b for each series. The modified Burgers model allowed a better prediction of the creep behaviour, with higher accuracy for the initial stages of creep (see Fig. 11b), confirmed with the reduction of the mean absolute percentage deviation. Once again, the tertiary creep stage observed on EP3 series (after the 0.3% of strain) cannot be predicted with the modified Burgers model, therefore, higher deviation between numerical and experimental results are observed on these stages of test. The experimental and numerical curves (strain *versus* time) are also presented in Fig. 12. This figure shows great correlation between the experimental results and the numerical model, with overlapping curves during the first and second creep stages (all 2400 h for EP1 and EP2 series, and up to 600 h in EP3 series).

From the analytical modelling it was possible to conclude that the values obtained for $E_M$, are highly correlated with the instantaneous tensile properties, and show clear influence from the preparation methods (see analysis on the $E_{(t = 0)}$ on section 3.2). The Maxwell's coefficient of dynamic viscosity defines the constant rate of creep strain variation (slop of the curve at the steady-state branch), with higher values leading to lower slope on the creep curve. On EP1 and EP2 series the $\eta_M$ is considerable higher on the V20 and V90 specimens (average of 41642 GPa h) than on REF specimens (24688.82 GPa h). On EP3 series the specimens with different preparation methods showed similar trend, with lower values for the REF specimens. However, EP3 series present significant lower $\eta_M$ values, when compared with EP1 and EP2 series. This parameter not only indicate that the preparation method has great influence on the creep development (when REF specimens are compared with V20 and V90 specimens, an increase of 53%, 86% and 107% is obtained for EP1, EP2 and EP3 series, respectably) but that the hygrothermal conditions from EP3 series lead to higher creep development, 3 to 9 times higher than on EP1 and EP2 series, depending on the preparation method. The Kelvin's modulus of elasticity shows the maximum creep strain developed from the Kevin-Voigt term, ($\varepsilon_K$) and the Kelvin's coefficient of dynamic viscosity defines the development rate of $\varepsilon_K$. In EP1 and EP2 series, REF specimens showed lower values for both parameters ($E_K = 5.61$ GPa and $\eta_K = 326.51$ GPa h) than V20 and V90 specimens ($E_K = 9.54$ GPa and $\eta_K = 770.65$ GPa h). EP3 series presents an average $E_K$ of 12.25 GPa and the lowest average $\eta_K$ (359.63 GPa h) of

**Table 4**
Modified Burgers equation parameters.

| Series | Specimen | N | MAPD [%] |
|--------|----------|-----|----------|
| EP1 | EP1_REF_1 | 0.53 | 0.86 |
| | EP1_REF_2 | 0.53 | 0.78 |
| | EP1_V20_1 | 0.54 | 0.83 |
| | EP1_V20_2 | 0.53 | 0.79 |
| | EP1_V90_1 | 0.53 | 0.77 |
| | EP1_V90_2 | 0.52 | 0.74 |
| EP2 | EP2_REF_1 | 0.59 | 0.85 |
| | EP2_REF_2 | 0.52 | 0.92 |
| | EP2_V20_1 | 0.50 | 0.83 |
| | EP2_V20_2 | 0.42 | 1.54 |
| | EP2_V90_1 | 0.49 | 0.93 |
| | EP2_V90_2 | 0.48 | 0.99 |
| EP3 | EP3_REF_1 | 0.46 | 2.93 |
| | EP3_REF_2 | 0.46 | 2.31 |
| | EP3_V20_1 | 0.38 | 3.90 |
| | EP3_V20_2 | – | – |
| | EP3_V90_1 | 0.38 | 0.90 |
| | EP3_V90_2 | 0.41 | 1.57 |

$n$ – parameter from the modified Burgers model; **MAPD** – mean absolute percentage deviation.
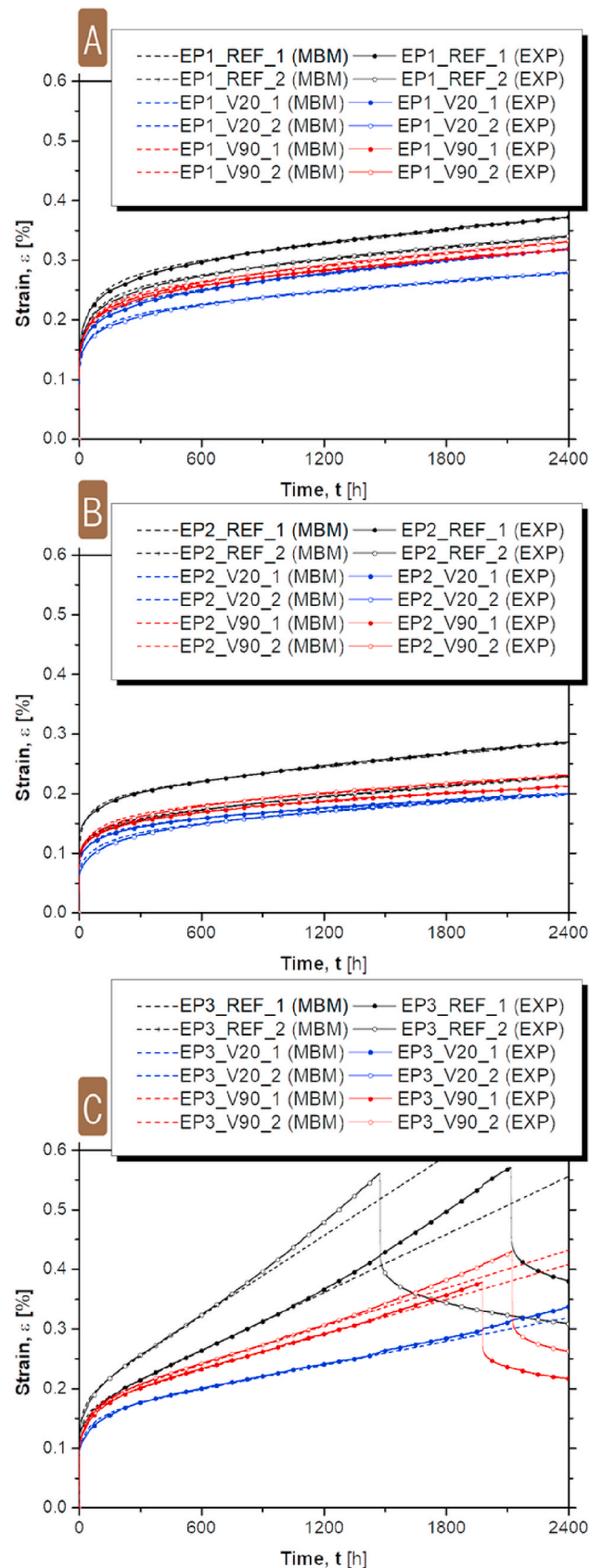


**Fig. 12.** Experimental (EXP) strain *versus* time and modified Burgers model (MBM) strain *versus* time: (a) EP1 series; (b) EP2 series; and (c) EP3 series.

all three series. It is noteworthy to stress that there is low variation on the parameters from EP1 and EP2 series, for specimens with the same preparation procedure. Based on the results from these two series, EP1 and EP2, it can be stated that this material exhibits linear viscoelastic/viscoplastic tensile behaviour up to sustained stress levels of 40%.

Finally, two main conclusions can be drawn from the analytical model: (i) the preparation method has great influence on the creep behaviour, with slower creep strain development for specimens subjected to the degassing procedure; (ii) the hygrothermal conditions have high influence on the creep behaviour of the adhesive, namely by increasing the slope of the creep curve on the steady-state branch (nearly 5.35 times higher).

## 4. Conclusions

This paper presented and analysed the results from an experimental programme aimed to further understand the tensile creep behaviour of a structural epoxy adhesive used for construction applications. New findings are added to the existing literature, namely at: (i) creep behaviour of epoxy adhesives manufactured using distinct processes of mixing (with and without degassing) and curing conditions (normal and accelerated); (ii) influence of hygrothermal conditions (98% of RH) on creep behaviour of epoxy prepared with different processes; and (iii) suitability of existing models to simulate the creep behaviour of epoxy adhesives prepared using different processes. The manufacturing procedure, curing conditions and the hygrothermal conditions were the main variables of this study. Based on the experimental results, an analytical analysis was carried out using the Burgers and the modified Burgers equations.

First, the tensile tests of epoxy adhesive demonstrated a significant increase on the instantaneous tensile properties with the degassing procedure (V20 and V90). When compared with the reference specimens (REF series), V20 specimens presented an increase on the average tensile strength and elastic modulus of 31% and 41%, respectively, whereas the V90 specimens show an even higher growth of 45% and 49%, respectively.

In the creep tests, the instantaneous elastic strain observed at the instance of loading, $\varepsilon_{(t\,=\,0)}$, was consistent with the quasi-static tensile tests. The hygrothermal conditions had great influence on the adhesive's creep behaviour. Similar behaviour was observed for specimens from EP1 and EP2 series (20 °C and 55% of relative humidity), with the development of creep up to the secondary creep stage in the 2400 h of sustained loading. Specimens exposed to 20 °C and 98% of relative humidity (EP3 series) presented the development of all three stages of creep (primary, secondary and tertiary) up to failure within the 2400 h of test (exception for EP3_V20_1, where failure was obtained after 3628 h of loading).

An analytical analysis was carried out to further understand the creep behaviour of all tested specimens. Two models were used: (i) the Burgers model and (ii) the modified Burgers model. Good correlations between the experimental and the numerical results were obtained for both models. However, a better fit was achieved with the latter model (average MAPD of 0.80%, 1.01% and 2.95% for EP1, EP2 and EP3 series, respectively) than in with the Burgers model (average MAPD of 2.62%, 2.60% and 3.26% for EP1, EP2 and EP3 series, respectively).

The analysis on the creep parameters $E_M$; $\eta_M$; $E_K$; and $\eta_K$, showed that the preparation method has great influence on the creep behaviour, with slower creep strain development for specimens subjected to the degassing procedure. This analysis also showed that the hygrothermal conditions have high influence on the creep behaviour of the adhesive, namely with the relative humidity increase (from 55% on EP1 and EP2 series to 98% on EP3 series), the slope of the creep curve on the steady-state branch was 5.35 times higher. Finally, in EP1 and EP2 series, specimens with the same preparation procedure exhibit linear viscoelastic/viscoplastic tensile behaviour up to sustained stress levels of 40%.

## References

[1] FIB. Externally applied FRP reinforcement for concrete structures. 2019.

[2] ACI 440.2R-08. Guide for the design and construction of externally bonded FRP systems for strengthening existing structures. 2008.

[3] Sena-Cruz JM, Barros JAO, Coelho MRF, Silva LFFT. Efficiency of different techniques in flexural strengthening of RC beams under monotonic and fatigue loading. Construct Build Mater 2012;29:175–82. https://doi.org/10.1016/j.conbuildmat.2011.10.044.

[4] Correia L, Sena-Cruz J, Michels J, França P, Pereira E, Escusa G. Durability of RC slabs strengthened with prestressed CFRP laminate strips under different environmental and loading conditions. Compos B Eng 2017;125:71–88. https://doi.org/10.1016/j.compositesb.2017.05.047.

[5] Correia L, Teixeira T, Michels J, Almeida JAPP, Sena-Cruz J. Flexural behaviour of RC slabs strengthened with prestressed CFRP strips using different anchorage systems. Compos B Eng 2015;81:158–70. https://doi.org/10.1016/j.compositesb.2015.07.011.

[6] Sena-Cruz J, Michels J, Harmanci YE, Correia L. Flexural strengthening of RC slabs with prestressed CFRP strips using different anchorage systems. Polymers 2015;7:2100–18. https://doi.org/10.3390/polym7101502.

[7] Silva P, Valente T, Azenha M, Sena-Cruz J, Barros J. Viscoelastic response of an epoxy adhesive for construction since its early ages: experiments and modelling. Compos B Eng 2017;116:266–77. https://doi.org/10.1016/j.compositesb.2016.10.047.

[8] Michels J, Sena-Cruz J, Christen R, Czaderski C, Motavalli M. Mechanical performance of cold-curing epoxy adhesives after different mixing and curing procedures. Compos B Eng 2016;98:434–43. https://doi.org/10.1016/j.compositesb.2016.05.054.

[9] Sousa JM, Correia JR, Cabral-Fonseca S. Durability of an epoxy adhesive used in civil structural applications. Construct Build Mater 2018;161:618–33. https://doi.org/10.1016/j.conbuildmat.2017.11.168.

[10] Costa I, Barros J. Tensile creep of a structural epoxy adhesive: experimental and analytical characterization. Int J Adhesion Adhes 2015;59:115–24. https://doi.org/10.1016/j.ijadhadh.2015.02.006.

[11] Cabral-Fonseca S, Correia JR, Custódio J, Silva HM, Machado AM, Sousa J. Durability of FRP - concrete bonded joints in structural rehabilitation: a review. Int J Adhesion Adhes 2018;83:153–67. https://doi.org/10.1016/j.ijadhadh.2018.02.014.

[12] Moussa O, Vassilopoulos AP, Keller T. Effects of low-temperature curing on physical behavior of cold-curing epoxy adhesives in bridge construction. Int J Adhesion Adhes 2012;32:15–22. https://doi.org/10.1016/j.ijadhadh.2011.09.001.

[13] Moussa O, Vassilopoulos AP, de Castro J, Keller T. Early-age tensile properties of structural epoxy adhesives subjected to low-temperature curing. Int J Adhesion Adhes 2012;35:9–16. https://doi.org/10.1016/j.ijadhadh.2012.01.023.

[14] Czaderski C, Martinelli E, Michels J, Motavalli M. Effect of curing conditions on strength development in an epoxy resin for structural strengthening. Compos B Eng 2012;43:398–410. https://doi.org/10.1016/j.compositesb.2011.07.006.

[15] Michels J, Widmann R, Czaderski C, Allahvirdizadeh R, Motavalli M. Glass transition evaluation of commercially available epoxy resins used for civil engineering applications. Compos B Eng 2015;77:484–93.

[16] Savvilotidou M, Vassilopoulos AP, Frigione M, Keller T. Development of physical and mechanical properties of a cold-curing structural adhesive in a wet bridge environment. Construct Build Mater 2017;144:115–24. https://doi.org/10.1016/j.conbuildmat.2017.03.145.

[17] Silva P, Fernandes P, Sena-Cruz J, Xavier J, Castro F, Soares D, et al. Effects of different environmental conditions on the mechanical characteristics of a structural epoxy. Compos B Eng 2016;88:55–63. https://doi.org/10.1016/j.compositesb.2015.10.036.

[18] S&P. Technical data sheet S & P resin 220 epoxy adhesive. Switzerland: Seewen; 2012.

[19] EN 12190. Products and systems for the protection and repair of concrete structures. Test methods. Determination of compressive strength of repair mortar 1999. 1999.

[20] International Organizational for Standardization. ISO 178:2002 - plastics – Determination of flexural properties. Hanser; 2002.

[21] BS EN 12615. Products and systems for the protection and repair of concrete structures. Test methods. Determination of slant shear strength 1999. 1999.

[22] International Organization for Standardization. ISO 527-2:2012 - plastics — determination of tensile properties — Part 2: test conditions for moulding and extrusion plastics. Geneva. 2012.

[23] International Organization for Standardization. ISO 527-1:2012 - plastics – Determination of tensile properties – Part 1: general principles. Geneva. 2012.

[24] Granja JL, Fernandes P, Benedetti A, Azenha M, Sena-Cruz J. Monitoring the early stiffness development in epoxy adhesives for structural strengthening. Int J Adhesion Adhes 2015;59:77–85. https://doi.org/10.1016/j.ijadhadh.2015.02.005.

[25] Majda P, Skrodzewicz J. A modified creep model of epoxy adhesive at ambient temperature. Int J Adhesion Adhes 2009;29:396–404. https://doi.org/10.1016/j.ijadhadh.2008.07.010.

[26] Godzimirski J, Rośkowicz M. Numerical analysis of long-lasting strength of adhesive bonds. Adv Manuf Sci Technol 2004;28:67–83.

## Paper 2

**TITLE:** DURABILITY OF EPOXY ADHESIVES AND CARBON FIBRE REINFORCED POLYMER LAMINATES USED IN STRENGTHENING SYSTEMS: ACCELERATED AGEING VERSUS NATURAL AGEING

**REFERENCE:**

# Durability of Epoxy Adhesives and Carbon Fibre Reinforced Polymer Laminates Used in Strengthening Systems: Accelerated Ageing versus Natural Ageing

**Ricardo Cruz** [1], **Luís Correia** [1], **Aloys Dushimimana** [1], **Susana Cabral-Fonseca** [2] and **José Sena-Cruz** [1,*]

[1] Institute for Sustainability and Innovation in Structural Engineering (ISISE)/Institute of Science and Innovation for Bio-Sustainability (IB-S), University of Minho, Azurém, 4800-058 Guimarães, Portugal; a51314@alumni.uminho.pt (R.C.); lcorreia@civil.uminho.pt (L.C.); aloysdushimimana@yahoo.fr (A.D.)

[2] Laboratório Nacional de Engenharia Civil, Materials Department, Av. do Brasil 101, 1700-066 Lisboa, Portugal; sbravo@lnec.pt

* Correspondence: jsena@civil.uminho.pt; Tel.: +351-253-510-200

**Abstract:** This work addresses the durability of structural epoxy adhesives and carbon fibre reinforced polymer (CFRP) laminates typically used in strengthening of existing reinforced concrete structures exposed to natural ageing. The experimental program included four natural (real) outdoor environments inducing ageing mainly caused by carbonation, freeze-thaw attack, elevated temperatures, and airborne chlorides from seawater. Moreover, a control (reference) environment (20 °C of temperature and 55% of relative humidity) and an environment involving water immersion of the materials under controlled temperature (20 °C of temperature) were also included in this investigation. The characterization involved the assessment of the physical, chemical and mechanical properties along a study period of up to two years. Furthermore, comparisons between the natural ageing tests developed in the scope of the present work and accelerated ageing tests existing in the literature were performed. Regarding to the epoxy adhesives, an increase in the glass transition temperature with the time was observed, while the tensile properties decreased, regardless of the outdoor environment. The CFRP laminates were marginally affected by the studied environments. Despite the remarkable dispersion of the results observed in the accelerated ageing tests for the period investigated, this testing protocol yielded higher mechanical degradation than under natural ageing.

**Keywords:** epoxy adhesive; CFRP laminate; durability; natural outdoor ageing; artificial accelerated ageing

## 1. Introduction

Structural repairing and strengthening of existing reinforced concrete (RC) structures with systems involving fibre reinforced polymer (FRP) materials are considered state-of-the-art in civil engineering. Carbon FRP (CFRP) materials are typically used due to, mainly, their superior mechanical properties (higher stiffness, strength and fatigue life, among others), and their great resistance to aggressive environments [1–7].

CFRP materials are commonly applied using the externally bonded reinforcement (EBR) technique or the near surface mounted (NSM) strengthening technique. The EBR technique uses laminate strips or sheets which are externally bonded to the surface of the structural member to be strengthened, while in the NSM technique the reinforcements (laminates or bars) are inserted into grooves cut into the concrete cover of the structural member. Typically, epoxy adhesives are used as the bonding agent. Both techniques are suitable for flexural and shear strengthening. In some cases, active techniques, e.g., prestressing, are required. The use of prestressing combines the advantages of FRP systems with external prestressing, which leads to more efficient use of concrete and CFRP and reduction on the deflection and crack width, amongst other advantages [8,9].

The knowledge on the durability of RC structures strengthened with CFRP is essential for structural safety. The durability has been intensively studied under laboratory conditions using accelerated ageing protocols. These types of protocol typically use higher stress levels, extreme environmental actions and/or size adjustments (i.e., a reduction of the sample thickness) in order to accelerate the degradation process and reduce the experimental time [10,11]. Then, the results are extrapolated to the real outdoor conditions and/or real-scaled elements. However, a very few studies on the durability have been performed under real outdoor conditions (natural ageing). Moreover, the relationship between accelerated ageing tests performed under laboratory conditions and natural ageing conditions for assessing the durability of these systems is not fully understood [12].

Typically, outdoor environments offer a combination of several degradation agents, such us moisture, temperature, and ultraviolet (UV) radiation. The absorption of moisture on composite materials can result from their exposure to precipitation, humidity or aqueous solutions diffused through other substrates. The degradation effect of moisture on composite materials can be understood by considering its effect on the constituent elements of the system, which are the fibre, the matrix and the fibre-matrix interphase. The absorption of moisture mainly damages the resin, which may lead to changes in the structure of the polymer [13]. Nevertheless, moisture can also deteriorate the interphase fibre-matrix, by reducing the fibre-matrix bond, and lead to the degradation at the fibre level. The diffusion of water in polymers and adhesives may lead to changes in their mechanical, physical, and chemical properties [14]. Physical ageing consists in a reversible change of material properties which can be recovered, in part, after drying (the property changes are also dependent on the temperature). Physical ageing includes a mechanism commonly known as plasticization, which results in the reduction in the modulus of elasticity and strength, and an increase in the ductility [15,16]. Another physical mechanism is swelling, which consists of volumetric changes as a result of the moisture content alone, independently of thermal expansion. Potentially, swelling can affect the fibre-matrix interface bond, leading to premature cracking or fibre separation [17]. The presence of water can also lead to a reduction of the glass transition temperature ($T_g$), that identifies the interval of temperature above which the mechanical properties (stiffness and strength) of the epoxy adhesive or polymer matrix drop drastically [3,16,17].

Regarding chemical ageing, it can occur after longer exposure to moisture. This is mostly an irreversible process of degradation which occurs in all constituent elements of the system (fibre, matrix and interface fibre-matrix) [13]. Finally, the mechanical degradation may result from the combination of different chemical and physical mechanisms, as swelling leads to microcracking in the weakened resin after hydrolysis as well as debonding effects at the interface [18]. The degradation level caused by moisture is highly influenced by the type of fibre reinforcement, and CFRP materials are relatively immune to the effects of moisture [3,10,16,17]. In fact, a recent study on the durability of CFRP laminate strips [10], reported a 3% reduction on the tensile strength and elastic modulus after 240-day exposure to full immersion in tap water. However, the synergy between moisture and other degradation agents can have a combined effect on CFRP laminates. In fact, Cabral-Fonseca et al. [19] investigated the synergistic effect of water-based environments, including immersion in: (i) demineralized water, (ii) water with 35 g/L of sodium chloride, and (iii) in an alkaline solution and different temperatures (60 °C, 40 °C and 23 °C), on the durability of three CFRP laminates typically used for construction applications. A reduction on the flexural strength was observed for all three environments. The results clearly showed higher rates of degradation at the more elevated temperature (60 °C), between 32% and 11% for the demineralized water. In contrast, epoxy adhesives are highly susceptible to moisture effects. Silva [10] carried out ageing tests on epoxy adhesive and observed relevant reductions of 14%, 47% and 38%, respectively, in the $T_g$, elastic modulus and tensile strength of the adhesive, after being fully immersed in water for a period of 480 days. In another investigation on the durability of a commercial epoxy adhesive, Sousa

et al. [20] reported high reductions on the flexural properties (strength: $-24\%$; and elastic modulus: $-30\%$) after immersion in water at 40 °C for two years.

The thermal effects on composites may be due to: (i) sub-zero temperatures, (ii) freeze-thaw cycles, (iii) thermal cycles, and/or (iv) elevated temperatures. Relevant literature review works about this topic can be found in [16,21–25]. The exposure to elevated temperatures leads, mainly, to softening of the resin (viscous response) and therefore, of the composite material. The stiffness and strength of resins and composite material are dependent of the temperature, and elevated temperatures near the glass transition temperature lead to softening and an increase in the viscoelasticity of the polymeric matrix of a FRP material or the adhesive. In contrast, the presence of elevated temperatures may lead to the positive post-cure phenomenon. As referred in [3], high temperatures can act as a post-cure of the material and thus increase $T_g$. In fact, an experimental work carried out by Cromwell et al. [26] showed an improvement on the tensile properties (strength and elastic modulus) of CFRP strips after exposure to a dry heat (60 °C) environment for periods of 6 and 18 weeks. An increase in moisture absorption and diffusion can also occur in the presence of elevated temperatures. Furthermore, the synergy between moisture and temperature might lead to higher degradation effects than each single individual environmental agent [16,21]. In general, thermal cycles lead to small changes on the stiffness and strength of FRP materials, unless the temperature variation is extremely high. On the other hand, in composite materials with high modulus resins, thermal cycles may lead to the appearance of microfractures. Regarding freeze-thaw cycles, the performance of reinforcing fibres, in general, is not affected. However, the performance of the resin and of the fibre-resin interface are reduced when FRP materials are exposed to freeze-thaw cycles, as a result of the difference in the coefficients of thermal expansion (CTE) between the polymer matrix and reinforcing fibres. Sub-zero temperatures can lead to the development of higher strength and stiffness values which can enhance the performance of polymer resin-based systems, however, freeze-thaw cycles (incursions to sub-zero temperatures) in the presence of moisture, can lead to increases in the degradation of the properties of the FRP materials. At their service temperatures, CFRPs are normally immune to thermal cycles [27]. However, since carbon fibers and the matrix resin present different CTEs, this might lead to matrix microcracking and might increase the degradation ratio. Silva [10] studied the effect of: (i) freeze-thaw cycles (temperature range: $-18$ °C to 20 °C; duration: 240 days) and (ii) thermal cycles (temperature range: 20 °C to 80 °C/$-15$ °C to 60 °C; duration: 240 days/180 days) on CFRP laminate strips, and reported negligible variations on the tensile strength, ultimate strain or stiffness of the laminate. However, the effect of the same environments on a cold-curing epoxy adhesive led to a significant reduction on the $T_g$ of the epoxy adhesive (of 23%), after the freeze-thaw ageing, as the curing process was interrupted due to the low temperatures, and an increase on the tensile properties (strength: 18% to 50%; elastic modulus: 5% to 25%), after the thermal cycles, due to post-curing phenomenon [10]. It should be referred that temperature is a key factor in the curing of the epoxy adhesive. Moussa et al. [28] studied the influence of low temperatures on the curing process of a cold-curing epoxy adhesive and observed a considerable increase in the curing time when lower temperatures were considered: for high temperatures (60 °C to 35 °C), full curing was attained after a few hours (3.7 to 1.6 h), whereas a low temperature (10 °C) led to longer curing periods (3 days).

Ultraviolet (UV) radiation can affect FRP structures used in outdoor applications. The influence of UV radiation on composite materials has been reported in several literature reviews [29–31]. FRP material damage by UV radiation mainly affects the components of the polymer matrix. As one of its functions is the transferring of stresses to and between the reinforcing fibres, the degradation caused in these component may strongly affect the mechanical properties of the composite material [29]. As demonstrated by some investigations on this topic [16], the effects of exposure to UV radiation, also known as photodegradation, on composite materials are mainly located in the top few microns of the surface, and affects mainly the aesthetic properties (loss of gloss and discolouration, often

referred to as yellowing). It has been shown that, in some cases, the damage to the material surface disproportionally affects the thermomechanical properties of FRP composites, leading to flaws and to fracture initiation at reduced stress levels when compared with those measured on unexposed material. It should be also mentioned that such flaws can lead to the ingress of moisture. Indeed, for outdoor environments, the effect of UV is often combined with the action of temperature, moisture, wind-borne abrasives, freeze-thaw cycling, and other environmental factors [16]. According to [3], carbon fibres are practically unaffected by UV radiation and, in general, the mechanical properties of composites are only slightly influenced by UV exposure. In an experimental study on the durability of three commercial CFRP laminate strips, Cabral-Fonseca et al. [19] observed photodegradation on the surface of the CFRP; however, the laminate did not show any variations on the flexural strength after 2000 h exposure to ultraviolet radiation. Sousa et al. [20] studied the effect of UV radiation, alongside with moisture and temperature cycles in an outdoor environment (Mediterranean climate), on commercial epoxy adhesives. The results showed inconsistent variations of the adhesive properties (shear modulus: +13%; shear strength: −7%; glass transition temperature: +2% reduction). A post-curing process during the outdoor ageing was reported as the cause that led to the increase in the shear strength. The effect of laboratory and outdoor environments on the flexural properties and curing of two epoxy adhesives was investigated by Frigione et al. [32,33]. The outdoor environment (in Salerno, Italy), which included UV radiation, along with temperature and humidity fluctuations, led to negligible variations of the mechanical properties of the adhesives.

Despite the significant number of studies that have been performed concerning the durability topic, gaps in the existing knowledge can be found, mainly concerning to the performance of this type of materials under natural ageing. Another important issue that needs to be addressed is the relationship between the effects of ageing under laboratory conditions (accelerated ageing) and outdoor conditions (natural ageing). This paper presents the results of an investigation on the durability of epoxy adhesives and CFRP laminates subjected to four outdoor environments inducing ageing mainly by exposure to carbonation, freeze-thaw attack, elevated temperatures, and airborne chlorides from seawater for up to two years. A control (reference) environment and an environment involving water immersion of the materials under controlled temperature were also included. Along the time of the experiments, the physical, chemical and mechanical properties of the materials were characterized, at certain timepoints, namely, after production (T0), and after one (T1) and two (T2) years of exposure. Furthermore, the results of natural ageing test developed in this work and accelerated ageing tests described in the literature were compared.

## 2. Materials, Experimental Program and Methods

### 2.1. Materials

#### 2.1.1. Epoxy Adhesives

This research work included the study of two commercial cold curing epoxy adhesives: (i) S&P Resin 220 epoxy adhesive, supplied by S&P® Clever Reinforcement Ibérica Lda. Company (Seixal, Portugal, hereupon referred as ADH1 adhesive; and, (ii) the trademarked Sikadur-30 epoxy adhesive, supplied by SIKA Schweiz AG (Zurich, Switzerland), henceforth referred to as ADH2 adhesive. Both epoxy adhesives are typically used in the context of strengthening concrete structures with CFRP laminates. Table 1 presents the characteristics declared by each supplier.

**Table 1.** Adhesives properties.

| Property | ADH1 Adhesive | | ADH2 Adhesive | |
|---|---|---|---|---|
| | Value | Test Method | Value | Test Method |
| Density, at 23 °C [g/cm$^3$] | 1.7–1.8 | *n*/a | 1.65 | *n*/a |
| Compression properties Strength [MPa] Modulus [GPa] | >70 *n*/a | EN 12190 [34] – | 75; 90 [1] 9.6 [2] | EN 196 [35] ASTM D 695-15 [36] |
| Flexural properties Modulus [GPa] | >7.1 | EN ISO 178 [37] | *n*/a | – |
| Tensile properties Strength [MPa] Modulus [GPa] | *n*/a *n*/a | – – | 26; 29 [1] 11.2 [2] | EN ISO 527-3 [38] EN ISO 527-3 [38] |
| Shear properties Strength [MPa] | >26 | EN 12615 [39] | 18 [4] | EN ISO 4624 [40] |
| Bond-strength by pull-off, on concrete [MPa] | 3 [3] | EN 13892-8 [41] | >4 [4] | EN 1542 [42] |
| $T_g$ [°C] | *n*/a | – | 52 [5] | EN 12614 [43] |

Notes: [1] 7 days at +10 °C; +35 °C; [2] at 23 °C; [3] 3 days at 20 °C; [4] 7 days at +23 °C; [5] 30 days at 30 °C.

### 2.1.2. CFRP Laminates

The CFRP laminate strips used in this research work are produced by S&P® Clever Reinforcement Ibérica Lda. Company and trademarked as CFK 150/2000. Prefabricated by pultrusion, these CFRP laminates are composed of unidirectional carbon fibres (fibre content higher than 68%) held together by a vinyl ester resin matrix. Two distinct geometries were analysed: (i) the laminate with the cross section of 10 mm by 1.4 mm, later referred as L10 strip, typically used with the NSM strengthening technique and (ii) the laminate with the cross section of 50 mm by 1.2 mm, hereupon referred to as L50 strip, normally used for external bonded applications (EBR). Both CFRP strips present a black and smooth external surface. According to the supplier, the mean value of the elastic modulus is higher than 170 GPa and characteristic tensile strength is higher than 2000 MPa [44].

### 2.2. Experimental Program

The experimental program was carried out in the framework of the "FRPlongDur—Long-term structural and durability performances of reinforced concrete elements strengthened in flexure with CFRP laminates" project. The main objective of the FRPLongDur project is to contribute to the knowledge on the long-term structural behaviour and durability performance of reinforced concrete RC elements strengthened in flexure with CFRP laminates under relevant artificial and real environmental conditions. Figure 1 shows the flowchart of the research project, which includes full-scale RC slabs strengthened in flexure with CFRP laminates throughout the NSM and EBR techniques, bond specimens and samples of the involved materials (concrete, epoxy adhesive and CFRP laminate). The present work addresses only the epoxy adhesives and the CFRP laminates.

Six different environmental conditions were studied (see also Table 2): two artificial environments (E1 and E2) and four outdoor environments (E3 to E6). The environment E1 was considered as the reference (controlled hygrothermal conditions, 20 °C/50% RH), while environment E2 intends to understand the effect water immersion under controlled temperature (approximately 20 °C). Despite the fact that all the remaining outdoor (natural) environmental conditions were located in Portugal, given the selected places (herein named experimental stations) it is expected to achieve specific ageing conditions, namely: E3—higher levels of concrete carbonation (due to the levels of $CO_2$ concentration since the experimental station is placed near the International Airport of Lisbon and near a critical highway); E4—freeze-thaw cycles, since the experimental station is located close to the highest mountain of Portugal ('Serra da Estrela'); E5—higher (elevated) service

temperatures and lower relative humidity; E6—higher levels of chlorides concentration and relative humidity, since the station is placed near the Atlantic Ocean.
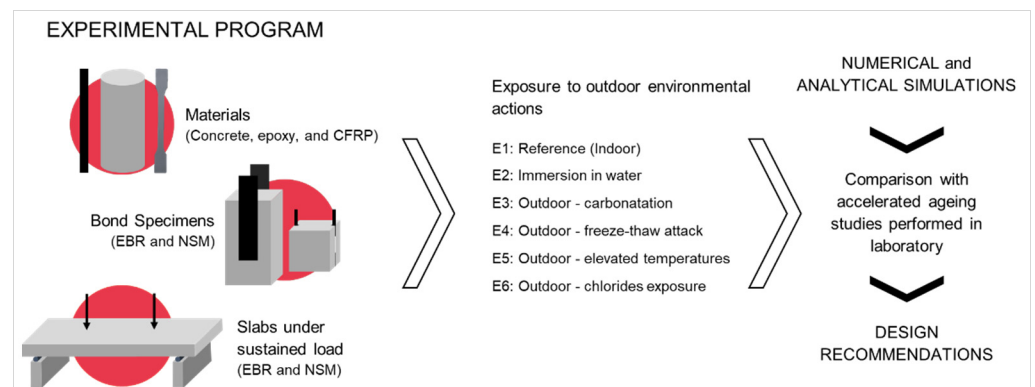


**Figure 1.** Flowchart of the FRPLongDur Project.

**Table 2.** Environments considered in the present study.

| Environment | Location | Description |
|---|---|---|
| E1 | University of Minho, Guimarães (41°27′11.5″ N 8°17′26.8″ W) | AE; Specimens under controlled hygrothermal conditions, 20 °C and 50% RH (reference environment) |
| E2 | University of Minho, Guimarães (41°27′08.1″ N 8°17′33.8″ W) | AE; Specimens under controlled hygrothermal conditions, 20 °C and 100% RH (immersed in tap water) |
| E3 | National Laboratory of Civil Engineering, Lisbon (38°45′41.7″ N 9°08′30.6″ W) | RE; Mild subtropical Mediterranean climate with short and mild winters and warm to hot summers; high levels of $CO_2$ |
| E4 | Lagoa Comprida Dam (EDP), Seia (40°21′55.8″ N 7°38′52.0″ W) | RE; Mild subtropical Mediterranean climate with low temperatures and snow during the wintertime and warm to hot summers |
| E5 | Factory of S&P Clever and Reinforcement, Elvas (38°53′33.5″ N 7°08′46.0″ W) | RE; Hot summer Mediterranean climate with high temperatures and drought specially during the summer |
| E6 | Port of Viana do Castelo (APDL), V. do Castelo (41°40′57.0″ N 8°49′28.3″ W) | RE; Mild subtropical Mediterranean climate with short and mild winters and warm to hot summers; high levels of chlorides concentration and RH |

To control the ambient temperature and relative humidity in each environment, sensors were installed close to the materials. During the recording of the data, some sensors faced technical issues. Due to that, the Portuguese Institute for the Sea and Environment (IPMA) provided the missing information. Table 3 presents the average ambient temperatures and relative humidity, as well as extreme values recorded between the years of 2018 and 2020 for each environment and trimester, while Figure 2 presents two examples of the temperatures and relative humidity recorded.

**Table 3.** Values of the temperature and relative humidity registered between the years 2018 and 2020 for the different environments studied.

| Environment | | Year 2018 | | Year 2019 | | | | Year 2020 | | | |
|---|---|---|---|---|---|---|---|---|---|---|---|
| | | July-September | October-December | January-March | April-June | July-September | October-December | January-March | April-June | July-September | October-December |
| E1 [a] | Temp. [°C] | 20.5 20.0–22.0 | 18.6 17.5–20.0 | 20.5 17.0–22.0 | 20.1 19.5–21.0 | 20.0 20.0–21.5 | 20.1 19.0–21.5 | 20.2 19.0–21.0 | 20.2 19.0–21.5 | – | – |
| | RH [%] | 69.9 55.0–79.5 | 62.7 53.5–67.5 | 50.7 35.5–69.5 | 60.6 49.0–74.0 | 71.5 56.5–77.5 | 63.8 51.5–75.0 | 54.3 41.5–60.5 | 62.5 48.5–75.5 | – | – |
| E2 [b] | Temp. [°C] | 24.3 24.1–24.5 | 21.4 19.7–25.0 | 20.6 18.6–21.4 | 21.2 19.8–23.9 | 21.6 20.9–22.4 | 19.8 17.6–21.6 | 20.0 [3] - | 20.0 [3] - | – | – |
| | RH [%] | 100.0 - | 100.0 - | 100.0 - | 100.0 - | 100.0 - | 100.0 - | 100.0 - | 100.0 - | – | – |
| E3 [c] | Temp. [°C] | 22.2 [1] 12.7–46.2 | 15.3 6.2–34.3 | 17.1 3.3–25.7 | 17.9 6.8–35.3 | 22.0 14.5–39.7 | 15.7 6.8–31.0 | 13.6 4.3–27.0 | 14.9 6.6–23.5 | – | – |
| | RH [%] | 66.2 [1] 14.0–100.0 | 78.5 11.0–100.0 | 71.0 12.0–100.0 | 67.1 13.0–100.0 | 66.8 20.0–100.0 | 81.6 19.0–100.0 | 78.3 22.0–100.0 | 80.5 34.0–100.0 | – | – |
| E4 [2][d] | Temp. [°C] | 18.0 7.4–32.4 | 7.8 −2.8–22.2 | 5.8 −4.7–18.5 | 10.2 −3.1–26.7 | 17.1 4.8–29.6 | 7.7 −2.3–24.6 | 6.1 −4.6–19.2 | 11.5 −3.6–27.0 | – | – |
| | RH [%] | 60.3 4.0–100.0 | 78.8 16.0–100.0 | 63.9 7.0–100.0 | 71.4 5.0–100.0 | 59.4 8.0–99.0 | 80.5 7.0–100.0 | 75.3 4.0–100.0 | 79.6 14.0–100.0 | – | – |
| E5 [2][e] | Temp. [°C] | 26.1 12.6–44.6 | 13.2 1.1–33.0 | 10.9 −1.9–26.2 | 19.3 4.7–38.0 | 25.0 11.7–39.9 | 14.5 3.1–34.7 | 11.6 0.3–25.3 | 19.2 2.1–39.0 | – | – |
| | RH [%] | 49.1 9.0–95.0 | 79.8 11.0–100.0 | 69.7 14.0–100.0 | 54.6 10.0–100 | 48.5 11.0–97.0 | 75.8 1.04–100.0 | 78.2 28.0–100.0 | 66.5 11.0–100.0 | – | – |
| E6 [a] | Temp. [°C] | – | – | 12.1 1.5–28.5 | 17.9 5.0–34.5 | 21.8 12.0–36.0 | 13.7 3.5.0–28.0 | 12.6 2.0–25.0 | 19.0 5.5–25.0 | 22.5 11.0–39.5 | 14.2 4.0–26 |
| | RH [%] | – | – | 76.1 18.0–100.0 | 69.0 26.5–99.0 | 71.0 22.0–99.0 | 88.1 45.0–100.0 | 82.8 38.5–100.0 | 75.8 33.5–100.0 | 70.2 28.5–99.5 | 86.7 42.0–100.0 |

Notes: For each environment, the mean value (first line) and the extreme minimum and maximum values (second line) are provided; [1] Also considered 26–30 June 2018; [2] Values obtained from IPMA (the IPMA's location station is 9 km apart E3 and 560 m apart E5); [3] Values obtained from the sensor installed on the experimental station; The following sensors were used to record the data: [a] EL-USB-2 EasyLog USB Data Logger (Akron, OH, USA) with a range of −35 to +80 °C for temperature and 0 to 100% for humidity (RH); [b] Carel PT100 Thermocouple (Padova, Italy) with a range of −50 to +250 °C for temperature; [c] Thies Clima 1.1005.54.000 (Göttingen, Germany) with a range of −30 to +70 °C for temperature and 0 to 100% for humidity (RH); [d] MicroStep-MIS PT100 (Bratislava, Slovakia) with a range of −50 to +70 °C for temperature and 0 to 100% for humidity (RH); [e] Vaisala HUMICAP®HMP155 (Vantaa, Finland) with a range of −80 to +60 °C for temperature and 0 to 100% for humidity (RH).
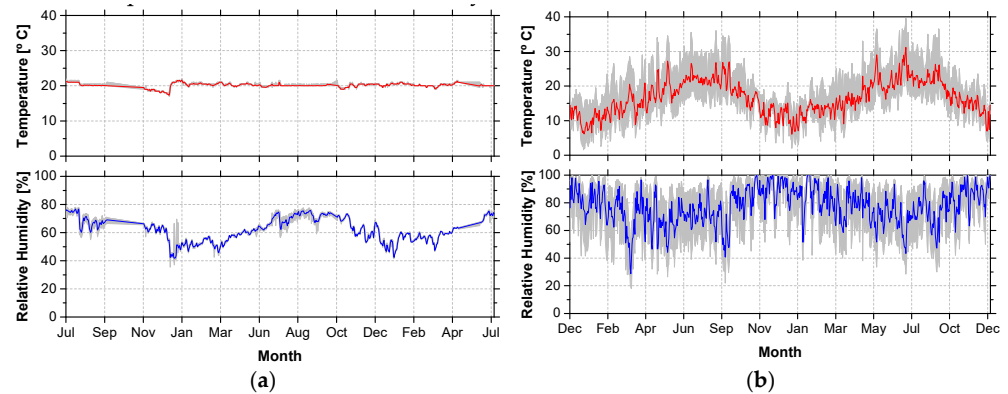
**Figure 2.** Temperature and relative humidity recorded in environments (**a**) E1 and (**b**) E6.

Figure 3 shows a schedule with the main tasks involved in this research. The manufacturing of the epoxy specimens and the preparation of the CFRP laminates took place approximately one year before the beginning of the ageing. During this period, all the specimens were kept in the environment E1. Initial assessment of the material's mechanical properties was performed at an early age (T0). Thus, epoxy specimens were tested seven days after production (June 2017), while CFRP laminates were tested in July 2017. The installation of the epoxy and CFRP laminate specimens in the experimental stations took place between June 2018 and December 2018 (see Figure 3). A view of two of the experimental stations is provided in Figure 4.



**Figure 3.** Timeframe of the developed work.



**Figure 4.** Experimental stations (**a**) E4 and (**b**) E3.

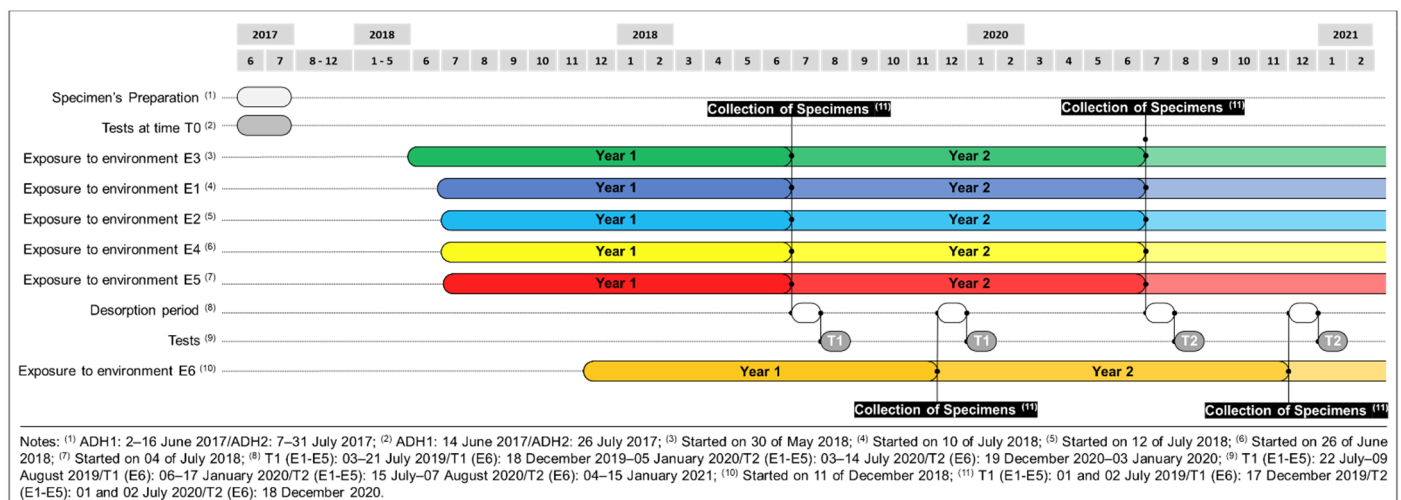After one (T1) and two (T2) years of exposure, 16 epoxy specimens (eight per type of adhesive) and eight CFRP laminate strips (6 of L10, and 2 of L50) were collected from each environment and tested. The test protocol included a desorption period. Epoxy specimens were sealed onsite and were only exposed to the desorption process one week before testing, with the hygrothermal conditions defined for E1. In the case of CFRP laminates, a three-week desorption period was adopted. During this period, the L50 CFRP strips were cut into the 15 mm wide test specimens. In the case of the specimens immersed in water (E2), no desorption process was adopted and all specimens were kept fully immersed all the time (only being removed immediately before testing). The transportation, desorption process, and test protocol used in both T1 and T2 experimental campaigns was the same, to achieve a direct results comparison and an accurate evaluation of the durability of the materials under each environment.

### 2.3. Methods

2.3.1. Epoxy Adhesives

The unaged (reference) and aged epoxy adhesives were submitted to physical, chemical and mechanical characterization using different methods and techniques, as follows:

The water absorption ability of the unaged epoxy adhesives was assessed by gravimetric measurements up to 10,000 h. Samples of adhesives ADH1 and ADH2 were immersed in water at three different temperatures: 20 °C, 40 °C and 60 °C, according to the ISO 62:2008 [45] methodology. Test specimens, with the same geometry used in DMA experiments (see below), were periodically removed from water and weighed, immediately after being superficially dried, using an analytic balance (AE240 Balance, Mettler Toledo, Greifensee, Switzerland), with 200 g range and readability of 0.1 mg). Subsequently, specimens were returned to the recipients for the continuation of the water absorption process.

- The chemical characterization of the unaged epoxy adhesives (cured at 23 °C during 7 days) was performed by Fourier transform infrared spectroscopy (FTIR), according to ASTM E 1252:1998 [46]. Samples were prepared by scraping the surface of tensile specimens (see below); powder obtained were mixed with dry spectroscopy grade potassium bromide and pressed into pellets. FTIR spectra were acquired with a Tensor 27 spectrometer (Bruker, Ettlingencity, Germany) collecting 32 scans at 0.6 cm/s, in the wavenumber range of 4000–450 cm$^{-1}$ with a spectral resolution of 4 cm$^{-1}$. The infrared spectra obtained were compared with spectra available in libraries in order to help the understanding of the position and intensity of the IR absorption bands.
- Dynamic mechanical analysis (DMA) for both unaged (cured at 23 °C, 7 days) and aged epoxy adhesives was carried out in order to evaluate the viscoelastic behaviour of adhesives and determine its glass transition temperature ($T_g$). The analysis followed ISO 6721-1/5:2019 [47,48]. Prismatic specimens with 4 mm × 10 mm × 60 mm were clamped between the movable and stationary fixtures in a dual cantilever configuration, using a Q800 dynamic mechanical analyser (TA Instruments, New Castle, DE, USA). The tests were conducted in air atmosphere, at a rate of 2 °C/min, from 25 °C to 150 °C. A constant frequency of 1 Hz and a maximum deformation of 15 μm were imposed. Per each adhesive, two replicates were tested. The $T_g$ was determined using two different methods: (i) as the extrapolated onset of the sigmoidal change in the storage modulus curve (E'), as per in the ASTM E 1640:2018 [49]; and (ii) from the peak of the tan δ curve.
- The tensile tests of both unaged and aged epoxy adhesives were carried out according to the EN ISO 527-2:2012 [50]. The geometry adopted ("type 1A"—as defined in EN ISO 527-2:2012 [50]) is shown in Figure 5. Tests were conducted on a servo-controlled testing machine (model: C11.DE.150KN.100.70.200, INEGI Sentur, Porto, Portugal), equipped with a 10 kN capacity load cell (with a linearity error less than 0.05% F.S.), under displacement control at a rate of 1 mm/min. In each series, composed of five or six specimens, the following strain measure devices were used: (i) a BFLA-5-3-3L

strain gauge (gauge length: 5 mm, TML, Tokyo, Japan) glued on the specimen's geometrical centre and (ii) a clip-on extensometer, with a gauge length of 50 mm (precision of $\pm 1$ µm) placed at the central region of constant width of each specimen. The elastic modulus was computed based on the slope between the 0.05% and 0.25% strain, on the stress-strain curve, as defined in the EN ISO 527-1:2019 standard [51].
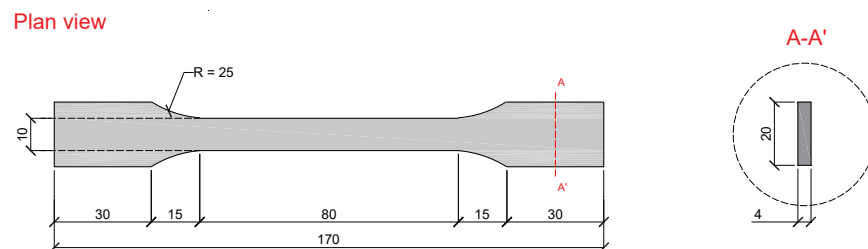


**Figure 5.** Geometry of the epoxy adhesive specimens used in the tensile tests. All units in (mm).

The fabrication of the epoxy adhesive specimens involved the following steps: (i) manually mixing of the two resin components; (ii) casting of homogenized compound into a Teflon mould; (iii) covering of the top surface of the moulds with acetate sheets and compaction with a steel roller (it should be stressed that all these procedures were executed with the necessary care in order to ensure that all specimens were manufactured with nominal geometry and homogeneity, avoiding the formation of voids and other types of defects); (iv) removal of specimens from the moulds one day after casting, and storage in a climatic chamber under controlled temperature and relative humidity (20 °C and 55% RH).

### 2.3.2. CFRP Laminates

The CFRP laminates were submitted to physical and mechanical characterization, using the following methods:

- The water absorption ability of the unaged CFRP laminates with similar procedures to those described for the epoxy adhesive up to 10,000 h, with water at 20 °C.
- The tensile tests of both unaged and aged epoxy adhesives were carried out according to the ISO 527-5:2009 norms [52]. Each specimen was 250 mm long, comprising an initial distance between grips of 150 mm. In order to avoid premature failure due to stress concentration upon the closing of the grips, aluminium tabs of 50 mm were glued to the ends of the CFRP specimens. Figure 6 shows the geometry of the CFRP laminate specimens. The tensile tests were carried out on a servo-controlled testing machine under displacement control with rate of 2 mm/min, equipped with a 200 kN capacity load cell (with a linearity error less than 0.05% F.S.). The following strain measuring devices were used: (i) a clip gauge of 50 mm gauge length (precision of $\pm 1$ µm) placed at the central region of constant width of each specimen; and (ii) one strain gauge TML BFLA-5-3-3L, glued on the geometrical centre of one specimen per series. Each series was composed of six specimens. The tensile elastic modulus ($E_f$), tensile strength ($f_f$), and strain at peak stress ($\varepsilon_f$) were determined according to ISO 527-5:2009 [52].
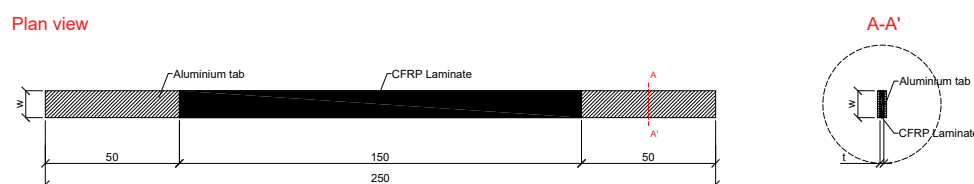


**Figure 6.** Geometry of the CFRP laminate strip specimens used in the tensile tests. All units in (mm).

While L10 CFRP strips were tested with their original cross-section geometry (10 mm × 1.4 mm), the L50 tested samples (250 mm × 15 mm × 1.2 mm) were extracted from the unaged/aged original plates (~350 mm × 50 mm × 1.2 mm).

## 3. Results and Discussion

### 3.1. Epoxy Adhesives

#### 3.1.1. Characterization before Exposure (T0)

Figure 7 shows the results of FTIR spectra for adhesives ADH1 and ADH2. The spectra show consistent peak characteristics of epoxy resin (E), in line with what is stated in the respective technical sheets (both adhesives are filled bicomponent thixotropic adhesives with a bisphenol-A-based resin with an aliphatic amine hardener); it is also possible to identify bands attributed to the presence of silicates (S) in both spectra, and carbonates (C) in ADH2 adhesive. Energy Dispersive X-ray Spectroscopy (EDX) analysis showed that the mineral filler of ADH1 adhesive is quartz [53], and ADH2 adhesive contains, as mineral fillers, calcite and quartz [54].
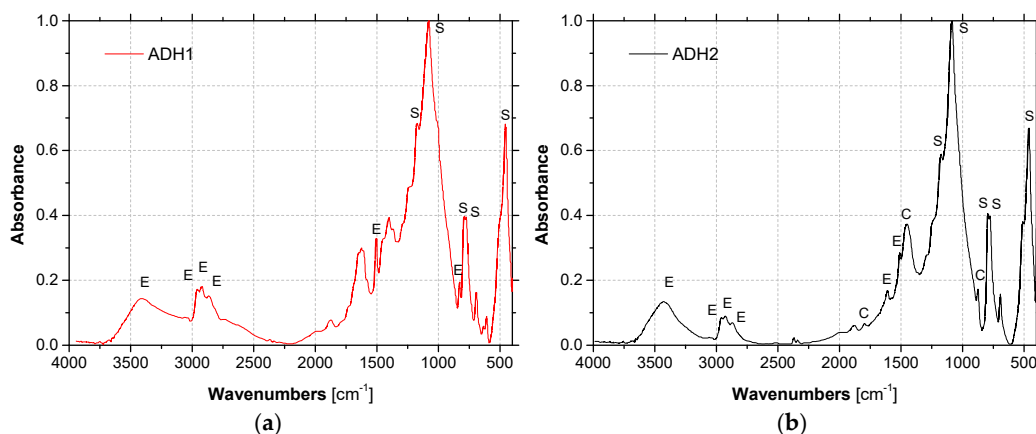


**Figure 7.** FTIR spectra of unaged adhesives (**a**) ADH1 and (**b**) ADH2 - assignment of IR peaks: E-epoxy, S-silicates and C-carbonates.

Figure 8 presents DMA experimental curves (storage modulus and tan δ versus temperature, two test specimens) for both adhesives ADH1 and ADH2, resulting from two consecutive temperature scans of material (cured at 23 °C for 7 days). Storage modulus curves present the typical sigmoidal shape of polymeric materials: after a glassy plateau, the storage modulus drops sharply and becomes practically null. The corresponding change in the experimental curve of tan δ is a peak.



**Figure 8.** DMA experimental curves of unaged adhesives (**a**) ADH1 and (**b**) ADH2—in two consecutive temperature runs.

The first run experimental curve of storage modulus curves started to exhibit a reduction at around 46.2 °C for ADH1 adhesive and 44.3 °C for ADH2 adhesive. On the other hand, tan δ curves exhibited a peak near 57.0 °C for ADH1 adhesive and 55.3 °C for ADH2 adhesive. A study carried out also by DMA with the same adhesives [55], but cured during only 3 days at 21 °C, led to slightly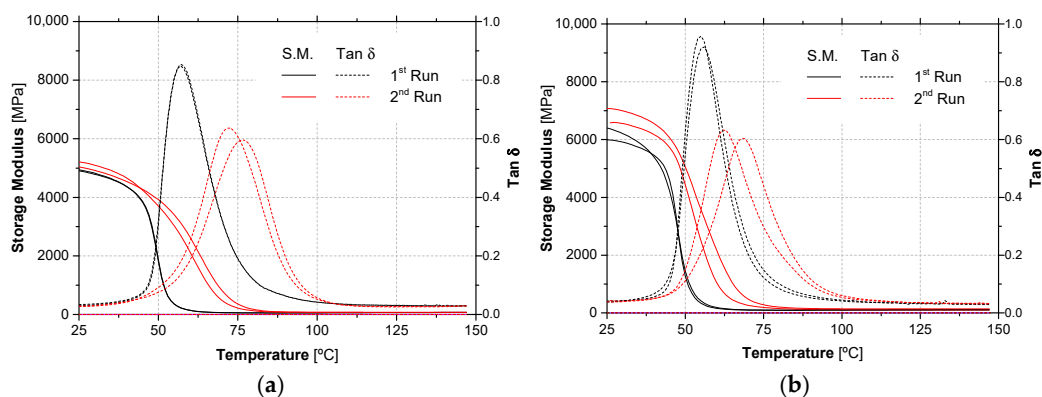 lower $T_g$ values, but of the same order of magnitude. The corresponding technical data sheet declared 52 °C for ADH2 adhesives, but those value was determined in samples cured at higher temperatures and measured by a distinct method (DSC instead DMA).

The second run experimental curves show an increment in $T_g$ values for both adhesives: 30% for ADH1 adhesive and 18% for ADH2 adhesive (considering the tan δ values), showing an important post-cure, particularly for ADH1 adhesive.

Figure 9 depicted the mass uptake of both adhesives, during water immersion at the three distinct temperatures, namely 20 °C, 40 °C and 60 °C.
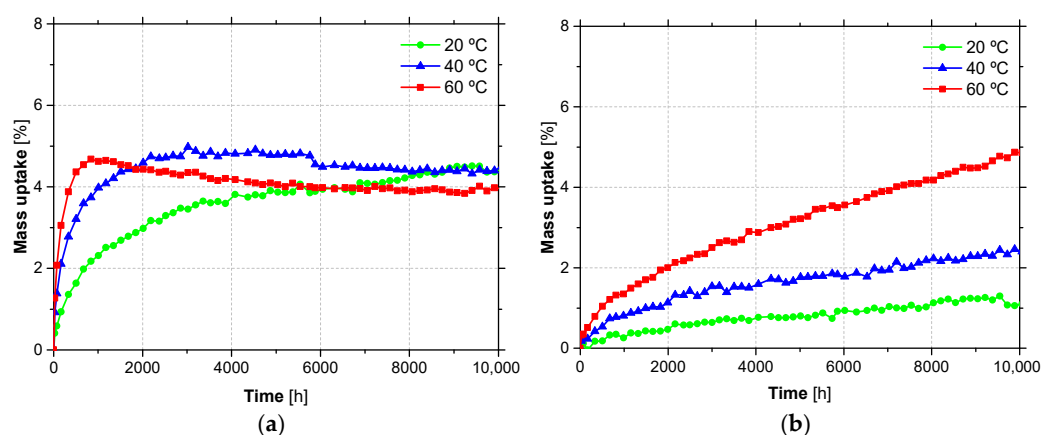


**Figure 9.** Water absorption of adhesives (**a**) ADH1 and (**b**) ADH2 at 20 °C, 40 °C and 60 °C.

As can be seen, the water absorption behaviour of the two adhesives is significantly distinct: while ADH1 adhesive shows a significant absorption rate during the early stages and reaches a steady state equilibrium (fully saturated state) after 5000 h, ADH2 adhesive presents a continuous increase of absorption, particularly for temperatures of 40 °C and 60 °C. As expected, by increasing the temperature, the water absorption increased. However, for immersion at 60 °C, ADH1 adhesive shows a mass loss, probably due to leaching of mineral filler by water. The different water absorption evidenced by the two adhesives, particularly in the initial phase, reflects distinct morphologies of its structure that are strongly affected by the content and nature of the mineral fillers. ADH1 adhesive appears to have a higher free volume to be occupied by water. For this reason, a very rapid initial increase is observed, which tends to settle after 5000 h and, as expected, higher water absorption rates are observed as the temperature increases. A study performed with ADH2 adhesive [56], where water immersion up to 36 months in similar temperatures (23 °C, 37.8 °C and 60 °C) were done, shows an analogous behaviour during the first 10,000 h.

In Section 3.1.2 presents the tensile properties of the epoxy adhesives (ADH1 and ADH2) obtained from the mechanical characterization (tested at T0), in terms of modulus of elasticity ($E_a$), tensile strength ($f_{a,ult}$) and corresponding strain ($\varepsilon_{a,ult}$). These results show that ADH2 adhesive presents higher mechanical properties, when compared to ADH1 adhesive. The obtained values are lower than the nominal values of the technical data sheet, which is not surprising because it is known that the mechanical properties of this type of adhesives can be affected by several factors occurring during the preparation of test specimens, including curing conditions. The results obtained are in line with those of other studies performed with the same adhesives [57].

### 3.1.2. Characterization after Exposure

As detailed in Section 2.3, for each adhesive (ADH1 and ADH2), environment (E1 to E6) and exposure period (T1 and T2), DMA tests were carried out in two replicates. Figure 10 presents the DMA experimental curves obtained.
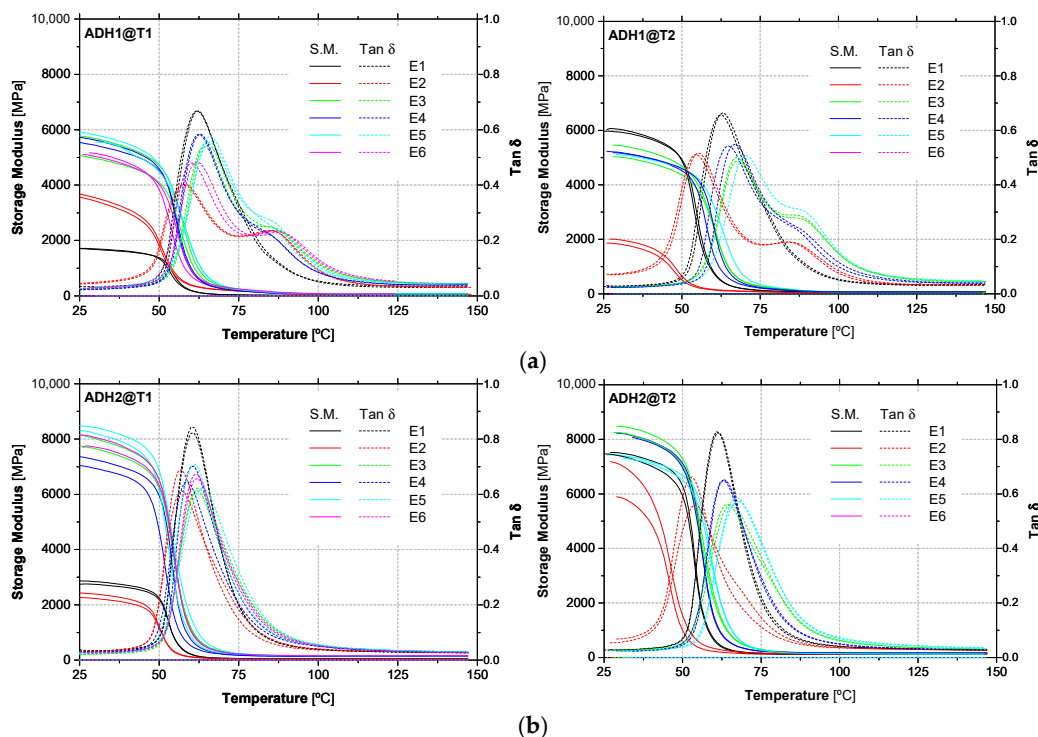


**Figure 10.** DMA experimental curves of adhesives (**a**) ADH1 and (**b**) ADH2, after one year (T1) and two (T2) years of exposure to the environments studied (E1 to E6).

For ADH1 adhesive, with respect to the peak point, an asymmetry on the right side of the tan δ curves is observed in all types of environments (except for environment E1). This phenomenon is particularly relevant for E2 (water immersion), where a second peak can be observed. This phenomenon (splitting of the tan δ peak curve) has been reported in other investigations (e.g., [56]) about the hygrothermal ageing of polymeric adhesives and is attributed to heterogeneous plasticization. In contrast with the responses observed for ADH1 adhesive, the experimental DMA curves of ADH2 adhesive do not show any asymmetries, related to the presence of water inside the material.

Table 4 presents the average values of $T_g$ obtained from (i) the onset of the storage modulus, $T_g$ (E'$_{onset}$), and from (ii) the tan δ $T_g$ (tan δ), for both adhesives (ADH1 and ADH2) and exposure periods (initial characterization—T0, T1 and T2), while Figure 11 presents the same values in the form of graphs, in addition to the initial characterization, considered as reference.

**Table 4.** Glass transition temperature of adhesives ADH1 and ADH2, after one year (T1) and two (T2) years of exposure to the environments studied (E1 to E6), including the reference (T0).

| Environment | $T_g$ (E'$_{onset}$) [°C] (CoV [%]) | | | $T_g$ (tan δ) [°C] (CoV [%]) | | |
|---|---|---|---|---|---|---|
| | T0 | T1 | T2 | T0 | T1 | T2 |
| **ADH1** | | | | | | |
| E1 | | 50.4 (1.1) | 50.5 (0.6) | | 62.0 (0.2) | 62.8 (0.6) |
| E2 | | 46.6 (0.1) | 43.2 (1.0) | | 57.9 (0.3) | 54.9 (0.6) |
| E3 | 46.2 (0.3) | 51.8 (0.2) | 54.1 (0.5) | 57.0 (0.2) | 64.5 (0.6) | 67.6 (0.1) |
| E4 | | 51.5 (0.3) | 54.9 (2.0) | | 62.7 (0.5) | 65.8 (1.5) |
| E5 | | 51.2 (1.1) | 56.2 (-) | | 65.9 (0.2) | 70.4 (-) |
| E6 | | 49.9 (1.6) | *n/a* | | 61.1 (1.4) | *n/a* |
| **ADH2** | | | | | | |
| E1 | | 49.9 (0.0) | 50.5 (0.4) | | 60.5 (0.1) | 61.2 (0.2) |
| E2 | | 46.8 (0.0) | 42.3 (0.8) | | 56.9 (0.3) | 53.5 (1.2) |
| E3 | 44.3 (1.0) | 50.1 (0.2) | 51.0 (0.4) | 55.3 (0.8) | 62.1 (0.5) | 64.9 (0.9) |
| E4 | | 49.3 (2.7) | 52.0 (0.5) | | 59.6 (1.5) | 63.2 (0.2) |
| E5 | | 48.9 (0.7) | 53.9 (0.5) | | 62.4 (2.2) | 67.4 (0.3) |
| E6 | | 50.3 (0.3) | *n/a* | | 61.8 (0.2) | *n/a* |
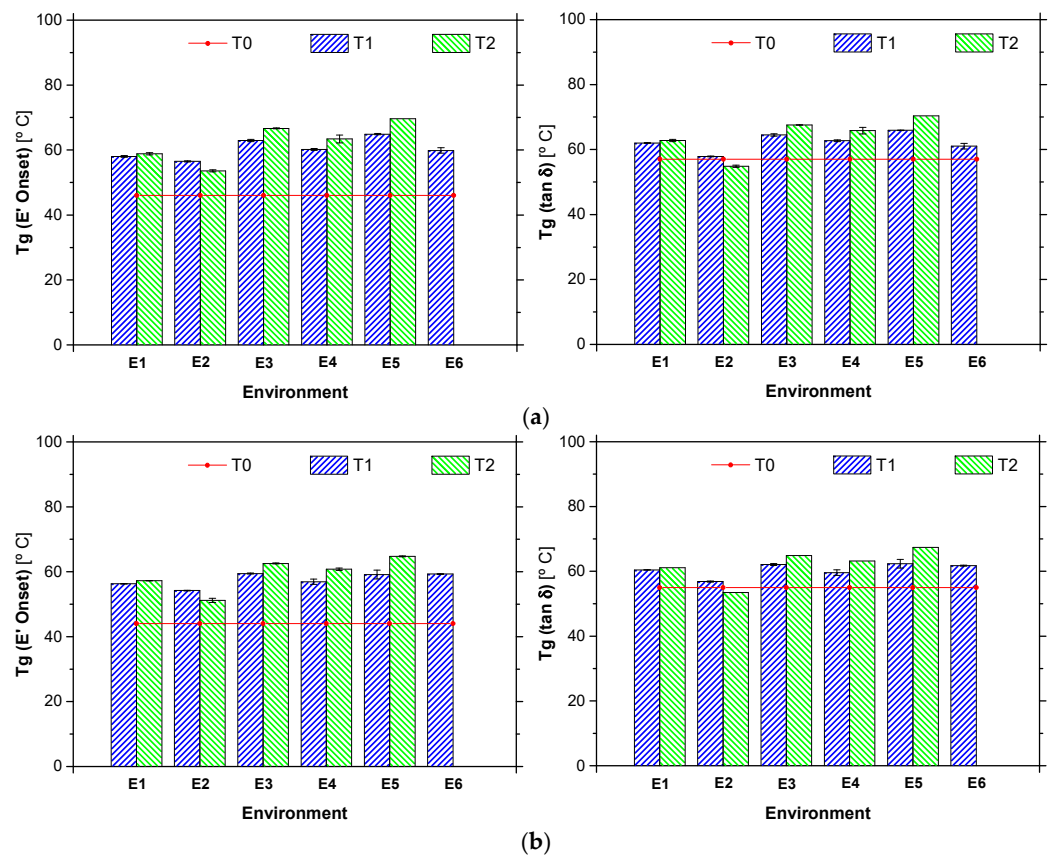


**Figure 11.** Glass transition temperature of adhesives (**a**) ADH1 and (**b**) ADH2, after one year (T1) and two (T2) years of exposure to the environments studied (E1 to E6), including the reference (cured at 23 °C, 7 days).

After two years of environmental exposure, the $T_g$ values of ADH1 adhesive for all outdoor environments (E3 to E6) are still higher than values obtained after curing under standard conditions for 7 days (T0). The reason for such behaviour may be related to the post-curing experienced by the material. When the first (T1) and second (T2) years of exposure are compared, it can be seen that the $T_g$ values are still increasing, for all outdoor environments. It should be noted, however, that environment E6, which presented the lowest $T_g$ values for time T1 (probably due to the higher relative humidity in this environment), was not reported and that may present a different trend. ADH1 adhesive exposed to environment E2 yielded to the lowest values of $T_g$. These results are consistent with the literature (e.g., [53]), where plasticization of the adhesive occurs due to water uptake yielding to a decrease in the $T_g$ value. Moreover, these results are also consistent with those obtained in tensile tests (see below), where a strong reduction on its tensile properties were observed for this environment.

Similarly to the ADH1 adhesive, in the case of ADH2 adhesive, higher values of $T_g$ were also observed for all the outdoor environments when compared with reference (curing under standard conditions during 7 days (T0). Moreover, there was an increase on the $T_g$ values over the last year (from T1 to T2). Also, for the environment E2, a non-negligible reduction in the $T_g$ values were observed (a decrease of 10.7% for $T_g$ (E'$_{onset}$) and 12.6% for $T_g$ (tan δ)), becoming the environment with the lowest values reported.

Table 5 presents the average results obtained from the tensile tests of ADH1 and ADH2 adhesives samples collected in each experimental station, after one (T1) and two (T2) years of environmental exposition. It is also included the values obtained at time T0 (adhesive tested 7 days after casting). Figure 12 shows graphical representation of the tensile strength and the elastic modulus of ADH1 and ADH2 adhesives obtained from the tests performed at T0, T1 and T2.

**Table 5.** Tensile properties of adhesives ADH1 and ADH2, after one (T1) and two (T2) years of exposure to the environment studied (E1 to E6), including the reference (T0).

| Environment | $f_{ult}$ [MPa] (CoV [%]) | | | $E_a$ [GPa] (CoV [%]) | | | $\varepsilon_{ult}$ [%] (CoV [%]) | | |
|---|---|---|---|---|---|---|---|---|---|
| | T0 | T1 | T2 | T0 | T1 | T2 | T0 | T1 | T2 |
| **ADH1** | | | | | | | | | |
| E1 | | 19.5 (1.8) | 18.2 (2.8) | | 6.6 (1.3) | 6.1 (1.4) | | 0.4 (13.0) | 0.3 (11.6) |
| E2 | | 7.2 (3.1) | 6.7 (2.7) | | 1.9 (5.2) | 1.6 (4.0) | | 1.1 (21.3) | 1.1 (11.9) |
| E3 | 19.9 (3.0) | 19.9 (3.1) | 17.4 (5.3) | 6.5 (3.0) | 6.7 (4.4) | 6.0 (5.4) | 0.4 (6.2) | 0.3 (11.1) | 0.3 (19.1) |
| E4 | | 20.1 (3.4) | 17.2 (4.3) | | 7.2 (1.4) | 5.4 (6.9) | | 0.3 (11.3) | 0.3 (12.8) |
| E5 | | 21.9 (5.2) | 18 (3.6) | | 7.5 (5.7) | 6.1 (5.0) | | 0.3 (11.2) | 0.3 (13.1) |
| E6 | | 17.7 (6.4) | 15.8 (4.3) | | 6.2 (5.4) | 5.0 (10.0) | | 0.3 (4.3) | 0.3 (12.9) |
| **ADH2** | | | | | | | | | |
| E1 | | 29.2 (3.8) | 26.2 (5.7) | | 9.6 (3.7) | 8.4 (3.6) | | 0.3 (18.5) | 0.4 (18.2) |
| E2 | | 13.9 (2.5) | 11.0 (7.6) | | 3.8 (7.4) | 3.1 (8.8) | | 0.3 (10.8) | 0.3 (11.7) |
| E3 | 24.8 (7.0) | 33.0 (3.6) | 27.7 (5.8) | 8.0 (8.2) | 10.6 (3.7) | 8.8 (5.3) | 0.4 (20.0) | 0.4 (14.7) | 0.3 (8.7) |
| E4 | | 31.5 (1.8) | 25.7 (5.7) | | 10.2 (1.6) | 8.1 (6.6) | | 0.4 (9.1) | 0.3 (15.8) |
| E5 | | 32.7 (4.6) | 28.6 (4) | | 10.4 (7.2) | 9.0 (4.7) | | 0.4 (10.3) | 0.3 (14.4) |
| E6 | | 34.0 (3.8) | 33.4 (3.8) | | 11.8 (2.1) | 10.9 (3.4) | | 0.3 (11.3) | 0.3 (3.5) |
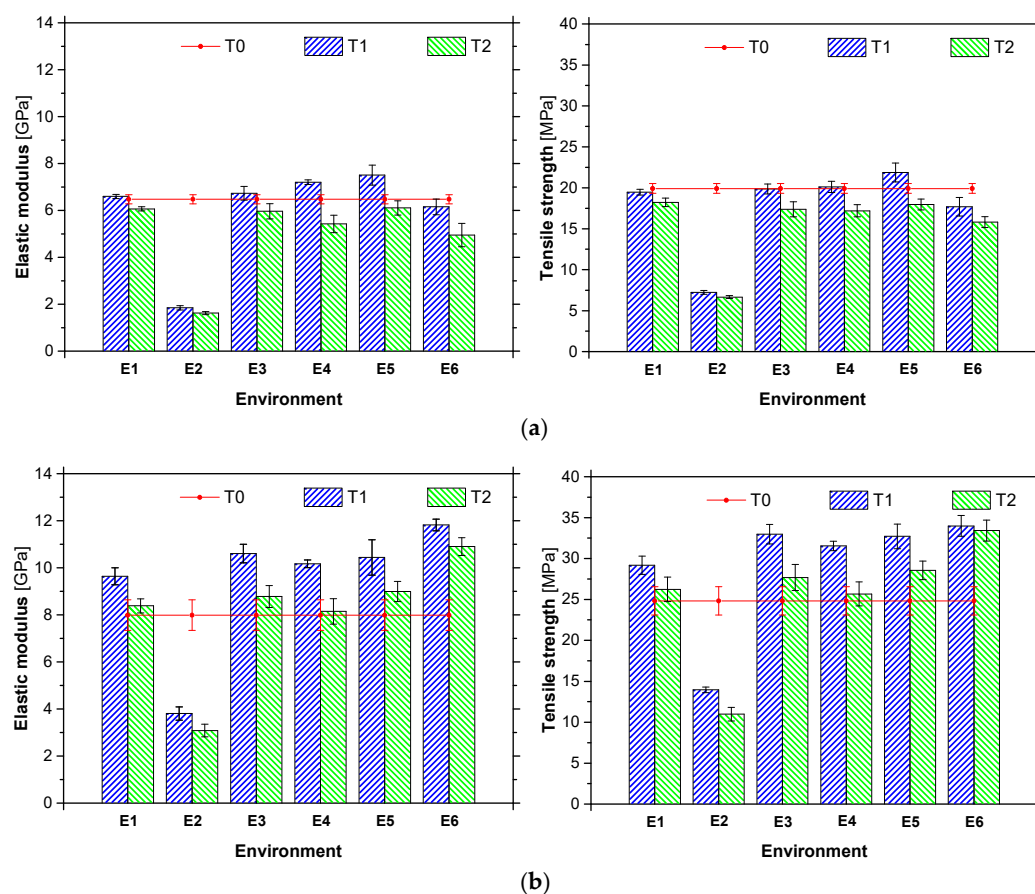
**Figure 12.** Elastic modulus and tensile strength of adhesives (**a**) ADH1 and (**b**) ADH2, after one (T1) and two (T2) years of exposure to the environment studied (E1 to E6), including the reference (T0).

The mechanical properties of the ADH1 adhesive at time T0 are in agreement with the results obtained in other similar works [53,58,59] and with the ones provided by the supplier [58]. Negligible variations in the values of $f_{ult}$ ($-2.0\%$) and $E_a$ ($+1.5\%$) were observed when the ADH1 adhesive was exposed to the E1 environment for one year (see Figure 12). From T0 to T2, a higher decrease in the mechanical properties was observed on $f_{ult}$ ($-8.5\%$) and $E_a$ ($-6.2\%$), indicating a reduction of the performance of the adhesive even under a controlled environment. The immersion in water (E2 environment) led to the greatest reduction in tensile properties: at T1, specimens exposed to the E2 environment presented a reduction of 62.8% and 72.0% on $f_{ult}$ and $E_a$, respectively, in comparison with the reference E1. This finding was already described in previous studies e.g., [16,20] where the authors showed that the absorption of water by the epoxy can cause plasticization (reduction of the elastic modulus and resistance) and swelling. These effects are more pronounced in the present case since the specimens were tested in a saturated state. From T1 to T2, a reduction on these tensile properties was also observed.

After one year of exposure (T1), ADH1 adhesive presented minor variations in the tensile properties for all outdoor environments (E3 to E6). The one-year exposure to environment E5 led to the highest increase in the mechanical properties of the adhesive ($f_{ult}$: +12.4%; and $E_a$: +13.8%, when compared with E1 specimens tested at T1), probably due to a post-curing phenomenon. As referred in [16,53], the exposure of the epoxy to temperatures higher than the initial curing temperature can lead to a post-curing process, improving the mechanical properties of the adhesive. However, in E6, there was a reduction of the epoxy mechanical properties probably as result of higher humidity registered at this site. During the second year of exposure (between T1 and T2) a general decrease in the tensile properties of ADH1 adhesive was observed in all outdoor environments: again, the

E6 environment yielded to the highest reduction on the properties of the adhesive ($f_{ult}$: −13.2%; and $E_a$: −18.4%), probably by the higher humidity, as referred above.

The mechanical properties of ADH2 adhesive at T0 are also in accordance with the values provided by the supplier [59], and with test results from similar works [60]. As shown in Figure 12, there was an increase in the tensile properties of ADH2 adhesive kept on the E1 environment after one year of exposure ($f_{ult}$: +17.7%; and $E_a$: +17.1%). This increase is an indicator that the curing process of ADH2 adhesive was not concluded after 7 days of curing (test at T0). During the second year of ageing (between T1 and T2), a decrease in the mechanical properties of ADH2 adhesive was observed ($f_{ult}$: −10.3%; and $E_a$: −12.5%) for specimens kept in the reference environment (E1), yet, these results obtained at T2 are higher than those obtained for the unaged (T0) specimens. Similarly to ADH1, the environment E2 led to strong reductions in $f_{ult}$ (−52.2% at T1) and $E_a$ (−60.5% at T1) of ADH2 adhesive, in comparison with the E1 environment, due to the abovementioned reasons. From the T1 to T2, a reduction in $f_{ult}$ of −21.3% and $E_a$ of −19.2% can be observed (for E2). All specimens exposed to the outdoor environments (E3-E6) present an increase in their mechanical properties after one year (T1): the highest increase was observed in E6 ($f_{ult}$: +16.5%; and $E_a$: +22.6%) and the smallest was observed in E4 ($f_{ult}$: +7.9%; and $E_a$: +6.3%), when compared with E1 specimens at time T1. The effect of relative high temperatures (even in short periods of time), might have caused a post-curing phenomenon. From T1 to T2, a reduction in the performance of the adhesive exposed to the outdoor environments was observed, especially in the E4 environment ($f_{ult}$: −18.6%; and $E_a$: −19.9%). However, the tensile properties of ADH2 adhesive are still higher after the two years of exposure to the outdoor environments, than when tested unaged (T0).

In short, the outdoor environments led to an increase in the mechanical properties of both adhesives (ADH1 and ADH2) during the first year (post-curing phenomenon might be the cause), and a significant decrease after the second year, in contrast with environments E1 and E2 where the degradation agents (moisture and temperature) were controlled, outdoor environments incorporate a synergy between moisture, UV radiation, temperature cycling, and chemical exposure. Although each selected outdoor environment is geographically distant and presents specific ageing conditions (see Section 2.2), the obtained results do not clearly show which one (or degradation agent) has the greatest influence on the adhesive properties. Finally, it should be noted that for both adhesives (ADH1 and ADH2) and exposure times (T1 and T2), immersion in water (E2) led to the greatest degradation of the tensile properties (up to −75%).

### 3.2. CFRP Laminates

CFRP laminates were fully immersed in water at 20 °C for a period of 10,000 h. Test specimens were weighed, on a weekly basis, using a high precision balance (Kern PFB 600-2, company, Balingen, Germany, with 600 g range and readability of 0.01 g), but no mass variation was detected. Considering that the average weigh of a L10 and L50 specimen was 5.52 g and 23.24 g, respectively, the measuring errors are equal to 0.18% for L10 strip and 0.04% for L50 strip. Therefore, it can be stated that the studied CFRP strips present great resistance to the water ingress. Table 6 presents the mean values of the tensile strength ($f_{fu}$), elastic modulus ($E_f$) and strain at peak stress ($\varepsilon_{fu}$) obtained for the L10 and L50 laminates, after one and two years of environmental exposure. This table also includes the values before ageing (T0), i.e., the reference values. Similarly, Figure 13 shows the mean values of the tensile strength and elastic modulus obtained at T1 and T2 experimental campaigns, alongside with the test results obtained at T0.

**Table 6.** Tensile properties of L10 and L50 laminates, after one (T1) and two (T2) years of exposure to the environment studied (E1 to E6), including the reference (T0).

| Environment | $f_{fu}$ [MPa] (CoV [%]) | | | $E_f$ [GPa] (CoV [%]) | | | $\varepsilon_{ult}$ [$\times 10^{-3}$] (CoV [%]) | | |
|---|---|---|---|---|---|---|---|---|---|
| | T0 | T1 | T2 | T0 | T1 | T2 | T0 | T1 | T2 |
| **Laminate L10** | | | | | | | | | |
| E1 | | 2674 (2.7) | 2528 (4.4) | | 179 (1.6) | 165 (2.7) | | 14.9 (3.2) | 15.3 (6.1) |
| E2 | | 2688 (3.4) | 2460 (7.1) | | 174 (0.7) | 168 (0.5) | | 15.5 (2.9) | 16.0 (12.5) |
| E3 | 2405 (3.8) | 2792 (3.7) | 2590 (5.4) | 164 (1.2) | 177 (1.8) | 172 (1.1) | 14.6 (3.8) | 15.8 (3.8) | 15.1 (5.1) |
| E4 | | 2758 (2.9) | 2617 (4.5) | | 175 (1.8) | 174 (4.5) | | 15.8 (2.3) | 15.0 (4.5) |
| E5 | | 2611 (5.0) | 2619 (5.3) | | 173 (2.0) | 176 (1.5) | | 15.1 (4.6) | 14.9 (5.2) |
| E6 | | 2667 (3.0) | 2640 (2.9) | | 171 (1.4) | 165 (4.2) | | 15.6 (2.9) | 16.0 (1.9) |
| **Laminate L50** | | | | | | | | | |
| E1 | | 2748 (2.6) | 2497 (1.7) | | 174 (2.8) | 164 (1.3) | | 15.8 (3.6) | 15.3 (1.9) |
| E2 | | 2750 (2.0) | 2594 (2.8) | | 177 (3.2) | 169 (2.3) | | 15.6 (3.9) | 15.5 (3.0) |
| E3 | 2527 (10.8) | 2778 (2.1) | 2735 (1.8) | 190 (9.3%) | 174 (2.7) | 175 (0.9) | 13.3 (13.6) | 16.0 (3.6) | 15.6 (1.2) |
| E4 | | 2760 (2.5) | 2703 (3.4) | | 176 (1.5) | 175 (0.8) | | 15.7 (2.8) | 15.4 (3.3) |
| E5 | | 2720 (3.9) | 2618 (3.6) | | 178 (1.2) | 175 (1.3) | | 15.3 (4.0) | 14.9 (2.6) |
| E6 | | 2665 (2.2) | 2554 (4.6) | | 169 (1.6) | 168 (6.0) | | 15.7 (2.6) | 15.2 (6.1) |
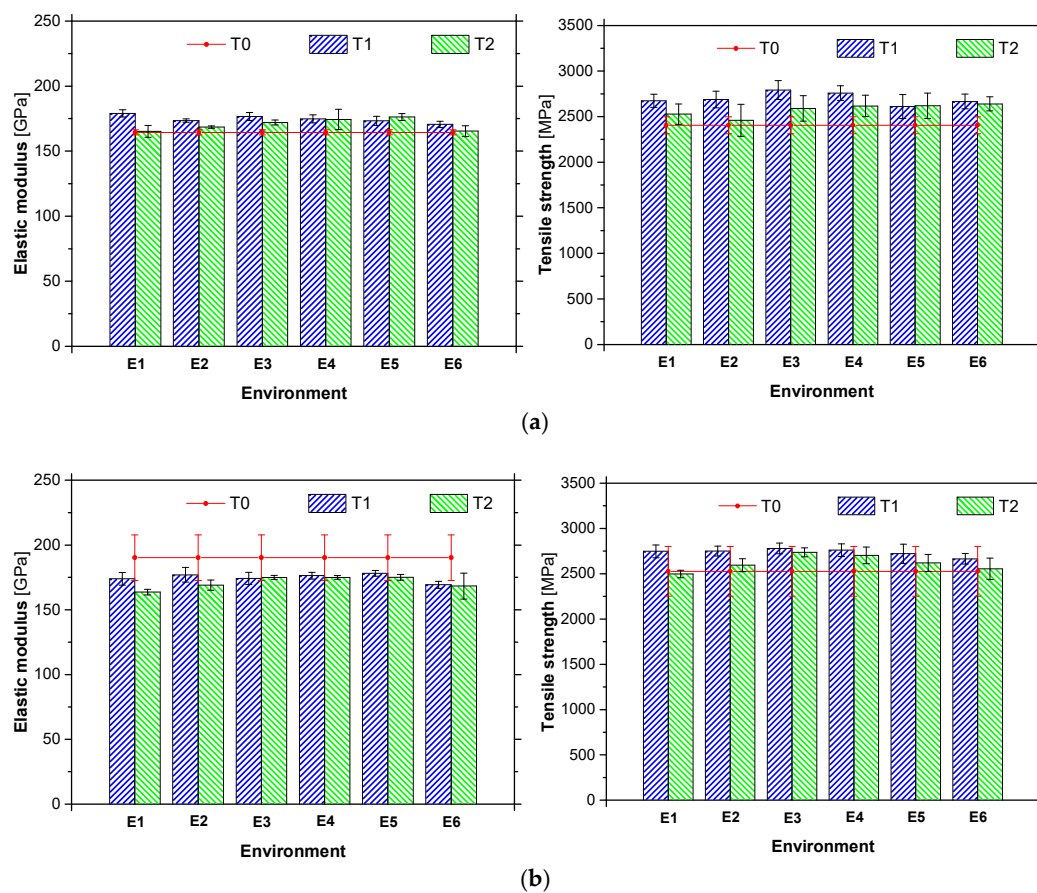


**Figure 13.** (**a**) Elastic modulus and tensile strength of (**a**) L10 and (**b**) L50 laminates, after one (T1) and two (T2) years of exposure to the environment studied (E1 to E6), including the reference (T0).

The values obtained for $f_{\mathrm{fu}}$ and $E_{\mathrm{f}}$ at the time T0 are in agreement with the ones claimed by the supplier. Regardless of the exposure period, in general the type of environment had a minor influence on the mechanical performance of the CFRP laminates (for the same period of exposure, the difference between the maximum and minimum value observed in the different environments is equal to 6.0%). However, when the period of exposure is considered, a tendency of decreasing mechanical properties with the increase of exposure time is observed (an average value of 3.6% was obtained)—a maximum variation of 9.3% was found for the environment E2 between T1 and T2. This variation (from T1 to T2) seems to be higher in the case of strength than in the case of elastic modulus. When T0 is considered in the analysis, in general, for T1 and T2 higher values of the mechanical properties are observed, probably due to a post-curing phase. Finally, regardless the type of environment, the CFRP laminates have presented a low reduction of their mechanical properties.

## 4. Accelerated Ageing versus Natural Ageing

In order to compare the accelerated ageing tests with natural ageing, two databases of accelerated ageing tests (one for epoxy adhesives and another for CFRP laminates) were developed by collecting data from the literature. Then, this data was compared with the results obtained from specimens under natural ageing, developed in the present work.

The database of results of accelerated ageing tests of epoxy adhesive presents the following characteristics:

- More than 105 series (each series composed of three to six specimens) were considered from 17 research works [20,53,56,61–75];
- In terms of types of exposure conditions, water immersion, thermal cycles, wet-dry cycles and freeze-thaw cycles were considered;
- Regardless the type of exposure condition, results obtained from tests under temperatures higher than $T_{\mathrm{g}}$—20 °C were disregarded;
- Water immersion included tap water, demineralised water and water with chlorides;
- Tensile (ISO 527-2, ASTM D638) or flexural (ISO 178, ASTM D790-92) test protocols were adopted for the characterization of the adhesives;
- Periods of exposure up to 21,600 h were found.

Figure 14 depicts the evolution of retention with the time of results in terms the elastic modulus and tensile strength, for epoxy adhesives tested under accelerated ageing protocols. The retention was defined as the ratio between the elastic modulus (or the tensile strength) after ageing and the reference elastic modulus (or the tensile strength), i.e., before ageing. These graphs also include the results of the accelerated ageing tests carried out in the scope of the present work (environment E2) and the results of natural ageing (environments E3 to E6).
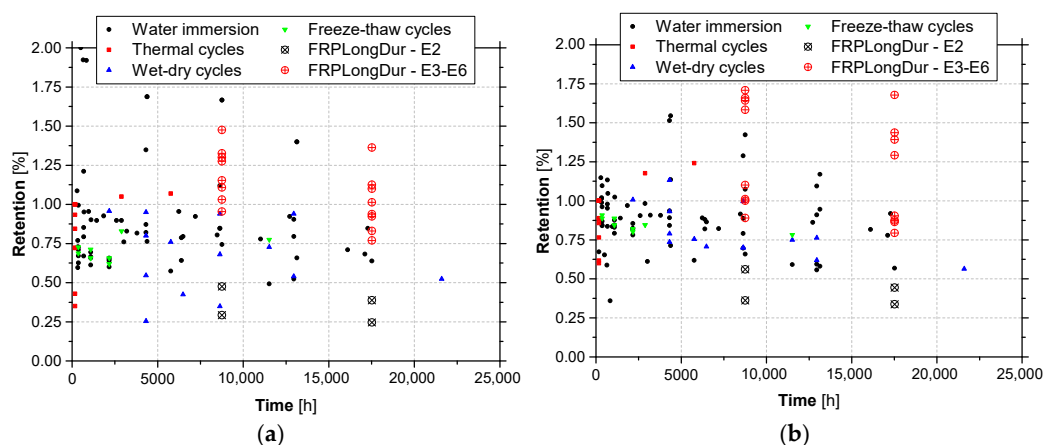


**Figure 14.** Retention values of (**a**) elastic modulus and (**b**) tensile strength of epoxy adhesives under accelerated ageing tests protocols versus natural ageing (E3 to E6).

Despite the dispersion of results, from these graphs it becomes clear that for similar periods of exposure, accelerated ageing tests yield lower values of the retention parameter, when compared with natural ageing. When retention values lower than 1.0 are considered, average retentions of the tensile strength equal to 0.72 (with a coefficient of variation, CoV = 27%) and 0.88 (CoV = 8.1%) are obtained, respectively, for accelerated ageing and natural ageing (E3 to E6); in the case of elastic modulus, these values are equal to 0.72 (CoV = 27%) and 0.88 (CoV = 4.4%).

When the results of environment E2 are compared with the remaining accelerated ageing tests, in general lower values of retention are obtained in the former tests. The principal reason relies on the fact that the specimens of environment E2 were tests in a wet state, just after being removed from the water recipients, without being submitted to any drying process.

Guidelines, such as ACI 440.2R-17 [5] or CNR-DT 200 R1/2013 [4] use durability conversion factors to account for the detrimental effects caused by the different types of exposure conditions. Based on the data collected from the accelerated ageing tests, non-conservatively estimated data values as a function of the conversion factor were determined and its graphical representation is provided in Figure 15a. Based on these results, for ensuring 10% of the non-conservative estimates, a conversion factor of 0.55 should be adopted.
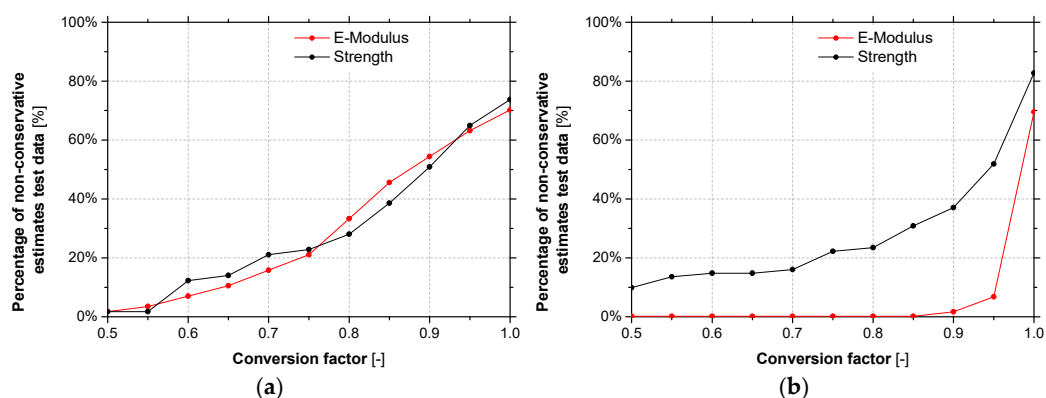


**Figure 15.** Percentage of non-conservatively estimated data points as function of the conversion factor for (**a**) epoxy adhesives and (**b**) CFRP laminates.

Regarding to the database of results of accelerated ageing tests of CFRP laminates, the following characteristics can be drawn:

- More than 63 (elastic modulus) and 76 (tensile strength) series—each series composed of three to six specimens—were considered from 14 research works [19,66,75–86];
- In terms of types of exposure conditions, water immersion, thermal cycles, wet-dry cycles and freeze-thaw cycles were considered;
- Regardless the type of exposure condition, results obtained from tests under temperatures higher than $T_g$—20 °C were disregarded;
- Water immersion included tap water, demineralised water and water with chlorides;
- Tensile (ISO 527-5, ASTM D3039/D3039M) or flexural (ISO 14125/ ASTM D7264) test protocols were adopted for the characterization of the CFRP laminates;
- Periods of exposure up to 20160 h were found.

Figure 16 depicts the evolution of retention with the time of results in terms the elastic modulus and tensile strength, for CFRP laminates tested under accelerated ageing protocols. These graphs also include the results of the accelerated ageing tests carried out in the scope of the present work (environment E2) and the results of natural ageing (environments E3 to E6).
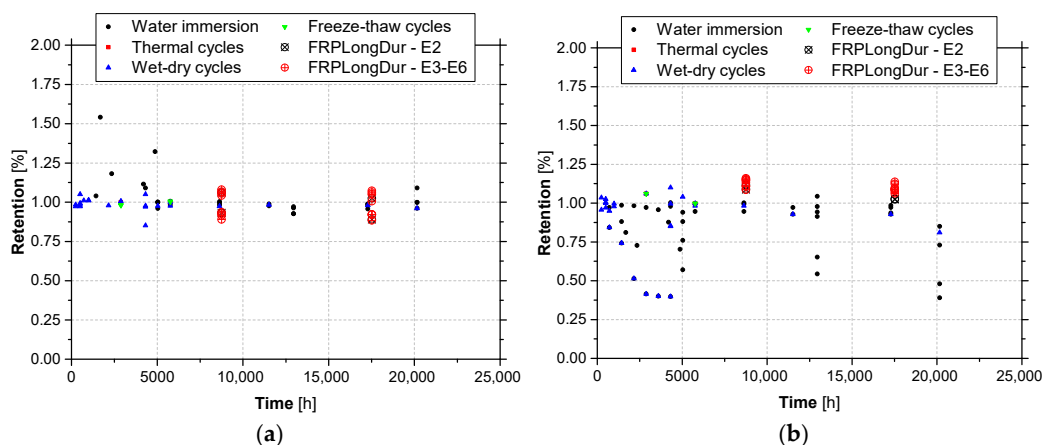
**Figure 16.** Retention values of (**a**) elastic modulus and (**b**) tensile strength of CFRP laminates under accelerated ageing tests protocols versus natural ageing (E3 to E6).

Again, despite the dispersion of results, from these graphs it becomes clear that for similar periods of exposure, in general accelerated ageing tests yield similar or lower values of the retention parameter, when compared with natural ageing. When retention values lower than 1.0 are considered, average retentions of the tensile strength equal to 0.74 (CoV = 42%) are obtained for accelerated ageing, while for natural ageing (E3 to E6) values higher than 1.0 are always obtained; in the case of elastic modulus, these values are equal to 0.97 (CoV = 2.8%) and 0.91 (CoV = 7.9%), respectively. The fact that retention values of elastic modulus for accelerated ageing higher than natural ageing ones are observed may be related to the results obtained in series L50 (see Section 3.2). Moreover, according to these results, the environmental actions have more impact on the strength than on the elastic modulus (see Figures 15b and 16).

## 5. Conclusions

This work addressed the durability of two structural epoxy adhesives (ADH1 and ADH2) and two CFRP laminates (L10 and L50) typically used in strengthening of existing reinforced concrete structures under natural ageing conditions. Four (natural) outdoor environments inducing ageing were adopted, mainly by carbonation (E3), freeze-thaw attack (E4), elevated temperatures (E5), and airborne chlorides from seawater (E6). Furthermore, a control (reference) environment (E1) and an environment involving water immersion of the materials under controlled temperature (E2) were also included in this investigation. The characterization involved the assessment to the physical, chemical and mechanical properties along the time, namely at an early stage (T0) and one (T1) and two (T2) years after exposure to the ageing conditions. Comparisons between the natural ageing tests developed in the scope of the present work and accelerated ageing tests existing in the literature were also performed.

Thus, from the studies carried out with the adhesives ADH1 and ADH2, the following main conclusions can be drawn:

- Results of FTIR spectra of unaged (T0) material have shown typical characteristics of epoxy resins (both adhesives are filled bicomponent thixotropic adhesives with a bisphenol-A-based resin and an aliphatic amine hardener);
- Water absorption tests up to 10,000 h of unaged (T0) material have revealed two completely different behaviors: (i) ADH1 adhesive shows a significant absorption rate at early stages and reaches a steady state equilibrium (fully saturated state) after 5000 h, regardless of the temperature (~5% of uptake), while ADH2 adhesive presented a continuous increase of absorption (at 10,000 h, values of uptake of ~1%, 2.5% and 5% were registered for temperatures of 20 °C, 40 °C and 60 °C, respectively);
- Values of glass transition temperature (based on the onset of sigmoidal change of storage modulus curve from DMA tests), $T_g$, of unaged (T0) material of 46.2 °C and

44.3 °C were obtained for ADH1 and ADH2, respectively; by performing a post-curing (2nd scan), values of 60.1 °C and 52.3 °C were obtained. Ageing up to two (T2) years, yielded to an increase in the $T_g$ of the adhesives, regardless of the environment;

- From the tensile tests, values of elastic modulus of 6.5 GPa and 8.0 GPa, and tensile strength of 19.9 MPa and 24.8 MPa, were obtained for the unaged (T0) ADH1 and ADH2, respectively. After one year of exposure (T1), adhesives ADH1 and ADH2 have shown negligible and significant (up to +48%) variations on the tensile properties, respectively, for all the environments (except E2). When compared with T1, for exposure time T2 both adhesives faced a decrease in the tensile properties (up to 25%) for all the environments (except E2). For both adhesives (ADH1 and ADH2) and exposure times (T1 and T2) environment E2 yielded to significant decrease in the tensile properties (up to −75%);
- Despite the dispersion of results, for similar periods of exposure, accelerated ageing tests yield lower values of the retention tensile properties, when compared with natural ageing.

From the studies carried out with the CFRP laminates L10 and L50, the following main conclusions can be highlighted:

- Water absorption tests up to 10,000 h of unaged (T0) material have revealed negligible water uptake values;
- From the tensile tests, values of elastic modulus of 164 GPa and 190 GPa, and tensile strength of 2405 MPa and 2527 MPa, were obtained for the unaged (T0) L10 and L50, respectively. After two years of exposure, CFRP laminates L10 and L50 have shown almost negligible variations of their tensile properties;
- Despite the dispersion of results, for similar periods of exposure, accelerated ageing tests yield similar or lower values of the retention tensile properties, when compared with natural ageing.

Despite the relevant outputs provided by this work, particularly in terms of durability of epoxy adhesives and CFRP laminates under natural ageing conditions, attempts to establish relationships between accelerated and natural ageing test conditions were unsuccessful as they could not to be derived. It may be possible to establish these relationships if longer periods of exposure to natural ageing are adopted. This should be pursued in future research works.

Construção e Indústria, S.A., Hilti Portugal-Produtos e Serviços, Lda., Artecanter—Indústria Criativa, Lda., and Tecnipor—Gomes&Taveira Lda.

## References

1. Bakis, C.E.; Bank, L.C.; Brown, V.L.; Cosenza, E.; Davalos, J.F.; Lesko, J.J.; Machida, A.; Rizkalla, S.H.; Triantafillou, T.C. Fiber-Reinforced Polymer Composites for Construction—State-of-the-Art Review. *J. Compos. Constr.* **2002**, *6*, 73–87. [CrossRef]
2. Zoghi, M. *The International Handbook of FRP Composites in Civil Engineering*; CRC Press: Boca Raton, FL, USA, 2013; ISBN 9780849320132.
3. FIB Bulletin 90. *Externally Applied FRP Reinforcement for Concrete Structures, Federation International du Beton Technical Report Prepared by a Working Party of the T5.1 FRP Reinforcement for Concrete Structures*; Federation Internationale du Beton: Lausanne, Switzerland, 2019; ISBN 9782883941311.
4. CNR. *Guide for the Design and Construction of Externally Bonded FRP Systems for Strengthening Existing Structures*; CNR-DT 200 R1/2013; Advisory Committee on Technical Recommendations for Construction: Rome, Italy, 2013; p. 144.
5. Committee 440. *Guide for the Design and Construction of Externally Bonded FRP Systems for Strengthening Concrete Structures*; ACI 440.2R-02; American Concrete Institute: Farmington Hills, MI, USA, 2017.
6. HB 305. *Design Handbook for RC Structures Retrofitted with FRP and Metal Plates: Beams and Slabs*; HB 305—2008; Standards Australia: Australia, Sydney, 2008.
7. CSA. *Canadian Highway Bridge Design Code*; CAN/CSA-S6-14; National Standard of Canada: Ontario, ON, Canada, 2014.
8. El-Hacha, R.; Elbadry, M. Strengthening concrete beams with externally prestressed carbon fiber composite cables. *Proc. Fiber-Reinf. Plast. Reinf. Concr. Struct.* **2001**, *4*, 699–708.
9. Correia, L.; Teixeira, T.; Michels, J.; Almeida, J.A.; Sena-Cruz, J. Flexural behaviour of RC slabs strengthened with prestressed CFRP strips using different anchorage systems. *Compos. Part B Eng.* **2015**, *81*, 158–170. [CrossRef]
10. Silva, P.M. Time-Dependent Behaviour and Durability of RC Slabs Strengthened with NSM CFRP strips. Ph.D. Thesis, University of Minho, Braga, Portugal, 2017.
11. Ghiassi, B. *Durability Analysis of Bond Between Composite Materials and Masonry Substrates*; University of Minho: Braga, Portugal, 2013.
12. Tatar, J.; Hamilton, H. Comparison of laboratory and field environmental conditioning on FRP-concrete bond durability. *Constr. Build. Mater.* **2016**, *122*, 525–536. [CrossRef]
13. Helbling, C.; Karbhari, V. Durability of composites in aqueous environments. In *Durability of Composites for Civil Structural Applications*; Elsevier: Amsterdam, The Netherlands, 2007; pp. 31–71.
14. Jones, F.R. Durability of reinforced plastics in liquid environments. In *Reinforced Plastics Durability*; Pritchard, G., Ed.; CRC: Boca Raton, FL, USA, 1999; pp. 70–110.
15. Thomson, K.W.; Wong, T.; Broutman, L.J. The plasticization of an epoxy resin by dibutylphthalate and water. *Polym. Eng. Sci.* **1984**, *24*, 1270–1276. [CrossRef]
16. Cabral-Fonseca, S.; Correia, J.; Custódio, J.; Silva, H.; Machado, A.; Sousa, J. Durability of FRP—concrete bonded joints in structural rehabilitation: A review. *Int. J. Adhes. Adhes.* **2018**, *83*, 153–167. [CrossRef]
17. Sen, R. Developments in the durability of FRP-concrete bond. *Constr. Build. Mater.* **2015**, *78*, 112–125. [CrossRef]
18. Wood, C.A.; Bradley, W.L. Determination of the effect of seawater on the interfacial strength of an interlayer E-glass/graphite/epoxy composite by in situ observation of transverse cracking in an environmental SEM. *Compos. Sci. Technol.* **1997**, *57*, 1033–1043. [CrossRef]
19. Cabral-Fonseca, S.; Nunes, J.P.; Rodrigues, M.P.; Eusébio, M.I. Durability of carbon fibre reinforced polymer laminates used to reinforced concrete structures. *Sci. Eng. Compos. Mater.* **2011**, *18*, 201–207. [CrossRef]
20. Sousa, J.M.; Correia, J.R.; Cabral-Fonseca, S. Durability of an epoxy adhesive used in civil structural applications. *Constr. Build. Mater.* **2018**, *161*, 618–633. [CrossRef]
21. Juska, T.; Dutta, P.; Carlson, L.; Weitsman, J. Thermal Effects. In *ASCE Gap Analysis for Durability of Fiber Reinforced Polymer Composites in Civil Infrastructure*; American Society of Civil Engineers: Reston, VA, USA, 2001; pp. 40–51. ISBN 0-7844-0578-6.
22. Gonilha, J.A.; Correia, J.R.; Branco, F.A.; Sena-Cruz, J. Durability of GFRP-concrete adhesively bonded connections: Experimental and numerical studies. *Eng. Struct.* **2018**, *168*, 784–798. [CrossRef]
23. Grammatikos, S.A.; Jones, R.G.; Evernden, M.; Correia, J.R. Thermal cycling effects on the durability of a pultruded GFRP material for off-shore civil engineering structures. *Compos. Struct.* **2016**, *153*, 297–310. [CrossRef]
24. Sousa, J.M.; Correia, J.R.; Cabral-Fonseca, S.; Diogo, A.C. Effects of thermal cycles on the mechanical response of pultruded GFRP profiles used in civil engineering applications. *Compos. Struct.* **2014**, *116*, 720–731. [CrossRef]
25. Heshmati, M.; Haghani, R.; Al-Emrani, M. Environmental durability of adhesively bonded FRP/steel joints in civil engineering applications: State of the art. *Compos. Part B Eng.* **2015**, *81*, 259–275. [CrossRef]
26. Cromwell, J.; Harries, K.; Shahrooz, B. Environmental durability of externally bonded FRP materials intended for repair of concrete structures. *Constr. Build. Mater.* **2011**, *25*, 2528–2539. [CrossRef]
27. ISIS Canada. *Durability of FRP Composites for Construction*; ISIS: Toronto, ON, Canada, 2006.

28. Moussa, O.; Vassilopoulos, A.P.; Keller, T. Effects of low-temperature curing on physical behavior of cold-curing epoxy adhesives in bridge construction. *Int. J. Adhes. Adhes.* **2012**, *32*, 15–22. [CrossRef]

29. Chin, J.W. Durability of composites exposed to ultraviolet radiation. In *Woodhead Publishing Series in Civil and Structural Engineering*; Woodhead Publishing: Cambridge, UK, 2007; pp. 80–97. ISBN 978-1-84569-035-9.

30. Layton, J. Weathering. In *Pritchard*; Woodhead Publishing: Cambridge, UK, 1999; ISBN 978-1-85573-320-6.

31. Sousa, J.M. Durability of Pultruded GFRP Profiles and Adhesively Bonded Connections Between GFRP Adherends. Ph.D. Thesis, University of Lisbon, Lisbon, Portugal, 2018.

32. Frigione, M.; Naddeo, C.; Acierno, D. Cold-Curing Epoxy Resins: Aging and Environmental Effects. I—Thermal Properties. *J. Polym. Eng.* **2001**, *21*, 23–52. [CrossRef]

33. Frigione, M.; Naddeo, C.; Acierno, D. Cold-Curing Epoxy Resins: Aging and Environmental Effects. Part II—Mechanical Properties. *J. Polym. Eng.* **2001**, *21*, 349–368. [CrossRef]

34. CEN. *EN 12190:1999 Products and Systems for the Protection and Repair of Concrete Structures. Test Methods. Determination of Compressive Strength of Repair Mortar*; CEN—Comité Européen de Normalisation: Brussels, Belgium, 1999.

35. CEN. *EN 196-1:2005 Methods of testing Cement—Determination of Strength*; CEN—Comité Européen de Normalisation: Brussels, Belgium, 2005; Volume 3.

36. *ASTM D695-15, Standard Test Method for Compressive Properties of Rigid Plastics*; ASTM D695-15: West Conshohocken, PA, USA, 2015.

37. ISO. *ISO 178:2002—Plastics—Determination of Flexural Properties*; International Organization for Standardization (ISO): Genève, Switzerland, 2002.

38. ISO. *ISO 527-3:2018—Plastics—Determination of Tensile Properties Part 3: Test Conditions for Films and Sheets*; International Organization for Standardization (ISO): Genève, Switzerland, 2018.

39. CEN. *EN 12615:1999 Products and Systems for the Protection and Repair of Concrete structures. Test methods. Determination of Slant Shear Strength*; CEN—Comité Européen de Normalisation: Brussels, Belgium, 1999.

40. ISO. *ISO 4624:2016—Paints and Varnishes—Pull-off Test for Adhesion*; International Organization for Standardization (ISO): Genève, Switzerland, 2016.

41. CEN. *EN 13892-8:2002 Methods of Test for Screed Materials. Determination of Bond Strength*; CEN-Comité Européen de Normalisation: Brussels, Belgium, 2002.

42. CEN. *EN 1542:1999 Products and Systems for the Protection and Repair of Concrete Structures. Test Methods. Measurement of Bond Strength by Pull-Off*; CEN—Comité Européen de Normalisation: Brussels, Belgium, 1999; Volume 10.

43. CEN. *EN 12614:2004 Products and Systems for the Protection and Repair of Concrete Structures. Test Methods. Determination of Glass Transition Temperatures of Polymers*; CEN—Comité Européen de Normalisation: Brussels, Belgium, 2004; Volume 12.

44. S&P CFRP Laminates. *Technical Datasheet*; S&P: Seewen, Switzerland, 2014.

45. ISO. *ISO 62:2008—Plastics—Determination of Water Absorption*; International Organization for Standardization (ISO): Genève, Switzerland, 2008.

46. ASTM International. *Practice for General Techniques for Obtaining Infrared Spectra for Qualitative Analysis*; ASTM International: West Conshohocken, PA, USA, 2013.

47. ISO. *ISO 6721-1:2019—Plastics—Determination of dynamic mechanical properties—Part 1: General Principles*; International Organization for Standardization (ISO): Genève, Switzerland, 2019.

48. International Organizational for Standardization. *ISO 6721-5:2019—Plastics—Determination of Dynamic Mechanical Properties—Part 5: Flexural Vibration—Non-Resonance Method*; International Organizational for Standardization: Geneva, Switzerland, 2019.

49. ASTM International. *ASTM E1640-18, Standard Test Method for Assignment of the Glass Transition Temperature by Dynamic Mechanical Analysis*; ASTM International: West Conshohocken, PA, USA, 2018.

50. ISO. *ISO 527-2:2012—Plastics—Determination of Tensile Properties—Part 2: Test conditions for Moulding and Extrusion Plastics*; International Organization for Standardization (ISO): Genève, Switzerland, 2012.

51. ISO. *ISO 527-1:2012—Plastics—Determination of Tensile Properties—Part 1: General Principles*; International Organization for Standardization (ISO): Genève, Switzerland, 2019.

52. ISO. *ISO 527-5:2009 Part 5: Test Conditions for Unidirectional Fibre-Reinforced Plastic composites. Plastic—Determ. Tensile Prop*; International Organization for Standardization (ISO): Genève, Switzerland, 2009; Volume 1.

53. Silva, P.; Fernandes, P.; Sena-Cruz, J.; Xavier, J.; Castro, F.; Soares, D.; Carneiro, V. Effects of different environmental conditions on the mechanical characteristics of a structural epoxy. *Compos. Part B Eng.* **2016**, *88*, 55–63. [CrossRef]

54. Cabral-Fonseca, S. *Durabilidade de Materiais Compósitos de Matriz Polimérica Reforçados com Fibras Usados na Reabilitação de Estruturas de Betão (Durability of Fibre Reinforced Polymer Composite Materials Used in the Rehabilitation of Concrete Structures)*; University of Minho: Braga, Portugal, 2008.

55. Michels, J.; Widmann, R.; Czaderski, C.; Allahvirdizadeh, R.; Motavalli, M. Glass transition evaluation of commercially available epoxy resins used for civil engineering applications. *Compos. Part B Eng.* **2015**, *77*, 484–493. [CrossRef]

56. Yang, Q.; Xian, G.; Karbhari, V.M. Hygrothermal ageing of an epoxy adhesive used in FRP strengthening of concrete. *J. Appl. Polym. Sci.* **2007**, *107*, 2607–2617. [CrossRef]

57. Michels, J.; Cruz, J.S.; Christen, R.; Czaderski, C.; Motavalli, M. Mechanical performance of cold-curing epoxy adhesives after different mixing and curing procedures. *Compos. Part B Eng.* **2016**, *98*, 434–443. [CrossRef]

58. S&P. *Technical Data Sheet S & P Resin 220 Epoxy Adhesive*; S&P: Seewen, Switzerland, 2012.
59. Sika Sikadur®. *30 Product Data Sheet*; SIKA: Dublin, Ireland, 2017.
60. Kwiecień, A. Stiff and flexible adhesives bonding CFRP to masonry substrates—Investigated in pull-off test and Single-Lap test. *Arch. Civ. Mech. Eng.* **2012**, *12*, 228–239. [CrossRef]
61. Lu, Z.; Xie, J.; Zhang, H.; Li, J. Long-Term Durability of Basalt Fiber-Reinforced Polymer (BFRP) Sheets and the Epoxy Resin Matrix under a Wet–Dry Cyclic Condition in a Chloride-Containing Environment. *Polymers* **2017**, *9*, 652. [CrossRef] [PubMed]
62. Zafar, A.; Bertocco, F.; Schjødt-Thomsen, J.; Rauhe, J. Investigation of the long term effects of moisture on carbon fibre and epoxy matrix composites. *Compos. Sci. Technol.* **2012**, *72*, 656–666. [CrossRef]
63. Zainuddin, S.; Hosur, M.; Zhou, Y.; Kumar, A.; Jeelani, S. Durability studies of montmorillonite clay filled epoxy composites under different environmental conditions. *Mater. Sci. Eng. A* **2009**, *507*, 117–123. [CrossRef]
64. Lettieri, M.; Frigione, M. Effects of humid environment on thermal and mechanical properties of a cold-curing structural epoxy adhesive. *Constr. Build. Mater.* **2012**, *30*, 753–760. [CrossRef]
65. Al-Safy, R.; Al-Mahaidi, R.; Simon, G.P.; Habsuda, J. Experimental investigation on the thermal and mechanical properties of nanoclay-modified adhesives used for bonding CFRP to concrete substrates. *Constr. Build. Mater.* **2012**, *28*, 769–778. [CrossRef]
66. Abu Hassan, S.; Gholami, M.; Ismail, Y.S.; Sam, A.R.M. Characteristics of concrete/CFRP bonding system under natural tropical climate. *Constr. Build. Mater.* **2015**, *77*, 297–306. [CrossRef]
67. Shrestha, J.; Ueda, T.; Zhang, D. Durability of FRP Concrete Bonds and Its Constituent Properties under the Influence of Moisture Conditions. *J. Mater. Civ. Eng.* **2015**, *27*, 4014009. [CrossRef]
68. Savvilotidou, M.; Vassilopoulos, A.; Frigione, M.; Keller, T. Effects of aging in dry environment on physical and mechanical properties of a cold-curing structural epoxy adhesive for bridge construction. *Constr. Build. Mater.* **2017**, *140*, 552–561. [CrossRef]
69. Ke, L.; Li, C.; He, J.; Dong, S.; Chen, C.; Jiao, Y. Effects of elevated temperatures on mechanical behavior of epoxy adhesives and CFRP-steel hybrid joints. *Compos. Struct.* **2020**, *235*, 111789. [CrossRef]
70. Cabral-Fonseca, S.; Nunes, J.P.; Rodrigues, M.P.; Eusébio, M.I. Durability of epoxy adhesives used to bond CFRP laminates to concrete structures. In Proceedings of the 17th International Conference Composite Materials—ICCM 17, Edinburgh, UK, 27–31 July 2009; pp. 1–8.
71. Frigione, M.; Aiello, M.; Naddeo, C. Water effects on the bond strength of concrete/concrete adhesive joints. *Constr. Build. Mater.* **2006**, *20*, 957–970. [CrossRef]
72. Moazzami, M.; Ayatollahi, M.; Akhavan-Safar, A.; da Silva, L. Experimental and numerical analysis of cyclic aging in an epoxy-based adhesive. *Polym. Test.* **2020**, *91*, 106789. [CrossRef]
73. Goglio, L.; Rezaei, M. Variations in mechanical properties of an epoxy adhesive on exposure to warm moisture. *J. Adhes. Sci. Technol.* **2012**, *28*, 1394–1404. [CrossRef]
74. Heshmati, M.; Haghani, R.; Al-Emrani, M. Durability of bonded FRP-to-steel joints: Effects of moisture, de-icing salt solution, temperature and FRP type. *Compos. Part B Eng.* **2017**, *119*, 153–167. [CrossRef]
75. Xie, J.; Lu, Z.; Guo, Y.; Huang, Y. Durability of CFRP sheets and epoxy resin exposed to natural hygrothermal or cyclic wet-dry environment. *Polym. Compos.* **2019**, *40*, 553–567. [CrossRef]
76. Dawood, M.; Rizkalla, S. Environmental durability of a CFRP system for strengthening steel structures. *Constr. Build. Mater.* **2010**, *24*, 1682–1689. [CrossRef]
77. Fernandes, P.; Silva, P.; Correia, L.; Sena-Cruz, J. Durability of an epoxy adhesive and a CFRP laminate under different exposure conditions. In Proceedings of the SMAR 2015—Third Conference on Smart Monitoring Assessment and Rehabilitation of Civil Structures, Antalya, Turkey, 7–9 September 2015.
78. Fernandes, P.; Sena-Cruz, J.; Xavier, J.; Silva, P.; Pereira, E. Durability of bond in NSM CFRP-concrete systems under different environmental conditions. *Compos. Part B Eng.* **2018**, *138*, 19–34. [CrossRef]
79. Hawileh, R.A.; Abdalla, J.A.; Hasan, S.S.; Ziyada, M.B.; Abu-Obeidah, A. Models for predicting elastic modulus and tensile strength of carbon, basalt and hybrid carbon-basalt FRP laminates at elevated temperatures. *Constr. Build. Mater.* **2016**, *114*, 364–373. [CrossRef]
80. Shi, J.-W.; Zhu, H.; Wu, G.; Wu, Z.-S. Tensile behavior of FRP and hybrid FRP sheets in freeze–thaw cycling environments. *Compos. Part B Eng.* **2014**, *60*, 239–247. [CrossRef]
81. Katogi, H.; Takemura, K.; Shimamura, Y. Mechanical Properties of Carbon Fiber Reinforced Plastics under Hot-Wet Environment. *Key Eng. Mater.* **2011**, *462-463*, 207–212. [CrossRef]
82. Kumar, B.G.; Singh, R.A.P.; Nakamura, T. Degradation of Carbon Fiber-Reinforced Epoxy Composites by Ultraviolet Radiation and Condensation. *J. Compos. Mater.* **2002**, *36*, 2713–2733. [CrossRef]
83. Lu, Z.; Li, J.; Xie, J.; Huang, P.; Xue, L. Durability of flexurally strengthened RC beams with prestressed CFRP sheet under wet–dry cycling in a chloride-containing environment. *Compos. Struct.* **2021**, *255*, 112869. [CrossRef]
84. Nguyen, T.-C.; Bai, Y.; Zhao, X.-L.; Al-Mahaidi, R. Durability of steel/CFRP double strap joints exposed to sea water, cyclic temperature and humidity. *Compos. Struct.* **2012**, *94*, 1834–1845. [CrossRef]
85. Sciolti, M.S.; Frigione, M.; Aiello, M.A. Wet Lay-Up Manufactured FRPs for Concrete and Masonry Repair: Influence of Water on the Properties of Composites and on Their Epoxy Components. *J. Compos. Constr.* **2010**, *14*, 823–833. [CrossRef]
86. Wu, P.; Xu, L.; Luo, J.; Zhang, X.; Bian, W. Influences of long-term immersion of water and alkaline solution on the fatigue performances of unidirectional pultruded CFRP plate. *Constr. Build. Mater.* **2019**, *205*, 344–356. [CrossRef]

## Paper 3

**TITLE:** DURABILITY OF BOND BETWEEN NSM CFRP STRIPS AND CONCRETE UNDER REAL-TIME FIELD AND LABORATORY ACCELERATED CONDITIONING

**REFERENCE:**

Cruz, R., Correia, L., Cabral-Fonseca, S., and Sena-Cruz, J. 2022. Durability of bond between NSM CFRP strips and concrete under real-time field and laboratory accelerated conditioning. *Journal of Composites for Construction*, 26(6), 04022074. https://doi.org/10.1061/(ASCE)CC.1943-5614.0001262.

# Durability of Bond between NSM CFRP Strips and Concrete under Real-Time Field and Laboratory Accelerated Conditioning

Ricardo Cruz[1]; Luís Correia[2]; Susana Cabral-Fonseca[3]; and José Sena-Cruz[4]

**Abstract:** This investigation addresses the durability of the adhesive bond between near-surface-mounted (NSM) carbon fiber-reinforced polymer (CFRP) strips and concrete, under real-time field conditioning and laboratory-accelerated conditioning. Four natural outdoor environments were considered in the experimental program to induce aging mainly by carbonation, freeze-thaw cycles, elevated temperatures, and airborne chlorides from seawater. Additionally, a control environment (20°C and 55% RH) and a water immersion environment under controlled temperature (20°C) were considered. The durability was studied mainly throughout the mechanical properties obtained from (1) the involved materials (concrete, epoxy adhesive, and CFRP strips); and (2) the bond specimens, with a period of exposure up to 2 years. The bond performance of NSM-CFRP strips to concrete was slightly affected by environments under investigation, being water immersion and freeze–thaw cycles the most deleterious ones. A maximum average bond strength decrease of approximately 12% was registered for the specimens immersed in water, while in the case of the outdoor environments, the maximum bond degradation (approximately 8%) occurred for the specimens of freeze–thaw cycles after 2-year exposure. **DOI:** [10.1061/(ASCE)CC.1943-5614.0001262](10.1061/(ASCE)CC.1943-5614.0001262). © *2022 American Society of Civil Engineers.*

**Author keywords:** Concrete; CFRP; Epoxy adhesive; Bond NSM; Durability; Real-time field conditioning; Laboratory-accelerated conditioning.

## Introduction

The use of carbon fiber-reinforced polymer (CFRP) materials in the strengthening of existing reinforced-concrete (RC) structures has been increasing over the last three decades, being considered state-of-art in civil engineering. Two main techniques are being used to apply these composite materials (FIB 2019): the externally bonded reinforcement (EBR) and the near-surface-mounted (NSM) techniques. While in the former, laminate strips or sheets are externally bonded to the surface of the structural element to be strengthened, in the latter, laminate strips or bars are inserted inside grooves on the concrete cover of the structural member. Both systems can be used for flexural and/or shear strengthening. Epoxy adhesives are typically used as a bonding agent. These systems can be applied through passive and active systems, that is, by prestressing application, which combines the advantages of using CFRP systems with external prestressing, resulting of a more efficient use of concrete and CFRP, and reduction on the deflection and crack width, among other advantages (El-Hacha and El-Badry 2001; Correia

et al. 2015). When compared with the EBR technique, NSM presents the following main advantages (De Lorenzis and Teng 2007; Coelho et al. 2015): (1) less probability of premature debonding, as the bonded contact area is higher, leading to more efficient use of the FRP materials—in many cases, FRP failure is achieved; (2) easy to extend the reinforcement to adjacent elements; (3) greater protection of the FRP against external aggressive agents or acts of vandalism; and (4) smaller visual impact. Therefore, the present work addresses only the NSM strengthening technique.

The durability of RC structures strengthened with CFRP materials has been intensively studied using accelerated conditioning protocols (ACP) under laboratory conditions (Fernandes et al. 2018). Nevertheless, several gaps in the existing knowledge can be found, namely on the performance of this type of strengthening solution under real-time field conditioning in outdoor conditions. Moreover, the relationship between laboratory-accelerated conditioning and real-time field conditioning is another important gap in the literature that must be better understood and still remains a challenge (Ashraf 2016; Tatar and Hamilton 2016). Some studies, e.g. (Hassan et al. 2015; Kabir et al. 2016; Mohd Hashim et al. 2016; Tatar and Hamilton 2016; Fernandes et al. 2018) include real-time field conditioning and laboratory-accelerated conditioning protocols and try to establish relationships between the aging effects of both types of exposure. There are other investigations that only address the durability under outdoor conditions (Al-Tamimi et al. 2015; Bhashya et al. 2015; Sen 2015; Hsieh et al. 2017). From the previous studies, no relationship between laboratory-accelerated conditioning and real-time field conditioning could be found. Nevertheless, in most cases, for similar test periods, the level of degradation reached in laboratory-accelerated conditioning is higher than in real-time field conditioning.

The former ASTM E632-82 (ASTM 1988) standard established some concepts and protocols for the development of laboratory-accelerated conditioning tests aiming at predicting the long-term in-service performance, that is, an aging test in which the

[1]Ph.D. Student, Dept. of Civil Engineering, Univ. of Minho, ISISE/IB-S, 4800-058 Guimarães, Portugal.

[2]Postdoctoral Researcher, Dept. of Civil Engineering, Univ. of Minho, ISISE/IB-S, 4800-058 Guimarães, Portugal.

[3]Auxiliary Researcher, Materials Dept., National Laboratory of Civil Engineering, 1700-066 Lisbon, Portugal. ORCID: https://orcid.org/0000-0001-6609-3228.

[4]Associate Professor, Dept. of Civil Engineering, Univ. of Minho, ISISE/IB-S, 4800-058 Guimarães, Portugal (corresponding author). ORCID: https://orcid.org/0000-0003-3048-1290. Email: jsena@civil.uminho.pt

degradation of materials is intentionally accelerated more than that aging expected in service for the same period of exposure to the degradation mechanisms. However, this approach presents some limitations, as it is difficult to develop laboratory-accelerated conditioning tests/protocols for predicting long-term in-service performance due to the following reasons: (1) the degradation mechanisms in the materials are complex, and in many cases are not well understood; (2) the degradation factors affecting performance are numerous and are difficult to quantify, which means that most of existing accelerated protocols do not consider all important factors and those considered seldom relate quantitatively to in-service exposure; and (3) the materials are frequently tested in configurations different from those used in-service. In addition, another difficulty comes from the fact that each one of the materials and interfaces composing the bond system (concrete, adhesive, FRP and concrete–adhesive and adhesive–FRP interfaces) present different degradation rates and degradation mechanisms (Tatar and Milev 2021).

The durability of the materials involved in this work (concrete, CFRP, and adhesive) has been extensively investigated, and several publications can be found in the literature (FIB 1983; CERF 2001; Cruz et al. 2021; CNR 2013; ACI 2017; Frigione and Lettieri 2018; Cromwell et al. 2011; Tatar and Milev 2021). The most relevant environmental degradation factors that affect these materials are: thermal effects, moisture, UV exposure, and chemicals. Therefore, when exposed to a single or a combination of degradation factors, the materials experience a sequence of chemical, mechanical, and/or physical changes leading to the alteration of one or more mechanical properties. Regarding the thermal effects, one primary concern is about elevated temperatures: due to the viscous response of both resins/adhesives and composites, as the temperature rises, the elastic and ultimate properties lower, particularly if the temperature reaches or surpasses the glass transition temperature of the material. In general, thermal cycles do not have detrimental effects on CFRP materials, while they may cause microfractures in some resins and adhesives. In general, freeze–thaw cycles do not cause any deleterious effect on the CFRP performance, while the cycles decrease the mechanical performance of adhesives and the fiber–matrix interface. For temperatures below 0°C, resin/adhesive systems may improve their performance in terms of strength and stiffness. Moisture absorption mostly affects the resins/adhesives through the following main degradation mechanisms: plasticization, swelling, relaxation, hydrolysis, and leaching. Consequently, resins/adhesives and composites can be significantly affected by the presence of moisture, yielding to the reduction of glass transition temperature, and strength and stiffness. Typically, the effects of exposure of CFRP composites to UV radiation are usually limited to the top few microns of the surface, affecting mainly their aesthetical properties. Finally, alkaline environments may cause degradation of the resin and the interface between CFRP composites and support.

The bond behavior of NSM–CFRP strips to concrete is highly important, as it is responsible for the stress transfer between the strengthening material and the substrate. Therefore, the investigation on the durability of the bond of these systems is essential, as its success is highly dependent on its durability. Very few articles can be found in the literature addressing this topic. Most of them are performed under laboratory-accelerated conditioning in laboratory conditions, whereas only one contains a component on real-time field conditioning. Fernandes et al. (2018) investigated the durability of bond between NSM–CFRP strips and concrete systems under different environmental conditions, including laboratory-accelerated conditioning (water immersion, wet/dry cycles, temperature cycles, and freeze–thaw cycles) and real-time field conditioning (wet/dry cycles in marine environment and warm and temperate environment from Mediterranean climate).

The evolution of bond strength was assessed by performing direct pull-out tests on the aged specimens for different periods of exposure up to 2 years. Results have shown that the exposure to the environments (which may be considered quite severe) did not result in an effective degradation of the bond strength. In most of the environments, the bond strength even increased. A maximum bond strength decrease of ~12% was observed in both the real outdoor environments. Conversely, a maximum increase of 8% was obtained with temperature cycles between −15°C and +60°C. According to the authors, the bond strength increase can be explained by the improvement observed in the mechanical properties of the epoxy adhesive itself, which lead to an improvement of the chemical adhesion between the CFRP strip and the adhesive.

Peng et al. (2019) undertook a study on the durability of the bond between the NSM–CFRP strips and concrete under freeze–thaw cycles. The following variables were studied: (1) the type of concrete (ordinary concrete, high-strength concrete, and concrete with additional frost resistance); (2) the geometry of CFRP strips [$16 \times 2.0$ (mm) and $16 \times 4.5$ (mm)]; and (3) the bond length (300 and 450 mm). After bond aging, the authors concluded that the freeze–thaw cycles (1) yielded in a considerable decrease in compressive strength of ordinary concrete, and (2) lead to a decrease in the bond strength of ~15%, with ordinary concrete. However, an increase in the bond strength (20%) was observed for specimens with concrete of high strength. Furthermore, the degradation of concrete was pointed out as the principal cause for the deterioration of the bond.

Garzón-Roca et al. (2015) performed an experimental program on the durability of the NSM–CFRP strips to concrete using direct pull-out tests, carried out for evaluating the bond behavior of specimens aged through wet–dry cycles. A total of 30 specimens were considered with the following three studied variables: bond length (60 and 90 mm), groove width (4 and 8 mm), and groove depth (15 and 25 mm). The specimens were subjected to 90 wet–dry cycles, each one lasting 24 h, consisting in wetting the specimens during 12 h by immersion in water with 3% of NaCl at $20 \pm 1$°C, followed by a drying period at about $30 \pm 1$°C. A maximum decrease of ~12% in the maximum pull-out force was observed.

Considering the existing investigations, it is still controversial the relationship between the effects caused by real-time field conditioning and laboratory-accelerated conditioning. Moreover, in addition to the attempts to compare the degradation caused by each type of environment, it should be highlighted that real-time field conditioning includes several environmental degradation factors acting simultaneously, for example moisture, thermal effects, and UV exposure, making it very difficult to reproduce them in the accelerated conditioning protocols. The execution of real-time field conditioning tests is more complex than laboratory-accelerated conditioning tests. As stated by Fernandes et al. (2018), performing real-time field conditioning tests requires longer testing periods and is more time consuming. Nevertheless, it is mandatory to develop this type of tests, as only these ones can provide effective knowledge about the real degradation mechanisms.

From the previous paragraphs, it becomes clear that there are gaps in the knowledge of the durability of the bond in NSM systems, namely regarding (1) the relationship between real-time field conditioning and laboratory-accelerated conditioning, (2) the durability of NSM technique itself, and (3) the influence of the type of environment on the durability of the NSM technique. Therefore, this work intends to provide new insights on the durability of the NSM bonding system, throughout an experimental investigation where aging was induced by exposure to carbonation, freeze–thaw, elevated temperatures, and airborne chlorides from seawater. The investigation also includes a reference (control)

environment and a water-immersion environment under controlled temperature. During the aging, three periods of analysis were considered, mainly: after specimen's production (T0), after 1 (T1) year of exposure, and after 2 (T2) years of exposure. Moreover, the results obtained from the real-time field conditioning were compared with laboratory-accelerated conditioning tests available in the existing literature. Considerations about the environmental conversion factors (also common known as environmental reduction factors) existing in guidelines, such as CAN/CSA-S6-06 (CSA 2006), ACI 440.2R-17 (ACI 2017), and CNR-DT 200 R1/2013 (CNR 2013), are also presented.

## Experimental Program, Materials, and Methods

### Experimental Program

This work was carried out in the scope of the FRPLongDur project. This project intends to investigate the long-term structural behavior and durability of RC elements strengthened in flexure with CFRP laminate strips under relevant laboratory-accelerated conditioning and real-time field conditioning environments for 10 years [further details about this project can be found in Cruz et al. (2021)]. This work is mainly devoted to the durability of bond between CFRP strips and concrete using the NSM-strengthening technique and follows the publication Cruz et al. (2021), where a work on the durability of epoxy adhesives and CFRP laminates was performed. To facilitate the comparison between the materials that compose the NSM system and the durability of the system itself, a selection of relevant results from Cruz et al. (2021) is presented in this paper.

A total of six different environments were considered: two artificial laboratory environments (E1 and E2), and four real outdoor environments (E3 to E6); Fig. 1 shows their main characteristics. The accelerated and the real-time field conditioning were materialized through experimental stations, especially developed for the installation of the specimens in the different environments. The environment E1 (reference environment) presents controlled

hygrothermal conditions (20°C/55% RH), and environment E2 consists of the immersion of the specimens in fresh water under controlled temperature (20°C). Environment E2 was adopted, (1) as an extreme environment in terms of moisture (typically design guidelines do not allow permanent immersion in water of FRP systems without proper protection), and (2) to allow comparisons with the other environments included in the study. Regarding to the outdoor environments, it is expected to be achieved the following specific aging conditions: E3, higher levels of concrete carbonation due to the elevated levels of $CO_2$ concentration from air pollution, since this experimental station is located close to the international airport of Lisbon and close to a highway with heavy traffic load; E4, freeze–thaw cycles, since the experimental station was placed at the highest mountain of Portugal ("Serra da Estrela"); E5, elevated service temperatures and lower relative humidity due to the climate characteristics of Elvas; and E6, high levels of airborne chlorides concentration and relative humidity, since the experimental station is located by the seaside (Atlantic Ocean).

To record the air temperature and relative humidity (RH) at each experimental station, sensors were installed at the experimental stations. Some sensors faced technical issues, and the record data were lost. Therefore, the missing data were provided by the Portuguese Institute for the Sea and Environment (IPMA). Table 1 presents the temperature and relative humidity registered at each environment (maximum, average, and minimum values) between the years of 2018 and 2020, by trimester. Fig. 2 provides two examples of the evolution of the temperature and relative humidity in experimental stations E1 and E3 during this period. The technical characteristics of the sensors used can be found in Cruz et al. (2021).

Fig. 3 presents the timeframe of the experimental work. Specimens preparation was concluded approximately 15 months before the beginning of the environmental exposure. During this period, all specimens were kept in a laboratory environment. An initial assessment of the specimens' mechanical properties was performed at early stages (T0). Therefore, the compressive strength and elastic modulus of the concrete were assessed 28 days after casting (December 2016), while the tensile strength of the concrete was
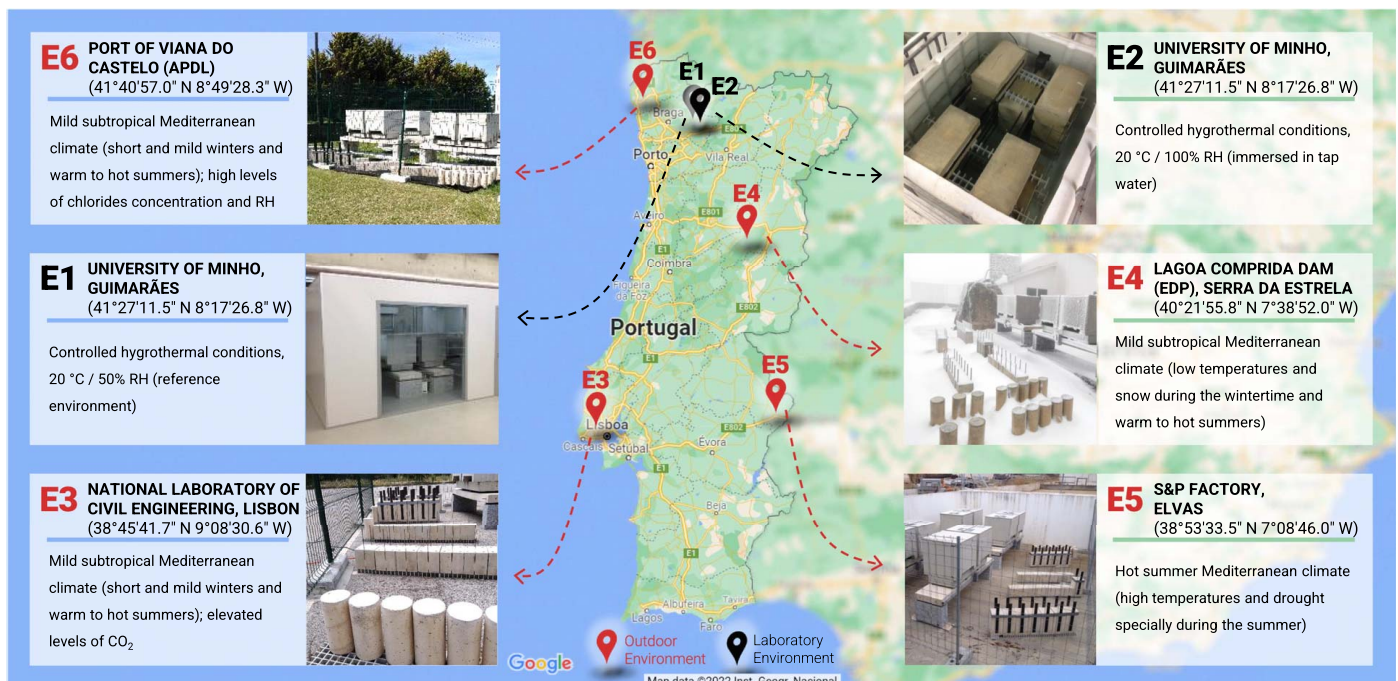


**E6 PORT OF VIANA DO CASTELO (APDL)**
(41°40'57.0" N 8°49'28.3" W)
Mild subtropical Mediterranean climate (short and mild winters and warm to hot summers); high levels of chlorides concentration and RH

**E1 UNIVERSITY OF MINHO, GUIMARÃES**
(41°27'11.5" N 8°17'26.8" W)
Controlled hygrothermal conditions, 20 °C / 50% RH (reference environment)

**E3 NATIONAL LABORATORY OF CIVIL ENGINEERING, LISBON**
(38°45'41.7" N 9°08'30.6" W)
Mild subtropical Mediterranean climate (short and mild winters and warm to hot summers); elevated levels of $CO_2$

**E2 UNIVERSITY OF MINHO, GUIMARÃES**
(41°27'11.5" N 8°17'26.8" W)
Controlled hygrothermal conditions, 20 °C / 100% RH (immersed in tap water)

**E4 LAGOA COMPRIDA DAM (EDP), SERRA DA ESTRELA**
(40°21'55.8" N 7°38'52.0" W)
Mild subtropical Mediterranean climate (low temperatures and snow during the wintertime and warm to hot summers)

**E5 S&P FACTORY, ELVAS**
(38°53'33.5" N 7°08'46.0" W)
Hot summer Mediterranean climate (high temperatures and drought specially during the summer)

**Fig. 1.** Environments included in this investigation. (Base map © Google, Map data ©2022 Inst. Geogr. Nacional; Images by authors.)

evaluated almost 2 years after casting (October 2018). The tensile properties of the epoxy adhesive were evaluated 7 days after the specimens' production, whereas the CFRP laminate tensile properties were evaluated after receipt from the manufacturer (March 2017). Also, pull-out tests were performed with bond NSM–CFRP-to-concrete specimens in October 2017 (8 months after strengthening application). The installation of specimens in the experimental stations took place between June 2018 and December 2018. Fig. 4 depicts the specimens placed in two of the experimental stations. In each outdoor location (E3 to E6), all bond specimens were placed with one groove aligned with the sunrise direction and the other with the sunset direction.

After 1 (T1) and 2 (T2) years of exposure in each experimental station, several test specimens were collected to be tested at the laboratory, namely, epoxy adhesive specimens, CFRP strips, concrete cylinders, and two bond NSM–CFRP to concrete specimens. The test protocol included a 3-week desorption period with the hygro-thermal conditions defined for E1 (E1 specimens continued in their conditioning during the desorption period). This desorption period was adopted to avoid the effect of misleading weather conditions when the specimens were collected (heavy rainfall), which may not represent the average degradation level along the year. For the specimens immersed in water (E2), no desorption phase took place, being all specimens immersed in water all the time (they were removed immediately before being tested). The same protocol of test preparation and execution was adopted for both experimental campaigns T1 and T2.

## Materials

Concrete, CFRP strips, and epoxy adhesive were the materials involved in this investigation. The next sections provide detailed information about these materials.

### Concrete

A concrete with a compressive characteristic strength (cylinder/cube) of 30/37 MPa (C30/37), exposure class XC4(P), water/cement ratio (CL) of 0.40, maximum aggregate size ($d_{max}$) of 12.5 mm, slump class S4 (slump of 160–210 mm), and produced with portland cement type CEM II/A–L 42.5R [Eurocode 2 (IPQ 1992)/EN 206-1 (CEN 2000)] was used to cast all the specimens from a single concrete batch of about 12 m³. Three different types of concrete specimens were adopted: (1) cylinders for the assessment of the compressive properties; (2) prisms for the assessment of the tensile properties and carbonation depth; and (3) cubes, for the assessment of the bond behavior of NSM–CFRP to concrete.

### CFRP

The CFRP strips used in this investigation were prefabricated by pultrusion, being composed of unidirectional carbon fibers (fiber content higher than 68%) and adhered by a vinyl–ester–resin matrix, with a $T_g$ of ~85°C (Cabral-Fonseca 2008). The CFRP strips had a rectangular cross-section geometry of 10 mm (wide) by 1.4 mm (thick). This is a typical geometry used in practical applications with the NSM strengthening technique. According to the supplier, the average

**Table 1.** Temperature and relative humidity recorded in the environments between the years 2018 and 2020

| Env. | Measured parameter | Year 2018 | | Year 2019 | | | | Year 2020 | | | |
|---|---|---|---|---|---|---|---|---|---|---|---|
| | | Jul to Sep | Oct to Dec | Jan to Mar | Apr to Jun | Jul to Sep | Oct to Dec | Jan to Mar | Apr to Jun | Jul to Sep | Oct to Dec |
| E1 | Temp. (°C) | 20.5 | 18.6 | 20.5 | 20.1 | 20.0 | 20.1 | 20.2 | 20.2 | — | — |
| | | 20.0–22.0 | 17.5–20.0 | 17.0–22.0 | 19.5–21.0 | 20.0–21.5 | 19.0–21.5 | 19.0–21.0 | 19.0–21.5 | | |
| | RH (%) | 69.9 | 62.7 | 50.7 | 60.6 | 71.5 | 63.8 | 54.3 | 62.5 | — | — |
| | | 55.0–79.5 | 53.5–67.5 | 35.5–69.5 | 49.0–74.0 | 56.5–77.5 | 51.5–75.0 | 41.5–60.5 | 48.5–75.5 | | |
| E2 | Temp. (°C) | 24.3 | 21.4 | 20.6 | 21.2 | 21.6 | 19.8 | 20.0[a] | 20.0[a] | — | — |
| | | 24.1–24.5 | 19.7–25.0 | 18.6–21.4 | 19.8–23.9 | 20.9–22.4 | 17.6–21.6 | – | – | | |
| | RH (%) | 100.0 | 100.0 | 100.0 | 100.0 | 100.0 | 100.0 | 100.0 | 100.0 | — | — |
| | | — | — | — | — | — | — | — | — | | |
| E3 | Temp. (°C) | 22.2[b] | 15.3 | 17.1 | 17.9 | 22.0 | 15.7 | 13.6 | 14.9 | — | — |
| | | 12.7–46.2 | 6.2–34.3 | 3.3–25.7 | 6.8–35.3 | 14.5–39.7 | 6.8–31.0 | 4.3–27.0 | 6.6–23.5 | | |
| | RH (%) | 66.2[b] | 78.5 | 71.0 | 67.1 | 66.8 | 81.6 | 78.3 | 80.5 | — | — |
| | | 14.0–100.0 | 11.0–100.0 | 12.0–100.0 | 13.0–100.0 | 20.0–100.0 | 19.0–100.0 | 22.0–100.0 | 34.0–100.0 | | |
| E4[c] | Temp. (°C) | 18.0[d] | 7.8 | 5.8 | 10.2 | 17.1 | 7.7 | 6.1 | 11.5 | — | — |
| | | 7.4–32.4 | −2.8–22.2 | −4.7–18.5 | −3.1–26.7 | 4.8–29.6 | −2.3–24.6 | −4.6–19.2 | −3.6–27.0 | | |
| | RH (%) | 60.3[d] | 78.8 | 63.9 | 71.4 | 59.4 | 80.5 | 75.3 | 79.6 | — | — |
| | | 4.0–100.0 | 16.0–100.0 | 7.0–100.0 | 5.0–100.0 | 8.0–99.0 | 7.0–100.0 | 4.0–100.0 | 14.0–100.0 | | |
| E5[c] | Temp. (°C) | 26.1 | 13.2 | 10.9 | 19.3 | 25.0 | 14.5 | 11.6 | 19.2 | — | — |
| | | 12.6–44.6 | 1.1–33.0 | −1.9–26.2 | 4.7–38.0 | 11.7–39.9 | 3.1–34.7 | 0.3–25.3 | 2.1–39.0 | | |
| | RH (%) | 49.1 | 79.8 | 69.7 | 54.6 | 48.5 | 75.8 | 78.2 | 66.5 | — | — |
| | | 9.0–95.0 | 11.0–100.0 | 14.0–100.0 | 10.0–100 | 11.0–97.0 | 1.04–100.0 | 28.0–100.0 | 11.0–100.0 | | |
| E6 | Temp. (°C) | — | — | 12.1 | 17.9 | 21.8 | 13.7 | 12.6 | 19.0 | 22.5 | 14.2 |
| | | | | 1.5–28.5 | 5.0–34.5 | 12.0–36.0 | 3.5.0–28.0 | 2.0–25.0 | 5.5–25.0 | 11.0–39.5 | 4.0–26 |
| | RH (%) | — | — | 76.1 | 69.0 | 71.0 | 88.1 | 82.8 | 75.8 | 70.2 | 86.7 |
| | | | | 18.0–100.0 | 26.5–99.0 | 22.0–99.0 | 45.0–100.0 | 38.5–100.0 | 33.5–100.0 | 28.5–99.5 | 42.0–100.0 |

Notes: For each environment and for each measured parameter, the mean value (first line) and the extreme minimum and maximum values (second line) are presented.
[a]Values obtained from the controller equipment installed on the experimental station in this trimester.
[b]Also included May 30–June 30, 2018.
[c]Values provided by IPMA (IPMA's station is located 9 km apart from E4 and 560 m apart from E5).
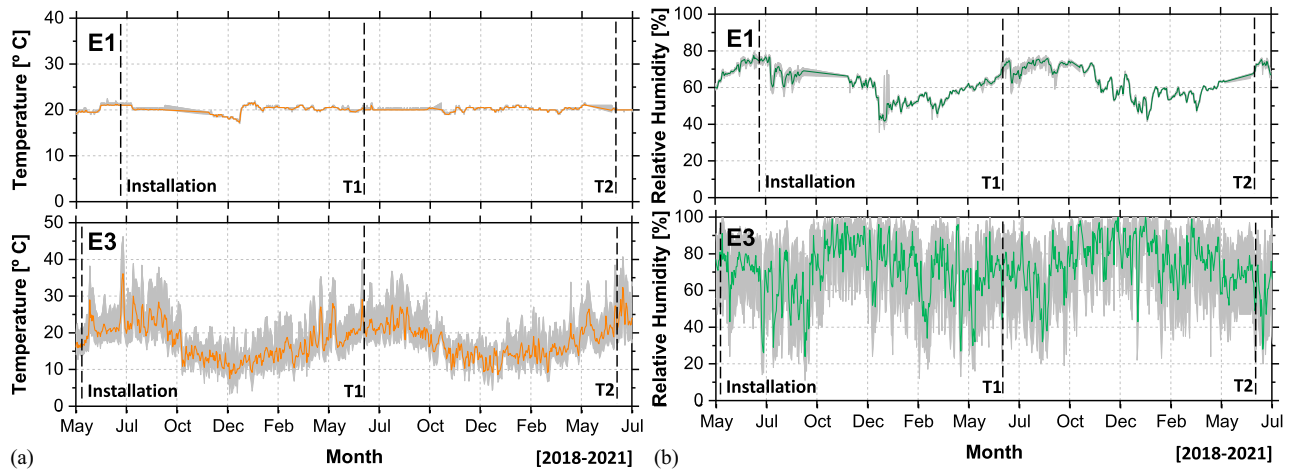[d]Also included June 26–30, 2018.

**Fig. 2.** Meteorological records collected at environments E1 and E3, between the years 2018 and 2020: (a) temperature; and (b) relative humidity.
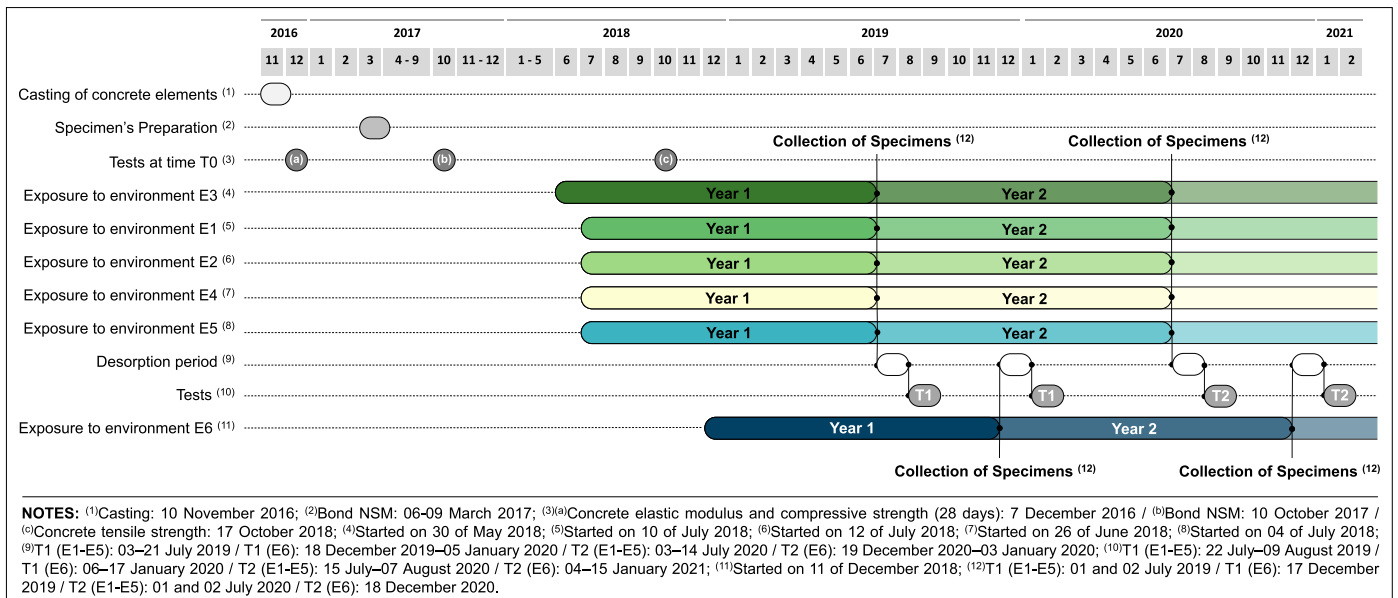


NOTES: [1]Casting: 10 November 2016; [2]Bond NSM: 06-09 March 2017; [3][a]Concrete elastic modulus and compressive strength (28 days): 7 December 2016 / [b]Bond NSM: 10 October 2017 / [c]Concrete tensile strength: 17 October 2018; [4]Started on 30 of May 2018; [5]Started on 10 of July 2018; [6]Started on 12 of July 2018; [7]Started on 26 of June 2018; [8]Started on 04 of July 2018; [9]T1 (E1-E5): 03–21 July 2019 / T1 (E6): 18 December 2019–05 January 2020 / T2 (E1-E5): 03–14 July 2020 / T2 (E6): 19 December 2020–03 January 2020; [10]T1 (E1-E5): 22 July–09 August 2019 / T1 (E6): 06–17 January 2020 / T2 (E1-E5): 15 July–07 August 2020 / T2 (E6): 04–15 January 2021; [11]Started on 11 of December 2018; [12]T1 (E1-E5): 01 and 02 July 2019 / T1 (E6): 17 December 2019 / T2 (E1-E5): 01 and 02 July 2020 / T2 (E6): 18 December 2020.

**Fig. 3.** Timeframe of the experimental work carried out.



**Fig. 4.** Specimens in the experimental stations: (a) E3; and (b) E4.

value of the elastic modulus and the characteristic tensile strength is higher than 170 GPa and 2,000 MPa, respectively (S&P 2014).

### Adhesive

A commercial cold-curing epoxy adhesive was used as the bonding agent between the CFRP strip and the concrete substrate. According to the supplier, the average value of the flexural elastic modulus is higher than 7.1 GPa (S&P 2015). The adhesive presents a tensile strength of 19.9 MPa (after 7 days of curing at 20°C) and a $T_g$ of 46.2°C (after 7 days of curing at 23°C) according to Cruz et al. (2021), where further details regarding this epoxy adhesive can also be found.

## Test Methods

The unaged (reference) and aged specimens were characterized using different methods and techniques, depending on the type of specimen and property to be assessed.

### Concrete

Cylindrical concrete specimens of 150 mm in diameter and 300 mm in height were used to evaluate the modulus of elasticity ($E_{cm}$) and compressive strength ($f_{cm}$) of concrete, according to NP EN 12390-13:2013 (IPQ 2013) and NP EN 12390-3:2011 (IPQ 2011) standards, respectively. All tests were conducted using a servo-controlled universal testing machine (UTM) with a 2,000 kN capacity. The initial characterization (T0) was performed 28 days after casting with four specimens (Fig. 3). Furthermore, the assessment of the average concrete compressive properties ($E_{cm}$ and $f_{cm}$) after 1 (T1) and 2 (T2) years of aging was achieved using three specimens, per year, from each environment. In total, 40 concrete cylinders were tested.

The evaluation of concrete tensile strength was carried out through pull-off tests with concrete prisms. The test setup followed the recommendations of the standard EN1542:1999 (BSI 1999). Matest E142 equipment was used, with a maximum pull-off force capacity of 16 kN, an accuracy of 1%, and a resolution of 10 N. These tests were performed using a loading rate of 1 MPa/s and a dolly size (diameter) of 50 mm. Four pull-off tests were performed for the initial characterization (T0), whereas a total of 48 pull-off tests were carried out to assess the concrete tensile strength after aging (four for each aging period—T1 and T2—and environment—E1 to E6).

The determination of carbonation depth in concrete was performed according to the LNEC E391:1993 (LNEC 1993) recommendation. Carbonation depth was assessed using a solution of phenolphthalein indicator that appears pink in contact with alkaline concrete (with a pH value higher than 9) and colorless at lower levels of pH. The tests were performed at T1 and T2, using two concrete core samples of 50 mm in diameter and 100 mm in height, per environment. Therefore, 26 tests were performed for the assessment of the carbonation depth. Note that the carbonation depth was not assessed at T0. In fact, all specimens were kept in the same environmental conditions (laboratory environment) before their exposure to the mentioned aging conditions.

### CFRP Strip and Epoxy Adhesive

The tensile properties of the CFRP strips and the epoxy adhesive were assessed at unaged (T0) and aged (T1 and T2) stages according to ISO 527-5:2009 (ISO 2009) and ISO 527-2:2012 (ISO 2012), respectively. For each environment and test stage (T0, T1, and T2), a minimum of six CFRP strips samples and five epoxy specimens were tested. Therefore, 78 and 65 specimens were used the assessment of the tensile properties of the CFRP strips and the epoxy adhesive, respectively. Further details about the assessment performed in these materials can be found in Cruz et al. (2021).

### NSM–CFRP to Concrete Bond Tests

The performance of bond NSM–CFRP to concrete was assessed by performing direct pull-out tests. Fig. 5 presents the geometry of specimens and the corresponding test configuration used. A concrete cubic block with a 200-mm edge was adopted, to which two CFRP strips (cross section of $10 \times 1.4$ mm) were bonded over a bond length of 60 mm in the faces parallel to the casting direction of the cubes, as shown in Fig. 5. A groove with a 15-mm depth and 5-mm width was made at the surface of the concrete block and, at its center, the CFRP strip was installed. The bond length of 60 mm was adopted to (1) avoid the failure of CFRP and (2) be sufficiently large to be representative of the system and minimize the influence of the inevitable effects (e.g., geometric irregularities), as demonstrated in previous research works (Fernandes et al. 2015, 2018; Ricardo Cruz et al. 2020).
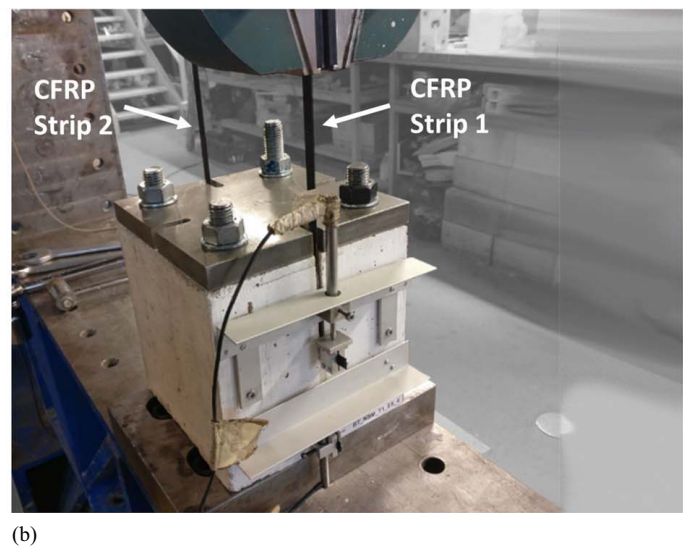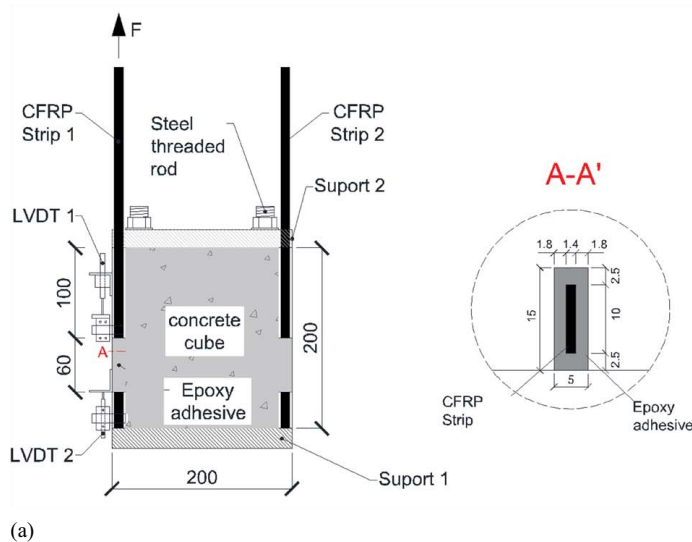


(a)

(b)

**Fig. 5.** Pull-out test of bond NSM–CFRP to concrete: (a) specimen's geometry and test configuration; and (b) photograph of the test. Note: all units in mm.

The application of the load was performed using a servo-controlled equipment. The slip at the loaded, $s_l$, and free, $s_f$, ends was measured using two LVDTs (range $\pm2.5$ mm and linearity error of $\pm0.05\%$ F.S.), respectively, LVDT1 and LVDT2. The load, $F$, was measured with a load cell placed between the grip and the actuator, with a static load-carrying capacity of 200 kN (linearity error of $\pm0.05\%$ F.S.). The tests were performed under displacement control at the loaded end section (LVDT1), with a rate of 0.12 mm/min. Four tests were performed per aging period and environment.

## Results and Discussion

### Materials

This section presents and discusses the results from the assessment of the material's mechanical properties along the time.

### Concrete

Table 2 details the tabulated results in terms of the mean values and corresponding coefficients of variation (CoV) of the concrete elastic modulus ($E_{cm}$) and compressive strength ($f_{cm}$), tensile strength ($f_{ctm}$), and carbonation depth, for the times T0, T1, and T2. Fig. 6 shows a graphical representation of these parameters.

Mechanical properties of concrete obtained at T0 were in agreement with the class of concrete strength C30/37 [Eurocode 2 (IPQ 1992)/EN 206-1 (CEN 2000)], with a $E_{cm} = 33$ GPa and $f_{cm} = 38$ MPa at 28 days of age. In general, the exposure of the concrete to the environments lead to an increase in compressive strength in relation to T0 results, except the immersed specimens (E2) that were tested in a saturated state, that is, without being submitted to any drying process before testing. While environment E1 did not cause any relevant change, the remaining environments yielded to the increase of the mechanical properties of the concrete, particularly at T2 in E4 (+21.2%) and E6 (+21.0%) specimens, probably as a result of the higher humidity of these environments (Table 1). In fact, the compressive strength of concrete increases in environments with high humidity, as it was reported by Mi et al. (2018). The maximum decrease in the compressive strength was verified for E2 specimens at T2 (−6.7% when compared with T0). This behavior can be justified by the fact that saturated concrete presents lower compressive strength than dry concrete (Zhou and Ding 2014; Zhang et al. 2020). In general, a higher variation in the compressive strength of the concrete than in its elastic modulus was observed. The highest variations in the elastic modulus were observed after 2 years of aging (T2) for environments E3 (−7.2%) and E6 (+12.0%).

When compared with T0, the tensile strength decreased after T1 and T2 periods of exposure with the highest reduction in E2 (70.5% retention), since the corresponding specimens were tested saturated. In fact, the presence of pore-water on concrete reduces the tensile strength, as demonstrated by Jin et al. (2012). Also, a nonnegligible tensile strength decrease was verified in E6 specimens. In general, similar values were obtained in the remaining outdoor specimens (E3–E5). Contrary to compressive strength, a general decrease in tensile strength was obtained, a fact that can be related to the higher reduction of surface mechanical properties than core zones, as shown by Rozsypalová et al. (2018).

As expected, the highest carbonation depth was obtained in the E3 specimens. A carbonation depth of ~7.5 mm was obtained in the other series, which is in agreement with other similar investigations for similar times of exposure and environmental conditions (e.g., Bouzoubaâ et al. 2010; Otieno et al. 2020). The lowest values were obtained in the E1 and E2 specimens, probably due to the reduced contact with $CO_2$, especially when immersed in water. All the outdoor environments have shown increases in the depth of carbonation [Table 2; Fig. 6(d)] when compared with the laboratory environments, particularly at T1. However, small variations on the increase of the carbonation depth can be observed between T1 and T2, which can be related to confinement imposed by COVID-19 pandemic during the second year of exposure (T2) and, consequently, a reduction in the air concentration of $CO_2$ anthropogenic.

### Epoxy Adhesive

Table 3 details the results in terms of the mean values and corresponding CoV of epoxy adhesive elastic modulus ($E_a$), tensile strength ($f_a$), and ultimate strain ($\varepsilon_a$), for the times T0, T1, and T2, while Fig. 7 shows these results graphically.

An elastic modulus of 6.5 GPa and a tensile strength of 19.9 MPa were obtained for the unaged (T0) specimens. At T1, small variations on the tensile properties for all the environments (except E2) were verified, with the highest increase obtained in E5 specimens ($E_a$ increased ~15% and $F_a$ increased ~10% in comparison with T0), probably due to the post-curing phenomenon (Silva et al. 2016). A significant reduction was obtained in E2 specimens (up to 75% in the elastic modulus), where specimens were tested saturated (without desorption before testing). This finding can be justified by the absorption of water by the epoxy, which causes plasticization (reduction of the elastic modulus and resistance) and swelling (Cabral-Fonseca et al. 2018; Sousa et al. 2018). In each environment, between T1 and T2, a general decrease in the tensile properties was verified for all the environments. The highest reduction in the tensile strength and elastic modulus of the adhesive was registered, respectively in the E5 (−17.8%) and in the E4 (−25.0%) environments. This highest decrease in $E_a$ is

**Table 2.** Mean values of the elastic modulus ($E_{cm}$) compressive strength ($f_{cm}$), tensile strength ($f_{ctm}$), and carbonation depth of concrete, after 1 (T1) and 2 (T2) years of exposure to the environment studied (E1 to E6), including the reference (T0)

| Environment | $E_{cm}$ (GPa) [CoV (%)] | | | $f_{cm}$ (MPa) [CoV (%)] | | | $f_{ctm}$ (MPa) [CoV (%)] | | | Carbonation depth (mm) [CoV (%)] | | |
|---|---|---|---|---|---|---|---|---|---|---|---|---|
| | T0 | T1 | T2 | T0 | T1 | T2 | T0 | T1 | T2 | T0 | T1 | T2 |
| REF | 29.1 (4.7) | — | — | 41.5 (4.4) | — | — | 3.4 (13.3) | — | — | — | — | — |
| E1 | — | 28.0 (0.7) | 28.7 (1.7) | — | 42.8 (2.4) | 43.3 (1.4) | — | 2.9 (10.4) | 3.2 (1.3) | — | 7.3 (19.9) | 7.7 (14.8) |
| E2 | — | 28.2 (2.8) | 27.7 (2.9) | — | 40.7 (0.7) | 38.7 (2.9) | — | 2.5 (5.3) | 2.4 (11.8) | — | 7.1 (15.2) | 5.5 (17.7) |
| E3 | — | 29.4 (0.8) | 27.0 (8.0) | — | 46.3 (0.9) | 46.0 (3.4) | — | 3.2 (3.6) | 2.8 (9.7) | — | 10.1 (5.5) | 9.3 (18.2) |
| E4 | — | 28.6 (3.4) | 29.7 (12.1) | — | 46.5 (3.4) | 50.3 (0.8) | — | 3.2 (13.5) | 3.1 (5.3) | — | 7.8 (7.5) | 8.4 (14.1) |
| E5 | — | 28.6 (2.7) | 29.1 (1.6) | — | 44.9 (1.0) | 48.2 (1.5) | — | 3.1 (6.3) | 3.1 (16.4) | — | 7.8 (10.9) | 8.0 (12.5) |
| E6 | — | 30.2 (3.7) | 32.6 (0.5) | — | 48.0 (2.4) | 50.2 (1.3) | — | 2.7 (4.4) | 2.8 (8.8) | — | 8.0 (14.1) | 7.3 (13.9) |
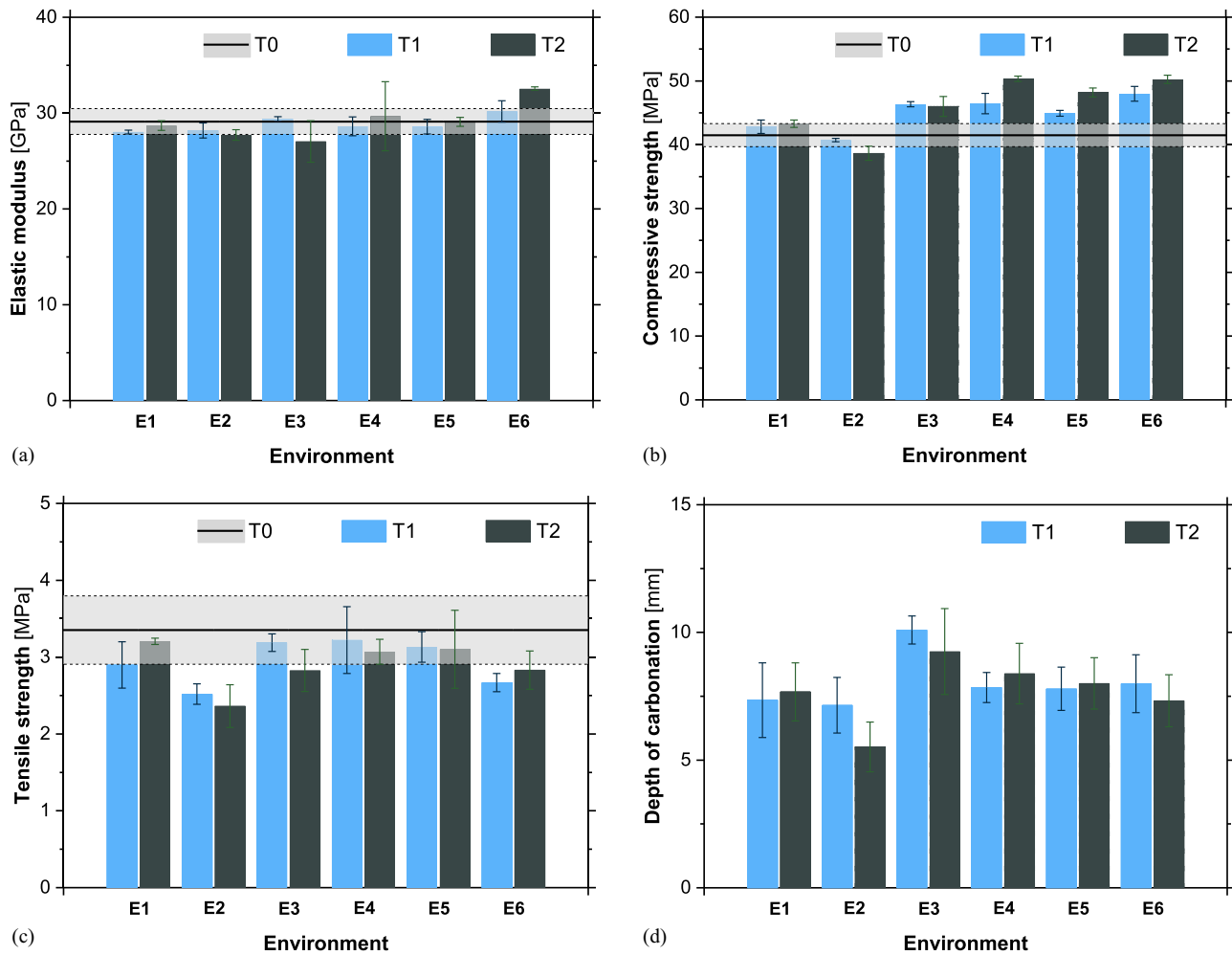
**Fig. 6.** Concrete properties: (a) elastic modulus; (b) compressive strength; (c) tensile strength; and (d) carbonation depth, after 1 (T1) and 2 (T2) years of exposure to the environment studied (E1 to E6), including the reference (T0).

**Table 3.** Mean values of the elastic modulus ($E_a$), tensile strength ($f_a$), and ultimate strain ($\varepsilon_a$) of the adhesive, after 1 (T1) and 2 (T2) years of exposure to the environment studied (E1 to E6), including the reference (T0)

| | $E_a$ (GPa) [CoV (%)] | | | $f_a$ (MPa) [CoV (%)] | | | $\varepsilon_a$ ($\times 10^{-3}$) [CoV (%)] | | |
|---|---|---|---|---|---|---|---|---|---|
| Environment | T0 | T1 | T2 | T0 | T1 | T2 | T0 | T1 | T2 |
| REF | 6.5 (3.0) | — | — | 19.9 (3.0) | — | — | 0.4 (6.2) | — | — |
| E1 | — | 6.6 (1.3) | 6.1 (1.4) | — | 19.5 (1.8) | 18.2 (2.8) | — | 0.4 (13.0) | 0.3 (11.6) |
| E2 | — | 1.9 (5.2) | 1.6 (4.0) | — | 7.2 (3.1) | 6.7 (2.7) | — | 1.1 (21.3) | 1.1 (11.9) |
| E3 | — | 6.7 (4.4) | 6.0 (5.4) | — | 19.9 (3.1) | 17.4 (5.3) | — | 0.3 (11.1) | 0.3 (19.1) |
| E4 | — | 7.2 (1.4) | 5.4 (6.9) | — | 20.1 (3.4) | 17.2 (4.3) | — | 0.3 (11.3) | 0.3 (12.8) |
| E5 | — | 7.5 (5.7) | 6.1 (5.0) | — | 21.9 (5.2) | 18.0 (3.6) | — | 0.3 (11.2) | 0.3 (13.1) |
| E6 | — | 6.2 (5.4) | 5.0 (10.0) | — | 17.7 (6.4) | 15.8 (4.3) | — | 0.3 (4.3) | 0.3 (12.9) |

Source: Data from Cruz et al. (2021).

probably a consequence of the high humidity of the environment E4 (Table 1).

**CFRP Strips**

Table 4 presents the tabulated results in terms of the mean values and corresponding CoV of CFRP strips elastic modulus ($E_f$), tensile strength ($f_f$), and ultimate strain ($\varepsilon_f$), for the times T0, T1, and T2, while in Fig. 8 a graphical representation of these parameters is shown.

An average elastic modulus of 164 GPa and an average tensile strength of 2,405 MPa were obtained for the unaged (T0) CFRP

strip specimens. These values are in agreement with the ones provided by the supplier. In general, for T1 and T2 times of testing (mainly at T1), higher values of the mechanical properties are observed than in T0, probably due to the post-curing phenomenon that may have overlapped the deleterious effects of the environmental degradation factors. According to Cabral-Fonseca (2008), the $T_g$ of the CFRP is ~85°C. Yet, considering that the CFRP material was exposed to direct sunlight, it is highly likely that the effective temperature in this material surpassed its $T_g$. In fact, considering the provisions included in Eurocode 1–Part 5 (IPQ 2009),
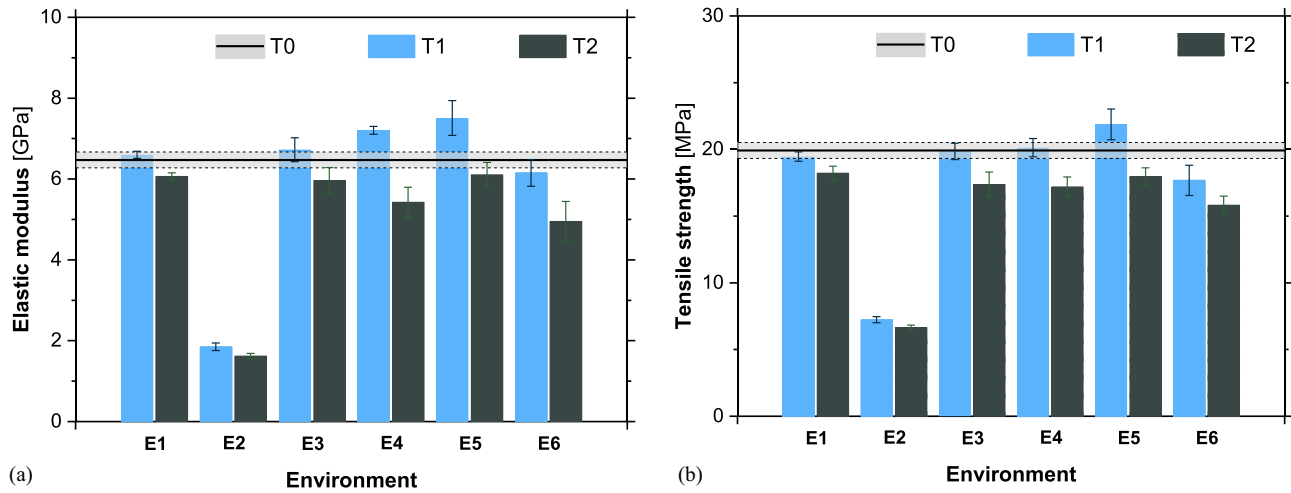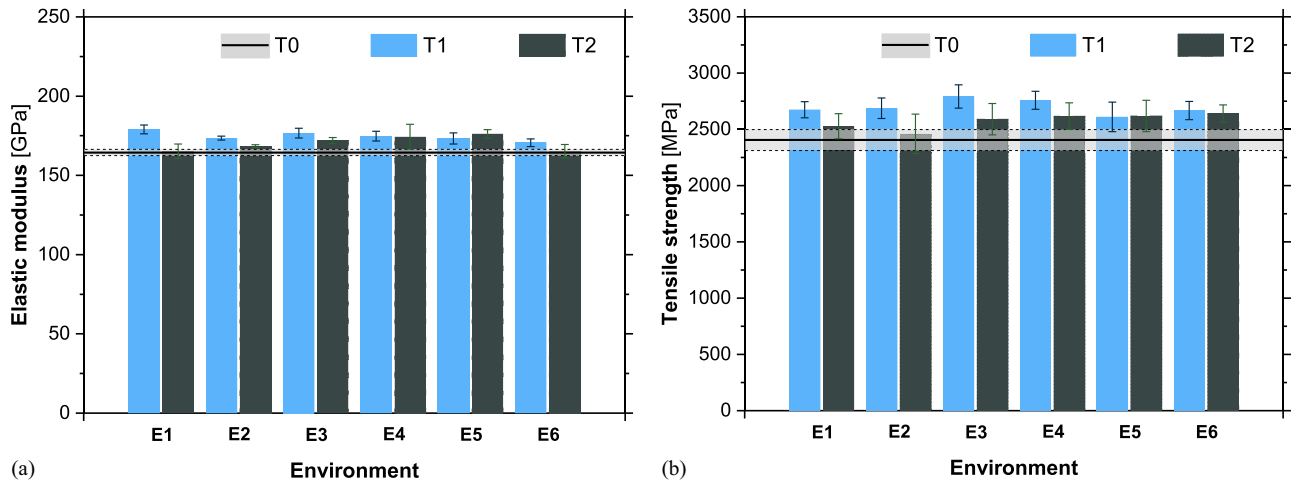
**Fig. 7.** Adhesive properties: (a) elastic modulus; and (b) tensile strength, after 1 (T1) and 2 (T2) years of exposure to the environment studied (E1 to E6), including the reference (T0).

**Table 4.** Mean values of the elastic modulus ($E_f$), tensile strength ($f_f$), and ultimate strain ($\varepsilon_f$) of the CFRP strips, after 1 (T1) and 2 (T2) years of exposure to the environment studied (E1 to E6), including the reference (T0)

| Environment | $E_f$ (GPa) [CoV (%)] | | | $f_f$ (MPa) [CoV (%)] | | | $\varepsilon_f$ (×10$^{-3}$) [CoV (%)] | | |
|---|---|---|---|---|---|---|---|---|---|
| | T0 | T1 | T2 | T0 | T1 | T2 | T0 | T1 | T2 |
| REF | 164 (1.2) | — | — | 2,405 (3.8) | — | — | 14.6 (3.8) | — | — |
| E1 | — | 179 (1.6) | 165 (2.7) | — | 2,674 (2.7) | 2,528 (4.4) | — | 14.9 (3.2) | 15.3 (6.1) |
| E2 | — | 174 (0.7) | 168 (0.5) | — | 2,688 (3.4) | 2,460 (7.1) | — | 15.5 (2.9) | 16.0 (12.5) |
| E3 | — | 177 (1.8) | 172 (1.1) | — | 2,792 (3.7) | 2,590 (5.4) | — | 15.8 (3.8) | 15.1 (5.1) |
| E4 | — | 175 (1.8) | 174 (4.5) | — | 2,758 (2.9) | 2,617 (4.5) | — | 15.8 (2.3) | 15.0 (4.5) |
| E5 | — | 173 (2.0) | 176 (1.5) | — | 2,611 (5.0) | 2,619 (5.3) | — | 15.1 (4.6) | 14.9 (5.2) |
| E6 | — | 171 (1.4) | 165 (4.2) | — | 2,667 (3.0) | 2,640 (2.9) | — | 15.6 (2.9) | 16.0 (1.9) |

Source: Data from Cruz et al. (2021).



**Fig. 8.** CFRP strips properties: (a) elastic modulus; and (b) tensile strength, after 1 (T1) and 2 (T2) years of exposure to the environment studied (E1 to E6), including the reference (T0). Results collected from Cruz et al. (2021).

when materials with a dark surface are exposed to relatively-high air temperatures (maximum of 46.2°C in E3) and direct sunlight, the temperature is expected to increase significantly (~88°C for the case of CFRP in E3). Regardless of the type of environmental exposure and duration, a minor variation on the mechanical performance of the CFRP strips was observed (considering the same period of exposure, a maximum difference of 6.0% was observed between the maximum and minimum value for the different environments). However, a tendency of decreasing in the mechanical properties from T1 to T2 is observed (an average value of 3.6% was verified and a maximum decrease of 9.3% was obtained in the E2 specimens from T1 to T2). This decrease (between T1

and T2) seems to be higher in the case of strength than in the case of elastic modulus. This decrease may be justified by the presence of humidity, supported by the results of environment E2. Contrary to T1, during T2 the post-curing phenomenon that could occur is probably not sufficient to overlap the deleterious effects of the environmental degradation factors.

### Pull-out Tests

Table 5 presents the main results in terms of the mean values and corresponding CoV of the pull-out tests of bond between NSM–CFRP-to-concrete after 1 (T1) and 2 (T2) years of environmental exposure, including the initial characterization (T0), where $K$ = initial stiffness, obtained from the slope of the linear fitting performed on the pull-out force versus loaded end slip ($F_l - s_l$) curves in the range 0 to 10 kN; $F_{max}$ = maximum pull-out force achieved during the test; and $s_{lmax}$ = loaded end slip at $F_{max}$. The observed failure modes are also included in Table 5, whereas Fig. 10 shows all the failure modes observed. Fig. 9(a) shows the typical responses in terms of the pullout force versus loaded end slip relationships ($F_l - s_l$), while in Figs. 9(b and c), the average $F_l - s_l$ per series are shown for the indoor and outdoor environments, respectively. Fig. 9(d) presents the evolution of the maximum pull-out force. Regarding the $F_l - s_l$, the typical shape observed in these curves presents mainly three components (Fernandes et al. 2015, 2018; Ricardo Cruz et al. 2020): (1) an ascending pre-peak branch, with a progressive decrease in stiffness due to the nonlinear behavior of the adhesive and increasing of damage in the laminate–adhesive interface until reaching the peak; (2) a descending post-peak branch due to the progressive increase of the damage previously referred; and (3) a branch where the force is almost constant until stopping the test, mainly governed by friction between the CFRP strip and concrete. Similar responses have been reported in previous works.

The failure modes were classified according to the following: (1) debonding failure at the interface between the CFRP laminate and adhesive (F/A); (2) cohesive failure in the adhesive (A); (3) adhesive failure at the interface between the adhesive and concrete (A/C); or (4) cohesive failure in concrete (C). In some cases, these failure modes included concrete cracking (CC) or concrete splitting (CS). In addition, one or more of the following damages could be also observed in the concrete splitting zone: cohesive failure of adhesive, adhesive cracking, failure of adhesive–concrete interface, or cohesive failure of concrete (Fig. 10).

The results obtained from the initial characterization (T0) are similar to the ones observed in previous works (Fernandes et al. 2018; Ricardo Cruz et al. 2020). For the adopted bond length (60 mm), the maximum pull-out force achieved corresponds to ~84% of the tensile strength of the CFRP strip. Failure with tensile rupture of the CFRP strip can be achieved if a bond length between 80 and 90 mm is adopted (Fernandes et al. 2015).

The initial stiffness ($K$) decreased within the first year of aging (from T0 to T1), whereas no significant variation could be observed between T1 and T2. During the test period (T0, T1, and T2), similar values of $F_{max}$ were observed for specimens exposed to E1 environment, whereas a decrease on $F_{max}$ was verified on E2 to E4 environments (especially in E2, with a decrease of 12.8% at T2). Small increases in $F_{max}$ were observed in E5 and E6 environments, particularly in E6 where it has increased 7.5% during the first year (T1). More complex failure modes were verified with the presence of high levels of humidity and with the increase in the time of exposure.

**Table 5.** Mean values of the initial stiffness ($K$), maximum pullout force ($F_{max}$) and corresponding loaded end slip ($s_{lmax}$) of pull-out tests of bond NSM–CFRP to concrete systems, after 1 (T1) and 2 (T2) years of exposure to the environment studied (E1 to E6), including the reference (T0)

| Env. | $K$ (kN/mm) [Cov (%)] | | | $F_{max}$ (kN) [Cov (%)] | | | $s_{lmax}$ (mm) [Cov (%)] | | | Failure mode | | |
|---|---|---|---|---|---|---|---|---|---|---|---|---|
| | T0 | T1 | T2 | T0 | T1 | T2 | T0 | T1 | T2 | T0 | T1 | T2 |
| REF | 141.5 (34.5) | — | — | 28.2 (2.5) | — | — | 0.54 (28.7) | — | — | F/A (3); F/A + CC (1) | — | — |
| E1 | — | 95.3 (6.6) | 104.8 (24.5) | — | 28.8 (1.9) | 28.0 (1.6) | — | 0.62 (3.6) | 0.56 (10.3) | — | F/A (2); F/A + CC (2) | F/A (3); F/A + CC (1) |
| E2 | — | 93.9 (13.8) | 111.1 (38.2) | — | 25.2 (1.1) | 24.6 (2.0) | — | 0.52 (6.3) | 0.49 (21.0) | — | A/C + CS (4) | F/A + CS (1); A + CS (1); A/C + CS (1); C + CS (1) |
| E3 | — | 128.5 (34.5) | 120.5 (27.3) | — | 27.7 (4.8) | 27.0 (3.0) | — | 0.56 (17.4) | 0.54 (8.6) | — | F/A (1); F/A + CC (2); F/A + CS (1) | F/A + CC (3); F/A + CS (1) |
| E4 | — | 95.0 (16.2) | 110.6 (17.0) | — | 27.7 (1.9) | 25.7 (3.6) | — | 0.62 (5.8) | 0.52 (6.3) | — | F/A + CS (4) | F/A + CC (2); F/A + CS (2) |
| E5 | — | 112.3 (33.3) | 110.3 (6.6) | — | 29.7 (1.1) | 28.1 (2.6) | — | 0.64 (10.4) | 0.57 (1.9) | — | F/A (1); F/A + CC (3) | F/A + CC (3); F/A + CS (1) |
| E6 | — | 113.2 (28.1) | 108.3 (4.8) | — | 30.5 (1.8) | 29.4 (4.8) | — | 0.63 (12.5) | 0.58 (13.4) | — | F/A + CC (3); F/A + CS (1) | F/A + CS (3) |

Failure modes: F/A = debonding failure at CFRP–adhesive interface; A/C = debonding failure at adhesive–concrete interface; C = cohesive failure of concrete; A = cohesive failure of adhesive; CC = concrete cracking; CS = concrete splitting.

Note: values between parentheses are the number of specimens where this failure mode occurred.
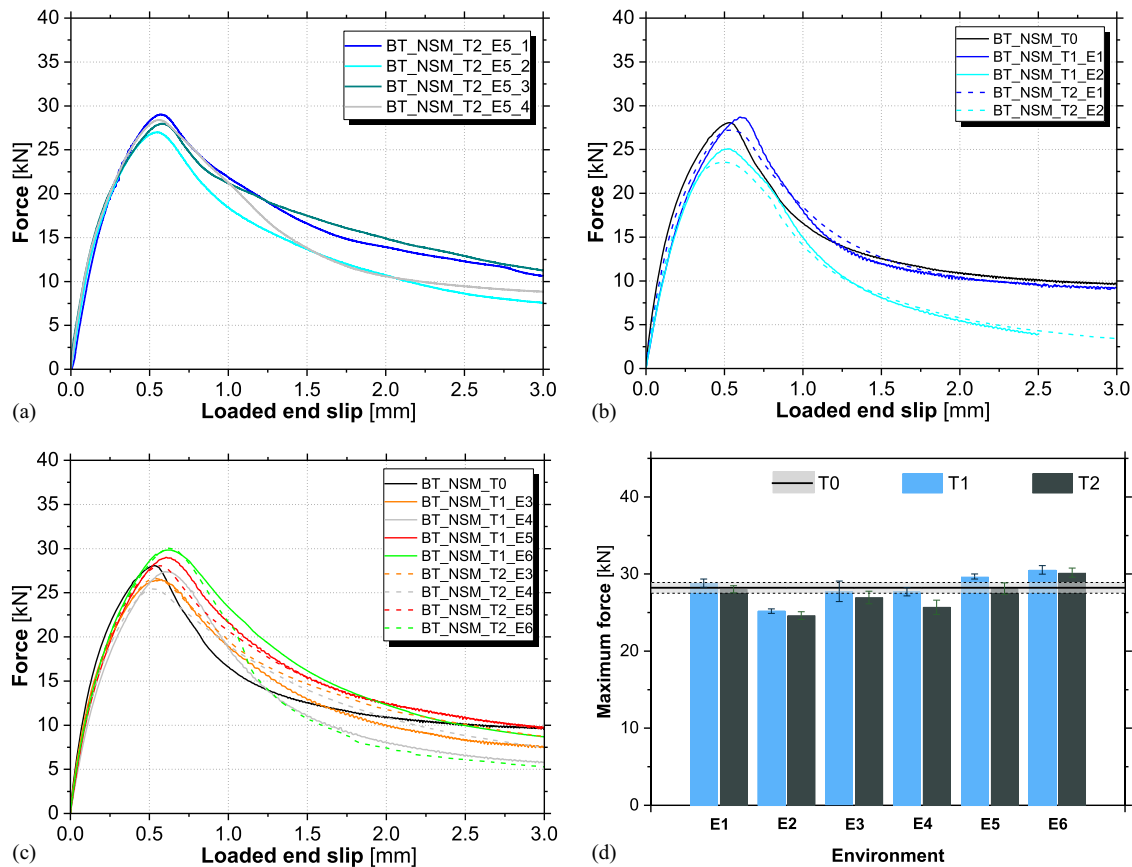
**Fig. 9.** Results of pull-out tests on bond NSM–CFRP to concrete: (a) force versus loaded end slip for E5 specimens after 2 (T2) years of exposure; (b) force versus loaded end slip (average curves of four specimens in each environment) for laboratory environments; (c) force versus loaded end slip for outdoor environments; and (d) maximum force after 1 (T1) and 2 (T2) years of exposure to the environment studied (E1 to E6), including the reference (T0).

**Effect of the Environmental Condition**

Regardless of the environment, the initial stiffness ($K$) decreased with aging. This observation was also reported by Fernandes et al. (2018), where the reduction of the adhesion strength at the laminate–adhesive interface was considered as the main cause. In general, debonding failure at the interface between the CFRP laminate and adhesive (F/A) was the dominant failure mode (except in environment E2). Therefore, regardless of the environment, the laminate–adhesive interface has a relevant role in the NSM bond system. In addition, taking into account the results obtained for the epoxy adhesive (Table 3; Fig. 7), no direct relationship can be established between the initial stiffness of the NSM system and tensile properties of the epoxy adhesive. This observation is evident particularly in the case of the E2 environment, where the elastic modulus of the epoxy adhesive decreased ∼75%, after 2 years of exposure (T2), and the corresponding reduction of the initial stiffness of the pull-out specimens was close to 21%.

Negligible variations in specimens of environment E1 were observed after 1 (T1) and 2 (T2) years of exposure, as they present similar $F_l - s_l$ curves, $F_{max}$, and failure modes. Comparing all environments, water immersion (E2) led to the highest decrease in $F_{max}$ (around 12% at T1 and T2, when compared with reference E1). In general, $s_{lmax}$ is directly proportional to $F_{max}$; therefore, the lowest $s_{lmax}$ values were also observed in E2 specimens. As mentioned, the E2 environment also led to the greatest degradation of the mechanical properties of involved materials, namely concrete, epoxy, and CFRP strips, which means that the decrease in the mechanical properties of the involving materials might lead to a

reduction in the strength of bond NSM–CFRP to concrete system. However, the exposure to water immersion led to a higher decrease at the material level (∼63% on the tensile strength of the adhesive and ∼25% on tensile strength of concrete, after 2 years) than with the NSM system (reduction of ∼12% on bond strength, after 2 years). This supports that the resisting mechanisms of the NSM technique do not directly depend on the individual mechanical performance of each corresponding material but from synergic effects. A dominant failure mode could not be seen in environment E2. Instead, a wider range of failure modes was observed (Table 5), showing higher degradation at the interfaces between adhesive and concrete. As stated by De Lorenzis and Teng (2007), the effectiveness of the NSM–CFRP-to-concrete system significantly depends on the mechanical properties of superficial concrete, which is normally the most degraded part. Consequently, the mentioned reduction at the material level led not only to the failure at the adhesive–concrete interface but also to cohesive failure in the concrete and adhesive.

The outdoor environments have shown no significant $F_{max}$ variations within the 2 years of aging. Comparing the reference E1 at both T1 and T2 times of testing with the specimens of outdoor environments (E3 to E6), a decrease of $F_{max}$ was verified in E3 and E4, with its highest reduction in E4 specimens at T2 (8.2%). On the contrary, a $F_{max}$ increase was obtained in E5 and E6, and the highest increase was observed on E6 specimens at T1 (5.9%). It can be argued that freeze–thaw cycles observed on E4 during the winter season are the principal degradation agent of the NSM bond system. These results do not preclude the existence or importance of the other degradation agents such as carbonation (E3),
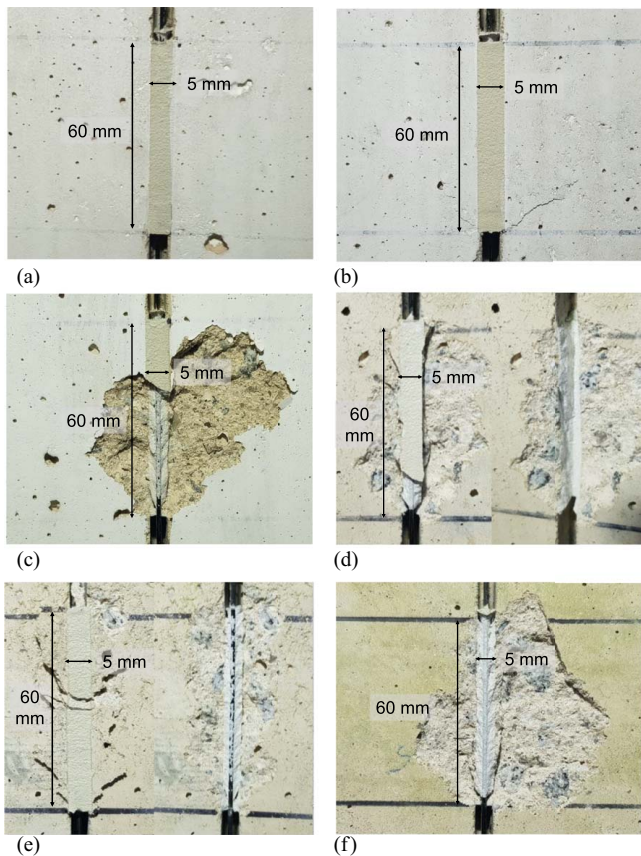
**Fig. 10.** Failure modes observed in pull-out tests of bond NSM–CFRP to concrete specimens: (a) debonding failure at CFRP laminate–adhesive interface (F/A); (b) debonding failure at CFRP laminate–adhesive interface with concrete cracking (F/A + CC); (c) debonding failure at CFRP laminate–adhesive interface with concrete splitting (F/A + CS); (d) cohesive failure in the adhesive with concrete splitting (A + CS); (e) debonding failure at adhesive–concrete interface with concrete splitting (A/C + CS); and (f) cohesive failure in the concrete with concrete splitting (C + CS).

elevated temperatures (E5), or chloride exposure (E6). However, it should be noted that all outdoor environments have several similarities (daily and seasonal hygro-thermal variations, UV radiation) and, therefore, the differences in the $F_{max}$ did not diverge greatly from each other. Moreover, the $F_{max}$ follows a resembling trend in all four outdoor environments, namely, it decreases from T1 to T2. In the outdoor environments, although the dominant failure mode remained F/A, it was typically coupled with concrete cracking (CC) or concrete splitting (CS). Furthermore, despite the weakest link of the bond between the CFRP strips and concrete continuing to be the laminate–adhesive interface, a higher concrete degradation was observed in all the outdoor environments.

**Effect of Time of Exposure**

A general decrease in the initial stiffness ($K$) was observed from T0 to T1, whereas between T1 and T2, $K$ continued to decrease but solely on environments E1, E2, and E4.

Under controlled conditions of the E1 environment, $F_{max}$ was similar at T0, T1, and T2 (a maximum variation of 2.8% was observed). Also, specimens exposed to this environment presented always the same failure mode (F/A). The environment E2 presented the greatest reduction on $F_{max}$ after one (~10.6%) and two

(~12.8%) years when compared with T0. However, when T1 and T2 are compared, a small variation (2.5%) was observed. Nevertheless, the exposure time was an important factor in environment E2, since significant differences were observed in terms of failure modes. In fact, within the second year of aging, cohesive failure at the adhesive and concrete was also observed, while in the first year, specimens failed mainly by adhesive failure at the interface between the adhesive and concrete. Over the aging period, some outdoor environments showed a decrease of $F_{max}$ (E3 and E4), whereas others showed an increase on the same property (E5 and E6). Nevertheless, all outdoor environments showed a reduction (~4.7%) on the maximum bond strength from the first year (T1) to the second year (T2). This reduction, greatest in E4 (~7.2%), indicates that time is a relevant factor in the degradation of the NSM bond system, as longer exposure periods can yield to higher degradation and, consequently, lower $F_{max}$. Finally, a remark on the failure modes at both test periods should be mentioned, as cracking in the concrete (CC) and concrete splitting (CS) become more evident from T1 to T2.

## Laboratory-Accelerated Conditioning versus Real-Time Field Conditioning and Design Guidelines

With the aim of establishing comparisons between laboratory-accelerated conditioning and real-time field conditioning, a database was created, composed of results from artificial laboratory-accelerated conditioning tests collected from the existing literature. Therefore, this database included results from pull-out tests of bond NSM–CFRP to concrete, with the following characteristics:

1. Number of test specimens: 48 pull-out tests from four research works, namely Sena-Cruz et al. (2012); Al-Mahmoud and Mechling (2014); Fernandes et al. (2018); Garzón-Roca et al. (2015);
2. Type of FRP: CFRP strips;
3. Test configuration: direct pull-out test and beam pull-out test;
4. Types of environmental conditions: freeze–thaw cycles, wet–dry cycles, temperature cycles, immersion in salt water, immersion in tap water, moisture and splash exposure;
5. Periods of exposure: up to 18,000 h (~2 years).

Preliminary analyses of the database and several attempts of establishing correlations in terms of bond strength retention between each individual accelerated-environmental condition (typically adopted in durability studies) and the real-time field conditioning environments studied in this work were carried out. However, due to the significant dispersion of the results and the reduced number of test data, no specific correlations could be found. Therefore, the graph in Fig. 11(a) includes the bond strength-retention values, with the time of all the results included in the database gathered. This graph also includes the results of the laboratory-accelerated conditioning tests (E2) and the results of real-time field conditioning (E3 to E6) carried out in this work. Despite the dispersion, it seems that there is a trend of a slight decrease in the bond strength retention with time, in both types of test protocols (real-time field conditioning and laboratory-accelerated conditioning). In addition, up to ~18,000 h, laboratory-accelerated conditioning tests yield similar average values of the retention (0.99) when compared with real-time field conditioning (1.00). However, when only retention values lower than 1.0 are considered, an average bond strength retention equal to 0.92 (CoV = 5.3%) and 0.95 (CoV = 3.8%) are obtained, respectively, for laboratory-accelerated conditioning and real-time field conditioning (E3 to E6).
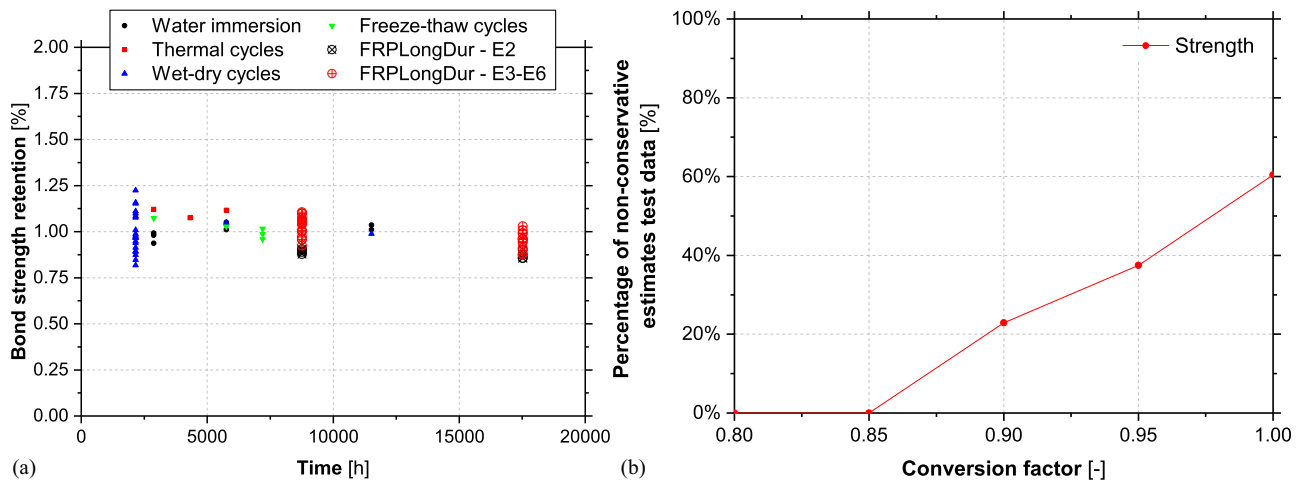
**Fig. 11.** Accelerated conditioning tests protocols versus real-time field conditioning on NSM: (a) retention values; and (b) percentage of non-conservatively estimated data points as a function of the conversion factor.

Fig. 11(b) presents the relationship between the percentage of nonconservative estimates test results from the bond NSM–CFRP to concrete database established (percentage of the cases where the adopted conversion factor is not conservative) and the corresponding conversion factor; in this study, only values of retention lower than 1.0 were considered. A conversion factor of 0.85 should be adopted for ensuring that the nonconservative estimates do not exceed 10%. In the work developed by Cruz et al. (2021), conversion factors of 0.85 and 0.55 were proposed for CFRP strips and epoxy adhesives, respectively, for outdoor applications. Comparing the conversion factor proposed in this study (0.85) with the values of conversion factors proposed by Cruz et al. (2021) for the CFRP strips (0.85) and epoxy adhesives (0.55), it can be concluded that the degradation of the bond system is similar to the degradation of the CFRP strip and lower than the degradation obtained for the case of the epoxy adhesive. The reason for this is related to the governing resisting mechanisms of the NSM–CFRP strips strengthening technique (Sena Cruz and de Barros 2004).

Guidelines such as CAN/CSA-S6-06 (CSA 2006), ACI 440.2R-17 (ACI 2017), or CNR DT 200 R1 (CNR 2013) include provisions to account for the durability aspects of FRP strengthening systems. However, specific provisions for the design of NSM–CFRP to concrete systems are included only in the CAN/CSA-S6-06 and ACI 440.2R-17. Generally, the service life prediction counting for the durability aspects is considered by means of the environmental conversion factors ($C_E$ for the case of ACI 440.2R-17; $\eta_a$ for the case of CNR DT 200 R1; CAN/CSA-S6-06 does not explicitly use environmental conversion factors), that reduces the ultimate tensile strain of the FRP material and does not account for the bond-strength reduction that can occur from the environmental exposure. In the case of flexural strengthening with NSM systems, the ACI 440.2R-17 proposes an environmental conversion factor of 0.85, for exterior or aggressive environmental conditions, when epoxy/carbon systems are used. Nevertheless, for calculating the FRP development length, a design bond strength value ($\tau_b$) of 6.9 MPa is provided. However, this approach does account for the different types of environmental conditions and, consequently, different levels of bond strength durability. As demonstrated in this work, the bond durability is affected by the type of conditioning and, therefore, this standard may need to be improved, where a value of 0.85 is suggested for the reduction of the bond NSM strength. Moreover, it should be highlighted that the environmental conversion factors proposed in ACI 440.2R-17 and CNR DT 200 R1 are not dependent on the type of strengthening system (e.g., EBR or NSM). Furthermore, from a formal point of view, the durability effects should be considered in the provisions for determining the nominal strengths (e.g., flexural strength, shear strength, or bond strength).

## Conclusions

This investigation addressed the durability of the bond of NSM–CFRP-to-concrete systems under real-time field conditioning conditions. Four natural outdoor environments (E3 to E6) were adopted for inducing aging mainly by carbonation (E3), freeze–thaw attack (E4), elevated temperatures (E5), and airborne chlorides from seawater (E6). A control (reference) environment (E1) and water immersion environment (E2), both under controlled hygrothermal and hydrothermal conditions, respectively, were also included in this work. The evolution of mechanical properties of the specimens was characterized along the time, namely at an early stage (T0) and after 1 (T1) and 2 (T2) years of exposure. A comparison between the results of real-time field conditioning tests developed in the scope of this work and results of laboratory-accelerated conditioning tests from the existing literature was also performed. Therefore, from the work carried out, the following conclusions can be stated:

1. When comparing with T0, after 1 and 2 years of exposure, the concrete compressive strength increased (except in E2), mainly in outdoor environments (up to +21%). Small variations were observed for elastic modulus (in between −7.8% and +12.0%);
2. The tensile strength of the superficial concrete decreased after 1 and 2 years of aging when compared with T0. The highest reduction in the tensile strength was observed in E2 specimens (∼30%), probably due to the fact that the specimens were tested saturated, while in the other exposures environments the reduction was about 12%;
3. Higher levels of carbonation depth were observed for outdoor environments when compared with laboratory environments. As expected, the highest carbonation depth was attained in E3 specimens, due to the presence of high levels of $CO_2$ concentration in this environment. While at T1, an increase in the carbonation depth was observed for all the outdoor environments, between T1 and T2, small variations were registered. The restrictions in terms of mobility imposed by COVID-19 pandemic may have a relevant role for these results.

4. Small variations on the epoxy tensile properties were verified for all the environments (excluding E2). The highest increase was obtained in E5 specimens at T1 ($E_a$ increased ~15% and $F_a$ increased ~10% in comparison with T0). The highest reduction on the tensile properties was observed in E2 specimens at T2 (~75% in $E_a$ in comparison with T0);

5. In general, the mechanical properties of the CFRP strips increased at T1 and T2 times of testing, in comparison with T0. The maximum tensile strength increase was registered for E3 between T0 and T1. Minor variations without statistical significance were observed when the effect of environmental exposure was considered;

6. From the pull-out tests of the unaged (T0) specimens, a maximum average tensile stress in the CFRP strip of 2,014.3 MPa was obtained, which corresponds to ~84% of its tensile strength. Immersion in water (environment E2) caused the highest reduction in the maximum tensile stress in the CFRP strip (~12% at both T1 and T2). Regarding the outdoor environments, the highest decrease in the maximum tensile stress in the CFRP strip was verified in E4 specimens at T2 (8.2%) whereas the highest increase was obtained in E6 specimens at T1 (5.9%);

7. Failure at the laminate–adhesive interface was observed in almost all the pull-out tests. The type and time of exposure seems to affect the observed failure modes. Debonding at the laminate–adhesive interface was the main failure mode observed in the majority of the pull-out tests. However, the type and time of exposure seems to affect the failure modes. Therefore, in the specimens expose to outdoor environments, the complexity of the failure modes has also increased from mostly adhesive at the laminate–adhesive interface to adhesive at the laminate–adhesive interface with concrete splitting;

8. Despite the dispersion of results, for similar periods of exposure, real-time field conditioning tests yielded to similar values of bond strength retention than the ones registered in laboratory-accelerated conditioning tests.

9. Assuming that laboratory-accelerated conditioning tests constitute an upper bound of real-time field conditioning and based on the database collected from the existing literature, a bond strength retention of 0.85 is suggested for the case of exterior or aggressive environmental conditions for NSM–CFRP to concrete systems.

Finally, regardless of the relevant outputs presented in this investigation, particularly in terms of durability of the bond of NSM–CFRP-to-concrete systems under real-time field conditioning, the attempts to establish relationships between accelerated and real-time field conditioning test conditions are not consistent, as the amount of results is small. Nevertheless, it may be possible to establish better relationships if longer periods of exposure to real-time field conditioning are implemented and more tests were conducted. This should be pursued in future research works.

## Data Availability Statement

Some or all data, models, or code that support the findings of this study are available from the corresponding author upon reasonable request (tests results of concrete, epoxy, CFRP strip, and pullout tests).

## Acknowledgments

## References

ACI (American Concrete Institute). 2017. *Guide for the design and construction of externally bonded FRP systems for strengthening concrete structures*. ACI 440.2R-17. Farmington Hills, MI: ACI.

Al-Mahmoud, F., and J.-M. Mechling. 2014. "Bond strength of different strengthening systems – concrete elements under freeze–thaw cycles and salt water immersion exposure." *Constr. Build. Mater.* 70: 399–409. https://doi.org/10.1016/j.conbuildmat.2014.07.039.

Al-Tamimi, A. K., R. A. Hawileh, J. A. Abdalla, H. A. Rasheed, and R. Al-Mahaidi. 2015. "Durability of the bond between CFRP plates and concrete exposed to harsh environments." *J. Mater. Civ. Eng.* 27 (9): 04014252. https://doi.org/10.1061/(ASCE)MT.1943-5533.0001226.

Ashraf, W. 2016. "Carbonation of cement-based materials: Challenges and opportunities." *Constr. Build. Mater.* 120: 558–570. https://doi.org/10.1016/j.conbuildmat.2016.05.080.

ASTM. 1988. *Standard practice for developing accelerated tests to aid prediction of the service life of building components and materials (withdrawn 2005)*. ASTM E632-82. West Conshohocken, PA: ASTM.

Bhashya, V., S. S. Kumar, R. Gopal, B. H. Bharatkumar, T. S. Krishnamoorthy, Nagesh, and N. R. Iyer. 2015. "Long term studies on FRP strengthened concrete specimens." *Indian J. Eng. Mater. Sci.* 22 (4): 465–472.

Bouzoubaâ, N. B., A. B. Bilodeau, B. T. Tamtsia, and S. F. Foo. 2010. "Carbonation of fly ash concrete: Laboratory and field data." *Can. J. Civ. Eng.* 37 (12): 1535–1549. https://doi.org/10.1139/L10-081.

BSI (British Standards Institution). 1999. *Products and systems for the protection and repair of concrete structures – Test methods – Measurement of bond strength by pull-off*. EN 1542. London: BSI.

Cabral-Fonseca, S. 2008. "Durabilidade de materiais compósitos de matriz polimérica reforçados com fibras usados na reabilitação de estruturas de betão." Ph.D. thesis, Dept. of Polymer Engineering, Univ. of Minho.

Cabral-Fonseca, S., J. R. Correia, J. Custódio, H. M. Silva, A. M. Machado, and J. Sousa. 2018. "Durability of FRP - concrete bonded joints in structural rehabilitation: A review." *Int. J. Adhes. Adhes.* 83: 153–167. https://doi.org/10.1016/j.ijadhadh.2018.02.014.

CEN (European Committee for Standardization). 2000. *Concrete — Part 1: Specification, performance, production and conformity*. EN 206-1. Brussels, Belgium: CEN.

CERF (Civil Engineering Research Foundation). 2001. *Gap analysis for durability of fiber reinforced polymer composites in civil infrastructure*. Reston, VA: CERF.

CNR (National Research Council). 2013. *Guide for the design and construction of externally bonded FRP systems for strengthening existing structures*. Advisory Committee on Technical Recommendations for Construction. CNR-DT 200 R1/2013. Rome: CNR.

Coelho, M. R. F., J. M. Sena-Cruz, and L. A. C. Neves. 2015. "A review on the bond behavior of FRP NSM systems in concrete." *Constr. Build. Mater.* 93: 1157–1169. https://doi.org/10.1016/j.conbuildmat.2015.05.010.

Correia, L., T. Teixeira, J. Michels, J. A. P. P. Almeida, and J. Sena-Cruz. 2015. "Flexural behaviour of RC slabs strengthened with prestressed CFRP strips using different anchorage systems." *Composites, Part B* 81: 158–170. https://doi.org/10.1016/j.compositesb.2015.07.011.

Cromwell, J. R., K. A. Harries, and B. M. Shahrooz. 2011. "Environmental durability of externally bonded FRP materials intended for repair of concrete structures." *Constr. Build. Mater.* 25 (5): 2528–2539. https://doi.org/10.1016/j.conbuildmat.2010.11.096.

Cruz, R., L. Correia, A. Dushimimana, S. Cabral-Fonseca, and J. Sena-Cruz. 2021. "Durability of epoxy adhesives and carbon fibre reinforced polymer laminates used in strengthening systems: Accelerated ageing versus natural ageing." *Materials* 14 (6): 1533. https://doi.org/10.3390/ma14061533.

CSA (Canadian Standard Association). 2006. *Canadian highway bridge design code*. CAN/CSA-S6-06. Toronto: CSA.

De Lorenzis, L., and J. G. Teng. 2007. "Near-surface mounted FRP reinforcement: An emerging technique for strengthening structures." *Composites, Part B* 38 (2): 119–143. https://doi.org/10.1016/j.compositesb.2006.08.003.

El-Hacha, R., and M. El-Badry. 2001. "Strengthening concrete beams with externally prestressed carbon fiber composite cables." In *Proc., 5th Int. Conf. on Fiber Reinforced Polymers for Reinforced Concrete Structures*. London: Thomas Telford Ltd.

Fernandes, P., J. Sena-Cruz, J. Xavier, P. Silva, E. Pereira, and J. Cruz. 2018. "Durability of bond in NSM CFRP-concrete systems under different environmental conditions." *Composites, Part B* 138: 19–34. https://doi.org/10.1016/j.compositesb.2017.11.022.

Fernandes, P. M. G., P. M. Silva, and J. Sena-Cruz. 2015. "Bond and flexural behavior of concrete elements strengthened with NSM CFRP laminate strips under fatigue loading." *Eng. Struct.* 84: 350–361. https://doi.org/10.1016/j.engstruct.2014.11.039.

FIB (Fédération Internationale du Béton). 1983. *Durability of concrete structures*. CEB - RILEM International Workshop. Final Rep. Copenhagen, Denmark: FIB.

FIB (Fédération Internationale du Béton). 2019. *Externally applied FRP reinforcement for concrete structures*. Fib Bulletin 90. Copenhagen, Denmark: FIB.

Frigione, M., and M. Lettieri. 2018. "Durability issues and challenges for material advancements in FRP employed in the construction industry." *Polymers* 10 (3): 247. https://doi.org/10.3390/polym10030247.

Garzón-Roca, J., J. M. Sena-Cruz, P. Fernandes, and J. Xavier. 2015. "Effect of wet–dry cycles on the bond behaviour of concrete elements strengthened with NSM CFRP laminate strips." *Compos. Struct.* 132: 331–340. https://doi.org/10.1016/j.compstruct.2015.05.053.

Hassan, S. A., M. Gholami, Y. S. Ismail, and A. R. M. Sam. 2015. "Characteristics of concrete/CFRP bonding system under natural tropical climate." *Constr. Build. Mater.* 77: 297–306. https://doi.org/10.1016/j.conbuildmat.2014.12.055.

Hsieh, C.-T., Y. Lin, and S.-K. Lin. 2017. "Impact-echo method for the deterioration evaluation of near-surface mounted CFRP strengthening under outdoor exposure conditions." *Mater. Struct.* 50 (1): 72. https://doi.org/10.1617/s11527-016-0944-z.

IPQ (Instituto Português da Qualidade). 1992. *Design of concrete structures - Part 1-1: General rules and rules for buildings*. EN 1992-1-1. Eurocode 2. Caparica, Portugal: IPQ.

IPQ (Instituto Português da Qualidade). 2009. *Actions on structures – Part 1–5: General actions – Thermalactions*. EN 1991-1-5. Eurocode 1. Caparica, Portugal: IPQ.

IPQ (Instituto Português da Qualidade). 2011. *Testing hardened concrete. Part 3: Compressive strength of test specimen*. EN 12390-3. Caparica, Portugal: IPQ.

IPQ (Instituto Português da Qualidade). 2013. *Testing hardened concrete. Part 13: Determination of secant modulus of elasticity in compression*. EN 12390-13. Caparica, Portugal: IPQ.

ISO. 2009. *Plastics—Determination of tensile properties. Part 5: Test conditions for unidirectional fibre-reinforced plastic composites*. ISO 527-5. Genève: ISO.

ISO. 2012. *Plastics—Determination of tensile properties. Part 2: Test conditions for moulding and extrusion plastics*. ISO 527-2. Genève: ISO.

Jin, L., X. Du, and G. Ma. 2012. "Macroscopic effective moduli and tensile strength of saturated concrete." *Cem. Concr. Res.* 42 (12): 1590–1600. https://doi.org/10.1016/j.cemconres.2012.09.012.

Kabir, M. I., R. Shrestha, and B. Samali. 2016. "Effects of applied environmental conditions on the pull-out strengths of CFRP-concrete bond." *Constr. Build. Mater.* 114: 817–830. https://doi.org/10.1016/j.conbuildmat.2016.03.195.

LNEC (National Laboratory for Civil Engineering). 1993. *Concrete – determination of carbonation resistance*. E391-1993. Lisboa, Portugal: LNEC.

Mi, Z., Y. Hu, Q. Li, and Z. An. 2018. "Effect of curing humidity on the fracture properties of concrete." *Constr. Build. Mater.* 169: 403–413. https://doi.org/10.1016/j.conbuildmat.2018.03.025.

Mohd Hashim, M. H., A. R. Mohd Sam, and M. Hussin. 2016. "Experimental investigation on the effect of natural tropical weather on interfacial bonding performance of CFRP-concrete bonding system." *J. Eng. Sci. Technol.* 11 (4): 584–604.

Otieno, M., J. Ikotun, and Y. Ballim. 2020. "Experimental investigations on the effect of concrete quality, exposure conditions and duration of initial moist curing on carbonation rate in concretes exposed to urban, inland environment." *Constr. Build. Mater.* 246: 118443. https://doi.org/10.1016/j.conbuildmat.2020.118443.

Peng, H., Y. Liu, C. S. Cai, J. Yu, and J. Zhang. 2019. "Experimental investigation of bond between near-surface-mounted CFRP strips and concrete under freeze-thawing cycling." *J. Aerosp. Eng.* 32 (1). https://doi.org/10.1061/(ASCE)AS.1943-5525.0000937.

Ricardo Cruz, J., J. Sena-Cruz, M. Rezazadeh, S. Serega, E. Pereira, A. Kwiecień, and B. Zając. 2020. "Bond behaviour of NSM CFRP laminate strip systems in concrete using stiff and flexible adhesives." *Compos. Struct.* 245: 112369. https://doi.org/10.1016/j.compstruct.2020.112369.

Rozsypalová, I., P. Daněk, and O. Karel. 2018. "The bond strength by pull-off and direct tensile strength of concrete damaged by elevated temperatures." *IOP Conf. Ser.: Mater. Sci. Eng.* 385: 012047. https://doi.org/10.1088/1757-899X/385/1/012047.

Sen, R. 2015. "Developments in the durability of FRP-concrete bond." *Constr. Build. Mater.* 78: 112–125. https://doi.org/10.1016/j.conbuildmat.2014.12.106.

Sena-Cruz, J., P. Fernandes, P. Silva, J. Xavier, J. Barros, and M. R. F. Coelho. 2012. "Bond behaviour of concrete elements strengthened with NSM CFRP laminate strips under wet–dry cycles." In *Proc., Bond in Concrete*, 1023–1030. Brescia, Italy: Manerbio.

Sena Cruz, J. M., and J. A. O. de Barros. 2004. "Bond between near-surface mounted carbon-fiber-reinforced polymer laminate strips and concrete." *J. Compos. Constr.* 8 (6): 519–527. https://doi.org/10.1061/(ASCE)1090-0268(2004)8:6(519).

Silva, P., P. Fernandes, J. Sena-Cruz, J. Xavier, F. Castro, D. Soares, and V. Carneiro. 2016. "Effects of different environmental conditions on the mechanical characteristics of a structural epoxy." *Composites, Part B* 88: 55–63. https://doi.org/10.1016/j.compositesb.2015.10.036.

Sousa, J. M., J. R. Correia, and S. Cabral-Fonseca. 2018. "Durability of an epoxy adhesive used in civil structural applications." *Constr. Build. Mater.* 161: 618–633. https://doi.org/10.1016/j.conbuildmat.2017.11.168.

S&P. 2014. *CFRP laminates*. Technical Datasheet. Seewen, Switzerland: S&P.

S&P. 2015. *Resin epoxy adhesive*. S&P 220. Technical Data Sheet. Seewen, Switzerland: S&P.

Tatar, J., and H. R. Hamilton. 2016. "Comparison of laboratory and field environmental conditioning on FRP-concrete bond durability." *Constr. Build. Mater.* 122: 525–536. https://doi.org/10.1016/j.conbuildmat.2016.06.074.

Tatar, J., and S. Milev. 2021. "Durability of externally bonded fiber-reinforced polymer composites in concrete structures: A critical review." *Polymers* 13 (5): 765. https://doi.org/10.3390/polym13050765.

Zhang, G., C. Li, H. Wei, M. Wang, Z. Yang, and Y. Gu. 2020. "Influence of humidity on the elastic modulus and axis compressive strength of concrete in a water environment." *Materials* 13 (24): 5696. https://doi.org/10.3390/ma13245696.

Zhou, J.-k., and N. Ding. 2014. "Moisture effect on compressive behavior of concrete under dynamic loading." *J. Cent. South Univ.* 21 (12): 4714–4722. https://doi.org/10.1007/s11771-014-2481-7.

# Paper 4

**TITLE:** DURABILITY OF BOND OF EBR CFRP LAMINATES TO CONCRETE UNDER REAL-TIME FIELD EXPOSURE AND LABORATORY ACCELERATED AGEING

**REFERENCE:**

Cruz, R., Correia, L., Cabral-Fonseca, S., and Sena-Cruz, J. 2022. Durability of bond of EBR CFRP laminates to concrete under real-time field exposure and laboratory accelerated ageing. Submitted to *Construction and Building Materials* in 05-10-2022.

# Durability of bond of EBR CFRP laminates to concrete under real-time field exposure and laboratory accelerated ageing

Ricardo Cruz[1], Luís Correia[2], Susana Cabral-Fonseca[3] and José Sena-Cruz[4*]

[1]PhD Student, Univ. of Minho, ISISE/IB-S, Depart. of Civil Engineering, Guimarães, Portugal

[2]Postdoctoral Researcher, Univ. of Minho, ISISE/IB-S, Depart. of Civil Engineering, Guimarães, Portugal

[3]Research Officer, National Laboratory of Civil Engineering, Materials Department, Lisbon, Portugal

[4]Associate Professor, Univ. of Minho, ISISE/IB-S, Department of Civil Engineering, Guimarães, Portugal

[*]Corresponding author (email: jsena@civil.uminho.pt; Tel. +351 253 510 200).

## ABSTRACT

The durability of bond between carbon fibre-reinforced polymer (CFRP) laminates and concrete with the externally bonded reinforcement (EBR) technique was investigated under real-time field exposure (RTFE) and accelerated ageing. The experimental program includes four outdoor environments inducing carbonation, freeze-thaw attack, extreme temperatures, and airborne chlorides from ocean. A laboratory environment (20 ℃/55% RH) was used as reference. Additionally, a water-immersion environment (20 ℃) was considered. The study comprises mainly the evaluation of durability of bond between EBR-CFRP laminates and concrete over two years. The maximum pullout force varied between -4.3% and +16.2% under RTFE whereas on water-immersed specimens, the maximum pullout force decreased ∼8%.

**Keywords:** durability; bond; EBR; real-time field exposure; laboratory accelerated aging; CFRP laminate; epoxy adhesive; concrete.

## 1. INTRODUCTION

The application of the externally bonded reinforcement (EBR) technique using carbon fibre-reinforced polymer (CFRP) materials for strengthening of reinforced concrete (RC) structures has become a widespread practice, especially over the last two decades. With the EBR technique, CFRP laminates or sheets are externally bonded to the tensile surface of the RC element, as a solution for flexural and/or shear strengthening. EBR with CFRP sheets has been also used for confining RC columns and joints. Epoxy adhesives are usually used as the bonding agent. Given the relevance of these strengthening techniques, several codes, e.g. ACI 440.2R-17 [1], CAN/CSA-S6-06 [2] include provisions for its design, while future ones, e.g. prEN 1992-1-1 [3] plan to include them.

The durability aspects of RC structures strengthened with CFRP systems have been investigated mainly at laboratory employing accelerated conditioning protocols (ACPs), whereas the investigations under real-time field exposure in outdoor environments are very scarce. Therefore, it represents an important lack of knowledge. Furthermore, the relationship between the effects of laboratory accelerated aging and real-time field exposure is another critical issue in the literature and needs to be better understood, e. g., [4, 5]. From the existing research, some studies only address the durability under real-time field exposure, and others include both types of exposure and attempt to correlate the effects of laboratory accelerated aging *versus* real-time field exposure. Ambiguous results concerning the relationship between field exposure and laboratory aging on FRP composites have been reported [6]. Some researchers have reported higher degradation in laboratory accelerated aging than in field exposure, e.g., [5, 7] while others have observed higher degradation under field exposure, e.g., [8-10].

A clear knowledge on the durability and long-term behaviour of the bond between EBR-CFRP laminates and concrete is essential for the long-term design of this strengthening system, as the bond assures the stress transfer between the strengthening system and the concrete substrate. The lack of consistent knowledge of these systems has been mentioned as a critical obstacle to the extensive use of these systems/materials in civil engineering applications, e.g. [11]. Additionally, up to now, design codes addressing the particular case of the durability of bond of EBR-FRP in RC structures are not available, and therefore, it represents an additional difficulty for the use of these systems; nevertheless, there are various design guidelines developed in different countries [6]. It should be highlighted that the short-term behaviour of the EBR-CFRP to concrete system has already been widely investigated, e. g. [12-15].

Several investigations addressing the durability of the materials that compose the EBR-CFRP to concrete systems (CFRP laminate, adhesive, and concrete) have been conducted. Moisture, thermal variations, UV radiation exposure, and chemical attacks are the most important environmental degradation factors which affect these materials, acting individually or combined. Nevertheless, the EBR-CFRP to concrete bond system is a complex multilayer system composed also by the corresponding interfaces between these three materials. Therefore, the assessment of the durability of the bonded joints became a complex process, as it is not so simple as studying the durability of each one of the system components separately [6]. The bonded joint is generally the highest critical aspect that affects the system efficiency [16]. According to Tatar and Milev [6], exposure to moisture has been reported, in general, as the most detrimental degradation factor for adhesion properties. The following works provide relevant investigations on the durability of EBR-CFRP to concrete system

Kabir et al. [17] developed an investigation on the time-dependent behaviour of bond between EBR-CFRP strips (made by wet lay-up with two plies of CFRP sheet) and concrete under three environments: (i) temperature cycles (5 hours at a constant temperature of 40 ℃ followed by 7 hours at gradual decrease to 30 ℃); (ii) wet-dry cycles (one week at around 95% RH and 30-32 ℃ followed by one week at normal lab condition at 20-23 ℃) and (iii) outdoor environment of Sydney, Australia, for up to 18 months. The authors used a single-lap shear test to evaluate the bond strength of control (unexposed) and exposed specimens and concluded that the maximum bond strength degradation (15.2%) was observed in the outdoor environment, which was attributed to the degradation of epoxy mechanical properties. Temperature cycles led to a non-significant deterioration, probably due to the lower range of cyclic temperatures applied (30-40 ℃), which were set below the glass transition temperature ($T_g$) of epoxy resin ($T_g = 47$ ℃). Wet-dry cycles led to a minimal deterioration of the bond strength of EBR-CFRP to concrete (maximum reduction of ~5% after one year of exposure). The failure modes changed in the case of wet-dry cycles (from thick concrete to very thin concrete layer attached to the FRP) and outdoor exposure (from thick layer of concrete to almost no concrete attached to debonded FRP), but not with thermal cycles (thick layer of concrete attached to the epoxy adhesive of the debonded FRP). The effective bond length increased due to exposure to all environments.

Hassan et al. [18] studied the bond behaviour of EBR-CFRP laminates to concrete system under various environmental conditions based on the natural tropical climate of Malaysia (extremely hot/wet environment). Double lap concrete-CFRP joints were prepared and then subjected to diverse types of exposure, including: (i) outdoor exposure under Malaysia's natural tropical climate

(the temperature and relative humidity varied between 23–35 ℃ and 60–95%, respectively); (ii) wet/dry cycles in plain water (24 cycles); (iii) wet/dry cycles (24 cycles) in salt water and, (iv) laboratory condition (with relative humidity between 75–90% and room temperature of 25–32 ℃), up to 6 months. After exposure, the double-lap shear tests were performed to investigate the bonding characteristics in detail. The results showed that the average bond strength degradation was minor (~2.1%) after exposure for 6 months to tropical outdoor conditions and even increased with wet/dry cycles in plain water and wet/dry cycles in salt water (average increase of ~6.7%).

Mohd Hashim et al. [19] investigated the effect of exposure to natural tropical climate on the interfacial bonding performance of EBR-CFRP to concrete system. Concrete prisms with two CFRP laminate strips bonded on opposite sides were exposed for 3, 6, and 9 months under (i) laboratory conditions, (ii) natural tropical climate exposure, (iii) wet-dry cycles (3 days wet followed by 4 days dry – 1 cycle/week) with 3.5% saltwater solution at room temperature and at 40 ℃ and, (iv) dual exposure composed by wet-dry cycles (room temperature and 40 ℃) with 3.5% saltwater solution followed by tropical climate exposure (3 days wet/4 days dry at laboratory followed by 7 days of tropical climate exposure – each cycle lasted 2 weeks). The results demonstrated that the combination of climate effects can improve the curing of the bonded joints and therefore leading to a better performance. Therefore, the bonding system was only slightly affected by the exposure to tropical climate/salt solution. No specific trend of bond strength evolution along the testing times (3, 6 and 9 months) was observed.

From the works previously described, it can be concluded that is not clear the comparison between the levels of aggressivity caused by laboratory *versus* real-time filed exposure. It should be stated

that with the laboratory accelerated aging protocols it is impossible to reproduce all the environmental degradation factors that act under real-time field exposure (natural). Additionally, the real-time field exposure requires longer test periods to extract valuable results of degradation in the system. Many authors have tried to establish comparisons between the effects caused by both types of aging, e. g. [10, 17-19]. Nevertheless, in several cases, the matrix of environmental degradation factors/times of exposure established by the authors are not adequate to directly compare the effects of both aging types (natural and artificial accelerated in laboratory). Despite such difficulties, it is of paramount relevance to develop real-time field exposure tests, as only these type of tests can provide effective knowledge on the real degradation mechanisms [10].

Existing guidelines accounts for the deleterious effects of environmental exposure. While codes e.g. ACI 440.2R-17 [1] and CNR-DT 200 R1/2013 [20] consider explicitly these durability effects through environmental conversion factors (also known as reduction factors), other codes only refer the need of considering durability effects, e.g. CAN/CSA-S6-06 [2], AASHTO FRPS-1 [21], ISIS Design Manual 4 [22], JSCE CES41 [23] and TR55 [24].

Considering the aforementioned statements, various gaps in the knowledge of durability of the EBR CFRP to concrete systems need to be investigated, mainly: (i) the performance of these systems under different real-time field exposure environments and ageing periods; and (ii) the relationship between the effects of real-time field exposure and laboratory accelerated aging. Thus, this investigation aims at studying of the durability of a EBR bonding system by means of an experimental work, which includes exposure to four outdoor environments for real-time field exposure (natural aging mainly by carbonation, freeze-thaw attack, extreme temperatures, and

6

airborne chlorides from the ocean) for up to two years. A reference (control) environment (20 ºC/55% RH) and a water immersion environment under controlled temperature (20 ºC) were also considered. The specimens were tested at three timepoints of aging: after production (T0) and after one (T1) and two (T2) years of exposure. A database composed of results of laboratory accelerated conditioning tests collected from the literature was created and compared with the results of real-time field exposure from this work. Finally, new insights in predicting the service life of the EBR-CFRP to concrete systems and suggestions for improving the existing guidelines, such as ACI 440.2R-17 [1] and CNR-DT 200 R1/2013 [20] were also developed.

## 2. EXPERIMENTAL PROGRAM, CONSTITUTIVE MATERIALS, AND METHODS

### 2.1 Experimental Program

This work presents the durability assessment of the bond between EBR-CFRP laminates and concrete and is linked with the investigation of Cruz et al. [25], where the durability of epoxy adhesives and CFRP laminates were studied. Both works were performed in the scope of the FRPLongDur project, which further details are presented in Cruz et al. [25]. For the easier comparison between the results of the involved materials on the EBR-CFRP to concrete system and the durability of the system itself, this work also includes a selection of relevant results (epoxy adhesive and CFRP laminate) of Cruz et al. [25].

The specimens were exposed to a total of six environments, including: two laboratory environments and four outdoor environments. Fig. 1 presents the relevant characteristics of these six environments and their geographical location. The laboratory environments included a

7

(i) reference/control (E1 environment) – controlled hygrothermal conditions (20 ℃/55% RH) and (ii) immersion in fresh water (E2 environment) with controlled temperature (20 ℃). The four real-time field exposure (outdoor/natural) environments were considered giving the specific characteristics that can be found in Portugal to achieve specific conditioning effects, namely: (iii) high levels of concrete carbonation (E3 environment), due to the elevated levels of concentration of anthropogenic $CO_2$ in this location, which is near to a highway with high traffic load and is also close to the International Airport of Lisbon; (iv) freeze-thaw attack (E4 environment), since specimens were installed in the highest mountain of Portugal ('Serra da Estrela'); (v) extreme service temperatures and lower values of relative humidity (E5 environment), characteristics of the climate of Elvas; and, (vi) high levels of airborne chlorides from sea water in the air and high relative humidity (E6 environment), since the test specimens were placed nearby to the Atlantic Ocean, in the coast of Viana do Castelo.
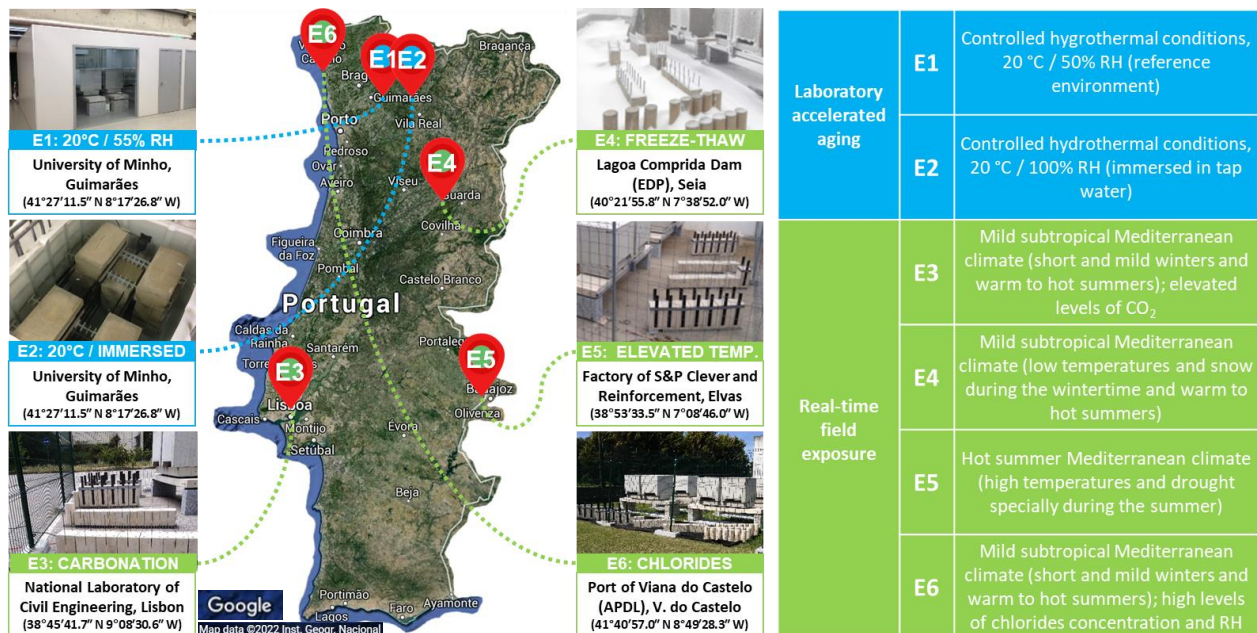


**Fig. 1.** Environments considered in this investigation. (Base map © Google, Map data ©2022 Inst.

Geogr. Nacional; Images by authors.)

The air temperature and relative humidity were continuously monitored at each location (technical details of these sensors can be found in Cruz et al. [25]). Fig. 2 shows the diary average temperatures and relative humidity recorded between 2018 and 2020 in each experimental station.
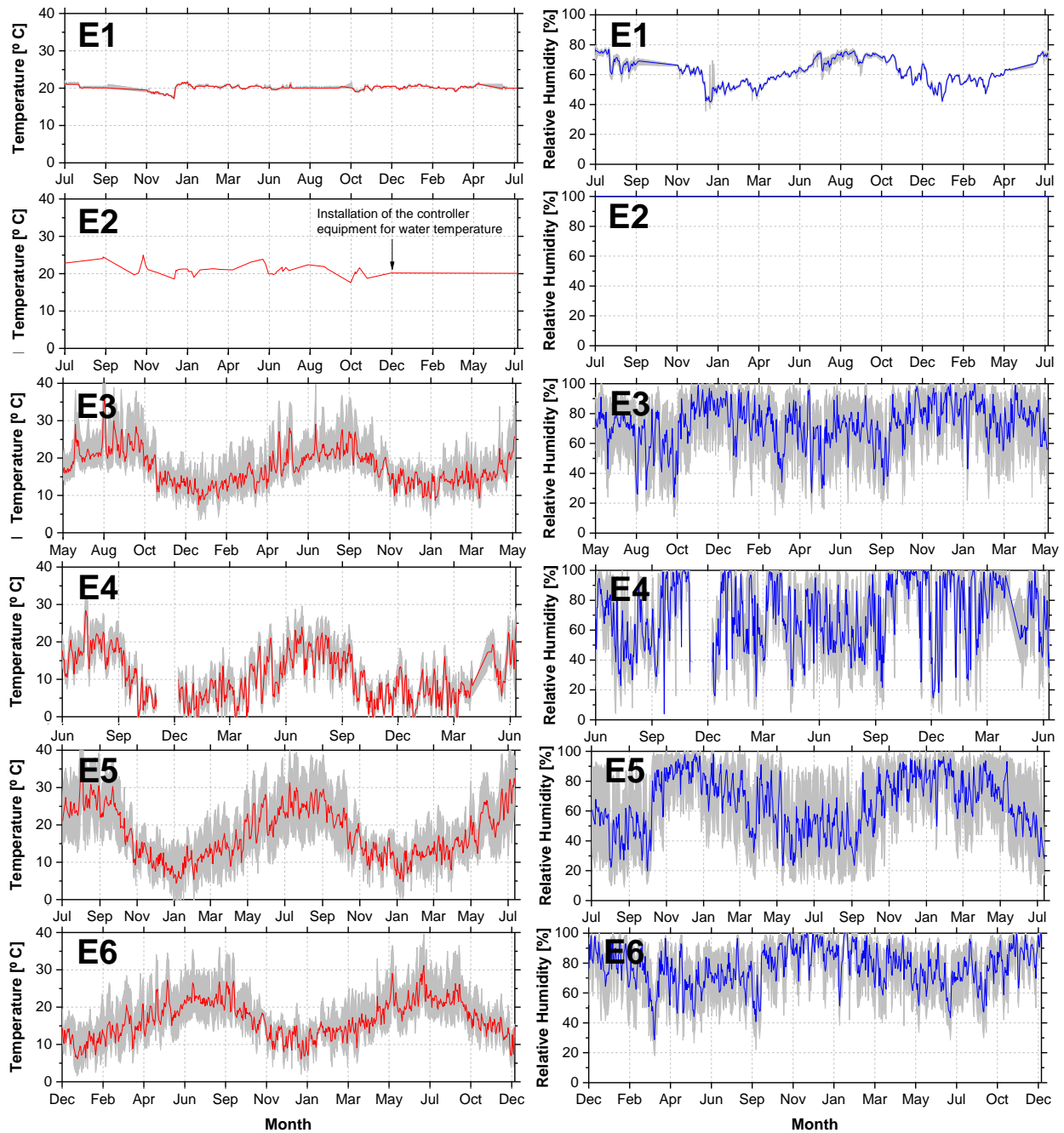
Notes: For each environment is presented the daily mean values (line) and the envelope extreme minimum and maximum values (grey line); E2: A controller equipment for the temperature of the water was installed on the experimental station in December 2019, setting the temperature at 20 ºC; E4 and E5: values provided by IPMA (IPMA's station is located 9 km apart from E4 and 560 m apart from E5).

**Fig. 2.** Air temperature and relative humidity recorded in the environments.

A timeline with the main steps developed in this work is presented in Fig. 3. Specimens were produced and then stored in the laboratory premises (~15 months) before the exposure to the

10

abovementioned environments. During this period, an experimental campaign (T0) was performed to evaluate the initial mechanical properties. The determination of the tensile properties of the CFRP laminates was performed when it arrived from the producer company (March 2017) whereas the mechanical characterization of the epoxy adhesive was performed 7 days after the production of specimens (curing age typically used for epoxy adhesives). The elastic modulus and compressive strength of concrete were evaluated 28 days after casting (December 2016), whereas its tensile strength was only assessed at ~2 years of age (October 2018), due to technical issues. The bond characterization on EBR-CFRP to concrete specimens was performed 8 months after the strengthening application (October 2017). The ageing of the bond specimens and material samples started in between June and December of 2018. It should be highlighted that in real-time field exposure (E3 to E6 environments), all bond specimens used the same orientation: one CFRP laminate positioned to sunrise direction and other to the sunset to get the maximum solar exposure.
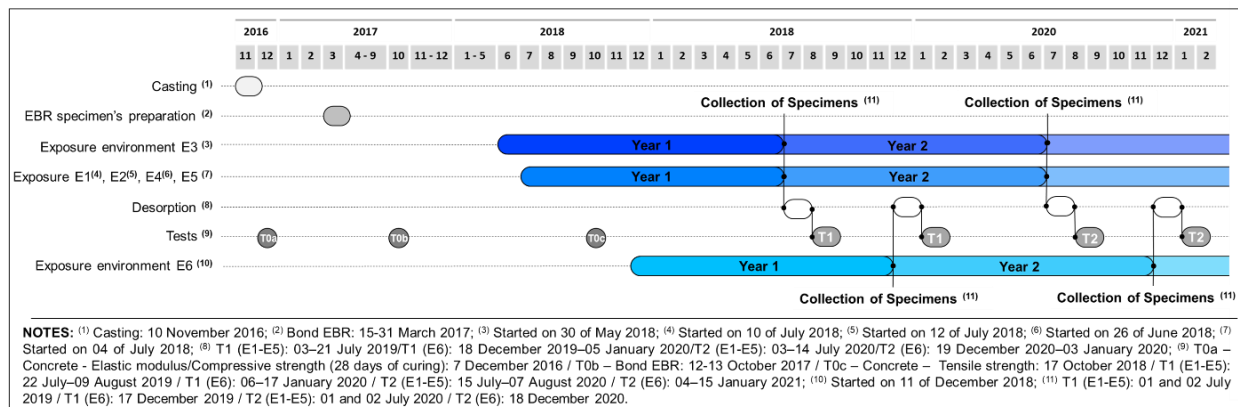


**Fig. 3.** Timeframe of the work carried out.

A set of materials samples and bond specimens were taken every year from each experimental station to be characterized at the laboratory, after one (T1) and two (T2) years of exposure. Each

set was composed by CFRP laminate strips, epoxy adhesive specimens, concrete cylinders, and EBR-CFRP to concrete bond specimens. After collecting these specimens, a desorption period of three weeks prior to the tests was adopted. This desorption phase was adopted to avoid the effect of punctual and instantaneous high level of humidity (e.g., rain) that the specimens may faced at the moment of their collecting. The desorption was achieved by placing the collected specimens inside a climatic chamber, with the E1 hygrothermal conditions. E1 specimens were kept under the same laboratory conditions during this period, while E2 specimens (immersed in water) were also kept fully immersed until testing. This protocol was adopted in both T1 and T2 times.

## 2.2 Materials

This section presents a detailed characterization of the involved materials used in this work, namely the CFRP laminate, epoxy adhesive and concrete.

### 2.2.1  CFRP laminate

A CFRP laminate prefabricated by pultrusion and composed by unidirectional carbon fibres (fibre content higher than 68%) and by a vinyl ester resin matrix was adopted in this work. This CFRP laminate has a black and smooth external surface. The rectangular cross-section geometry is 50 mm wide by 1.2 mm thick. It should be mentioned that this type of cross-section geometry is commonly used in EBR-CFRP strengthening applications. According to the technical datasheet provided by the supplier [26], this CFRP has a characteristic elastic modulus greater than 170 GPa and a characteristic tensile strength higher than 2000 MPa.

*2.2.2   Adhesive*

A commercial cold curing epoxy adhesive was adopted as bonding agent to fix the CFRP laminate to concrete. Based on the previous work [25], this epoxy adhesive presents a tensile strength of ~20 MPa, an elastic modulus of ~6.5 GPa (both mean tensile properties after 7 days of curing at 20 ℃) and a $T_g$ of 46.2 ℃ (after 7 days of curing at 23 ℃). Furthermore, according to the datasheet provided by the supplier [27], the adhesive's flexural elastic modulus is higher than 7.1 GPa. Further details regarding the characteristics of this epoxy adhesive used can also be found in Cruz et al. [25].

*2.2.3   Concrete*

A single batch of a concrete was used to cast all the specimens: (i) cylinders for compression tests, and (ii) prisms for bond EBR-CFRP to concrete specimens. The later specimens were also used to assess to the concrete's tensile properties and its carbonation depth. For that purpose, a ready-mix concrete was ordered with the following characteristics: standard cylinder compressive characteristic strength of 30 MPa (37 MPa in standard cube), exposure class XC4(P) (cyclic wet and dry), water/cement ratio (CL) of 0.40, maximum aggregate size of 12.5 mm, slump class S4 (Eurocode 2 [3]/EN 206-1 [28])

**2.3 Test Methods**

Different methods were adopted depending on the material/property to be evaluated on both unaged (reference/control) and aged specimens.

13

### 2.3.1   CFRP laminate and adhesive

The elastic modulus ($E_a$ and $E_f$) and tensile strength ($f_a$ and $f_f$) of the epoxy adhesive and CFRP laminate were assessed following the ISO 527-2:2012 [29] and ISO 527-5:2009 [30], respectively. Per stage (T0, T1 and T2) and environment (E1-E6), at least five epoxy specimens and six CFRP laminates were tested. Additional information regarding other physical and mechanical properties assessed are detailed in Cruz et al. [25].

### 2.3.2   Concrete

The elastic modulus ($E_{cm}$) and compressive strength ($f_{cm}$) of concrete were assessed using cylinders of 150/300 mm (diameter/height), according to NP EN 12390-13:2013 [31] and NP EN 12390-3:2011 [32] standards, respectively. The initial characterization (T0 tests) was conducted 28 days after casting, using 4 specimens (see Fig. 3). After one and two (T1/T2) years of conditioning, 3 specimens per environment were tested.

The tensile strength of the concrete ($f_{ctm}$) was determined by means of pull-off tests conducted on the bottom face (perpendicular to the cast direction) of concrete prisms according to EN 1542:1999 [33] standard. For each environment (E1-E6) and time of testing (T0, T1 and T2), four tests (two per concrete prism) were performed. The tests were conducted using a machine Matest E142, with a capacity of 16 kN (maximum pull-off force), accuracy of 1% and resolution of 10 N. These tests were carried out with a loading rate of 1 MPa/s and using a dolly of 50 mm diameter.

The carbonation depth of concrete was determined according to LNEC E391:1993 [34] standard. The method is based on the pH reduction that occurs on the carbonated concrete caused by the $CO_2$

14

of the atmosphere. A solution of phenolphthalein indicator was used to measure the carbonation depth. This solution becomes pink in contact with basic (alkaline) concrete (pH higher than 9) while continues transparent at lower levels of pH. This characterization was conducted after one and two (T1 and T2) years of conditioning but not on the initial characterization (T0). Two samples of concrete of 50/100 mm (diameter/height) were extracted from the concrete prisms per environment and testing time.

### 2.3.3 EBR-CFRP to concrete bond tests

Fig. 4 presents the geometry of bond EBR-CFRP to concrete specimens and the corresponding single-lap shear test configuration. Concrete prisms of 400 mm × 200 mm × 200 mm were adopted with two CFRP laminates (of 50 mm × 1.2 mm cross-section) bonded in each opposite face of the concrete prism and parallel to the casting direction, according to the EBR technique (2 laminates/prism). Prior the CFRP application, the concrete surface was prepared using sand blast method. A bond length of 220 mm was adopted, remaining 100 mm free (unbonded) from the extremity of the concrete prism to avoid premature failure by concrete rip off at the loaded end. The adopted bond length (220 mm) is higher than the theoretical effective length ($l_e$) equal to 101 mm according to the CNR-DT 200 R1/2013 [20]. The tests were conducted with the specimens installed horizontally on a steel plate with 70 mm × 300 mm × 550 mm (Support 1), fixed to a stiff testing steel closed frame system. Other steel plate (Support 2) was designed to ensure negligible horizontal displacements in the loading direction. A prismatic steel bar (Support 3) was placed in the rear top part of the specimen to minimize vertical displacements. The tests were performed using a servo-controlled equipment. The applied force ($F$) was measured through a load cell with a maximum load carrying capacity of 200 kN (linearity error of 0.05% F.S.), installed between the

actuator and the grip used to pull the CFRP strip. The relative displacement between the CFRP and the concrete (slip) at the loaded end section ($s_l$) and free end section ($s_f$) was measured using two linear variable displacement transducers (LVDTs), LVDT1 and LVDT2 respectively, with a stroke of ±10 mm (linearity error of 0.24% F.S.). The tests were performed under displacement control at the loaded end through LVDT1 with a rate of 0.12 mm/min. For each environment (E1-E6) and testing time (T0, T1 and T2), 4 tests were performed (see Fig. 3).



(a)                                                                                          (b)
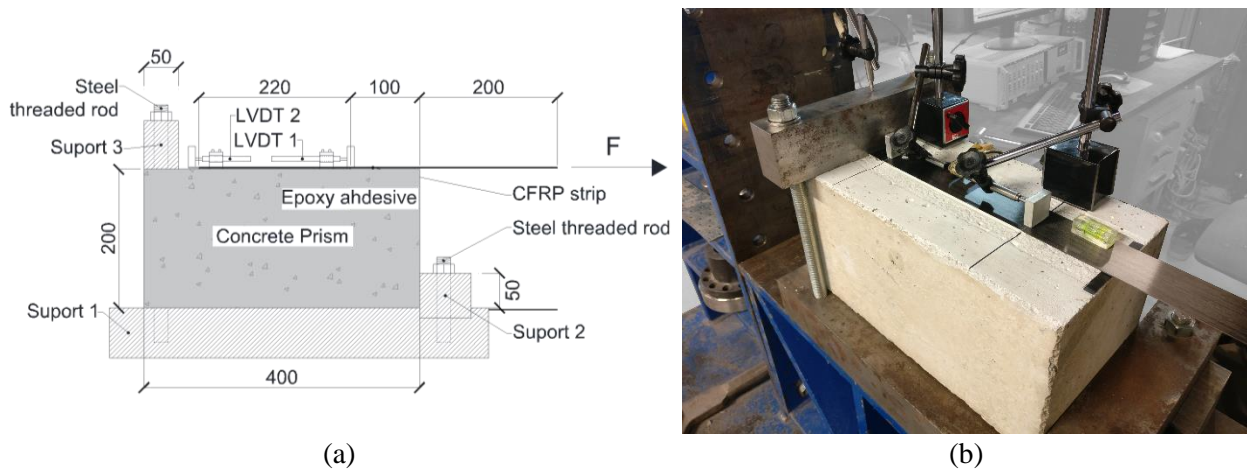
**Fig. 4.** Pull-out shear test of bond EBR-CFRP to concrete: (a) specimen's geometry and test configuration and (b) photograph of the test. Note: All units in [mm].

## 3. RESULTS AND DISCUSSION

### 3.1 Materials

The results obtained from the evaluation of the mechanical properties of the materials alongside the time are presented and discussed in this section. In this publication, the values of the material's mechanical properties are presented graphically. The detailed presentation of the nominal values are available elsewhere [25].

*3.2.1   CFRP laminate*

Fig. 5 shows the average values of elastic modulus ($E_f$) and tensile strength ($f_f$) obtained for the CFRP laminates at times T0, T1 and T2.
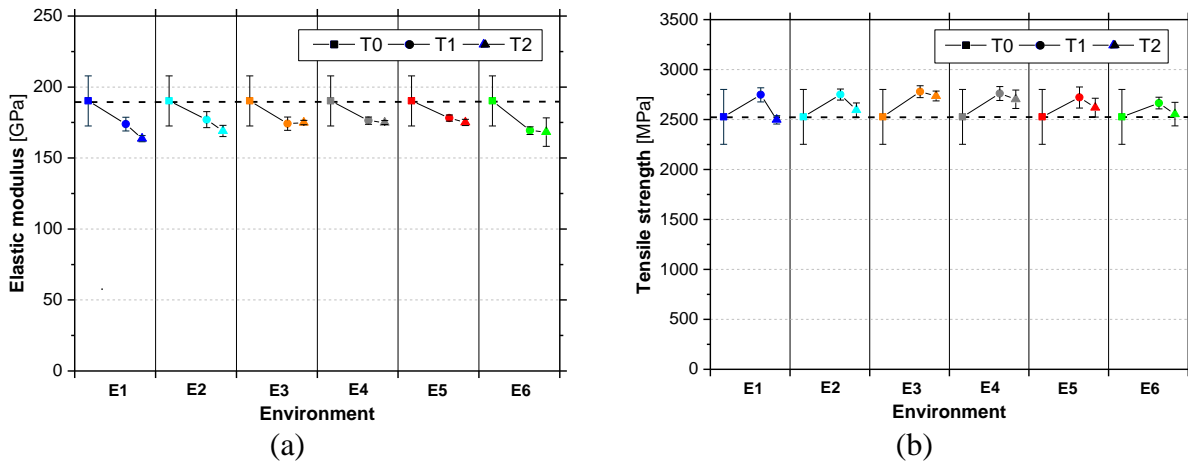


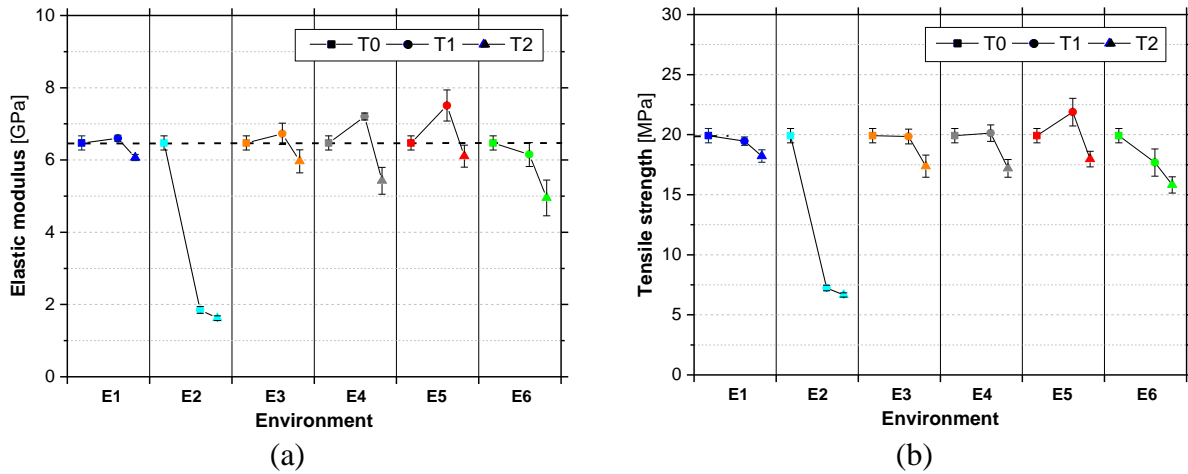**Fig. 5.** CFRP laminate tensile properties: (a) elastic modulus and (b) tensile strength at the initial characterization (T0) and after one and two years (T1/T2) of exposure to environments E1-E6. Source: Data from Cruz et al. [25].

In the initial characterization (T0) of the CFRP laminate, an elastic modulus ($E_f$) of 190 GPa (CoV = 9.3%) and a tensile strength ($f_f$) of 2527 MPa (CoV = 10.8%) were obtained. These values fit with the characterization published by the CFRP producer [26]. Regardless of the type of exposure and duration, small variations on the tensile mechanical properties of the CFRP laminate were observed, particularly on the elastic modulus with a tendency of decreasing with the time. Between T0 and T1, in all environments, a decrease in the elastic modulus was observed, which was statistically significant according to the ANOVA test. The maximum p-value of the 6 series (T0 against the each one of the 6 environments of T1) was 0.004 (p-value < 0.05 it means that the mean results differ significantly between series). This decreased continued for the second year of exposure (between T1 and T2) for specimens exposed to laboratory environments, but not for the

real-time field specimens, which showed an almost negligible variation. A general increase in tensile strength was observed in the period T0-T1 (significant statistic differences between mean values were verified according to the ANOVA test – maximum p-value = 0.007) whereas in the period T1-T2, a decrease in all the environments was observed, especially in specimens of laboratory environments. The increase observed in the period T0-T1 can be a consequence of the matrix post-curing phenomenon that may occurred in the CFRP laminate from the sun exposure, since this material presents a dark surface which leads to elevated temperatures inside the material (higher than the air temperature). Therefore, it is probable that the detrimental effects of the environmental degradation factors have been balanced by the post-curing during the first year of exposure. The general decrease on the tensile mechanical properties of the CFRP in the period T1-T2 seems percentual higher in tensile strength than in elastic modulus, as also observed by Fernandes et al. [10]. This finding can be attributed to the environmental degradation factors that acted on the CFRP laminate in T1-T2. On the contrary to T1, during T2, the post-curing phenomenon that could occur is probably not sufficient to overcome the environmental degradation factors. Finally, it should be highlighted that the evolution of the mechanical properties along time are very similar, regardless the type of exposure.

*3.2.2   Adhesive*

Fig. 6 shows the average values of the elastic modulus ($E_a$) and tensile strength ($f_a$) obtained in the epoxy adhesive at times T0, T1 and T2.

**Fig. 6.** Adhesive tensile properties: (a) elastic modulus and (b) tensile strength at the initial characterization (T0) and after one and two years (T1/T2) of exposure to environments E1-E6. Source: Data from Cruz et al. [25].

In the initial characterization (T0), an elastic modulus ($E_a$) of 6.5 GPa and a tensile strength ($f_a$) of 19.9 MPa were obtained. Excluding E2, between T0 and T1, the tensile properties of the epoxy adhesive have shown small variations (the highest increase was observed in E5 environment – $E_a$ increased ~15% and $f_a$ increased ~10 %, when compared with T0). These improvements can be explained by the post-curing that may faced during the first year due to the temperature exposure to the sun. The tensile properties of the adhesive specimens exposed to E2 drastically decreased (up to 75% in $E_a$). The difference in $E_a$ and $f_a$ is between T0 and T1 for E2 specimens is statistically significant by performing a variance analysis ANOVA test. This finding can be related also with testing specimens in a saturated state (without desorption phase). From the existing literature, e.g. [16, 35], the incorporation of water by the epoxy adhesives can cause swelling and plasticization, yielding to the reduction of the $E_a$ and $F_a$. Between T1 and T2, a general reduction on the tensile properties was observed (maximum $f_a$ reduction was registered in the E5 environment – 17.8% while the maximum $E_a$ reduction was registered in the E4 environment – 25.0%). The high humidity recorded in E4 experimental station (see Fig. 2) is probably the main cause for the

19

reduction observed in the $E_a$ for these specimens. The ANOVA test confirmed that both $E_a$ and $f_a$ differs significantly between T1 and T2 for all the environments.

### 3.2.3   Concrete

Fig. 7 presents the average results of the elastic modulus ($E_{cm}$), compressive strength ($f_{cm}$), tensile strength ($f_{ctm}$) and carbonation depth on the initial characterization (T0) and after one and two years (T1 and T2) of exposure.



(a)                                                      (b)

(c)                                                      (d)
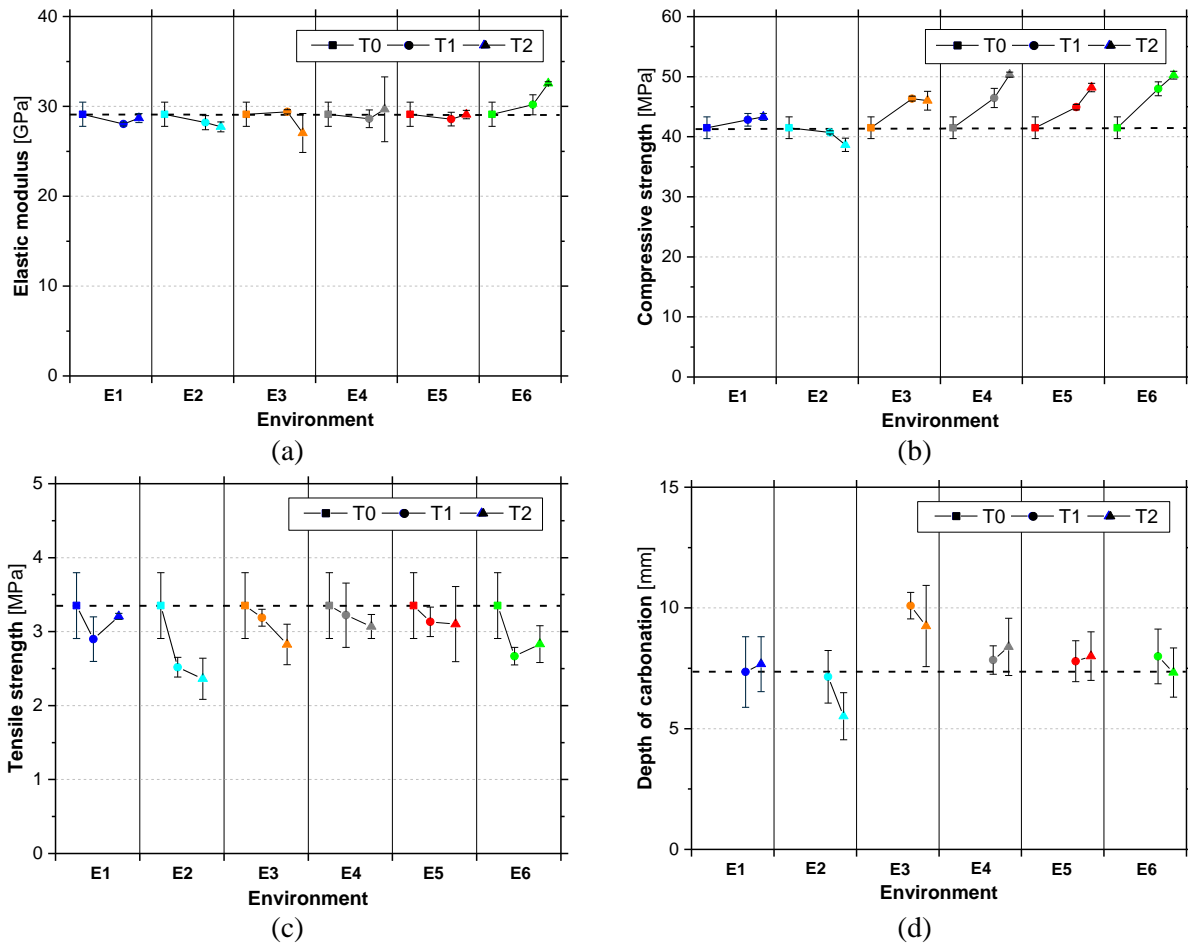
**Fig. 7.** Concrete's mechanical/physical properties: (a) elastic modulus, (b) compressive strength, (c) tensile strength and (d) carbonation depth obtained at the initial characterization (T0) and after one and two years (T1/T2) of exposure to environments E1-E6.

In the initial characterization of the mechanical properties of concrete (T0), conducted with 28 days of age, an elastic modulus ($E_{cm}$) of 29 GPa and a compressive strength ($f_{cm}$) of 42 MPa were obtained. The impact of the aging on $f_{cm}$ is higher than on $E_{cm}$. Small $E_{cm}$ variations were observed in specimens exposed to laboratory environments which, according to an ANOVA test, were statically insignificant between T0 and T1 and between T1 and T2. However, the real-time field exposure led to $E_{cm}$ variations in between -7.2% (E3 at T2) and +12.0% (E6 at T2) when compared with T0 results. This latter $E_{cm}$ increase can indicate an improvement due to the exposure to a high humidity conditioning. The real-time field exposure led to an increase in the concrete's compressive strength (comparing with T0). The highest $f_{cm}$ increase was obtained in E4 (+21.2%) and E6 (+21.0%) environments at T2 (comparison with T0). This finding can be explained by the higher relative humidity (see Fig. 2), which is in agreement with other authors, e.g. [36]. The $f_{cm}$ did increase considerably in E1 environment (maximum increase of ~4% at T2). In the case of E2 environment, a $f_{cm}$ decrease was recorded, especially at T2 (6.7% in relation to T0), which can be explained by the lower compressive strength of saturated concrete when compared with dry concrete [37, 38]. However, it should be highlighted that $f_{cm}$ variations in E1 and E2 specimens are not statistically relevant from the ANOVA test performed.

Contrary to the compressive strength ($f_{cm}$), a general decrease in the tensile strength ($f_{ctm}$) was obtained at T1 and T2 conditioning times in comparison with T0. This finding indicated higher decrease of superficial mechanical properties when compared with the core's mechanical properties, as shown by Rozsypalová et al. [39]. The highest $f_{ctm}$ reduction was verified in E2 environment at T2 (-29.5%), however, these specimens were also tested saturated. The presence of

water in concrete pores decreases $f_{\text{ctm}}$, as referred by Jin et al. [40]. A considerable $f_{\text{ctm}}$ decrease was also verified in E6 environment at T1 (-20.6%). Similar values were obtained in the remaining environments (E1/E3-E5). It should be highlighted that the variations between T0-T1 and between T1-T2 (except E2) are not statistically relevant from the ANOVA test performed.

The real-time field exposure caused higher levels of carbonation depth than laboratory accelerated aging. Concrete exposed to E3 environment presented the highest carbonation depth (~10 mm), as expected, due to its location (near a highway and the International Airport of Lisbon). An average increase of ~30% was registered in the testing times T1 and T2, when compared with the E1 (used as reference). In the remaining series, a carbonation depth of ~7.5 mm of was obtained, which is in line with similar investigations, e. g. [41, 42]. Material exposed to E2 environment for 2 years (T2) recorded the lowest value, probably by reduced contact with $CO_2$ due to the immersion in water. Smaller increases in carbonatation depth compared to the values verified in E1 (maximum increase of 9.6% in E6 at T1) were obtained in the remaining outdoor environments. In fact, the outdoor environments lead to minor carbonation depth variations between T1 and T2, which can be a result of the reduction in the air concentration of anthropogenic $CO_2$ due to the confinement imposed by COVID-19 pandemic during the second year of exposure.

### 3.2 EBR-CFRP to concrete bond tests

Table 1 presents the main results (average values of four tests) of the single-lap shear tests from the initial characterization (T0) and after one and two years (T1/T2) of exposure to environments E1-E6, namely: $K$ is the initial stiffness of the force *versus* loaded end slip curve ($F_1 - s_1$) – obtained

from the slope of a linear fitting performed on these curves in between 0 to 10 kN; $F_{max}$ is the maximum pull-out shear force reached by the specimen during the whole test; $s_{lmax}$ is the loaded end slip attained at $F_{max}$; FM represents the failure modes observed. Fig. 8(a) and Fig. 8(b) present the average $F_l – s_l$ per series, for laboratory and real-time field exposure, respectively (average curves). Fig. 8(c) shows a typical force *versus* loaded end slip relationships ($F_l – s_l$). These curves presented the following behavior: first, an ascending branch appears until the debonding load is reached (maximum load supported by the effective length according to CNR-DT 200 R1/2013 CNR [20]); this branch with decreasing stiffness is initially linear up to 30-40% of $F_{max}$; the debonding that begins to occur beyond this value of 30-40% of $F_{max}$ is responsible by the stiffness degradation, which starts to occur when the shear strength is reached at the loaded end [14]; second, the slip at the loaded end increases until failure, with an almost constant force, as already observed in similar investigations [13, 14, 43]. In some tests, after the debonding load, a sudden decrease in force and increase in loaded end slip was observed, as result of a sudden detachment of an initial bonded zone, which probably corresponds to the effective bond length (see Fig. 8(c)). Fig. 8(d) presents the maximum force obtained from the bond tests performed at T0, T1 and T2.

**Table 1.** Main results of the pull-out shear tests on the bond EBR-CFRP to concrete system at the initial characterization (T0) and after one and two years (T1 and T2) of exposure to environments E1-E6.

| Env. | $K$ [kN/mm] | | | $F_{max}$ [kN] (CoV [%]) | | | $s_{lmax}$ [mm] (CoV [%]) | | | FM | | |
|---|---|---|---|---|---|---|---|---|---|---|---|---|
| | T0 | T1 | T2 | T0 | T1 | T2 | T0 | T1 | T2 | T0 | T1 | T2 |
| E1 | | 241.5 (2.7) | 282.1 (13.0) | | 29.9 (13.8) | 27.7 (11.0) | | 0.4 (16.6) | 0.3 (25.9) | | C [1]; C + F/A [3] | C [4] |
| E2 | | 275.6 (20.3) | 311.7 (38.4) | | 27.9 (8.4) | 31.1 (10.0) | | 0.2 (12.4) | 0.2 (8.7) | | C [4] | C [3]; C + F/A [1] |
| E3 | 292.8 (14.6) | 302.7 (9.5) | 329.5 (39.5) | 30.2 (13.3) | 31.8 (6.7) | 35.1 (9.1) | 0.5 (28.7) | 0.4 (44.7) | 0.4 (28.1) | C + F/A [2]; C [2] | C [3]; C + F/A [1] | C [4] |
| E4 | | 355.6 (26.0) | 305.5 (8.8) | | 28.9 (8.4) | 34.4 (11.1) | | 0.2 (32.6) | 0.3 (6.1) | | C [4] | C [4] |
| E5 | | 240.6 (6.2) | 251.9 (6.1) | | 29.7 (11.5) | 30.1 (5.9) | | 0.4 (29.8) | 0.4 (25.0) | | C [2]; C + F/A [2] | C [4] |
| E6 | | 276.0 (15.5) | 373.8 (11.1) | | 30.2 (13.5) | 29.2 (6.0) | | 0.3 (15.3) | 0.3 (31.0) | | C [4] | C [4] |

Failure modes (FM): C = cohesive failure of concrete; C + F/A = cohesive failure of concrete and debonding at laminate-adhesive interface; the value between square brackets is the number of specimens where the failure mode was observed.
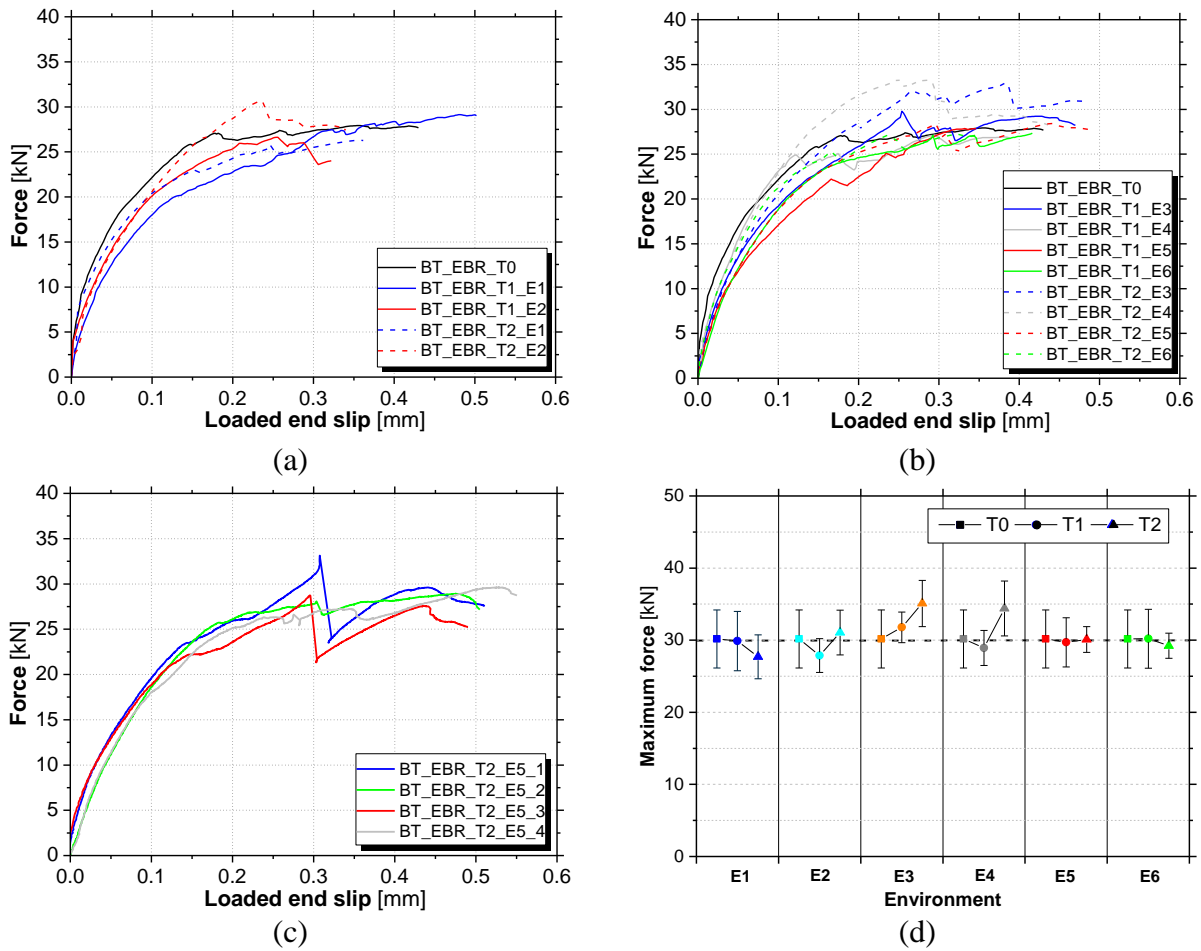
**Fig. 8.** Results of single-lap shear tests on bond EBR-CFRP to concrete specimens: (a) Force *vs.* loaded end slip (average curves of 4 specimens/environment) for laboratory accelerated aging; (b) Force *vs.* loaded end slip (average curves of 4 specimens/environment) for real-time field exposure; (c) Force *vs.* loaded end slip for E5 environment at T2; (d) Maximum pull-out shear force at the initial characterization (T0) and after one and two years (T1 and T2) of exposure on the environments E1-E6.

Fig. 9 presents the two types of failure modes observed in bond EBR-CFRP to concrete tests: (i) cohesive failure in the concrete (C), which was the dominant failure mode and (ii) cohesive failure in the concrete with simultaneous debonding at the laminate-adhesive interface (C + F/A), also observed in some test specimens (see Table 1).

**Fig. 9.** Failure modes observed in the pull-out shear bond EBR tests: (a) C – cohesive failure of concrete and (b) C + F/A - cohesive failure of concrete and debonding at laminate-adhesive interface.

The initial characterization (T0) of the bond EBR-CFRP to concrete specimens provided results in agreement with related preceding works, e.g. [14, 43]. An average maximum force of 30.2 kN was reached, with cohesive failure of the concrete (C) as the dominant failure mode. In two specimens, the detachment at the laminate-adhesive interface (F/A) was also observed in approximately half of the bond length. The average maximum tensile stress obtained in the CFRP laminate was 503 MPa (~20% of the ultimate tensile strength of the CFRP strip), which is in agreement with the result obtained using the formulation proposed by the CNR-DT 200 R1/2013 [20] (505 MPa). The initial stiffness ($K$) varies with the environment and period of exposure. In general, the real-time field exposure leads to a higher initial stiffness. A tendency of $F_{max}$ increase was verified in specimens of E3 and E4 environments (specially in E3, where $F_{max}$ increased 16.2% at T2 in comparison with T0). The increase in the time of exposure seems to cause the change of the failure mode, from C + F/A to C.

### 3.2.4   Effect of the environmental exposure type

A decrease in the initial stiffness ($K$) was observed between the initial characterization (T0) and T1 for E1 environment. The E2 environment seems to do not affected the initial stiffness. In general, the real-time field exposure has led to an increase in the initial stiffness (in comparison with T0 or with E1 at T1 and T2), except in the case of E5 series, which has showed lower $K$ values.

The exposure to E1 environment caused only a negligible variation in $F_{max}$ after one year (T1) of exposure. However, a $F_{max}$ decrease of 8.3% was observed at T2. The specimens immersed in water (E2) recorded a $F_{max}$ decreased at T1 (6.7%) followed by an increase at T2 (12.2%) when compared with the E1 environment (reference) for the same period of exposure. The $F_{max}$ on specimens of E1 and E2 environments did not statistically differs significantly with the ANOVA test between T0-T1 and T1-T2. It should be highlighted that the tensile properties of the epoxy adhesive faced a strong reduction in the E2 environment, justified by plasticization and swelling effects, which had not been observed in the bond EBR-CFRP to concrete system. Therefore, for the studied period, it seems that the overall behaviour of the bond of EBR-CFRP to concrete systems does not fully depend only on the mechanical properties of the adhesive, as the magnitude of strength reduction observed in the adhesive was not verified in the bonding system. Furthermore, due to the small variations in the mechanical properties of the remaining constitutive materials, the overall durability of the EBR system is probable not substantially dependent of the individual properties of each material, even with water absorption and testing in a saturated state. The $F_{max}$ increase observed at T2 can be related with the adhesive plasticization, which may reduce the interfacial peaks of shear stress (responsible by the premature debonding of the CFRP laminate) and lead to a better and more uniform distribution of the shear stresses along the whole bond length (also

observed by Hassan et al. [18]) yielding to an increase in the maximum force, as already observed in EBR-CFRP strengthening using flexible adhesives, e.g. Kwiecień [44].

Regarding to the real-time field exposure (environments E3-E6), $F_{max}$ did not change significantly after one year of conditioning (T1) in comparison with the reference E1. Variations of $F_{max}$ in between +6.4% (E3) and -3.3% (E4) were observed. Higher variations were observed after two years of conditioning (T2), with strong $F_{max}$ increases of +26.7% and +24.2%, respectively, in E3 and E4 environments (comparting to E1 at T2). Therefore, after a two-year conditioning (T2), the maximum strength has increased in immersed (E2) and outdoor (E3 and E4) environments, which indicates a bond strength improvement of the EBR-CFRP to concrete system in the conditions of this study. Nevertheless, by performing the ANOVA test between T0-T1 (minimum p-value = 0.424 for E2 environment) and T1-T2 (minimum p-value = 0.081 for E4 environment) it was possible to conclude that $F_{max}$ did not significantly statistically differs on outdoor specimens.

Considering only the evolution of the mechanical properties of the constitutive materials exposed to outdoor environments (see "Materials" section), the observed $F_{max}$ increase in the EBR-CFRP to concrete system can be related with the: (i) increase in the compressive strength of concrete (also observed by Kabir et al. [17]), (ii) decrease in the superficial tensile strength of concrete, (iii) improvement of the interface characteristics, and (iv) reduction of the elastic modulus of the adhesive. As stated before, the reduction of the adhesive's elastic modulus allows to a better and more uniform distribution of the shear stress along the active bond length which leads to the increasing of the maximum strength. The diary and seasonal fluctuations of temperature and humidity faced in outdoor exposure can lead to development of shear stresses at the interfaces due

to the different thermal expansion coefficients of the constitutive materials. These stresses can lead to the bond damage and even to debonding of the CFRP strip. However, the temperature and humidity of the tested environments do not seem to be significant to the point where it impacts the interfaces. As stated by Cabral-Fonseca et al. [16], the effects of freeze-thaw cycles are controversial, as some authors found deterioration of the bonding system and others stated small effects on FRP-concrete bond. In the present investigation, the bond strength observed on E4 environment increased after two-year exposure. The non-deleterious effects may be justified by the reduced range of extreme temperatures and the corresponding number of cycles faced by this outdoor environment, when compared with other works from the literature. Finally, for a given testing period (T1 or T2) the same failure modes were observed in all environments, even in E2 environment (where specimens were tested saturated).

### 3.2.5  *Effect of time of exposure*

During the first year of exposure (between T0 and T1), a general decrease on the initial stiffness ($K$) was observed, except for E4 environment. Then, on the second year (between T1 and T2), a tendency of increase in the initial stiffness ($K$) occurred, regardless of the environment. The highest increase was verified in E6 environment (35%), which can be related with the increase in the elastic modulus of concrete in E6 at T2. Nevertheless, E4 environment induced a reduction of the initial stiffness in this interval.

The maximum force remained almost constant along the time in E1, E2, E5 and E6 environments (maximum decrease of ~8.3% in E1 at T2), whereas $F_{max}$ increased in E3 and E4 environments, especially during the second year of exposure (maximum increase of ~16.2% in E3). After two

stages of evaluation (T1 and T2), no clear trend of evolution in $F_{max}$ was observed in E2, E4, E5 and E6 environments. Nevertheless, a continuously $F_{max}$ decrease and a continuous $F_{max}$ increase was observed in E1 and E3 environment, respectively.

Comparing the failure modes observed on series corresponding to T0, T1 and T2, it became clear that the C + F/A tends to change to cohesive in the concrete (C) with the increase of the exposure time. This finding may be related with the change in the mechanical properties of the concrete surrounding the adhesive-concrete (A/C) interface and due to the improvement of laminate-adhesive (F/A) interface along the time.

## 4. LABORATORY VERSUS FIELD EXPOSURE AND DESIGN GUIDELINES

A database of laboratory accelerated aging tests was established to perform comparisons between the results from laboratory accelerated aging (collected in the existing literature) and real-time field exposure (obtained in the present work). Therefore, results from the EBR systems obtained on EBR-CFRP to concrete bond tests were gathered. This database presents the following main characteristics:

- Database size: 50 test results, collected from five research works [45-49];
- Type of FRP: pultruded CFRP laminates with thicknesses between 1.2 and 1.4 mm and elastic modulus between 155 and 176 GPa;
- Type of adhesive: epoxy adhesives;
- Concrete compressive strength: between 25 and 50 MPa;
- Bond lengths: ranging from 100 to 600 mm;

30

- Test configurations: single-lap shear test and beam test;

- Types of exposure conditions: freeze-thaw cycles (in water and 90% RH), immersion in water (tap and salt water), sun exposure (thermal cycles) and saline splash exposure (salt fog cycles);

- Periods of exposure: up to 18000 hours (~2 years).

A preliminary analysis of the database's results and attempts of correlating the bond strength retention observed for each specific accelerated aging type (found in literature) with real-time field exposure conditions were performed. The bond strength retention was computed as the ratio between the strength after exposure and reference strength (before exposure). Nevertheless, no specific correlations could be obtained due to the significant dispersion of the results and reduced number of test results.

Fig. 10(a) presents the relationship between the evolution of bond strength retention and time of exposure, obtained for the results of laboratory accelerated conditioning that compose the database. The results of laboratory accelerated aging of the E2 environment (black circles) and the results of real-time field exposure of the E3-E6 environments (red circles) are also presented. In general, a considerable dispersion of the results can be observed, without a clear trend of evolution with the time. The dispersion in real-time field exposure is lower than in laboratory accelerated aging, with a retention value close to 1.0 (RTFE). Accelerated aging protocols by water immersion tends to yield lower values of bond strength retention when compared with real-time field exposure, whereas thermal cycles (sun exposure) tend to give higher values, even for short periods of

exposure. When only bond strength retention values lower than 1.0 are considered, average retentions of strength equal to 0.84 (with a coefficient of variation, CoV = 9.4%) and 0.93 (CoV = 4.9%) are obtained, respectively, for laboratory accelerated aging and real-time field exposure (E3-E6 environments). From these results, it becomes clear that, up to ~18000 hours, laboratory accelerated aging yield to lower bond strength retention than real-time field exposure.

Fig. 10(b) presents the relationship between non-conservative estimated data values (percentage of the cases where the adopted conversion factor is not conservative) of the database collected and the conversion factor (only retention values lower than 1.0 were considered in this work). Based in this approach, a bond strength conversion factor of 0.75 should be used for ensuring at least 10% of the non-conservative estimates with the EBR system. In the investigation developed by Cruz et al. [25], which addressed on the durability of the CFRP laminate and epoxy adhesive, strength conversion factors of 0.85 and 0.55 were proposed, respectively. Comparing the conversion factor proposed in this work (0.75) for the EBR system with the values of conversion factors proposed by Cruz et al. [25] for the CFRP strips (0.85) and epoxy adhesives (0.55), it can be concluded that the degradation of the bond EBR system is higher than the degradation of the CFRP laminate itself and lower than the degradation of the epoxy adhesive.
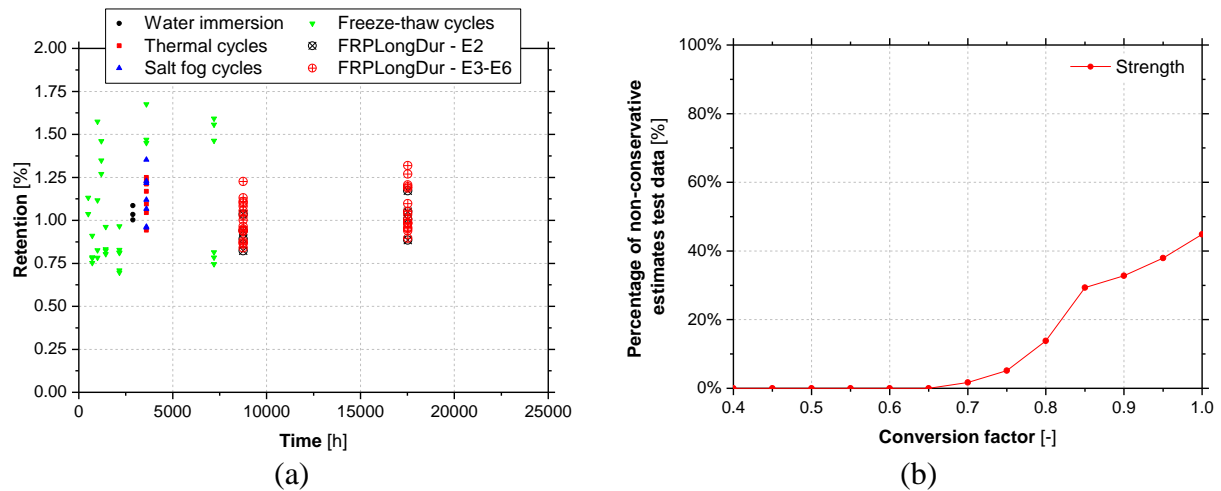
**Fig. 10.** Laboratory accelerated aging versus real-time field exposure on bond EBR-CFRP to concrete systems: (a) retention values and (b) percentage of non-conservatively estimated data versus conversion factor.

The durability of the FRP strengthening systems is explicitly accounted in the existing guidelines ACI 440.2R-17 [1] and CNR-DT 200 R1/2013 [20]. These guidelines provide environmental conversion (or reduction) factors ($C_E$ for the case of ACI 440.2R-17, $\eta_a$ for the case of CNR DT 200 R1/2013) to predict the service life of the FRP strengthening system considering generic types of environmental exposure. Nevertheless, these guidelines do not provide conversion factors for specific types of exposure. Furthermore, in ACI 440.2R-17 and CNR-DT 200 R1/2013, a same conversion factor of 0.85 is proposed for exterior and aggressive environmental conditions using epoxy/carbon systems (including EBR and NSM techniques). However, these design conversion factors only reduce the ultimate tensile strength/strain of the FRP material and do not consider the eventual reduction on the bond strength of the FRP-concrete systems, which, as demonstrated in this investigation, is affected by the type of conditioning. Therefore, these guidelines should be improved to consider either (i) the bond strength degradation and (ii) more specific types of environmental exposure.

## 5. CONCLUSIONS

The results of an investigation on the durability of bond in EBR-CFRP to concrete systems under real-time field exposure was described in this paper. The experimental program included a total of six exposure environments. Two laboratory conditions under controlled hygrothermal/ hydrothermal conditions were considered: (i) a control (reference) environment (E1) and (ii) water immersion environment (E2). Four types of real-time field exposure were included for inducing aging mainly by carbonation (E3), freeze-thaw attack (E4), elevated temperatures (E5), and airborne chlorides from seawater (E6). Experimental campaigns were performed along the time to assess the evolution of the mechanical characteristics of materials and bond at specific time points, namely at an early stage (T0) before conditioning and after one and two years (T1/T2) of conditioning. The results obtained from real-time field exposure developed in this work and results of laboratory accelerated aging from the existing literature were compared. An analysis of the appropriateness of these results when compared with the existing guidelines was also developed. From this work, the following conclusions can be pointed out:

*EBR-CFRP to concrete bond tests:*

- A maximum force of 30.2 kN was obtained on the initial characterization (T0), which corresponds to only ~20% of the tensile strength of the CFRP laminate;

- At T1 and T2, no trend of evolution in the bond strength was obtained for laboratory aging (E1 and E2), with a maximum bond strength variation in E2 environment at T1 (decrease of 8.3% in comparison with T0). Regarding to real-time field exposure, a tendency of increasing in the

bond strength at T2 was verified in E3 and E4 environments (highest increase of +16.2% in E3 environment in comparison with T0); negligible variations were obtained in E5 and E6 environments (maximum decrease of ~3.3% in E6 at T2);

- The cohesive failure in the concrete (C) was observed in all the test specimens; In some tests, debonding at the laminate-adhesive interface (F/A) was also verified in addition to the cohesive failure in the concrete (C); This complementary component F/A was common in the first testing period (T0) and tends to disappear with the exposure and increase in the time of exposure;

*Laboratory versus field exposure and design guidelines:*

- Despite the dispersion of results, for similar periods, the real-time filed exposure yielded higher values of bond strength retention than laboratory accelerated aging (considering only retention values lower than 1.0);

- An environmental conversion factor of 0.75 is suggested for the case of exterior or aggressive environmental conditions for accounting the bond strength durability of the EBR-CFRP to concrete system (for the design purposes, the real bond strength should be decreased in 25%). The existing guidelines should be improved to account for the bond strength degradation.

## ACKNOWLEDGEMENTS

## REFERENCES

[1] ACI, Guide for the design and construction of externally bonded FRP systems for strengthening concrete structures, ACI 440.2R-17. American Concrete Institute. Farmington Hills (MI)2017.
[2] CSA, Canadian Highway Bridge Design Code, CAN/CSA-S6-06. Canadian Standards Association. Toronto, Toronto, 2006.
[3] IPQ, NP EN EN 1992-1-1. Eurocode 2: design of concrete structures - Part 1-1: general rules and rules for buildings, Instituto Português da Qualidade (IPQ). Caparica, Portugal. 20101992.
[4] W. Ashraf, Carbonation of cement-based materials: Challenges and opportunities, Construction and Building Materials 120 (2016) 558-570.
[5] J. Tatar, H.R. Hamilton, Comparison of laboratory and field environmental conditioning on FRP-concrete bond durability, Construction and Building Materials 122 (2016) 525-536.
[6] J. Tatar, S. Milev, Durability of Externally Bonded Fiber-Reinforced Polymer Composites in

Concrete Structures: A Critical Review, Polymers 13(5) (2021) 765.

[7] M. Lettieri, M. Frigione, Natural and artificial weathering effects on cold-cured epoxy resins, Journal of Applied Polymer Science 119(3) (2011) 1635-1645.

[8] V.M. Karbhari, K. Ghosh, Comparative durability evaluation of ambient temperature cured externally bonded CFRP and GFRP composite systems for repair of bridges, Composites Part A: Applied Science and Manufacturing 40(9) (2009) 1353-1363.

[9] G.M. Odegard, A. Bandyopadhyay, Physical aging of epoxy polymers and their composites, Journal of Polymer Science Part B: Polymer Physics 49(24) (2011) 1695-1716.

[10] P. Fernandes, J. Sena-Cruz, J. Xavier, P. Silva, E. Pereira, J. Cruz, Durability of bond in NSM CFRP-concrete systems under different environmental conditions, Composites Part B: Engineering 138 (2018) 19-34.

[11] V.M. Karbhari, J.W. Chin, D. Hunston, B. Benmokrane, T. Juska, R. Morgan, J.J. Lesko, U. Sorathia, D. Reynaud, Durability gap analysis for fiber-reinforced polymer composites in civil infrastructure, Journal of Composites for Construction 7(3) (2003) 238-247.

[12] A. Bilotta, F. Ceroni, M. Di Ludovico, E. Nigro, M. Pecce, G. Manfredi, Bond efficiency of EBR and NSM FRP systems for strengthening concrete members, Journal of Composites for Construction 15 (2011) 757-772.

[13] C. Mazzotti, A. Bilotta, C. Carloni, F. Ceroni, T. D'Antino, E. Nigro, C. Pellegrino, Bond between EBR FRP and concrete. In: Pellegrino C, Sena-Cruz J, editors. RILEM State-of-the-Art Reports, vol. 19, Dordrecht: Springer Netherlands; 2016, p. 39–96. , (2016).

[14] I. Iovinella, A. Prota, C. Mazzotti, Influence of surface roughness on the bond of FRP laminates to concrete, Construction and Building Materials 40 (2013) 533-542.

[15] C. Pellegrino, J. Sena-Cruz, Design Procedures for the Use of Composites in Strengthening of Reinforced Concrete Structures : State-of-the-Art Report of the RILEM Technical Committee 234-DUC, 2016. https://search.ebscohost.com/login.aspx?direct=true&scope=site&db=nlebk&db=nlabk&AN=105 6106.

[16] S. Cabral-Fonseca, J.R. Correia, J. Custódio, H.M. Silva, A.M. Machado, J. Sousa, Durability of FRP - concrete bonded joints in structural rehabilitation: A review, International Journal of Adhesion and Adhesives 83 (2018) 153-167.

[17] M.I. Kabir, R. Shrestha, B. Samali, Effects of applied environmental conditions on the pull-out strengths of CFRP-concrete bond, Construction and Building Materials 114 (2016) 817-830.

[18] S.A. Hassan, M. Gholami, Y.S. Ismail, A.R.M. Sam, Characteristics of concrete/CFRP bonding system under natural tropical climate, Construction and Building Materials 77 (2015) 297-306.

[19] M.H. Mohd Hashim, A.R. Mohd.Sam, M. Hussin, Experimental investigation on the effect of natural tropical weather on interfacial bonding performance of CFRP-concrete bonding system, 11 (2016) 584-604.

[20] CNR, CNR-DT 200 R1/2013. Guide for the design and construction of externally bonded FRP systems for strengthening existing structures., 2013.

[21] AASHTO, Guide Specifications for Design of Bonded FRP Systems for Repair and Strengthening of Concrete Bridge Elements, AASHTO-FRPS-1. American Association of State Highway and Transportation Officials, Washington, DC, USA, 2010.

[22] ISIS, Strengthening Reinforced Concrete Structures with Externally-Bonded Fibre Reinforced Polymers (FRPs), Design Manual 4 (Man. No. 4). FRP Rehabilitation of Reinforced Concrete

Structures. Intelligent Sensing for Innovative Structures (ISIS). ISIS Canada; Neale, K.W. (Ed.) University Sherbrooke: Sherbrooke, QC, Canada, 2012.2012.

[23] JSCE, Recommendations for Upgrading of Concrete Structures with Use of Continuous Fiber Sheets, Concrete Engineering Service 41. Japan Society of Civil Engineers. Tokyo, Japan, 20012001.

[24] CS, Design Guidance for Strengthening Concrete Structures Using Fibre Composite Materials, Concrete Society TR55. 3rd ed.; Concrete Society Technical Reports 55 (TR55); Camberley: Surrey, UK, 20122012.

[25] R. Cruz, L. Correia, A. Dushimimana, S. Cabral-Fonseca, J. Sena-Cruz, Durability of Epoxy Adhesives and Carbon Fibre Reinforced Polymer Laminates Used in Strengthening Systems: Accelerated Ageing versus Natural Ageing, Materials 14(6) (2021) 1533.

[26] S&P, S&P CFRP Laminates. Technical Datasheet, Seewen, Switzerland, 2014.

[27] S&P, S&P 220 Resin epoxy adhesive. Technical Data Sheet, Seewen, Switzerland, 2015.

[28] CEN, EN 206-1. Concrete — Part 1: Specification, performance, production and conformity, European Committee for Standardization (CEN). 20002000.

[29] ISO, ISO 527-2. Plastics—Determination of Tensile Properties. Part 2: Test Conditions for Moulding and Extrusion Plastics, International Organization for Standardization (ISO): Genève, Switzerland, 2012.2012.

[30] ISO, ISO 527-5. Plastics—Determination of Tensile Properties. Part 5: Test Conditions for Unidirectional Fibre-Reinforced Plastic Composites, International Organization for Standardization (ISO): Genève, Switzerland, 2009.2009.

[31] IPQ, NP EN 12390-13. Testing Hardened Concrete. Part 13: Determination of Secant Modulus of Elasticity in Compression, Instituto Português da Qualidade (IPQ). Caparica, Portugal. 20132013.

[32] IPQ, NP EN 12390-3. Testing Hardened Concrete. Part 3: Compressive Strength of Test Specimen, Instituto Português da Qualidade (IPQ). Caparica, Portugal. 20112011.

[33] BSI, Products and systems for the protection and repair of concrete structures - Test methods - Measurement of bond strength by pull-off, EN 1542. STANDARD by British-Adopted European Standard. British Standards Institution (BSI). 19991999.

[34] LNEC, LNEC. Concrete – determination of carbonation resistance. E391-1993, Portuguese specification from LNEC. 19931993.

[35] J.M. Sousa, J.R. Correia, S. Cabral-Fonseca, Durability of an epoxy adhesive used in civil structural applications, Construction and Building Materials 161 (2018) 618-633.

[36] Z. Mi, Y. Hu, Q. Li, Z. An, Effect of curing humidity on the fracture properties of concrete, Construction and Building Materials 169 (2018) 403-413.

[37] G. Zhang, C. Li, H. Wei, M. Wang, Z. Yang, Y. Gu, Influence of Humidity on the Elastic Modulus and Axis Compressive Strength of Concrete in a Water Environment, Materials 13(24) (2020) 5696.

[38] J.-k. Zhou, N. Ding, Moisture effect on compressive behavior of concrete under dynamic loading, Journal of Central South University 21(12) (2014) 4714-4722.

[39] I. Rozsypalová, P. Daněk, O. Balkanský, The bond strength by pull-off and direct tensile strength of concrete damaged by elevated temperatures, IOP Conference Series: Materials Science and Engineering 385 (2018) 012047.

[40] L. Jin, X. Du, G. Ma, Macroscopic effective moduli and tensile strength of saturated concrete, Cement and Concrete Research 42(12) (2012) 1590-1600.

[41] N.B. Bouzoubaâ, A.B. Bilodeau, B.T. Tamtsia, S.F. Foo, Carbonation of fly ash concrete: laboratory and field data, Canadian Journal of Civil Engineering 37(12) (2010) 1535-1549.

[42] M. Otieno, J. Ikotun, Y. Ballim, Experimental investigations on the effect of concrete quality, exposure conditions and duration of initial moist curing on carbonation rate in concretes exposed to urban, inland environment, Construction and Building Materials 246 (2020) 118443.

[43] S. Soares, J. Sena-Cruz, J. Cruz, P. Fernandes, Influence of Surface Preparation Method on the Bond Behavior of Externally Bonded CFRP Reinforcements in Concrete, Materials 12 (2019) 414.

[44] A. Kwiecień, Stiff and flexible adhesives bonding CFRP to masonry substrates—Investigated in pull-off test and Single-Lap test, Archives of Civil and Mechanical Engineering 12(2) (2012) 228-239.

[45] P. Colombi, G. Fava, C. Poggi, Bond strength of CFRP–concrete elements under freeze–thaw cycles, Composite Structures 92(4) (2010) 973-983.

[46] K. Al-Tamimi Adil, A. Hawileh Rami, A. Abdalla Jamal, A. Rasheed Hayder, R. Al-Mahaidi, Durability of the Bond between CFRP Plates and Concrete Exposed to Harsh Environments, Journal of Materials in Civil Engineering 27(9) (2015) 04014252.

[47] M.F. Green, L.A. Bisby, Y. Beaudoin, P. Labossière, Effect of freeze-thaw cycles on the bond durability between fibre reinforced polymer plate reinforcement and concrete, Canadian Journal of Civil Engineering 27(5) (2000) 949-959.

[48] Y. Pan, G. Xian, H. Li, Effects of Freeze-Thaw Cycles on the Behavior of the Bond between CFRP Plates and Concrete Substrates, Journal of Composites for Construction 22(3) (2018) 04018011.

[49] F. Al-Mahmoud, J.-M. Mechling, M. Shaban, Bond strength of different strengthening systems – Concrete elements under freeze–thaw cycles and salt water immersion exposure, Construction and Building Materials 70 (2014) 399-409.

# Paper 5

**TITLE:** LONG-TERM FLEXURAL BEHAVIOUR OF SLABS STRENGTHENED WITH CFRP LAMINATE SYSTEMS UNDER DIFFERENT ACCELERATED AND NATURAL ENVIRONMENTAL CONDITIONS

**REFERENCE:**

Cruz, R., Correia, L., Dushimimana, A., Cabral-Fonseca, S., and Sena-Cruz, J. 2022. Long-term flexural behaviour of slabs strengthened with CFRP laminate systems under different accelerated and natural environmental conditions. Paper to be submitted.

# Long-term flexural behaviour of slabs strengthened with CFRP laminate systems under different accelerated and natural environmental conditions

Ricardo Cruz[1], Luís Correia[1], Aloys Dushimimana[1], Susana Cabral-Fonseca[2] and

José Sena-Cruz[1*]

[1]University of Minho, ISISE/IB-S, Department of Civil Engineering, Guimarães, Portugal

[2]LNEC, National Laboratory of Civil Engineering, Materials Department, Lisboa, Portugal

[*]Corresponding author (Email: jsena@civil.uminho.pt; Tel. +351 253 510 200).

**ABSTRACT**

The durability and long-term flexural behaviour of reinforced concrete (RC) slabs strengthened with carbon fibre reinforced polymer (CFRP) laminate systems were assessed under laboratory and natural environments. The non-prestressed externally bonded reinforcement (EBR) and near surface mounted (NSM), and the prestressed mechanical anchorage (MA) and gradient method anchorage (GA) strengthening techniques solutions were studied. Laboratory exposure included a reference (control) environment and a water immersion environment, both under controlled conditions whereas natural exposure includes four environments promoting ageing mostly by carbonation, freeze-thaw attack, elevated temperatures, and airborne chlorides from the ocean seawater. Short-term flexural tests, at an early stage, were performed to determine the load-carrying capacity of the CFRP-strengthened RC slabs and, therefore, design the level of sustained load to be used on the long-term flexural creep tests performed under the different environmental conditions studied. These tests allowed to investigate the time-dependent behaviour due to the

synergic effects of a continuous stress state imposed by a gravity-sustained loading and of specific environmental exposure types. The laboratory slabs present the smallest mid-span displacement growth over time whereas the outdoor slabs faced the higher mid-span displacement increase. Similar creep displacements were observed in all outdoor environments during the three-year exposure. Therefore, higher creep coefficients were observed on outdoor slabs than on laboratory slabs. Also, higher creep coefficients were verified with the prestressed MA and GA systems than with non-prestressed EBR and NSM solutions. Additionally, the EBR slabs presented higher creep coefficient values than NSM ones. Finally, the long-term creep coefficients obtained in this work are compared with a literature formulation and existing guidelines. The approaches employed revealed a conservative estimation for the non-prestressed slabs; nevertheless, they are not suitable with various prestressed slabs, mainly the slabs of GA system under outdoor exposure.

## 1. INTRODUCTION

Over the last decades, the solution based on the application of Carbon Fibre Reinforced Polymer (CFRP) materials for strengthening reinforced concrete (RC) structures has been widely used. These systems can be applied mainly throughout the Externally Bonded Reinforcement (EBR) and the Near Surface Mounted (NSM) techniques. In the former, the CFRP strips or sheets are applied on the concrete surface of the RC element to be strengthened, while in the latter, the pultruded CFRP strips or bars are introduced inside grooves pre-opened on the concrete cover of the RC structural element. Both techniques have been used for flexural and shear strengthening. For fixing the CFRP laminate strip to the concrete, an epoxy adhesive is typically applied as a bonding agent. Additionally, these techniques can be also applied using active systems by prestressing the CFRP strip. The pre-stressed systems merge the advantages of using these strengthening techniques with the benefits of the external prestressing, such as more efficient use of concrete and CFRP, reduction in the deflection and crack width, among other advantages, e.g. (El-Hacha and El-Badry 2001; Correia et al. 2015).

The steel bars used in RC structures are susceptible to corrosion that severely affects their serviceability and safety. The steel corrosion phenomenon is accompanied with an increase in their volume and expansion, which leads to the cracking of concrete and, consequently, a reduction of the service life of RC structures (Shin and Kim 2002). The level of damage depends on the type of environmental exposure and on the type of structure as well, being more relevant in harsh environments, e.g., marine environments and structures exposed to de-icing agents (Arockiasamy et al. 2000). The strengthening with CFRP laminate strips can be a solution for this type of problems.

There are some gaps in the existing knowledge concerning the strengthening of RC structures with these systems, namely their durability and long-term performance. A clear understanding on this topic is essential for the long-term prediction on the designing these strengthening solutions. The lack of valuable knowledge on these systems has been highlighted as a critical obstacle for the extensive use of these materials/systems in civil/structural engineering applications (Karbhari et al. 2003).

A structure exposed under outdoor conditions is vulnerable to degradation agents. The most relevant environmental degradation factors are the moisture (from precipitation, humidity or aqueous solutions diffused across other substrates), temperature (thermal variations), ultraviolet radiation (UV) and chemicals, which can act individually or combined. Detailed information reading this topic can be found elsewhere (Cruz et al. 2021). These environmental degradation factors are the reason for the outdoor environments chosen in this work. However, an RC slab strengthened with CFRP laminates is a complex multi-material system with the respective interfaces between materials. Therefore, the assessment of durability and long-term behaviour is a complex work.

Several studies concerning the durability of RC structures strengthened with CFRP strips can be found in the literature, mainly using artificial accelerated ageing protocols under laboratorial conditions. Nevertheless, studies performed under natural ageing in outdoor conditions are very scarce, which represents a gap in the existing knowledge. Moreover, the relationship between the results of accelerated and natural ageing is very difficult to establish and, therefore, needs to be better understood. Therefore, these limitations remain a challenge, even in other research subjects

of durability (Ashraf 2016; Tatar and Hamilton 2016; Frigione and Rodríguez-Prieto 2021). Nevertheless, some investigations including natural and accelerated ageing and trying to establish relationships between the ageing effects of both types of exposure are already present in the literature, e.g. (Hassan et al. 2015; Kabir et al. 2016; Mohd Hashim et al. 2016; Tatar and Hamilton 2016; Fernandes et al. 2018; Cruz et al. 2021). On the literature, the magnitude of degradation observed with each type of ageing is yet controversial and needs to be better understood.

Another limitation is related with the scarcity of information on long-term response of RC structures strengthened with CFRP strips under sustained loading, mainly when exposed to outdoor environments (Blaschko and Zehetmaier 2008; Hong and Park 2016; Breveglieri and Czaderski 2022). The deformation due to creep and shrinkage are usually several times higher than the instantaneous (elastic) deformation in RC structures. In the case of prestressed concrete members, the losses in the CFRP pre-strain occurs mainly due to creep and shrinkage of concrete (Arockiasamy et al. 2000). In the following paragraphs, relevant research for the topic is presented.

El Maaddawy et al. (2007) developed an investigation designed to assess the performance of RC beams repaired with CFRP sheets under corrosive environmental conditions. The authors tested a total of 16 beams (152 mm × 254 mm × 3200 mm). The beams were initially electrochemically corroded and later, part of them was repaired in flexure with a CFRP sheet along with a continuous wrapping. Subsequently, this group of the beams was subjected to an additional corrosion exposure. Finally, six beams were exposed to additional corrosion under a sustained load to simulate service conditions. The authors realized that the presence of the sustained load and associated flexural cracks during the post-repair corrosion exposure slightly increased the steel mass loss rate, which

further reduced the beam yielding load by approximately 4% but it had no noticeable effect on the beam ultimate strength.

Al Chami et al. (2009) performed an investigation on the time-dependent behaviour of CFRP strengthened concrete beams. The authors used a total of twenty-six reinforced concrete beams (100 mm × 150 mm × 1800 mm) with and without bonded CFRP laminates. The main parameters of this study were: (i) the level of sustained load (from 59% to 78% of the ultimate static capacities of the unstrengthened beams) and (ii) the strengthening scheme (different strengthening ratios to evaluate the contribution of the external strengthening on the creep resistance of the beams). The results prove that CFRP strengthening is efficient for increasing the load carrying capacity of the beams; however, there is virtually no improvement in performance regarding the long-term deflections. The authors concluded also that the most important factors that influence both creep rate and long-term deflection are the level of sustained load and the compressive strength of the concrete.

Li et al. (2021) developed an experimental study for assessing the prestress loss on the CFRP of RC beams strengthened with a prestressed CFRP plate subjected to sustained loading and continuous wetting condition. They considered a total of 8 RC beams strengthened by a prestressed CFRP plate with prestress levels of 20% and 40% of the CFRP tensile strength. The specimens were sustainedly loaded using two load levels (94 kN and 120 kN) under wet or dried environments for 170 days. The time-dependent prestress loss was monitored as well as, deflection, concrete strain, and crack propagation. The authors concluded that adhesive bonding was weakened by the moisture penetration, being the specimens with lower prestress levels more susceptible to the wet

condition due to the more severe cracking of concrete. The specimens under the wet condition have shown greater deflection increase (up to 20%) for the case of 20% prestress level. Nevertheless, regardless of the environmental exposure, the maximum crack widths of 40% prestressed specimens remained less than 0.2 mm even subjected to high sustained load level, which is within the limitation of the prestressed concrete structures. Deng et al. (2021) performed a study that came up in the scope of the investigation developed by Li et al. (2021). The authors additionally present the results of deflection up to 360 days for the specimens of the higher load level (120 kN). In this interval (170-360 days), the deflection was almost constant.

Lee et al. (2021) developed an investigation on the durability of FRP-concrete bond after sustained load for up to 13 years. They adopted small-scale plain concrete notched beams strengthened with CFRP sheets for testing in flexure to assess the change in debonding onset strain after being sustained loaded in indoor and outdoor environments for as long as 13 years. The authors concluded the following: (i) for indoor conditioning, the debonding onset strain was almost unaffected in the beams after 13 years of exposure; (ii) for outdoor conditioning, including freeze-thaw cycles, rain, hot weather, and ultraviolet exposure, clear reductions in the strain at the beginning of debonding were verified, especially 6 years after the beginning of conditioning. Moreover, the beams revealed higher bond degradation on outdoor environment (~60–75%) than on indoor environment (negligible variation), despite the outdoor beams having less than half the sustained load of the outdoor beams.

A two-part study on the RC slabs strengthened with prestressed and non-prestressed externally bonded CFRP strips under long-term environmental exposure (outdoor and laboratory) and

sustained loading was developed by Breveglieri and Czaderski , C. (Breveglieri and Czaderski 2021; Breveglieri and Czaderski 2022). In the first part (Breveglieri and Czaderski 2022), the strengthened RC slabs (5000 mm × 1000 mm × 220 mm) were loaded and exposed to outdoor environment for four years to evaluate the effects of exposure to elevated temperatures and solar radiation. The authors concluded that the elevated temperatures reached in the adhesive did not have significant impact on the service performance of non-prestressed slabs; however, it could result in the failure of the prestressed system. Therefore, the non-prestressed specimens have demonstrated a reasonable behaviour, nevertheless, a significant increase in CFRP strain was verified along the time. Due to the elevated temperatures and sustained loads, a premature failure was observed in the prestressed slab with the strips anchored with the gradient anchorage (GA) method. In the second part (Breveglieri and Czaderski 2021), the laboratory experiments are presented and discussed. Failure tests were performed to determine the ultimate strengths of the slabs. The results demonstrated that long-term exposure (thermal cycles and sustained load) does not affect the load-carrying capacity of the strengthened RC elements. Furthermore, an additional slab with an identical strengthening configuration was tested after being subjected to thermal cycles under a heavy sustained load under laboratory conditions, allowing us to better understand and verify the results obtained during the long-term experiments.

Considering the existing investigations, it remains unclear the structural effects under natural exposure when compared with laboratory accelerated exposure. Moreover, besides the attempts of the authors in establishing relationships between the damage caused by each type of exposure, these attempts were not successfully reached in many of the existing investigations, due to (i) the environmental conditions chosen, that cannot be used to compare the effects of accelerated and

natural ageing or (ii) by the times of exposure chosen which are not adequate to establish comparisons. Therefore, it is of paramount relevance to develop natural ageing tests, since only this type of tests can provide effective knowledge in the real degradation mechanisms, despite the limitations stated and others, such as the long testing periods and more time consuming (Fernandes et al. 2018).

This paper presents the results of an investigation on the long-term performance of RC slabs strengthened with CFRP strips using the EBR and NSM techniques with passive and active (prestressed) systems. The performance of the slabs was assessed under a sustained loading when exposed to four outdoor environments, inducing ageing mainly by carbonation, freeze-thaw attack, elevated temperatures, and airborne chlorides from seawater up to three years. A reference (control) environment (20 ºC/55% RH) and an environment consisting in water immersion under controlled temperature (20 ºC) were also included. The load carrying capacity of the RC strengthened slabs was evaluated after production. After loading and during the exposure period of 3 years, the slabs were periodically monitored in terms of mid-span deflection. Finally, an attempt on predicting the long-term creep coefficient for this type of strengthening systems is also assessed.

## 2. EXPERIMENTAL PROGRAM, MATERIALS, SPECIMENS AND TEST METHODS

### 2.1. Experimental program

The experimental program of this work is part of the work performed in the scope of the project "FRPLongDur - Long-term structural and durability performances of reinforced concrete elements strengthened in flexure with CFRP laminates", which includes the exposure to relevant artificial

accelerated and real outdoor conditions. Several types of specimens at three different scale levels were adopted, namely: (i) materials (concrete, epoxy adhesive and CFRP laminate), (ii) bond between EBR and NSM CFRP laminates and concrete and, (iii) full-scale RC slabs strengthened with CFRP laminates including EBR (passive and active) and NSM techniques. Further details regarding this project can be found in Cruz et al. (2021). This work follows the publications on the durability of epoxy adhesives and CFRP laminates (Cruz et al. 2021) and bond between CFRP laminates and concrete with EBR and NSM (Cruz et al. 2022) techniques, during the first two years of exposure. Therefore, this publication includes the results of long-term behaviour of full-scale RC slabs strengthened with CFRP laminates using the EBR (prestressed and non-prestressed) and NSM techniques for 3 years.

Fig. 1 presents the six types of environments adopted: (i) E1 and E2 - laboratory accelerated environments and (ii) E3 to E6 - real outdoor environments. An experimental station located in Portugal was built for each environment to install the specimens. Environment E1 (reference) was set with controlled hygrothermal conditions (20 ºC/55% RH); environment E2 aims at investigating the effect of continuous immersion in tap water with controlled hydrothermal conditions (20 ºC/100% RH). Each one of the outdoor environments was designed in order to reach the following specific ageing conditions: E3 – is characterized by elevated levels of concrete carbonation from the elevated $CO_2$ concentration in this experimental station, located in neighbouring to the International Airport of Lisbon and adjacent to a highway with heavy traffic load; E4 – is characterized by freeze-thaw cycles, since the experimental station was placed in the highest mountain of Portugal ('Serra da Estrela'); E5 – is characterized by elevated service temperatures and lower relative humidity, since the experimental station is located in 'Elvas' which

is characterized by this type of climate; E6 – is characterized by high levels of sea water airborne chlorides concentration and relative humidity, since the experimental station is located near the Atlantic Ocean. A brief description of each environment is provided in Fig. 1.
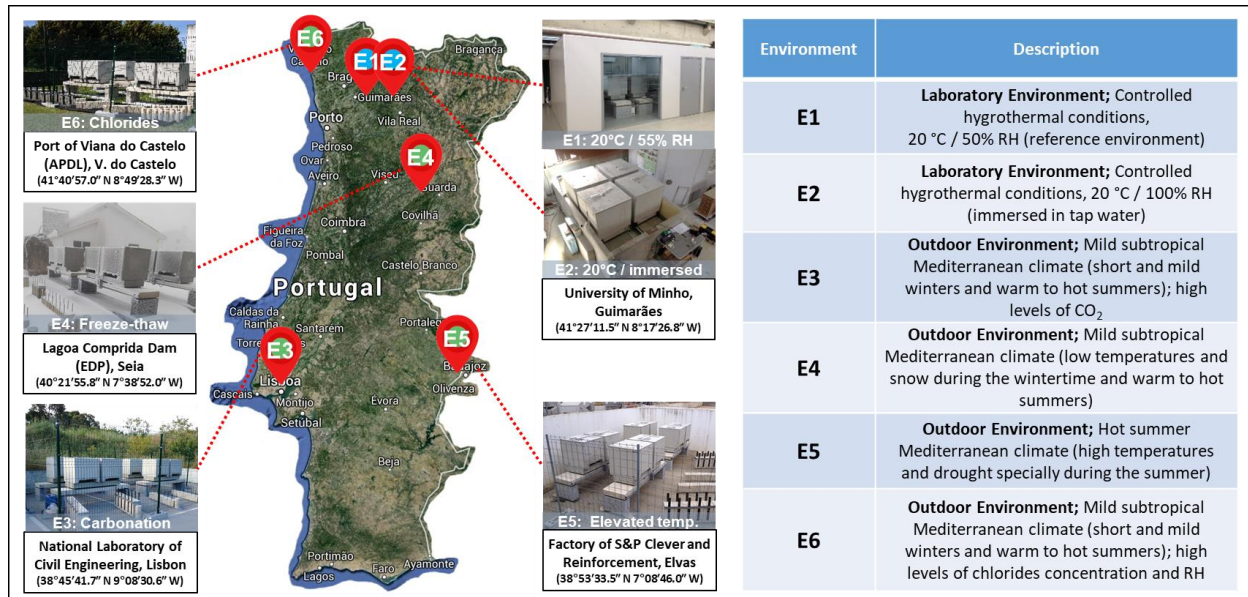


**Fig. 1.** Environments included in this work.

Fig. 2 presents a time schedule of the main steps that compose this work. The RC slabs were strengthened approximately 6 months after casting. The slabs' preparation was concluded approximately 8 months before loading/starting the environmental exposure. During all this period, the specimens were kept in the laboratory environment. The slab's load carrying capacity was evaluated 5 months after strengthening, in October 2017. The installation of specimens (including placement and application of the gravity load) in the experimental stations took place between January and December 2018 (see Fig. 2). Fig. 3 provides a view of the slabs under the creep test, installed in two of the experimental stations.
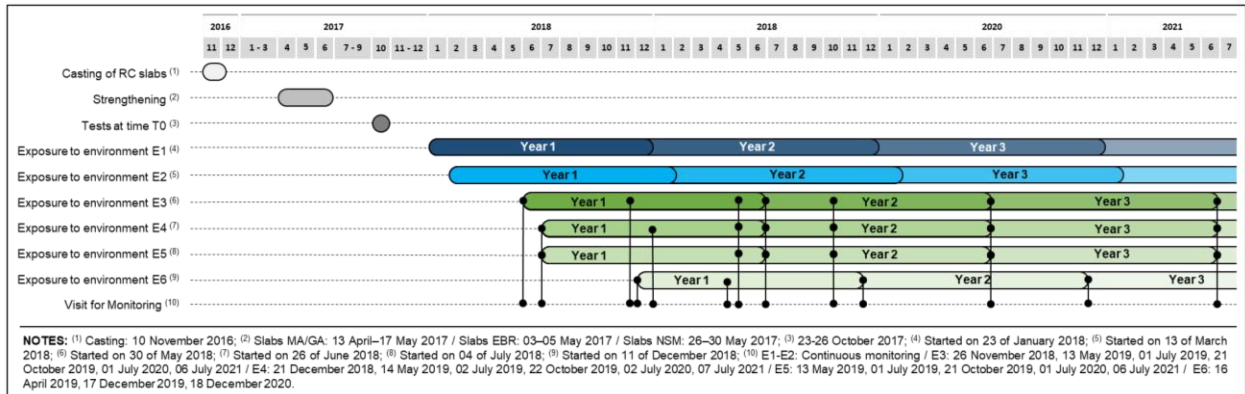
**Fig. 2.** Time schedule of the experimental work carried out.



| (a) | (b) |

**Fig. 3.** Total assembly of the slabs under flexural creep tests in the experimental stations (a) E1 and (b) E4.

A sensor to record the temperature and relative humidity of the air was installed in each experimental station, close to the slabs. Fig. 4 presents two examples of the temperatures and relative humidity registered in two experimental stations – laboratory and outdoor, respectively, E1 and E5. Tab. 1 presents the average temperature and relative humidity recorded in all the experimental stations between the years of 2018 and 2021 (per environment and trimester).
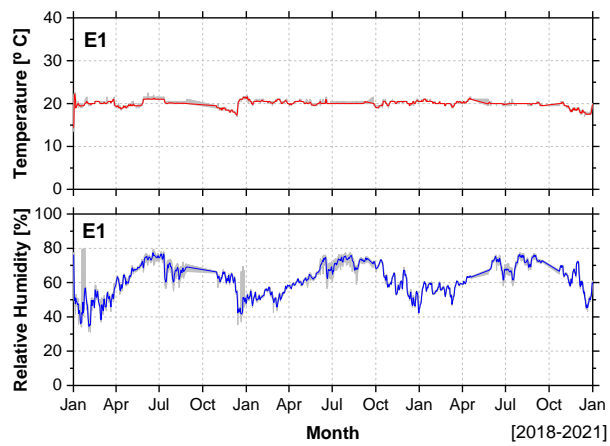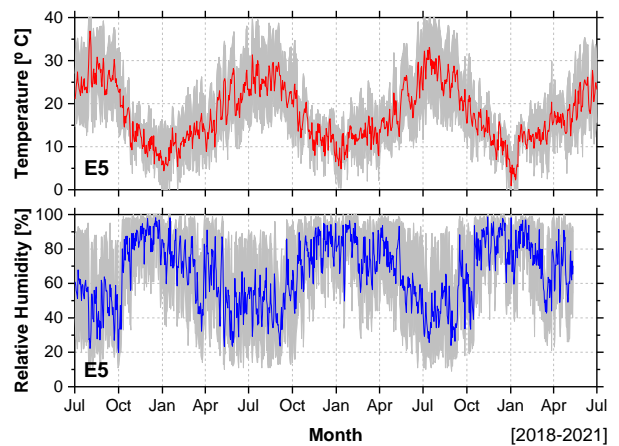
**Fig. 4.** Meteorologic records collected on (a) E1 (laboratory) and (b) E5 (outdoor) environments.

**Tab. 1.** Temperatures and relative humidity registered per environment between 2018 and 2021.

| Environment | | Year 2018 | | | | Year 2019 | | | | Year 2020 | | | | Year 2021 | | | |
|---|---|---|---|---|---|---|---|---|---|---|---|---|---|---|---|---|---|
| | | Jan-Mar | Apr-Jun | Jul-Sep | Oct-Dec | Jan-Mar | Apr-Jun | Jul-Sep | Oct-Dec | Jan-Mar | Apr-Jun | Jul-Sep | Oct-Dec | Jan-Mar | Apr-Jun | Jul-Sep | Oct-Dec |
| E1[a] | Temp. [°C] | 19.9 / 13.5-22.5 | 19.8 / 18.5-22.5 | 20.5 / 20.0-22.0 | 18.6 / 17.5-20.0 | 20.5 / 17.0-22.0 | 20.1 / 19.5-21.0 | 20.0 / 20.0-21.5 | 20.1 / 19.0-21.5 | 20.2 / 19.0-21.0 | 20.2 / 19.0-21.5 | 20.0 / 19.5-21.0 | 19.1 / 17.5-22.0 | -- | -- | -- | -- |
| | RH [%] | 47.0 / 31.0-79.5 | 62.6 / 43.0-77.0 | 69.9 / 55.0-79.5 | 62.7 / 53.5-67.5 | 50.7 / 35.5-69.5 | 60.6 / 49.0-74.0 | 71.5 / 56.5-77.5 | 63.8 / 51.5-75.0 | 54.3 / 41.5-60.5 | 62.5 / 48.5-75.5 | 70.8 / 58.0-77.5 | 65.8 / 56.5-73.5 | -- | -- | -- | -- |
| E2[b] | Temp. [°C] | 17.1 / 11.6-21.0 | 20.2 / 16.0-22.2 | 24.3 / 24.1-24.5 | 21.4 / 19.7-25.0 | 20.6 / 18.6-21.4 | 21.2 / 19.8-23.9 | 21.6 / 20.9-22.4 | 19.8 / 17.6-21.6 | 20.0[3] / - | 20.0[3] / - | 20.0[3] / - | 20.0[3] / - | -- | -- | -- | -- |
| | RH [%] | 100.0 / - | 100.0 / - | 100.0 / - | 100.0 / - | 100.0 / - | 100.0 / - | 100.0 / - | 100.0 / - | 100.0 / - | 100.0 / - | 100.0 / - | 100.0 / - | -- | -- | -- | -- |
| E3[c] | Temp. [°C] | -- | -- | 22.2[1] / 12.7-46.2 | 15.3 / 6.2-34.3 | 17.1 / 3.3-25.7 | 17.9 / 6.8-35.3 | 22.0 / 14.5-39.7 | 15.7 / 6.8-31.0 | 13.6 / 4.3-27.0 | 18.3 / 6.6-34.2 | 23.2 / 14.8-40.7 | 15.2 / 3.1-28.8 | 12.7 / 1.4-25.2 | 18.1 / 9.7-33.8 | -- | -- |
| | RH [%] | -- | -- | 66.2[1] / 14.0-100.0 | 78.5 / 11.0-100.0 | 71.0 / 12.0-100.0 | 67.1 / 13.0-100.0 | 66.8 / 20.0-100.0 | 81.6 / 19.0-100.0 | 78.3 / 22.0-100.0 | 73.5 / 24.0-100.0 | 63.7 / 16.0-100.0 | 80.8 / 25.0-100.0 | 77.0 / 22.0-100.0 | 69.5 / 17.0-100.0 | -- | -- |
| E4[3][d] | Temp. [°C] | -- | -- | 18.0 / 7.4-32.4 | 7.8 / −2.8-22.2 | 5.8 / −4.7-18.5 | 10.2 / −3.1-26.7 | 17.1 / 4.8-29.6 | 7.7 / −2.3-24.6 | 6.1 / −4.6-19.2 | 11.5 / −3.6-27.0 | 18.1 / 3.9-29.5 | 6.4 / −3.7-19.5 | 4.3 / −6.4-16.5 | 10.4 / 0.4-24.2 | -- | -- |
| | RH [%] | -- | -- | 60.3 / 4.0-100.0 | 78.8 / 16.0-100.0 | 63.9 / 7.0-100.0 | 71.4 / 5.0-100.0 | 59.4 / 8.0-99.0 | 80.5 / 7.0-100.0 | 75.3 / 4.0-100.0 | 79.6 / 14.0-100.0 | 55.5 / 7.0-100.0 | 82.1 / 13.0-100.0 | 76.1 / 11.0-100.0 | 72.2 / 6.0-100.0 | -- | -- |
| E5[3][e] | Temp. [°C] | -- | -- | 26.1 / 12.6-44.6 | 13.2 / 1.1-33.0 | 10.9 / −1.9-26.2 | 19.3 / 4.7-38.0 | 25.0 / 11.7-39.9 | 14.5 / 3.1-34.7 | 11.6 / 0.3-25.3 | 19.2 / 2.1-39.0 | 26.2 / 11.2-41.4 | 13.8 / −2.3-31.6 | 11.1 / −4.1-29.8 | 19.1 / 3.8-35.4 | -- | -- |
| | RH [%] | -- | -- | 49.1 / 9.0-95.0 | 79.8 / 11.0-100.0 | 69.7 / 14.0-100.0 | 54.6 / 10.0-100.0 | 48.5 / 11.0-100 | 75.8 / 1.04-97.0 | 78.2 / 28.0-100.0 | 66.5 / 11.0-100.0 | 45.9 / 9.0-99.0 | 77.7 / 19.0-100.0 | 74.8 / 21.0-100.0 | 68.4 / 17.0-100.0 | -- | -- |
| E6[a][d] | Temp. [°C] | -- | -- | -- | -- | 12.1 / 1.5-28.5 | 17.9 / 5.0-34.5 | 21.8 / 12.0-36.0 | 13.7 / 3.5-28.0 | 12.6 / 2.0-25.0 | 19.0 / 5.5-25.0 | 22.5 / 11.0-39.5 | 14.2 / 4.0-26.0 | 10.6[2] / −1.1-28.7 | 15.2[2] / 4.3-31.1 | 18.3[5] / 10.8-33.0 | 12.8[2] / 3.3-26.8 |
| | RH [%] | -- | -- | -- | -- | 76.1 / 18.0-100.0 | 69.0 / 26.5-99.0 | 71.0 / 22.0-99.0 | 88.1 / 45.0-100.0 | 82.8 / 38.5-100.0 | 75.8 / 33.5-100.0 | 70.2 / 28.5-99.5 | 86.7 / 42.0-100.0 | 80.7[2] / 23.0-99.0 | 78.1[2] / 26.0-98.0 | 80.4[5] / 23.0-98.0 | 84.8[2] / 22.0-100.0 |

Notes: first line present the mean value and second line includes the extreme values (minimum-maximum); [1]Also included 30 May - 30 June 2018; [2] Values provided by IPMA (IPMA's stations are located 9 km apart from E4, 560 m apart from E5 and 4 km apart from E6); [3] Values obtained from the water's temperature controller equipment installed in this trimester; Sensors: [a]EL-USB-2 EasyLog USB Data Logger (temperature (T) range: -35 to +80 °C; relative humidity (RH) range: 0 to 100%); [b]Carel PT100 Thermocouple (T range: -50 to +250 °C); [c]Thies Clima 1.1005.54.000 (T range: -30 to +70 °C; RH range: 0 to 100%); [d]MicroStep-MIS PT100 (T range: -50 to +70 °C)/MicroStep-RHT175 (RH range: 0 to 100%); [e]Vaisala HUMICAP®HMP155 (T range: -80 to +60 °C; RH range: 0 to 100%.)

The slabs of laboratory environments (E1 and E2) were continuously monitored using an acquisition system while the slabs of outdoor environments (E3 to E6) were manually monitored from time-to-time by performing visits to the experimental stations at key-times. In these cases, the continuous acquisition system was only used during the day of installation.

**2.2. Materials: detailing and mechanical characterization**

This work involved the use of concrete, steel rebars, CFRP strips and an epoxy adhesive. Detailed information about these materials is presented in the next sections.

2.2.1. Concrete

A single ready-mix batch (~12 m$^3$) of concrete with a compressive characteristic strength (cylinder/cube) of 30/37 MPa (C30/37), exposure class XC4(P), water/cement ratio (CL) of 0.40, maximum aggregate size (d$_{max}$) of 12.5 mm, slump class S4 (slump of 160-210 mm) (Eurocode 2) and produced with a portland cement type CEM II/A-L 42.5R (Eurocode 2 (IPQ 2010) and EN 206-1 (CEN 2000)) was used to cast all the cylinders to evaluate the concrete's compressive mechanical properties and full-scale RC slabs for flexural creep tests. Four cylindrical concrete specimens with 150 mm of diameter and 300 mm of height were used to assess the elastic modulus and compressive strength of concrete (28 days after casting) according to NP EN 12390-13:2013 (IPQ 2013) and NP EN 12390-3:2011 (IPQ 2011) standards, respectively. Tab. 2 presents the results obtained for the elastic modulus ($E_{cm}$) and compressive strength ($f_{cm}$).

2.2.2. Steel rebars

Steel rebars of class A400 NR SD (Eurocode 2 (IPQ 2010)) with 8 mm (Ø8) and 6 mm (Ø6) of diameter were used as internal reinforcement of the RC slabs. Two batches of steel were applied (Batch 1 for EBR, MA and GA slabs; Batch 2 for NSM slabs). The tensile properties of steel reinforcement were evaluated according to NP EN ISO 6892-1:2012 (ISO 2012) standard. Four samples of each bar type used, with a total length of 500 mm, were tested. Tab. 2 presents the results obtained for the elastic modulus ($E_s$), yield strength ($f_y$), and ultimate tensile strength ($f_u$).

### 2.2.3. Epoxy adhesive

The commercial cold curing epoxy adhesive with the trademark *S&P Resin 220 epoxy adhesive*, supplied by *S&P® Clever Reinforcement Ibérica Lda* company was employed as bonding agent between CFRP strips and concrete. This adhesive presents an average value of the flexural elastic modulus higher than 7.1 GPa, according to the technical datasheet provided by the supplier (S&P 2015). In this study, the mechanical properties of this adhesive were assessed according to according to ISO 527-2:2012 (ISO 2012) standard, after 7 days of curing at 20 ºC and 55% RH. Tab. 2 presents the results obtained for elastic modulus ($E_a$), tensile strength ($f_a$), and ultimate tensile strain ($\varepsilon_a$).

### 2.2.4. CFRP laminate strips

The CFRP strips produced by *S&P® Clever Reinforcement Ibérica Lda. Company* with the trademark CFK 150/2000 were used in this investigation. These CFRP strips are prefabricated by pultrusion, being composed of unidirectional carbon fibres (with a fibre content superior to 68%) and adhered by a vinyl ester resin matrix. This material shows a black and smooth external surface. Three different rectangular cross-section geometries were used in this work (width × thickness [mm]): (i) 10 × 1.4 (L10), (ii) 50 × 1.2 (L50) and (iii) 100 × 1.2 (L100). These are typical geometries currently adopted in practical applications. According to the mechanical characteristics provided by the supplier, the average value of the elastic modulus is higher than 170 GPa and the characteristic tensile strength is higher than 2000 MPa (S&P 2014). In this work, the CFRP tensile properties were evaluated using six samples for each type of CFRP cross-section geometry according to ISO 527-5:2009 (ISO 2009). Tab. 2 presents the results obtained for the elastic modulus ($E_f$), tensile strength ($f_f$), and ultimate tensile strain ($\varepsilon_f$).

**Tab. 2.** Average results of material characterization.

| Concrete | | $E_{cm}$ [GPa] (CoV [%]) | $f_{cm}$ [MPa] (CoV [%]) | -- |
|---|---|---|---|---|
| (28 days) | | 29.1 (4.7) | 41.5 (4.4) | -- |
| **Steel** | | $E_s$ [GPa] (CoV [%]) | $f_y$ [MPa] (CoV [%]) | $f_u$ [MPa] (CoV [%]) |
| Batch 1 | Ø6 | 209 (7.7) | 551 (0.8) | 635 (0.5) |
| | Ø8 | 220 (1.6) | 544 (1.8) | 670 (0.9) |
| Batch 2 | Ø6 | 228 (3.2) | 604 (0.5) | 698 (0.3) |
| | Ø8 | 241 (5.3) | 548 (3.6) | 687 (0.7) |
| **Adhesive** | | $E_a$ [GPa] (CoV [%]) | $f_a$ [MPa] (CoV [%]) | $\varepsilon_a$ [×10$^{-3}$] (CoV [%]) |
| (7 days) | | 6.5 (3.0) | 19.9 (3.0) | 4.0 (6.2) |
| **CFRP** | | $E_f$ [GPa] (CoV [%]) | $f_f$ [MPa] (CoV [%]) | $\varepsilon_f$ [×10$^{-3}$] (CoV [%]) |
| L10 | | 164 (1.2) | 2405 (3.8) | 14.6 (3.8) |
| L50 | | 190 (9.3) | 2527 (10.8) | 13.3 (13.6) |
| L100 | | 188 (8.0) | 2620 (2.9) | 14.0 (7.6) |

Note: CoV represents the Coefficient of Variation.

## 2.3. Slabs specimens' geometry

Fig. 5 presents the cross-section geometry of the slab's specimens of this investigation. A base RC slab (reference slab) was adopted for all the strengthened specimens (see Fig. 5(a)), with 2600 mm long and a cross-section geometry of 600 mm (width) by 120 mm (height). The bottom steel reinforcement in tension zone was materialized by 5 bars of 8 mm diameter (5Ø8) and the top steel reinforcement in the compression zone was composed of 3 steel bars of 6 mm of diameter (3Ø6). Steel stirrups of 6 mm diameter longitudinally spaced by 300 mm (Ø6@300) were also adopted. A 20 mm concrete cover was set. This base RC slab was strengthened by bonding 2200 mm long CFRP strips with distinct rectangular cross-section geometry according to the strengthening technique used. The main objective of the CFRP strengthening solutions was to double the load carrying capacity of the base RC slab (without CFRP). These slabs were strengthened using the non-prestressed EBR and NSM techniques and the prestressed MA and GA systems.

On the EBR slabs, a CFRP strip with a cross-section of 100 mm wide by 1.2 mm thick was bonded in the concrete cover (see Fig. 5(b)). The NSM system was composed by 4 CFRP strips with a cross-section of 10 mm by 1.4 mm installed inside the concrete cover (see Fig. 5(c)). The application of these systems is easier compared to the prestressed ones. In both the prestressed MA and GA systems, a CFRP strip of 50 mm by 1.2 mm cross-section with a pre-strain level of ~0.4% was adopted (see Fig. 5(b)). After the prestress application, the method of fixing the CFRP strip to concrete is different in these two techniques. The MA system comprises the installation of metallic anchorage plates at the ends of the CFRP strip. These anchorage plates of 200 mm wide and 270 mm long and made of aluminium are fixed to the concrete by anchor bolts and, therefore, a confinement is applied at the ends of the CFRP strip to avoid slippage. The strengthening on MA system is concluded 24 hours removing all the support devices. The GA system is based on the application of the gradient method (after prestressing) at the ends of the CFRP strip. The gradient method consists of the accelerated curing of the epoxy adhesive with high temperatures in a length of 600 mm dived in 3 sectors of 200 mm long each one. The sectors were heated successively, each one by a period of 15 min, after cooling the previous one and releasing a part of the applied force on the CFRP strip (~1/3 in each sector). It should be highlighted that a pre-strain of ~0.4% was imposed, however, a tendency of pre-strain loss was verified after strengthening. Detailed information regarding the prestressed systems can be found in (Correia et al. 2015; Correia et al. 2017).
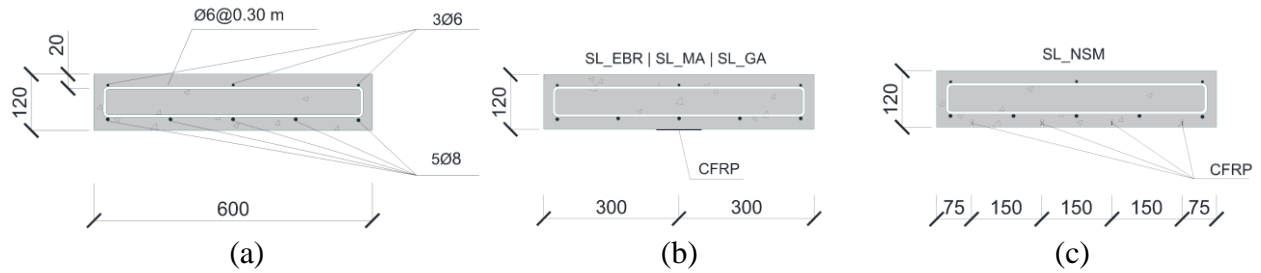
**Fig. 5.** Cross-section geometries of the slabs: (a) base RC slab (reference) (SL_REF); (b) EBR system (SL_EBR), MA system (SL_MA), GA system (SL_GA) and (c) NSM system (SL_NSM). Note: all dimensions in [mm].

## 2.4. Test Methods

2.4.1. Short-term flexural tests - initial characterization

A total of 5 RC slabs were tested in the slab's initial mechanical characterization with monotonic tests up to failure, including one reference base slab (SL_REF) without CFRP strengthening and four strengthened slabs, one per strengthening technique considered (SL_EBR, SL_NSM, SL_MA and SL_GA). Fig. 6 presents a longitudinal view of the slabs specimens and the test configuration adopted on the monotonic tests up to failure, which corresponds to a four-point bending scheme with the two forces applied centrally and spaced 300 mm from the mid-span section. The total span is equal to 2400 mm and the shear span is 900 mm (i.e., 7.5 times the thickness of the slab). The tests were performed using a servo-controlled equipment under displacement control at the internal transducer displacement of the actuator with a rate of 1.2 mm/min. The instrumentation included: (i) one load cell to record the applied load ($F$); (ii) 5 linear variable differential transducers (LVDTs) to monitor the vertical deflection along the longitudinal axis of the slab; (iii) a minimum of 8 strain gauges to measure the strain in the CFRP, steel reinforcement and top concrete. A load cell (maximum measuring capacity of 200 kN and a linearity error of ±0.05%) was placed between the actuator and the steel profile which distribute the load to the point loads. Three of the LVDTs

19

were placed in the pure bending zone (range of ±75 mm and a linearity error of ±0.10%) and the remaining two were installed at mid-distance between the supports and the line of the loads (range of ±25 mm and a linearity error of ±0.10%). For monitor the strains along the CFRP strips and on the bottom steel reinforcement, strain gauges TML BFLA-5-3 were used, whereas for measuring the strains on the concrete, it was applied strain gauges TML PFL-30-11-3L. Two strain gauges, SG1 and SG4 were placed near the end of CFRP strip (in EBR and NSM slabs, 200 mm away from the extremities of the CFRP strip; in the MA slab, 50 mm away from the anchor plate; and, in the GA slab, 50 mm away from the extremity of the gradient zone). Another two strain gauges were adopted: SG2 on the CFRP strip at mid-span and SG3 under the load line. The strain on the bottom steel reinforcement was measured using another strain gauge (SG5) glued at mid-span, on the middle steel rebar (in the transversal direction). The strain on concrete under compression was measured using a strain gauge (SG6) placed at mid-span on the top surface of the slab. The evolution of the crack width was measured in 3 cracks in the pure bending zone using a handheld USB microscope (VEHO VMS-004 D microscope), with a native resolution of 640 × 480 pixels and magnification capacity up to 400 times. In this work, a magnification factor of 20 times was adopted. The measurements were performed up to a pre-defined load to assure the safety of the operator.
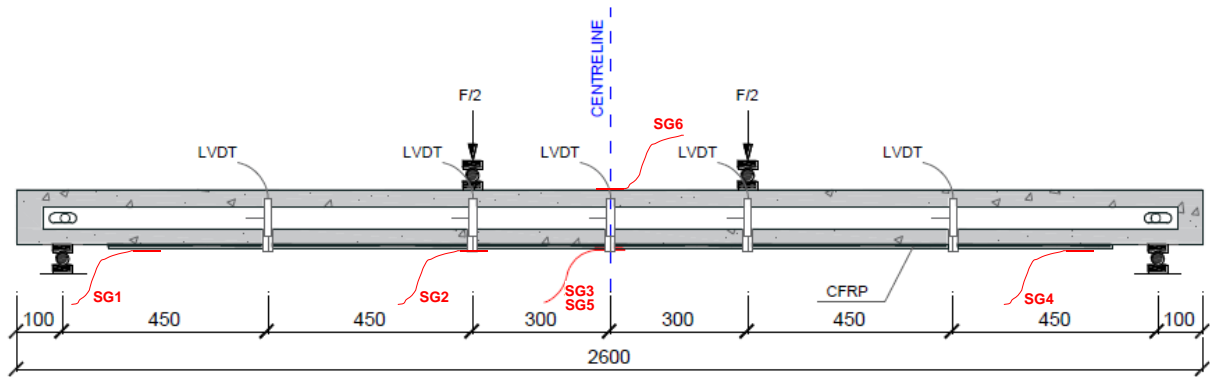
**Fig. 6.** Test configuration adopted in the monotonic tests up to failure. Note: All units in [mm].

### 2.4.2. Durability and long-term flexural creep tests

For study the long-term flexural creep behaviour of the CFRP strengthened slabs, a total of 24 specimens were tested. Each environment complained four slabs, one per strengthening technique. The slabs were submitted to a constant long-term gravity sustained load, as the slabs are usually loaded in real structures. Fig. 7 presents the flexural creep test configuration and the respective instrumentation for the long-term monitoring. This test scheme consists of a four-point bending test configuration similar to the one used in the monotonic tests up to failure (see Section 2.4.1). The total gravity sustained load applied was ~23.8 kN, materialized through a support RC slab (~3.8 kN) installed on the steel bars of the loading points. Two concrete blocks (~10 kN each one) were installed on this support RC slab. To allow rotation of the slab, two steel bars (roll) were placed on top of the supports (granite blocks). The loading points were materialized using two steel (roll) bars, each one placed 300 mm distant from mid-section of the RC slab. To record the mid-span vertical deflection, two devices were used: (i) a LVDT (range of ±75 mm and linearity of ±0.10%), installed permanently in laboratory experimental stations (E1 and E2) and only used in the outdoor environments (E3-E4) during the installation process and, (ii) one mechanical dial

21

gauge (measuring range of 40 mm and graduation value of 0.01 mm).
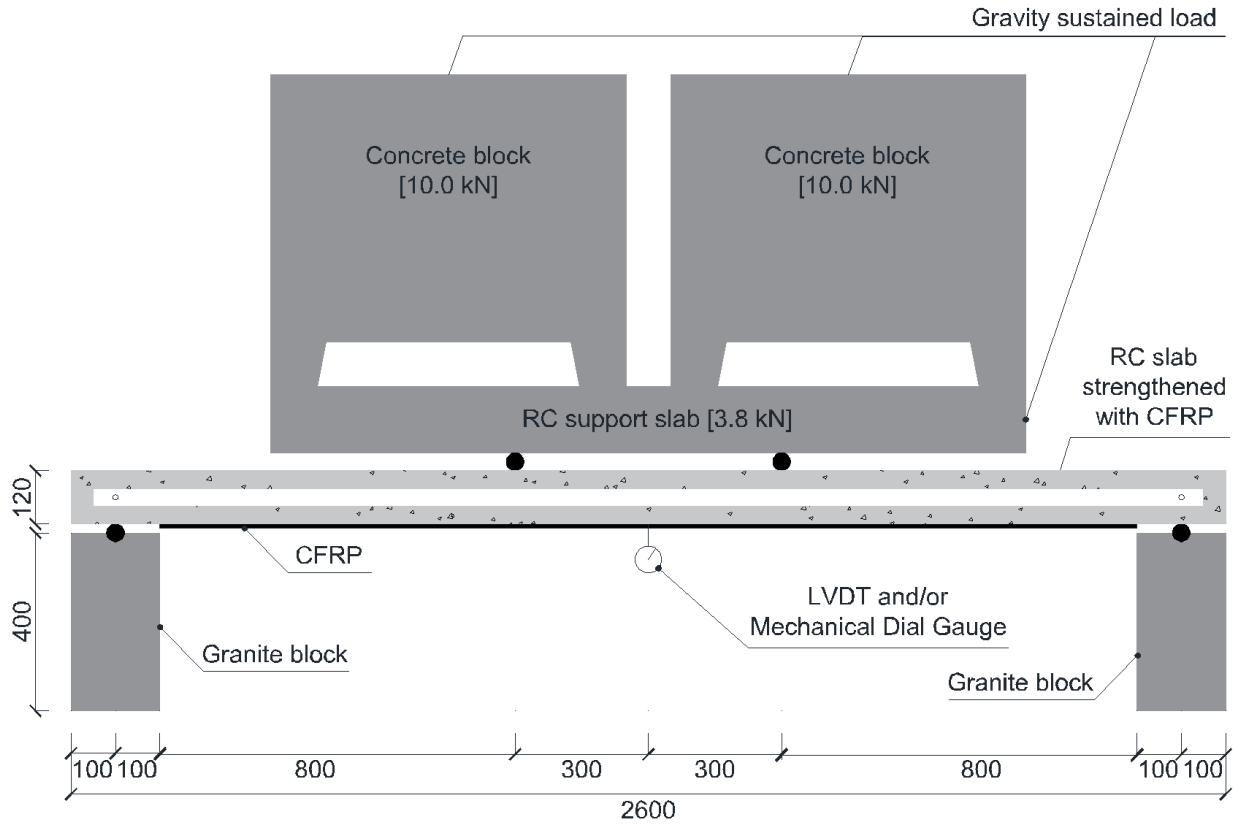


**Fig. 7.** Test configuration adopted for study the synergic effects of creep and 6 different exposure environments. Note: All units in [mm].

## 3. RESULTS AND DISCUSSION

### 3.1. **Short-term flexural test**s

Tab. 3 presents the main results obtained from the monotonic flexural tests up to failure on the slabs of the initial characterization. In this table, $K_I$, $K_{II}$ and $K_{III}$ represent the flexural stiffness at the elastic, cracked and yielding stages, respectively. These parameters were determined by computing the slope of the corresponding branch using two representative points. $F_{cr}$, $F_y$ and $F_{max}$ are the cracking, yielding and maximum loads recorded during the test, respectively. $\delta_{cr}$, $\delta_y$, $\delta_{max}$

22

are the mid-span vertical displacements at $F_{cr}$, $F_y$, $F_{max}$. $\varepsilon_{fmax}$ is the strain attained in the CFRP strip at $F_{max}$; $F_{max}/F_y$ and $\delta_{max}/\delta_y$ are the ductility parameters. Finally, the last column includes the observed failure modes (FM). Fig. 8 presents the relationships of applied force *versus* mid-span vertical displacements obtained. These relationships present the typical behaviour observed in RC slabs strengthened in flexure with CFRP systems, e.g. (Correia et al. 2015; Cruz et al. 2020).

**Tab. 3.** Main results of monotonic tests up to failure of the slabs of initial characterization.

| Specimen | Stiffness | | | Crack initiation | | Yielding | | Failure | | | Efficiency Parameters | | FM |
|---|---|---|---|---|---|---|---|---|---|---|---|---|---|
| | $K_I$ | $K_{II}$ | $K_{III}$ | $\delta_{cr}$ | $F_{cr}$ | $\delta_y$ | $F_y$ | $\delta_{max}$ | $F_{max}$ | $\varepsilon_{fmax}$ | $F_{max}/F_y$ | $\delta_{max}/\delta_y$ | |
| | [kN/mm] | | | [mm] | [kN] | [mm] | [kN] | [mm] | [kN] | [x10$^{-3}$] | [-] | [-] | [-] |
| SL_REF | 7.5 | 1.3 | -- | 1.2 | 12.3 | 19.6 | 28.8 | 120.5 | 31.0 | -- | -- | -- | -- |
| SL_EBR | 10.8 | 1.9 | 1.0 | 1.3 | 12.6 | 24.6 | 53.2 | 41.2 | 66.5 | 6.6 | 1.2 | 1.7 | D |
| SL_NSM | 9.1 | 1.4 | 0.4 | 2.4 | 14.4 | 22.3 | 39.9 | 74.4 | 62.3 | 14.1 | 1.6 | 3.3 | F |
| SL_MA | 10.6 | 1.6 | 0.6 | 2.0 | 20.4 | 22.2 | 49.7 | 79.2 | 67.6 | 12.2 | 1.4 | 3.6 | F |
| SL_GA | 10.0 | 1.6 | 0.6 | 2.0 | 20.0 | 23.3 | 52.0 | 38.3 | 60.0 | 7.0 | 1.2 | 1.6 | D |

Failure Modes (FM): D = CFRP strip debonding; F = CFRP rupture.
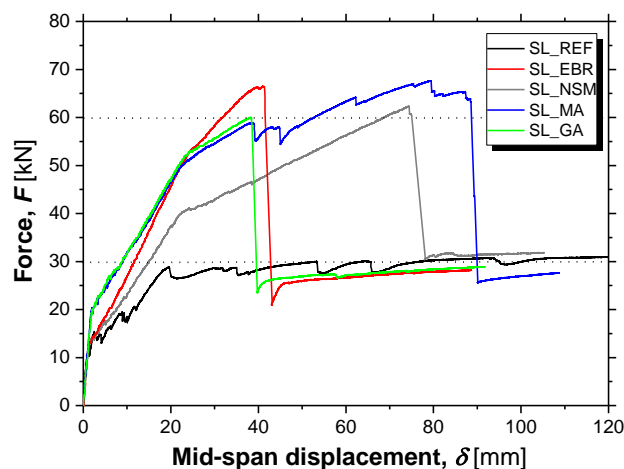


**Fig. 8.** Force *vs.* mid-span displacement obtained on the slabs of short-term tests.

In general, three test stages can be observed, mainly, (i) elastic ($K_I$), (ii) cracked ($K_{II}$) and (iii) post steel yielding ($K_{III}$). Flexural stiffness $K_I$ is similar in all slabs, as low amount of strengthening was adopted. The cracking of the concrete in the cracked phase reduces the flexural stiffness to $K_{II}$. The strengthening delays the crack initiation ($\delta_{cr}$, $F_{cr}$), specially on the prestressed slabs (the cracking force is ~62% higher in prestressed slabs than in the non-prestressed). The steel yielding occurred for a similar load ($F_y$) and mid-span deflections ($\delta_y$) in all the strengthened slabs, except on the SL_NSM, where the $F_y$ was ~77% of the observed in other slabs. This finding can be related with the less flexural stiffness ($K_{II}$) and less effectiveness in the flexural strength provided by the NSM configuration adopted when compared with the other systems used. After steel yielding, the CFRP strengthening plays a relevant role in the flexural stiffness $K_{III}$, as it becomes responsible to carry the additional increments of load (steel exhibits small hardening modulus).

Fig. 9 present the failure modes observed. The slab SL_REF failed by crushing of top concrete at mid-span. SL_EBR and the prestressed slab SL_GA failed by CFRP debonding. SL_NSM failed by CFRP rupture, for the maximum load of 62.3 kN. Similarly, the prestressed slab SL_MA also failed by CFRP rupture when $F_{max} = 67.6$ kN. The two prestressed slabs exhibit a similar behaviour until steel yielding. At this test stage, the debonding of the CFRP laminate starts to occur, however, the metallic anchor plates in the SL_MA avoided the premature detachment of CFRP strip, whereas in the SL_GA (gradient anchorage), the initial CFRP strip debonding was rapidly transformed into the complete strip detachment. The CFRP strengthening allows to increase the ultimate load carrying capacity of the slabs in +115%, +101%, +118% and +94%, respectively for slabs SL_EBR, SL_NSM, SL_MA and SL_GA, in comparison to SL_REF. From the previous values, it can be concluded that the initial objective of double the ultimate load of the SL_REF with the

CFRP strengthening (~60 kN) was generally achieved.



(a)                                                                   (b)

(c)                                                                   (d)
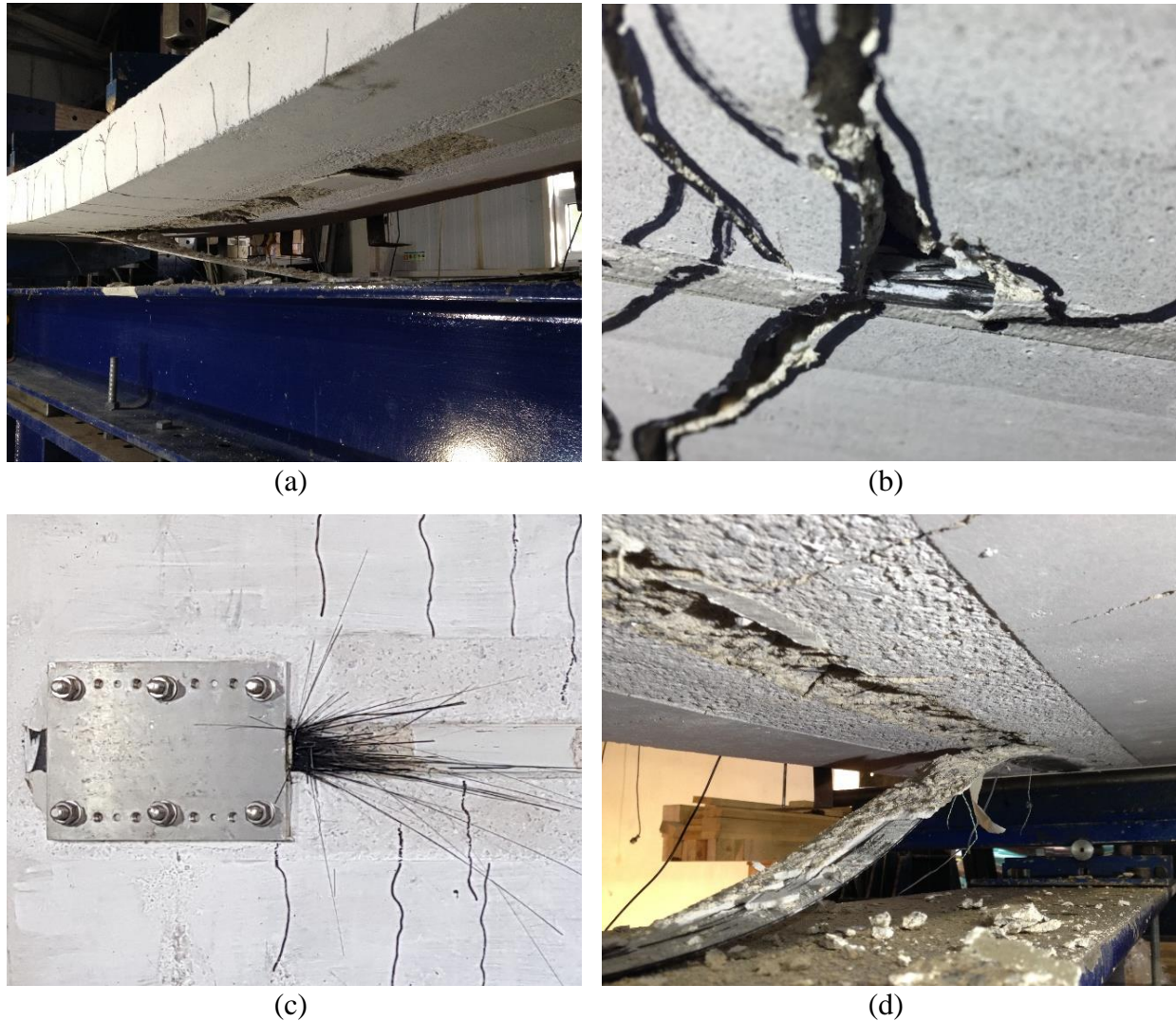
**Fig. 9.** Failure modes observed in monotonic flexural tests up to failure on the CFRP strengthened slabs: (a) SL_EBR: CFRP strip detachment from concrete; (b) SL_NSM: CFRP strips failure; (c) SL_MA: CFRP strip failure; (d) SL_GA: CFRP strip detachment from concrete. Note: SL_REF slab failed by crushing of the top concrete under compression at mid-span.

Fig. 10 presents the relationships between the applied force and strain in the CFRP strip and top concrete under compression in the tested slabs. The ultimate tensile strain was achieved on SL_NSM (1.4%) and SL_MA (1.6%), with a value very close to the ultimate tensile strain of the

CFRP laminate (~1.5%) in the SL_NSM and a value higher than the ultimate tensile strain of the CFRP laminate (~1.3%) in the case of SL_MA. On SL_EBR and SL_GA, the tensile strength of the CFRP strip was not achieved due to the premature detachment of the CFRP strip with a strain of ~0.7% and ~1.1%. Therefore, the strain at the detachment is ~0.4% higher on SL_GA than on SL_EBR, corresponding to the pre-strain level. A higher ultimate strain in the concrete for the prestressed specimens was observed as well as on SL_NSM. Therefore, prestressing of CFRP strips has improved the slab's overall performance and has also assured a more efficient use of the materials.
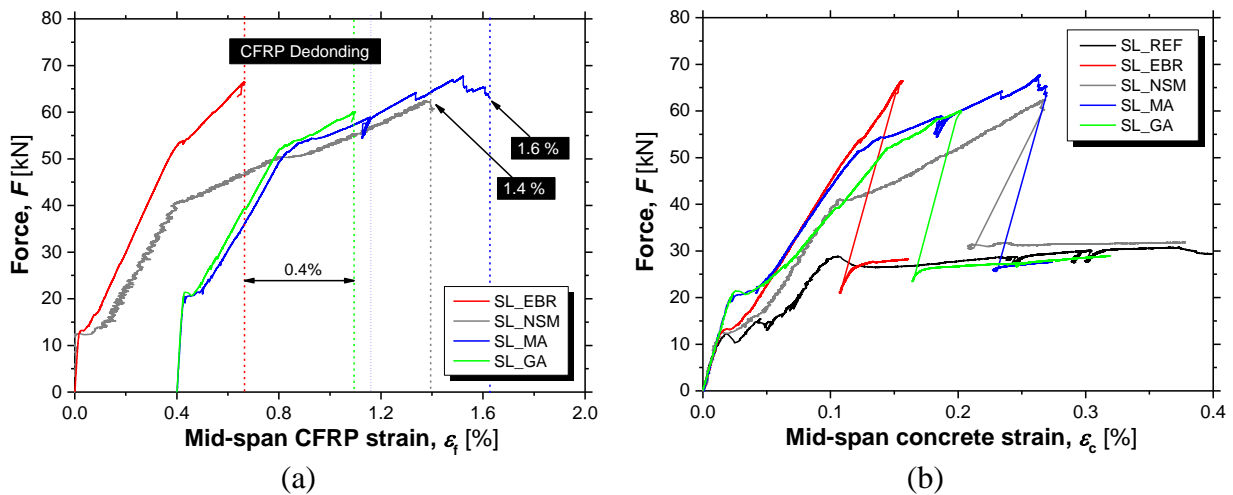


**Fig. 10.** Force *versus* material mid-span strain: (a) CFRP strip and (b) concrete.

### 3.2. Durability and long-term flexural creep tests

Tab. 4 presents the main parameters obtained in the long-term flexural creep tests of the RC CFRP strengthened slabs. In this table, $\delta_{el}$ represents the elastic deformation (mid-span vertical deflection immediately after installing of the gravity sustained load), $\delta_f$ is the total mid-span deflection recorded during the loaded period, $\delta_{cr,f}$ is the corresponding mid-span deflection recorded due to

the creep ($\delta_f$ - $\delta_{el}$), $\phi_f$ is the creep coefficient and finally, $\phi_\infty$ is the predicted long-term creep coefficient. Tab. 4 also presents the time, $t$, in hours, corresponding to the last recorded measurement. The time of the last record was selected as close as possible to the time corresponding to 3 years of testing (~26000 h).

The creep coefficient, $\phi_f$, was computed based on the following expression:

$$\phi_f = \frac{\delta_{cr,f}}{\delta_{el}} = \frac{\delta_f - \delta_{el}}{\delta_{el}} \tag{1}$$

**Tab. 4.** Instantaneous deflections and creep results of the slabs after a three-year of testing.

| Env. | EBR $\delta_{el}$ [mm] | $\delta_f$ [mm] | $\delta_{cr,f}$ [mm] | $\phi_f$ [-] | $\phi_\infty$ [-] | NSM $\delta_{el}$ [mm] | $\delta_f$ [mm] | $\delta_{cr,f}$ [mm] | $\phi_f$ [-] | $\phi_\infty$ [-] | MA $\delta_{el}$ [mm] | $\delta_f$ [mm] | $\delta_{cr,f}$ [mm] | $\phi_f$ [-] | $\phi_\infty$ [-] | GA $\delta_{el}$ [mm] | $\delta_f$ [mm] | $\delta_{cr,f}$ [mm] | $\phi_f$ [-] | $\phi_\infty$ [-] | Time [h] |
|---|---|---|---|---|---|---|---|---|---|---|---|---|---|---|---|---|---|---|---|---|---|
| E1 | 7.3 | 14.2 | 6.8 | 0.9 | 1.0 | 10.3 | 19.3 | 8.9 | 0.9 | 0.9 | 4.7 | 10.4 | 5.7 | 1.2 | 1.3 | 4.4 | 10.7 | 6.2 | 1.4 | 1.5 | 26304 |
| E2 | 8.3 | 13.4 | 5.0 | 0.6 | 0.6 | 11.3 | 18.6 | 7.3 | 0.7 | 0.7 | 4.8 | 10.5 | 5.8 | 1.2 | 1.3 | 5.1 | 9.7 | 4.6 | 0.9 | 1.0 | 27696 |
| E3 | 8.4 | 17.4 | 9.0 | 1.1 | 1.1 | 11.0 | 21.6 | 10.6 | 1.0 | 1.0 | 4.8 | 13.4 | 8.6 | 1.8 | 2.1 | 4.6 | 15.1 | 10.5 | 2.3 | 2.5 | 26208 |
| E4 | 8.5 | 17.0 | 8.4 | 1.0 | 1.1 | 12.1 | 21.8 | 9.7 | 0.8 | 0.9 | 5.1 | 13.7 | 8.6 | 1.7 | 1.8 | 5.3 | 14.2 | 8.9 | 1.7 | 1.8 | 26568 |
| E5 | 7.9 | 16.8 | 8.9 | 1.1 | 1.2 | 12.1 | 23.9 | 11.8 | 1.0 | 1.1 | 5.7 | 15.6 | 9.9 | 1.8 | 1.9 | 4.8 | 15.0 | 10.2 | 2.1 | 2.4 | 26352 |
| E6 | 8.5 | 15.9 | 7.4 | 0.9 | 0.9 | 10.4 | 20.2 | 9.8 | 1.0 | 1.0 | 5.1 | 13.1 | 8.0 | 1.6 | 1.7 | 3.4 | 12.6 | 9.2 | 2.7 | 2.9 | 26448 |
| Average | 8.2 (5.3) | 15.8 (9.5) | 7.6 (18.2) | 0.9 (18.1) | 1.00 (18.9) | 11.2 (6.5) | 20.9 (8.6) | 9.7 (14.4) | 0.9 (13.3) | 0.9 (13.0) | 5.0 (6.6) | 12.8 (14.2) | 7.8 (19.9) | 1.5 (15.7) | 1.7 (18.4) | 4.6 (13.2) | 12.9 (16.2) | 8.3 (25.8) | 1.8 (32.0) | 2.0 (33.0) | -- |

Note: the values between parentheses are the Coefficients of Variation (CoV (%)).

As detailed in section 2.4.2, the monitoring of the mid-span deflection included a reductant system composed by LVDTs and mechanical dial gauges on environments E1 and E2. In the case of the outdoor environments, the same redundant system was used only during the installation phase. Thus, the LVDTs were removed at the end of the installation work. The use of LVDTs during the installation allowed to confirm the accuracy of the measurements provided by the mechanical dial gauges. Fig. 11 presents of the results obtained with both measurement systems, where the

27

mid-span deflection is plotted against the time for slabs of E1 and E2 environments up to ~26000h.

As can be seen, both systems provide similar values.
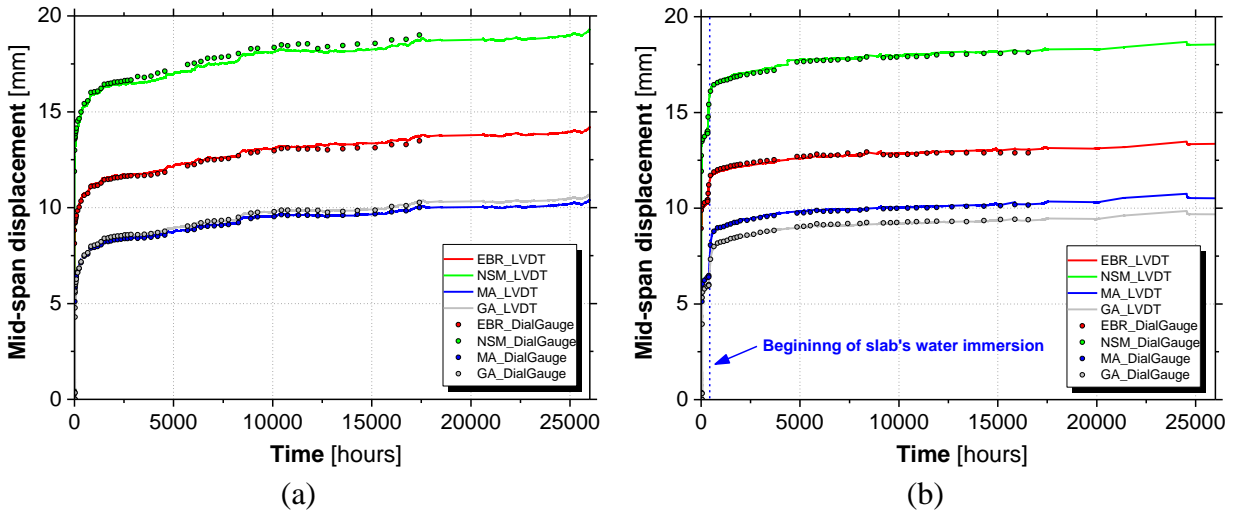


**Fig. 11.** Comparison of the mid-span displacement records provided by LVDTs and mechanical dial gauges for the (a) E1 and (b) E2 environments.

The elastic deformations ($\delta_{el}$) are, in general, in agreement with the expected elastic deformation provided by the quasi-static monotonic flexural tests up to failure of the short-term characterization (see Section 2.4.1). In environment E2, an abrupt increase on the mid-span displacement at about 350 hours of the slab's creep tests was registered due to the water immersion (see Fig. 11(b)). The existence of cracks in the bottom of the slab causes differential water absorption, and consequently volumetric variation, yielding to this steepest displacement growth. Water immersion also causes other minor effects on the vertical displacement, namely by opposing the self-weight of the slab with the water uplift (approximately 1.8 kN), and by promoting a re-adjustment in the supports.

Fig. 12 presents the evolution of the mid-span displacement along the time (up to ~26000 hours)

as function of (i) strengthening system and (ii) the environment. In general, the typical primary and secondary creep stages were observed. The primary creep stage had the duration of ~3000 hours, whereas the secondary creep stage was observed during the remaining duration of the creep test. Fluctuations in the mid-span deflection can be observed along the time, mainly in outdoor due to the variations in the local temperature and relative humidity.
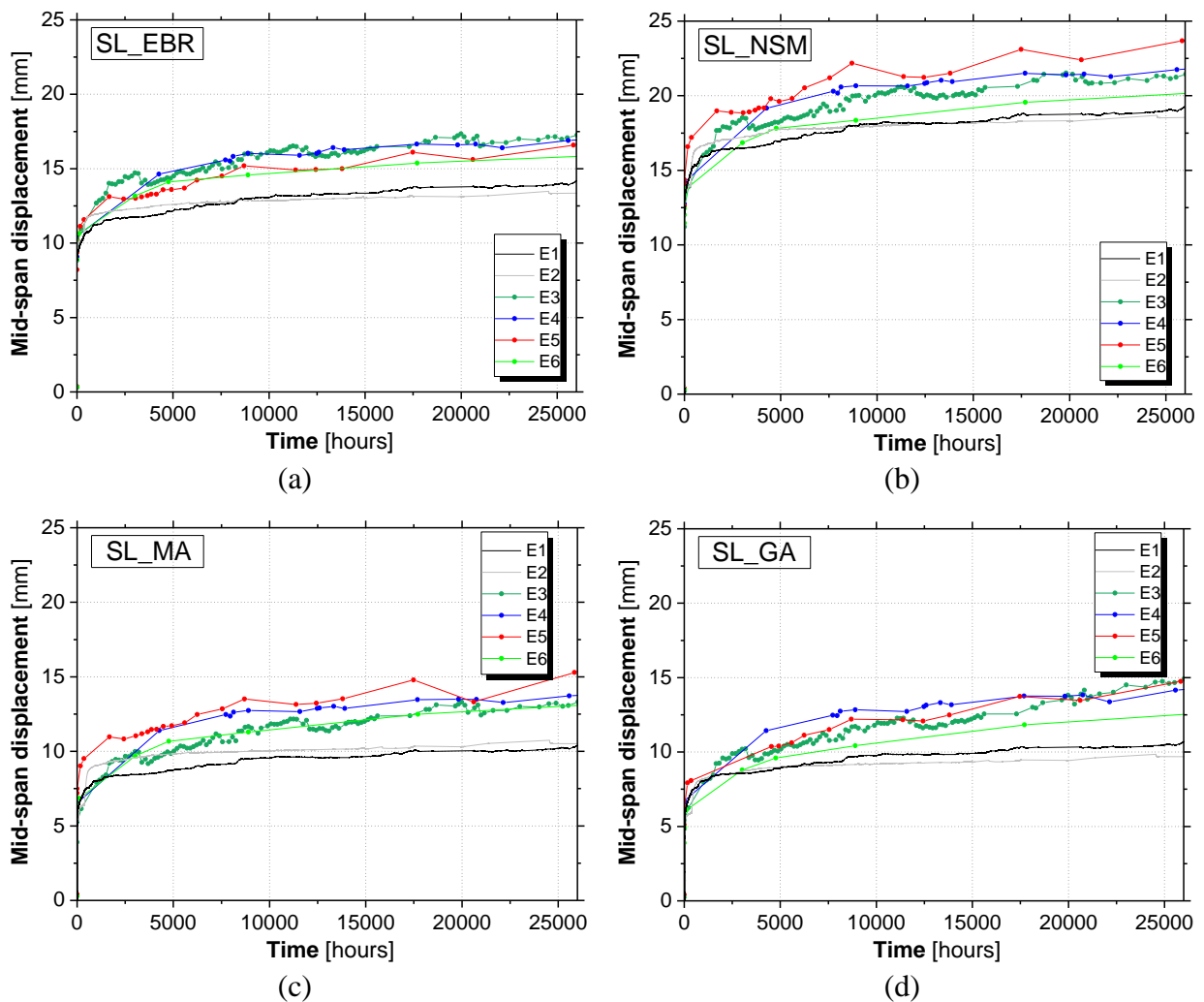


**Fig. 12.** Evolution of the mid-span displacement per strengthening technique in each environment: (a) EBR; (b) NSM; (c) MA and (d) GA.

*Influence of the environment*

The slabs of environments E1 and E2 present the smallest mid-span displacement growth overtime. The immersion of E2 slabs causes a sudden increase of the mid-span displacement. Nevertheless, this increase does not reflect a higher mid-span displacement in the final stages of the creep tests (~3 years). The creep coefficient is lower in slabs of E2 environment than in slabs of E1 environment. This finding is probably related with the better performance of the top concrete under compression in the E2 slabs due to the higher humidity faced, which has been attributed as the main responsible by the creep displacements in this type of structures. It seems that humidity does not affect neither the performance CFRP laminate and adhesive nor the interfaces between the constitutive materials.

With the data collected during the first three years of exposure, it is not clear which outdoor environment accelerates more the creep displacements. In general, slabs exposed to outdoor environments (E3 to E6) have higher mid-span vertical displacement growth than laboratory slabs (E1 and E2), which might be caused by the temperature and relative humidity fluctuations. As demonstrated by Li et al. (2021), the presence of humidity increases the mid-span deflection.

The E5 environment has caused the higher creep coefficients on non-prestressed slabs (EBR and NSM) whereas on prestressed slabs, the maximum creep coefficients were verified in E3 and E6 environments, respectively for MA and GA slabs. It should be stressed that a higher creep coefficient was also obtained for GA slab on E3 environment. Therefore, it seems that creep on non-prestressed slabs accelerates with higher temperatures whereas on non-prestressed slabs, the environments with a combination of elevated temperatures/humidity are responsible for higher

creep effects. On the contrary, the lower creep coefficients were obtained for E4 and E6 environments, which can indicate that environments with longer periods of significant humidity reduces the creep impact. A pronounced mid-span increase on the GA slab of E3 environment verified that starts ~17500 h after loading and culminates on the failure of this slab by CFRP detachment ~26000 h (3 years) after loading (see Fig. 13). This premature failure can be a result of prestress on the CFRP, loading condition as well as it can result from the temperature cycles faced by this slab which could cause different thermal expansion in the materials at the interfaces and therefore accelerate the CFRP detachment. It should be highlighted that, in the study conducted by Breveglieri and Czaderski (Breveglieri and Czaderski 2022) using also slabs strengthened with the GA system under sustained load in outdoor conditions, the CFRP detachment was also observed. Final remark for the substantial difference in the midspan displacement value recorded on the failure (~15 mm) when compared with the midspan displacement obtained at failure on the GA slab of the short-term flexural tests (~38 mm).



**Fig. 13.** CFRP detachment on GA slab of E3 environment ~26000 h (3 years) after loading.

*Influence of the strengthening system*

The elastic deformation ($\delta_{el}$) was higher on non-prestressed slabs, as expected. Higher $\delta_{el}$ values were obtained on NSM (~11.2 mm) slabs than on EBR (~8.2 mm). The $\delta_{el}$ obtained on prestressed slabs is lower than on non-prestressed slabs, being similar for both types of techniques used: MA (~5.0 mm) and GA (~4.6 mm). As mentioned before, $\delta_{el}$ values are very similar to the values of the midspan vertical displacement obtained on the short-term flexural tests for a force corresponding to the value of the gravity load (~23.5 kN) installed on the slabs. Additionally, although a CFRP laminate with a larger width (of 100 mm) have been applied on EBR slabs, the $\delta_{el}$ obtained on MA/GA (CFRP laminate 50 mm wide) slabs is substantially lower than the $\delta_{el}$ of EBR slabs due to effect of prestress itself, including camber deflection (~0.6 mm).

The average mid-span deflection due to the creep ($\delta_{cr,f}$) is similar in EBR (~7.6 mm), MA (~7.8 mm) and GA (~8.3 mm) slabs. A higher $\delta_{cr,f}$ was obtained on NSM slabs (~9.7 mm), which reveals higher creep deflections with the NSM solution designed. The creep coefficient ($\phi_f$) is higher with the prestressed systems MA (~1.54) and GA (~1.84) than with non-prestressed solutions EBR (~0.93) and NSM (~0.87). It should be highlighted that the creep coefficient is highly influenced by the $\delta_{el}$, which is the lowest with prestressed slabs. The $\phi_f$ tends to be higher on EBR than on NSM, nevertheless, the obtained values are very close. Therefore, a tendency for higher creep behaviour was observed on the prestressed solutions, with less performance on GA system than on MA system, probably by the higher capacity of the mechanical anchorage (steel plates) than of the gradient anchorage (accelerated curing of the adhesive). Therefore, although prestressing leads to the lowest long-term mid-span deflection ($\delta_f$), the creep coefficient in these specimens is the highest. In general, similar behaviour was observed on the prestressed slabs in

each environment.

*Creep coefficients and existing design guidelines*

The additional time-dependent deflection resulting from creep and shrinkage of a RC concrete element can be calculated by the following expression provided by the ACI 318-19 standard (ACI 2019):

$$\delta_{\text{creep}} = \frac{S}{1 + 50.\,\rho'} \cdot \delta_{\text{el}} \tag{2}$$

being $S$ a time-dependent factor and $\rho'$ the compression reinforcement ratio, obtained from the following expression:

$$\rho' = \frac{A_s'}{b.\,d} \tag{3}$$

being $A_s'$ the area of the compression reinforcement, $b$ the width of the cross-section of the RC slabs and $d$ the distance between the top compression fibre and the centroid of the longitudinal tensile reinforcement.

Considering the exposure time of this study (3 years), the AC1 318-19 standard (ACI 2019) predicts a creep coefficient of ~1.7 for non-prestressed flexural members, by interpolating the time-dependent factor $S$. Considering the values provided in Tab. 4, the value provided in AC1 318-19 is more close to the prestressed systems than to the non-prestressed systems, which means that the creep of concrete is more pronounced in the prestressed systems, being the main responsible by the creep deflection is this cases. This standard does not account for the prestressed systems and, also,

the influence of the type of environmental exposure faced by the structure on the creep coefficient.

The long-term creep coefficient, $\phi_\infty$ (see Tab. 4) was estimated considering the experimental results plotted as the inverse of the time by applying a linear fitting procedure. The values obtained varied between the large range of 0.64 and 2.93. As expected, the values estimated in E2 are lower than the ones of E1 and the values of outdoor environments are higher than the values of laboratory environments. Other authors have already studied the long-term deflection of RC elements strengthened with non-prestressed CFRP laminates, e.g. (Arockiasamy et al. 2000; Al Chami et al. 2009), obtaining smaller creep coefficients than the AC1 318-19 standard. In fact, according to Al Chami et al. (2009), the long-term creep coefficient should be ~1.2.

Fig. 14 presents the creep coefficients obtained after 3 years of exposure ($\phi_f$) and the long-term creep coefficient ($\phi_\infty$). Additionally, for comparison proposes, it is also presented the expected long-term creep coefficient for RC elements according to the AC1 318-19, and long-term creep coefficient for RC elements strengthened with CFRP according to the work performed by Al Chami et al. (Al Chami et al. (2009)).

First, it can be observed that both slabs with non-prestressed systems (EBR and NSM) presented lower creep coefficients than prestressed ones (MA and GA) as well lower values than the ones expected in the literature. In fact, the mid-span displacement evolution due to creep over the time is similar across all externally bonded slabs (EBR, MA, and GA) and slightly higher with the NSM slabs (see Fig. 12). The prestressed slabs have shown higher creep coefficients due to their significantly lower elastic mid-span deflections than on non-prestressed slabs. However, the results

obtained only surpass the value provided by AC1 318-19 mainly in GA slabs of E3, E5 and E6 environments. Therefore, in general, the creep deflections of the slabs were within an expected range.
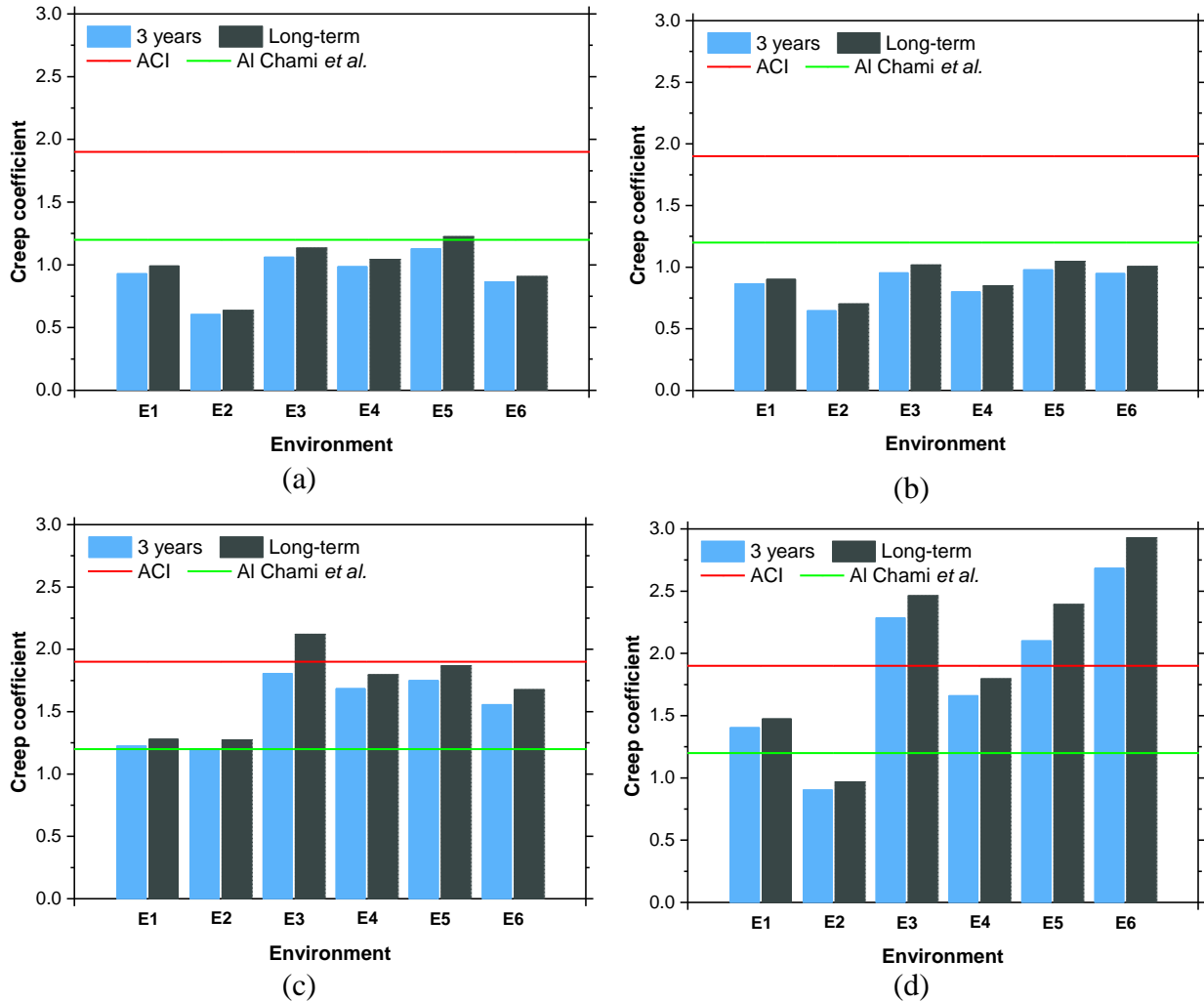


**Fig. 14.** Creep coefficients after 3 years ($\phi_f$) and long-term creep coefficients ($\phi_\infty$) of the slabs: (a) EBR; (b) NSM; (c) MA and (d) GA.

It should be noted that the creep coefficient is higher in outdoor slabs (E3-E6) than in the laboratory slabs (E1 and E2), especially with prestressed systems. With the non-prestressed systems, similar

results were obtained on E1 and outdoor (E3-E6) slabs. A small tendency of higher creep coefficients can be observed in slabs of E3 and E5 environments. On the contrary, the lower creep coefficients were obtained for E2 slabs. Although, there is not a clear environment that led to higher creep coefficients, the temperature and humidity fluctuations aligned with other chemical (e.g., presence of chlorides) and physical agents (e.g., freeze-thaw cycles), have a significant effect on the creep displacements.

In general, the long-term creep coefficient is slightly higher than the 3-year creep coefficient. This outcome is an indicator that the creep displacement is stabilizing with the increase in time.

## 4. CONCLUSIONS

This investigation addressed the long-term flexural behaviour of RC slabs strengthened with CFRP laminate systems under different accelerated and natural environmental conditions. Non-prestressed (EBR and NSM) and prestressed (MA and GA) strengthening solutions were studied. A reference (control) environment (E1) and an environment consisting in water immersion (E2), both under controlled exposure conditions were adopted in this work. To evaluate the effects of the natural exposure, four outdoor environments were considered for inducing ageing targeting carbonation (E3), freeze-thaw attack (E4), elevated temperatures (E5), and airborne chlorides from the ocean seawater (E6). The load carrying capacity of the RC slabs with the distinct strengthening solutions and of a RC slab without CFRP strengthening was assessed by performing short-term flexural tests at an early stage. These tests allowed to confirm the load carrying capacity designed for the slabs and therefore set the level of sustained load to install on the durability and long-term flexural creep tests. The synergic effects of a continuous stress state imposed by a gravity sustained

loading and of specific type of an environmental exposure (6 types) was evaluated by means of the slabs' flexural creep tests. The time-dependant flexural behaviour of the slabs was monitored being controlled the mid-span deflection. Finally, for each type of strengthening, the creep coefficient for 3 years of exposure was estimated as well as the long-term creep coefficient. Therefore, the following conclusions can be pointed out:

- The load carrying capacity obtained on the short-term flexural tests confirmed the objective of double the load carrying capacity of the non-strengthened RC slab; the cracking load is similar on the non-strengthened RC slab and non-prestressed solutions EBR and NSM whereas the prestressed solutions MA and GA allowed to increase the cracking load; the yielding load was similar on the non-prestressed EBR slab and prestressed MA and GA whereas non-prestressed NSM solution has recorded the lowest cracking load;

- The failure modes observed on the short-term flexural tests include the debonding of the CFRP laminate strip from the concrete on EBR and GA slabs and the CFRP laminate rupture by achievement of its maximum tensile strength on NSM and MA system; The non-strengthened REF slab failed by crushing at the mid-span's top concrete under compression;

- On the long-term flexural creep test in the distinct environments, the laboratory slabs present the smallest mid-span displacement growth overtime, with a creep coefficient lower in E2 slabs than in E1slabs. This finding can indicate that humidity does not affect neither the performance CFRP laminate of adhesive nor the interfaces between the materials.

- The slabs on outdoor environments have a higher mid-span displacement increase than laboratory slabs, probably due the temperature and relative humidity effects. None of the

outdoor environments has shown a clear increase on the creep displacements after a three-year exposure than the others; Nevertheless, it is clear the existence of higher creep coefficients on outdoor slabs than on laboratory slabs.

- Higher creep coefficients were obtained on the prestressed systems (MA and GA) than with non-prestressed solutions (EBR and NSM). The EBR slabs presented higher creep coefficient values than NSM. Therefore, a higher creep behaviour was found with the prestressed solutions (with better performance with MA system than with GA system); Nevertheless, in general, similar time-dependent behaviour was observed on the prestressed slabs (MA and GA);

- Comparing the long-term creep coefficients obtained in this work with the ones provided by the literature including existing guidelines, it can be concluded that only in a reduced number of environments/strengthening solution, the former surpasses the latter, mainly on prestressed GA slabs of the outdoor environments.

**REFERENCES**

ACI (American Concrete Institute). 2019. *Building Code Requirements for Structural Concrete*, ACI 318-19. An ACI Standard. American Concrete Institute. Farmington Hills (MI).

Al Chami, G., Thériault, M., and Neale, K. W. 2009. "Creep behaviour of CFRP-strengthened reinforced concrete beams." *Construction and Building Materials*, 23(4), 1640-1652.

Arockiasamy, M., Chidambaram, S., Amer, A., and Shahawy, M. 2000. "Time-dependent deformations of concrete beams reinforced with CFRP bars." *Composites Part B: Engineering*, 31(6), 577-592.

Ashraf, W. 2016. "Carbonation of cement-based materials: Challenges and opportunities." *Construction and Building Materials*, 120, 558-570.

Blaschko, M., and Zehetmaier, G. 2008. "Strengthening the Röslautal Bridge Using Innovative Techniques, Germany." *Structural Engineering International*, 18(4), 346-350.

Breveglieri, M., and Czaderski, C. 2021. "RC slabs strengthened with externally bonded CFRP strips under long-term environmental exposure and sustained loading. Part 2: Laboratory experiments." *Composites Part C: Open Access*, 6, 100210.

Breveglieri, M., and Czaderski, C. 2022. "Reinforced concrete slabs strengthened with externally bonded carbon fibre-reinforced pol-ymer strips under long-term environmental exposure and sustained loading. Part 1: outdoor experiments." *Composites Part C: Open Access 2021.*, 7.

CEN (European Committee for Standardization). 2000. *EN 206-1. Concrete — Part 1: Specification, performance, production and conformity*, European Committee for Standardization (CEN). 2000.

Correia, L., Sena-Cruz, J., Michels, J., França, P., Pereira, E., and Escusa, G. 2017. "Durability of RC slabs strengthened with prestressed CFRP laminate strips under different environmental

and loading conditions." *Composites Part B: Engineering*, 125, 71-88.

Correia, L., Teixeira, T., Michels, J., Almeida, J. A. P. P., and Sena-Cruz, J. 2015. "Flexural behaviour of RC slabs strengthened with prestressed CFRP strips using different anchorage systems." *Composites Part B: Engineering*, 81, 158-170.

Cruz, J. R., Seręga, S., Sena-Cruz, J., Pereira, E., Kwiecień, A., and Zając, B. 2020. "Flexural behaviour of NSM CFRP laminate strip systems in concrete using stiff and flexible adhesives." *Composites Part B: Engineering*, 195, 108042.

Cruz, R., Correia, L., Cabral-Fonseca, S., and Sena-Cruz, J. 2022. "Durability of Bond between NSM CFRP Strips and Concrete under Real-Time Field and Laboratory Accelerated Conditioning." *Journal of Composites for Construction*, 26(6), 04022074.

Cruz, R., Correia, L., Dushimimana, A., Cabral-Fonseca, S., and Sena-Cruz, J. 2021. "Durability of Epoxy Adhesives and Carbon Fibre Reinforced Polymer Laminates Used in Strengthening Systems: Accelerated Ageing versus Natural Ageing." *Materials*, 14(6), 1533.

Deng, J., Li, X., Wang, Y., Xie, Y., and Huang, C. 2021. "RC beams strengthened by prestressed CFRP plate subjected to sustained loading and continuous wetting condition: Flexural behaviour." *Construction and Building Materials*, 311, 125290.

El-Hacha, R., and El-Badry, M. 2001. *Strengthening Concrete Beams with Externally Prestressed Carbon Fiber Composite Cables*.

El Maaddawy, T., Soudki, K., and Topper, T. 2007. "Performance Evaluation of Carbon Fiber-Reinforced Polymer- Repaired Beams Under Corrosive Environmental Conditions." *Aci Structural Journal*, 104, 3-11.

Fernandes, P., Sena-Cruz, J., Xavier, J., Silva, P., Pereira, E., and Cruz, J. 2018. "Durability of bond in NSM CFRP-concrete systems under different environmental conditions." *Composites Part B: Engineering*, 138, 19-34.

Frigione, M., and Rodríguez-Prieto, A. 2021. "Can Accelerated Aging Procedures Predict the Long Term Behavior of Polymers Exposed to Different Environments?" *Polymers*, 13(16), 2688.

Hassan, S. A., Gholami, M., Ismail, Y. S., and Sam, A. R. M. 2015. "Characteristics of concrete/CFRP bonding system under natural tropical climate." *Construction and Building Materials*, 77, 297-306.

Hong, S., and Park, S.-K. 2016. "Long-term behavior of fiber-reinforced-polymer-plated concrete beams under sustained loading: Analytical and experimental study." *Composite Structures*, 152, 140-157.

IPQ (Instituto Português da Qualidade). 2010. *NP EN EN 1992-1-1. Eurocode 2: design of concrete structures - Part 1-1: general rules and rules for buildings*, Instituto Português da Qualidade (IPQ). Caparica, Portugal. 2010.

IPQ (Instituto Português da Qualidade). 2011. *NP EN 12390-3. Testing Hardened Concrete. Part 3: Compressive Strength of Test Specimen*, Instituto Português da Qualidade (IPQ). Caparica, Portugal. 2011.

IPQ (Instituto Português da Qualidade). 2013. *NP EN 12390-13. Testing Hardened Concrete. Part 13: Determination of Secant Modulus of Elasticity in Compression*, Instituto Português da Qualidade (IPQ). Caparica, Portugal. 2013.

ISO (International Organization for Standardization). 2009. *ISO 527-5. Plastics—Determination of Tensile Properties. Part 5: Test Conditions for Unidirectional Fibre-Reinforced Plastic Composites*, International Organization for Standardization (ISO): Genève, Switzerland,

2009.

ISO (International Organization for Standardization). 2012. *ISO 527-2. Plastics—Determination of Tensile Properties. Part 2: Test Conditions for Moulding and Extrusion Plastics*, International Organization for Standardization (ISO): Genève, Switzerland, 2012.

ISO. 2012. "NP EN ISO 6892–1. Metallic materials. Tensile testing. Part 1: method of test at room temperature. Instituto Português da Qualidade (IPQ). Caparica, 2012."

Kabir, M. I., Shrestha, R., and Samali, B. 2016. "Effects of applied environmental conditions on the pull-out strengths of CFRP-concrete bond." *Construction and Building Materials*, 114, 817-830.

Karbhari, V. M., Chin, J. W., Hunston, D., Benmokrane, B., Juska, T., Morgan, R., Lesko, J. J., Sorathia, U., and Reynaud, D. 2003. "Durability gap analysis for fiber-reinforced polymer composites in civil infrastructure." *Journal of Composites for Construction*, 7(3), 238-247.

Lee, J., Kim, J., Bakis, C. E., and Boothby, T. E. 2021. "Durability assessment of FRP-concrete bond after sustained load for up to thirteen years." *Composites Part B: Engineering*, 224, 109180.

Li, X., Deng, J., Wang, Y., Xie, Y., Liu, T., and Rashid, K. 2021. "RC beams strengthened by prestressed CFRP plate subjected to sustained loading and continuous wetting condition: Time-dependent prestress loss." *Construction and Building Materials*, 275, 122187.

Mohd Hashim, M. H., Mohd.Sam, A. R., and Hussin, M. 2016. "Experimental investigation on the effect of natural tropical weather on interfacial bonding performance of CFRP-concrete bonding system." 11, 584-604.

S&P. 2014. "S&P CFRP Laminates. Technical Datasheet."Seewen, Switzerland.

Shin, C. B., and Kim, E. K. 2002. "Modeling of chloride ion ingress in coastal concrete." *Cement and Concrete Research*, 32(5), 757-762.

Tatar, J., and Hamilton, H. R. 2016. "Comparison of laboratory and field environmental conditioning on FRP-concrete bond durability." *Construction and Building Materials*, 122, 525-536.

# ANNEX II – COMPILATION OF TEST RESULTS

## Part 1 – Materials: Concrete

Table 1.1 - Total results of the elastic modulus ($E_{cm}$) compressive strength ($f_{cm}$), tensile strength ($f_{ctm}$), and carbonation depth of concrete, after one (T1) and two (T2) years of exposure to the environment studied (E1 to E6), including the reference (T0).

| Env. | Specimen Number | $E_{cm}$ [GPa] | | | $f_{cm}$ [MPa] | | | $f_{ctm}$ [MPa] | | | Carbonation depth [mm] | | |
|---|---|---|---|---|---|---|---|---|---|---|---|---|---|
| | | T0 | T1 | T2 | T0 | T1 | T2 | T0 | T1 | T2 | T0 | T1 | T2 |
| REF | 1 | - | – | – | 38.80 | – | – | 3.80 | – | – | – | – | – |
| | 2 | 27.56 | – | – | 42.71 | – | – | 3.83 | – | – | – | – | – |
| | 3 | 30.04 | – | – | 42.16 | – | – | 2.63 | – | – | – | – | – |
| | 4 | 29.76 | – | – | 42.29 | – | – | 3.15 | – | – | – | – | – |
| | Average | 29.12 | – | – | 41.49 | – | – | 3.35 | – | – | – | – | – |
| | StDev | 1.36 | – | – | 1.81 | – | – | 0.45 | – | – | – | – | – |
| | Cov (%) | 4.66 | – | – | 4.36 | – | – | 13.28 | – | – | – | – | – |
| E1 | 1 | – | 28.23 | – | – | 41.35 | – | – | 2.65 | 3.16 | – | 8.24 | 7.87 |
| | 2 | – | 28.09 | 29.19 | – | 43.44 | 43.45 | – | 2.66 | - | – | 6.46 | 7.48 |
| | 3 | – | 27.76 | 28.21 | – | 43.66 | 43.01 | – | 3.40 | 3.19 | – | – | – |
| | 4 | – | – | – | – | – | – | – | 2.88 | 3.26 | – | – | – |
| | Average | – | 28.03 | 28.70 | – | 42.82 | 43.23 | – | 2.90 | 3.20 | – | 7.35 | 7.67 |
| | StDev | – | 0.20 | 0.49 | – | 1.04 | 0.22 | – | 0.30 | 0.04 | – | 1.46 | 1.14 |
| | Cov (%) | – | 0.70 | 1.72 | – | 2.43 | 0.51 | – | 10.45 | 1.28 | – | 19.89 | 14.81 |
| E2 | 1 | – | 27.35 | 28.42 | – | 41.06 | 38.88 | – | 2.69 | 2.03 | – | 6.81 | 5.63 |
| | 2 | – | 29.25 | 27.67 | – | 40.40 | 40.06 | – | 2.47 | 2.52 | – | 7.48 | 5.40 |
| | 3 | – | 27.96 | 27.07 | – | 40.74 | 37.33 | – | 2.33 | 2.73 | – | – | – |
| | 4 | – | – | – | – | – | – | – | 2.58 | 2.17 | – | – | – |
| | Average | – | 28.19 | 27.72 | – | 40.73 | 38.76 | – | 2.52 | 2.36 | – | 7.15 | 5.52 |
| | StDev | – | 0.79 | 0.55 | – | 0.27 | 1.12 | – | 0.13 | 0.26 | – | 1.09 | 0.98 |
| | Cov (%) | – | 2.80 | 1.99 | – | 0.66 | 2.88 | – | 5.26 | 11.76 | – | 15.23 | 17.68 |
| E3 | 1 | – | 29.10 | 23.99 | – | 46.12 | 47.68 | – | 3.05 | 2.68 | – | 9.99 | 7.78 |
| | 2 | – | 29.66 | 28.83 | – | 46.90 | – | – | 3.36 | 2.59 | – | 10.20 | 10.72 |
| | 3 | – | 29.40 | 28.28 | – | 46.01 | 44.45 | – | 3.19 | – | – | – | – |
| | 4 | – | – | – | – | – | – | – | 3.15 | 3.21 | – | – | – |
| | Average | – | 29.39 | 27.04 | – | 46.34 | 46.07 | – | 3.19 | 2.83 | – | 10.10 | 9.25 |
| | StDev | – | 0.23 | 2.16 | – | 0.40 | 1.61 | – | 0.11 | 0.27 | – | 0.55 | 1.68 |
| | Cov (%) | – | 0.79 | 8.00 | – | 0.86 | 3.50 | – | 3.56 | 9.70 | – | 5.46 | 18.17 |
| E4 | 1 | – | 27.69 | 33.35 | – | 46.33 | 50.35 | – | 2.88 | 3.00 | – | 7.94 | 8.58 |
| | 2 | – | 28.21 | 24.78 | – | 44.57 | 50.40 | – | 3.09 | – | – | 7.74 | 8.19 |
| | 3 | – | 29.97 | 30.88 | – | 48.47 | 50.77 | – | 2.96 | 2.91 | – | – | – |
| | 4 | – | – | – | – | – | – | – | 3.96 | 3.29 | – | – | – |
| | Average | – | 28.62 | 29.67 | – | 46.45 | 50.51 | – | 3.22 | 3.07 | – | 7.84 | 8.39 |
| | StDev | – | 0.98 | 3.60 | – | 1.60 | 0.19 | – | 0.43 | 0.16 | – | 0.59 | 1.18 |
| | Cov (%) | – | 3.42 | 12.13 | – | 3.44 | 0.37 | – | 13.49 | 5.29 | – | 7.49 | 14.12 |
| E5 | 1 | – | 27.78 | 29.26 | – | 44.28 | 49.35 | – | 3.06 | 3.37 | – | 7.40 | 7.53 |
| | 2 | – | 29.60 | 29.57 | – | 45.37 | 48.58 | – | 3.43 | 3.74 | – | 8.19 | 8.47 |
| | 3 | – | 28.37 | 28.46 | – | 45.15 | 47.96 | – | 2.88 | 2.39 | – | – | – |
| | 4 | – | – | – | – | – | – | – | 3.15 | 2.90 | – | – | – |
| | Average | – | 28.58 | 29.10 | – | 44.93 | 48.63 | – | 3.13 | 3.10 | – | 7.79 | 8.00 |
| | StDev | – | 0.76 | 0.47 | – | 0.47 | 0.57 | – | 0.20 | 0.51 | – | 0.85 | 1.00 |
| | Cov (%) | – | 2.65 | 1.61 | – | 1.04 | 1.18 | – | 6.35 | 16.38 | – | 10.91 | 12.54 |
| E6 | 1 | – | 30.41 | 32.51 | – | 48.91 | 49.55 | – | 2.47 | 2.87 | – | 8.03 | 6.99 |
| | 2 | – | 31.42 | 32.79 | – | 48.71 | 50.09 | – | 2.79 | 3.21 | – | 7.95 | 7.65 |
| | 3 | – | 28.72 | 32.38 | – | 46.33 | 51.10 | – | 2.69 | 2.71 | – | – | – |
| | 4 | – | – | – | – | – | – | – | 2.72 | 2.53 | – | – | – |
| | Average | – | 30.18 | 32.56 | – | 47.98 | 50.24 | – | 2.67 | 2.83 | – | 7.99 | 7.32 |
| | StDev | – | 1.11 | 0.17 | – | 1.17 | 0.64 | – | 0.12 | 0.25 | – | 1.13 | 1.02 |
| | Cov (%) | – | 3.69 | 0.53 | – | 2.45 | 1.28 | – | 4.43 | 8.79 | – | 14.13 | 13.93 |

## Part 2 – Materials: CFRP laminate strips

Table 2.1 - Total values of the elastic modulus (*E*), tensile strength (*f*), and ultimate strain (*ε*) of the L10 CFRP strips, after one (T1) and two (T2) years of exposure to the environment studied (E1 to E6), including the reference (T0).

| Env. | Specimen Number | *E* [GPa] | | | *f* [MPa] | | | *ε* [×10⁻³] | | |
|---|---|---|---|---|---|---|---|---|---|---|
| | | T0 [R1/R2] | T1 | T2 | T0 [R1/R2] | T1 | T2 | T0 [R1/R2] | T1 | T2 |
| REF | 1 | 163.45/166.35 | – | – | 2431.24/2271.84 | – | – | 14.87/13.66 | – | – |
| | 2 | 164.77/166.77 | – | – | 2348.27/2396.83 | – | – | 14.25/14.37 | – | – |
| | 3 | 163.45/161.07 | – | – | 2429.54/2299.79 | – | – | 14.86/14.28 | – | – |
| | 4 | 168.11/163.97 | – | – | 2483.30/2384.69 | – | – | 14.77/14.54 | – | – |
| | 5 | 161.78/163.14 | – | – | 2368.60/2434.67 | – | – | 14.64/14.92 | – | – |
| | 6 | 165.19/164.96 | – | – | 2367.27/2648.66 | – | – | 14.33/16.06 | – | – |
| | Average | 164.42 | – | – | 2405.39 | – | – | 14.63 | – | – |
| | StDev | 1.95 | – | – | 92.61 | – | – | 0.55 | – | – |
| | Cov (%) | 1.19 | – | – | 3.85 | – | – | 3.76 | – | – |
| E1 | 1 | – | 183.60 | 168.00 | – | 2600.47 | 2612.39 | – | 14.16 | 15.55 |
| | 2 | – | 179.82 | 160.71 | – | 2625.19 | 2541.78 | – | 14.60 | 15.82 |
| | 3 | – | 175.41 | 168.42 | – | 2626.09 | 2448.82 | – | 14.97 | 14.54 |
| | 4 | – | 175.84 | 166.98 | – | 2698.91 | 2635.51 | – | 15.35 | 15.78 |
| | 5 | – | 179.32 | 169.77 | – | 2672.74 | 2324.04 | – | 14.90 | 13.69 |
| | 6 | – | 180.42 | 157.46 | – | 2818.98 | 2607.04 | – | 15.62 | 16.56 |
| | Average | – | 179.07 | 165.22 | – | 2673.73 | 2528.26 | – | 14.94 | 15.32 |
| | StDev | – | 2.79 | 4.52 | – | 72.72 | 110.29 | – | 0.48 | 0.94 |
| | Cov (%) | – | 1.56 | 2.73 | – | 2.72 | 4.36 | – | 3.18 | 6.14 |
| E2 | 1 | – | 174.41 | - | – | 2819.77 | 2163.62 | – | 16.17 | 15.54 |
| | 2 | – | 175.56 | 170.05 | – | 2798.34 | 2687.13 | – | 15.94 | 15.80 |
| | 3 | – | 172.57 | 167.25 | – | 2695.21 | - | – | 15.62 | 20.29 |
| | 4 | – | 174.14 | 168.09 | – | 2619.90 | 2434.03 | – | 15.04 | 14.48 |
| | 5 | – | 172.22 | 168.66 | – | 2612.90 | 2445.23 | – | 15.17 | 14.50 |
| | 6 | – | 172.18 | 168.35 | – | 2583.01 | 2567.98 | – | 15.00 | 15.25 |
| | Average | – | 173.51 | 168.48 | – | 2688.19 | 2459.60 | – | 15.49 | 15.98 |
| | StDev | – | 1.27 | 0.91 | – | 92.10 | 174.34 | – | 0.45 | 1.99 |
| | Cov (%) | – | 0.73 | 0.54 | – | 3.43 | 7.09 | – | 2.91 | 12.46 |
| E3 | 1 | – | 179.30 | 169.97 | – | 2736.84 | 2629.25 | – | 15.26 | 15.47 |
| | 2 | – | 173.36 | 174.32 | – | 2605.64 | 2708.04 | – | 15.03 | 15.53 |
| | 3 | – | 179.92 | 173.91 | – | 2842.12 | 2769.19 | – | 15.80 | 15.92 |
| | 4 | – | 177.71 | 169.59 | – | 2780.91 | 2453.11 | – | 15.65 | 14.46 |
| | 5 | – | 171.49 | 173.22 | – | 2871.93 | 2366.71 | – | 16.75 | 13.66 |
| | 6 | – | 178.23 | 170.72 | – | 2917.01 | 2615.01 | – | 16.37 | 15.32 |
| | Average | – | 176.67 | 171.96 | – | 2792.41 | 2590.22 | – | 15.81 | 15.06 |
| | StDev | – | 3.13 | 1.92 | – | 102.00 | 139.53 | – | 0.59 | 0.76 |
| | Cov (%) | – | 1.77 | 1.12 | – | 3.65 | 5.39 | – | 3.76 | 5.08 |
| E4 | 1 | – | 170.77 | 170.45 | – | 2732.86 | 2744.70 | – | 16.00 | 16.10 |
| | 2 | – | 177.60 | 189.73 | – | 2670.47 | 2712.82 | – | 15.04 | 14.30 |
| | 3 | – | 173.19 | 170.93 | – | 2738.21 | 2620.41 | – | 15.81 | 15.33 |
| | 4 | – | 171.65 | 168.15 | – | 2690.10 | 2412.42 | – | 15.67 | 14.35 |
| | 5 | – | 179.20 | - | – | 2903.71 | - | – | 16.20 | - |
| | 6 | – | 176.28 | 172.62 | – | 2809.46 | 2593.55 | – | 15.94 | 15.02 |
| | Average | – | 174.78 | 174.38 | – | 2757.47 | 2616.78 | – | 15.78 | 15.02 |
| | StDev | – | 3.11 | 7.81 | – | 78.71 | 116.53 | – | 0.37 | 0.67 |
| | Cov (%) | – | 1.78 | 4.48 | – | 2.85 | 4.45 | – | 2.34 | 4.46 |
| E5 | 1 | – | 171.13 | 175.51 | – | 2616.55 | 2458.74 | – | 15.29 | 14.01 |
| | 2 | – | 169.78 | 174.80 | – | 2372.26 | 2776.29 | – | 13.97 | 15.88 |
| | 3 | – | 176.50 | 175.42 | – | 2529.86 | 2791.96 | – | 14.33 | 15.92 |
| | 4 | – | 178.37 | 180.18 | – | 2715.08 | 2625.65 | – | 15.22 | 14.57 |
| | 5 | – | 174.93 | 179.28 | – | 2760.76 | 2625.65 | – | 15.78 | 14.65 |
| | 6 | – | 168.87 | 172.36 | – | 2673.85 | 2437.21 | – | 15.83 | 14.14 |
| | Average | – | 173.26 | 176.26 | – | 2611.39 | 2619.25 | – | 15.07 | 14.86 |
| | StDev | – | 3.54 | 2.68 | – | 129.63 | 137.52 | – | 0.70 | 0.77 |
| | Cov (%) | – | 2.04 | 1.52 | – | 4.96 | 5.25 | – | 4.62 | 5.16 |
| E6 | 1 | – | 172.43 | 169.03 | – | 2764.95 | 2437.21 | – | 16.04 | 14.14 |
| | 2 | – | – | 169.68 | – | - | 2676.01 | – | – | 15.83 |
| | 3 | – | 172.35 | 169.20 | – | 2704.88 | 2740.68 | – | 15.69 | 16.15 |
| | 4 | – | – | 162.02 | – | - | 2699.52 | – | – | 15.95 |
| | 5 | – | 166.52 | 158.71 | – | 2651.70 | 2507.57 | – | 15.92 | 15.48 |
| | 6 | – | 171.31 | 163.63 | – | 2548.08 | 2612.61 | – | 14.87 | 16.46 |
| | Average | – | 170.65 | 165 .38 | – | 2667.41 | 2640.40 | – | 15.63 | 15.97 |
| | StDev | – | 2.43 | 4.19 | – | 79.69 | 75.74 | – | 0.45 | 0.30 |
| | Cov (%) | – | 1.42 | 2.53 | – | 2.99 | 2.87 | – | 2.91 | 1.88 |

Notes:

R1 – Roll number 1 of CFRP laminate

R2 – Roll number 2 of CFRP laminate

R1 – used for producing the CFRP strips for environmental ageing; used on the RC slabs strengthened with the NSM tecqnique.

R2 – used on the NSM-CFRP bond specimens.

Table 2.2 - Total values of the elastic modulus ($E_l$), tensile strength ($f_l$), and ultimate strain ($\varepsilon_l$) of the L50 CFRP strips, after one (T1) and two (T2) years of exposure to the environment studied (E1 to E6), including the reference (T0).

| Env. | Specimen Number | $E_l$ [GPa] | | | $f_l$ [MPa] | | | $\varepsilon_l$ [×10³] | | |
|---|---|---|---|---|---|---|---|---|---|---|
| | | T0 [R1/R2/R3] | T1 | T2 | T0 [R1/R2/R3] | T1 | T2 | T0 [R1/R2/R3] | T1 | T2 |
| **REF** | 1 | 2700.25/2717.08/2133.63 | – | – | 196.12/190.00/187.95 | | – | 13.77/14.30/11.35 | – | – |
| | 2 | 2759.70/ 2789.26/2164.67 | – | – | 185.66/175.11/176.65 | | – | 14.86/15.93/12.25 | – | – |
| | 3 | 2504.97/ 2763.60/2138.56 | – | – | 189.88/–/175.47 | | – | 13.19/–/12.19 | – | – |
| | 4 | 2682.28/ 2687.42/2096.87 | – | – | 220.58/171.21/197.24 | | – | 12.16/15.70/10.63 | – | – |
| | 5 | 2538.92/ 2873.45/2080.91 | – | – | 234.00/172.70/177.12 | | – | 10.85/16.64/11.75 | – | – |
| | 6 | –/ 2629.22/2690.21 | – | – | –/181.55/212.15 | | – | –/14.48/12.68 | – | – |
| | Average | 190.21 | – | – | 2526.53 | – | – | 13.30 | – | – |
| | StDev | 17.63 | – | – | 273.71 | – | – | 1.81 | – | – |
| | Cov (%) | 9.27 | – | – | 10.83 | – | – | 13.59 | – | – |
| **E1** | 1 | – | 181.53 | 162.36 | – | 2697.81 | 2436.28 | – | 14.86 | 15.01 |
| | 2 | – | 167.41 | 161.27 | – | 2780.05 | 2469.31 | – | 16.61 | 15.31 |
| | 3 | – | 171.13 | 166.33 | – | 2795.67 | 2546.87 | – | 16.34 | 15.31 |
| | 4 | – | 169.67 | 166.90 | – | 2611.67 | 2474.02 | – | 15.39 | 14.82 |
| | 5 | – | 176.42 | 162.12 | – | 2800.20 | 2504.69 | – | 15.87 | 15.45 |
| | 6 | – | 177.04 | 162.62 | – | 2800.61 | 2553.54 | – | 15.82 | 15.70 |
| | Average | – | 173.87 | 163.60 | – | 2747.67 | 2497.45 | – | 15.81 | 15.27 |
| | StDev | – | 4.87 | 2.18 | – | 70.59 | 42.28 | – | 0.58 | 0.29 |
| | Cov (%) | – | 2.80 | 1.33 | – | 2.57 | 1.69 | – | 3.64 | 1.88 |
| **E2** | 1 | – | 180.74 | 171.59 | – | 2696.21 | 2559.81 | – | 14.92 | 14.92 |
| | 2 | – | 185.16 | 172.26 | – | 2726.82 | 2536.88 | – | 14.73 | 14.73 |
| | 3 | – | 177.52 | 171.72 | – | 2835.52 | 2742.90 | – | 15.97 | 15.97 |
| | 4 | – | 166.57 | 171.15 | – | 2724.68 | 2616.41 | – | 16.36 | 15.29 |
| | 5 | – | 176.44 | 165.96 | – | 2699.49 | 2539.17 | – | 15.30 | 15.30 |
| | 6 | – | 175.70 | 161.66 | – | 2817.72 | 2570.36 | – | 16.04 | 15.90 |
| | Average | – | 177.02 | 169.06 | – | 2750.07 | 2594.26 | – | 15.55 | 15.35 |
| | StDev | – | 5.65 | 3.93 | – | 55.56 | 71.50 | – | 0.61 | 0.46 |
| | Cov (%) | – | 3.19 | 2.32 | – | 2.02 | 2.76 | – | 3.90 | 3.00 |
| **E3** | 1 | – | 179.18 | 176.65 | – | 2731.37 | 2744.18 | – | 15.24 | 15.53 |
| | 2 | – | 171.65 | 171.84 | – | 2850.35 | 2666.01 | – | 16.61 | 15.51 |
| | 3 | – | 179.67 | 176.29 | – | 2858.50 | 2802.24 | – | 15.91 | 15.90 |
| | 4 | – | 175.43 | 175.50 | – | 2700.40 | 2790.46 | – | 15.39 | 15.90 |
| | 5 | – | 165.76 | 174.70 | – | 2783.93 | 2699.38 | – | 16.79 | 15.45 |
| | 6 | – | 173.49 | 174.87 | – | 2744.41 | 2708.56 | – | 15.82 | 15.49 |
| | Average | – | 174.20 | 174.98 | – | 2778.16 | 2735.14 | – | 15.96 | 15.63 |
| | StDev | – | 4.73 | 1.57 | – | 59.27 | 49.00 | – | 0.57 | 0.19 |
| | Cov (%) | – | 2.72 | 0.90 | – | 2.13 | 1.79 | – | 3.59 | 1.22 |
| **E4** | 1 | – | 175.50 | 177.10 | – | 2702.44 | 2750.12 | – | 15.40 | 15.53 |
| | 2 | – | 175.97 | 174.99 | – | 2810.42 | 2869.86 | – | 15.97 | 16.40 |
| | 3 | – | 173.19 | 174.03 | – | 2848.72 | 2624.00 | – | 16.45 | 15.08 |
| | 4 | – | 181.65 | 176.52 | – | 2812.86 | 2653.98 | – | 15.49 | 15.04 |
| | 5 | – | 175.86 | 173.18 | – | 2651.50 | 2590.64 | – | 15.08 | 14.96 |
| | 6 | – | 175.75 | 174.04 | – | 2733.81 | 2728.66 | – | 15.56 | 15.68 |
| | Average | – | 176.32 | 174.98 | – | 2759.96 | 2702.88 | – | 15.66 | 15.45 |
| | StDev | – | 2.57 | 1.41 | – | 69.50 | 93.09 | – | 0.44 | 0.50 |
| | Cov (%) | – | 1.46 | 0.80 | – | 2.52 | 3.44 | – | 2.82 | 3.25 |
| **E5** | 1 | – | 181.05 | 178.28 | – | 2845.06 | 2718.80 | – | 15.71 | 15.25 |
| | 2 | – | 176.53 | 172.33 | – | 2800.23 | 2448.70 | – | 15.86 | 14.21 |
| | 3 | – | 177.16 | 174.14 | – | 2809.61 | 2592.65 | – | 15.86 | 14.89 |
| | 4 | – | 181.24 | 176.99 | – | 2604.64 | 2681.92 | – | 14.37 | 15.15 |
| | 5 | – | 177.15 | 173.74 | – | 2569.60 | 2647.91 | – | 14.51 | 15.24 |
| | 6 | – | 175.70 | - | – | 2692.66 | - | – | 15.33 | - |
| | Average | – | 178.14 | 175.10 | – | 2720.30 | 2618.00 | – | 15.27 | 14.95 |
| | StDev | – | 2.18 | 2.20 | – | 105.50 | 94.28 | – | 0.62 | 0.39 |
| | Cov (%) | – | 1.22 | 1.25 | – | 3.88 | 3.60 | – | 4.05 | 2.62 |
| **E6** | 1 | – | 175.01 | 186.79 | – | 2693.96 | 2682.93 | – | 15.39 | 14.36 |
| | 2 | – | 168.39 | 169.85 | – | 2723.61 | 2381.71 | – | 16.17 | 14.02 |
| | 3 | – | 168.93 | 173.48 | – | 2691.50 | 2556.89 | – | 15.93 | 14.74 |
| | 4 | – | 166.40 | 160.93 | – | 2684.47 | 2525.96 | – | 16.13 | 15.70 |
| | 5 | – | 168.94 | 162.43 | – | 2540.68 | 2717.86 | – | 15.04 | 16.73 |
| | 6 | – | 168.25 | 156.36 | – | 2654.99 | 2458.51 | – | 15.78 | 15.72 |
| | Average | – | 169.32 | 168.31 | – | 2664.87 | 2553.97 | – | 15.74 | 15.21 |
| | StDev | – | 2.68 | 10.02 | – | 59.03 | 117.66 | – | 0.41 | 0.93 |
| | Cov (%) | – | 1.58 | 5.95 | – | 2.22 | 4.61 | – | 2.58 | 6.10 |

Notes:
R1 – Roll number 1 of CFRP laminate
R2 – Roll number 2 of CFRP laminate
R3 – Roll number 3 of CFRP laminate

R1 – used for producing the CFRP strips for environmental ageing; used on the EBR-CFRP bond specimens.
R2 – used on the RC slabs strengthened with the MA and GA techniques.
R3 – not used.

Table 2.3 - Failure modes observed with the L10 CFRP strips, after one (T1) and two (T2) years of exposure to the environment studied (E1 to E6), including the reference (T0).
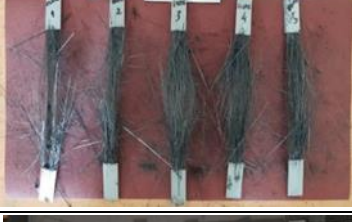
| Env. | Failure Modes – CFRP Laminate Strips L10 | | |
|---|---|---|---|
| | T0 | T1 | T2 |
| REF | N/A | – | – |
| E1 | – |  |  |
| E2 | – |  |  |
| E3 | – |  |  |
| E4 | – |  |  |
| E5 | – |  |  |
| E6 | – |  |  |

Table 2.4 - Failure modes observed with the L50 CFRP strips, after one (T1) and two (T2) years of exposure to the environment studied (E1 to E6), including the reference (T0).

| Env. | Failure Modes – CFRP Laminate Strips L50 | | |
|------|------|------|------|
| | T0 | T1 | T2 |
| REF | N/A | – | – |
| E1 | – |  |  |
| E2 | – |  |  |
| E3 | – |  |  |
| E4 | – |  |  |
| E5 | – |  |  |
| E6 | – |  |  |

## Part 3 – Materials: Epoxy adhesives

Table 3.1 - Total values of the elastic modulus ($E_a$), tensile strength ($f_a$), and ultimate strain ($\varepsilon_a$) of the adhesive S&P Resin 220 epoxy adhesive (ADH1), after one (T1) and two (T2) years of exposure to the environment studied (E1 to E6), including the reference (T0).
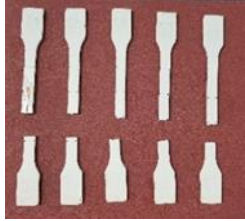
| Env. | Specimen Number | $E_a$ [GPa] | | | $f_a$ [MPa] | | | $\varepsilon_a$ [%] | | |
|---|---|---|---|---|---|---|---|---|---|---|
| | | T0 | T1 | T2 | T0 | T1 | T2 | T0 | T1 | T2 |
| REF | 1 | 6.27 | – | – | 19.40 | – | – | 0.44 | – | – |
| | 2 | 6.50 | – | – | 20.44 | – | – | 0.43 | – | – |
| | 3 | 6.78 | – | – | 20.59 | – | – | 0.45 | – | – |
| | 4 | 6.33 | – | – | 19.24 | – | – | 0.39 | – | – |
| | 5 | 5.78 | – | – | 16.65 | – | – | 0.28 | – | – |
| | 6 | 6.39 | – | – | 18.66 | – | – | 0.30 | – | – |
| | Average | 6.47 | – | – | 19.92 | – | – | 0.43 | – | – |
| | StDev | 0.20 | – | – | 0.60 | – | – | 0.03 | – | – |
| | Cov (%) | 3.04 | – | – | 3.02 | – | – | 6.15 | – | – |
| E1 | 1 | – | 6.62 | 6.01 | – | 19.22 | 18.43 | – | 0.32 | 0.34 |
| | 2 | – | 6.45 | 6.15 | – | 19.04 | 17.88 | – | 0.34 | 0.31 |
| | 3 | – | 6.67 | - | – | 19.94 | - | – | 0.39 | - |
| | 4 | – | - | 6.15 | – | - | 18.96 | – | - | 0.37 |
| | 5 | – | 6.65 | 5.96 | – | 19.66 | 17.62 | – | 0.43 | 0.28 |
| | Average | – | 6.60 | 6.07 | – | 19.47 | 18.22 | – | 0.37 | 0.33 |
| | StDev | – | 0.09 | 0.08 | – | 0.36 | 0.52 | – | 0.05 | 0.04 |
| | Cov (%) | – | 1.33 | 1.38 | – | 1.83 | 2.85 | – | 12.97 | 11.65 |
| E2 | 1 | – | 1.68 | 1.53 | – | 6.97 | 6.41 | – | 0.89 | 1.08 |
| | 2 | – | 1.92 | 1.64 | – | 7.35 | 6.62 | – | 1.30 | 1.11 |
| | 3 | – | 1.93 | 1.58 | – | 7.54 | 6.54 | – | 1.24 | 1.38 |
| | 4 | – | 1.82 | 1.72 | – | 6.98 | 6.87 | – | 0.77 | 1.06 |
| | 5 | – | 1.91 | 1.63 | – | 7.34 | 6.85 | – | 1.08 | 1.09 |
| | Average | – | 1.85 | 1.62 | – | 7.24 | 6.7 | – | 1.06 | 1.14 |
| | StDev | – | 0.10 | 0.07 | – | 0.23 | 0.18 | – | 0.23 | 0.14 |
| | Cov (%) | – | 5.16 | 4.03 | – | 3.13 | 2.68 | – | 21.35 | 11.86 |
| E3 | 1 | – | 6.94 | - | – | 19.73 | - | – | 0.32 | - |
| | 2 | – | - | - | – | - | - | – | - | - |
| | 3 | – | 6.91 | 6.10 | – | 20.23 | 17.95 | – | 0.37 | 0.32 |
| | 4 | – | 6.84 | 6.27 | – | 20.54 | 18.10 | – | 0.36 | 0.37 |
| | 5 | – | 6.22 | 5.52 | – | 18.92 | 16.08 | – | 0.29 | 0.25 |
| | Average | – | 6.73 | 5.96 | – | 19.86 | 17.38 | – | 0.34 | 0.31 |
| | StDev | – | 0.30 | 0.32 | – | 0.62 | 0.92 | – | 0.04 | 0.06 |
| | Cov (%) | – | 4.39 | 5.37 | – | 3.10 | 5.30 | – | 11.10 | 19.12 |
| E4 | 1 | – | 7.05 | 5.23 | – | 19.95 | 16.98 | – | 0.29 | 0.36 |
| | 2 | – | 7.26 | 4.98 | – | 20.40 | 16.59 | – | 0.28 | 0.28 |
| | 3 | – | 7.31 | - | – | 21.01 | - | – | 0.31 | - |
| | 4 | – | 7.20 | 5.87 | – | 19.14 | 18.32 | – | 0.24 | 0.35 |
| | 5 | – | - | 5.62 | – | - | 16.90 | – | - | 0.31 |
| | Average | – | 7.20 | 5.43 | – | 20.13 | 17.20 | – | 0.28 | 0.33 |
| | StDev | – | 0.10 | 0.37 | – | 0.68 | 0.74 | – | 0.03 | 0.04 |
| | Cov (%) | – | 1.36 | 6.88 | – | 3.38 | 4.31 | – | 11.34 | 12.79 |
| E5 | 1 | – | 8.13 | - | – | 23.09 | - | – | 0.33 | - |
| | 2 | – | 7.15 | 5.62 | – | 20.09 | 17.23 | – | 0.29 | 0.34 |
| | 3 | – | 7.07 | 6.31 | – | 21.70 | 17.56 | – | 0.27 | 0.30 |
| | 4 | – | - | 6.41 | – | - | 18.95 | – | - | 0.36 |
| | 5 | – | 7.69 | 6.09 | – | 22.64 | 18.15 | – | 0.34 | 0.41 |
| | Average | – | 7.51 | 6.11 | – | 21.88 | 17.97 | – | 0.31 | 0.35 |
| | StDev | – | 0.43 | 0.30 | – | 1.15 | 0.65 | – | 0.03 | 0.05 |
| | Cov (%) | – | 5.71 | 4.98 | – | 5.25 | 3.64 | – | 11.16 | 13.11 |
| E6 | 1 | – | - | 5.40 | – | - | 16.40 | – | - | 0.37 |
| | 2 | – | - | 4.59 | – | - | 14.63 | – | - | 0.36 |
| | 3 | – | 5.69 | 5.34 | – | 16.10 | 16.51 | – | 0.28 | 0.40 |
| | 4 | – | 6.36 | 4.15 | – | 18.26 | 15.65 | – | 0.27 | 0.29 |
| | 5 | – | 6.41 | 5.26 | – | 18.69 | 15.91 | – | 0.26 | 0.30 |
| | Average | – | 6.15 | 4.95 | – | 17.68 | 15.82 | – | 0.27 | 0.34 |
| | StDev | – | 0.33 | 0.50 | – | 1.14 | 0.67 | – | 0.01 | 0.04 |
| | Cov (%) | – | 5.36 | 10.04 | – | 6.42 | 4.26 | – | 4.33 | 12.90 |

Table 3.2 - Total values of the elastic modulus ($E_a$), tensile strength ($f_a$), and ultimate strain ($\varepsilon_a$) of the adhesive Sikadur-30 (ADH2), after one (T1) and two (T2) years of exposure to the environment studied (E1 to E6), including the reference (T0).

| Env. | Specimen Number | $E_a$ [GPa] | | | $f_a$ [MPa] | | | $\varepsilon_a$ [‰] | | |
|---|---|---|---|---|---|---|---|---|---|---|
| | | T0 | T1 | T2 | T0 | T1 | T2 | T0 | T1 | T2 |
| REF | 1 | 7.09 | – | – | 22.66 | – | – | 0.50 | – | – |
| | 2 | 8.90 | – | – | 26.09 | – | – | 0.32 | – | – |
| | 3 | 8.10 | – | – | 25.96 | – | – | 0.41 | – | – |
| | 4 | 8.29 | – | – | 27.34 | – | – | 0.51 | – | – |
| | 5 | 7.32 | – | – | 24.24 | – | – | 0.70 | – | – |
| | 6 | 8.21 | – | – | 22.68 | – | – | 0.25 | – | – |
| | Average | 7.99 | – | – | 24.83 | – | – | 0.45 | – | – |
| | StDev | 0.65 | – | – | 1.73 | – | – | 0.09 | – | – |
| | Cov (%) | 8.15 | – | – | 6.97 | – | – | 19.99 | – | – |
| E1 | 1 | – | 9.05 | 8.32 | – | 28.94 | 24.51 | – | 0.44 | 0.40 |
| | 2 | – | 9.96 | 8.62 | – | 31.10 | 28.23 | – | 0.35 | 0.42 |
| | 3 | – | 10.00 | 8.76 | – | 29.51 | 26.97 | – | 0.29 | 0.33 |
| | 4 | – | 9.40 | 7.90 | – | 28.68 | 27.00 | – | 0.32 | 0.37 |
| | 5 | – | 9.80 | 8.32 | – | 27.71 | 24.43 | – | 0.29 | 0.26 |
| | Average | – | 9.64 | 8.38 | – | 29.19 | 26.23 | – | 0.34 | 0.36 |
| | StDev | – | 0.36 | 0.30 | – | 1.12 | 1.50 | – | 0.06 | 0.07 |
| | Cov (%) | – | 3.74 | 3.56 | – | 3.84 | 5.73 | – | 18.55 | 18.23 |
| E2 | 1 | – | 4.12 | - | – | 13.93 | - | – | 0.36 | - |
| | 2 | – | 3.45 | 2.88 | – | 13.72 | 9.80 | – | 0.34 | 0.32 |
| | 3 | – | 3.62 | 3.47 | – | 13.62 | 11.54 | – | 0.34 | 0.29 |
| | 4 | – | 4.05 | 2.90 | – | 14.51 | 11.59 | – | 0.28 | 0.26 |
| | 5 | – | - | - | – | - | - | – | - | - |
| | Average | – | 3.81 | 3.08 | – | 13.95 | 10.98 | – | 0.33 | 0.29 |
| | StDev | – | 0.28 | 0.27 | – | 0.35 | 0.83 | – | 0.04 | 0.03 |
| | Cov (%) | – | 7.42 | 8.84 | – | 2.48 | 7.59 | – | 10.77 | 11.70 |
| E3 | 1 | – | 10.27 | 8.95 | – | 33.48 | 29.10 | – | 0.44 | 0.33 |
| | 2 | – | 10.93 | 8.12 | – | 31.28 | 24.96 | – | 0.30 | 0.28 |
| | 3 | – | 10.79 | 8.49 | – | 34.54 | 28.27 | – | 0.34 | 0.30 |
| | 4 | – | 10.02 | 9.52 | – | 31.94 | 29.20 | – | 0.40 | 0.34 |
| | 5 | – | 11.02 | 8.80 | – | 33.67 | 26.89 | – | 0.35 | 0.34 |
| | Average | – | 10.61 | 8.78 | – | 32.98 | 27.68 | – | 0.37 | 0.32 |
| | StDev | – | 0.39 | 0.47 | – | 1.19 | 1.59 | – | 0.05 | 0.03 |
| | Cov (%) | – | 3.69 | 5.34 | – | 3.62 | 5.75 | – | 14.70 | 8.70 |
| E4 | 1 | – | - | 9.21 | – | - | 28.45 | – | - | 0.36 |
| | 2 | – | 9.97 | 7.84 | – | 30.71 | 25.31 | – | 0.35 | 0.37 |
| | 3 | – | 10.16 | 8.07 | – | 31.97 | 25.51 | – | 0.41 | 0.28 |
| | 4 | – | - | 7.77 | – | - | 24.19 | – | - | 0.26 |
| | 5 | – | 10.38 | 7.85 | – | 31.93 | 24.91 | – | 0.40 | 0.35 |
| | Average | – | 10.17 | 8.15 | – | 31.54 | 25.68 | – | 0.39 | 0.32 |
| | StDev | – | 0.17 | 0.54 | – | 0.58 | 1.46 | – | 0.04 | 0.05 |
| | Cov (%) | – | 1.63 | 6.62 | – | 1.85 | 5.69 | – | 9.14 | 15.78 |
| E5 | 1 | – | 11.25 | 8.80 | – | 35.46 | 29.65 | – | 0.39 | 0.35 |
| | 2 | – | 10.97 | 8.51 | – | 32.64 | 26.46 | – | 0.35 | 0.37 |
| | 3 | – | 10.71 | 9.60 | – | 31.20 | 29.34 | – | 0.31 | 0.41 |
| | 4 | – | 10.15 | 9.39 | – | 32.79 | 29.07 | – | 0.39 | 0.28 |
| | 5 | – | 9.13 | 8.66 | – | 31.46 | 28.27 | – | 0.33 | 0.32 |
| | Average | – | 10.44 | 8.99 | – | 32.71 | 28.56 | – | 0.35 | 0.35 |
| | StDev | – | 0.75 | 0.42 | – | 1.51 | 1.14 | – | 0.04 | 0.05 |
| | Cov (%) | – | 7.17 | 4.73 | – | 4.61 | 4.01 | – | 10.28 | 14.40 |
| E6 | 1 | – | 11.43 | 10.81 | – | 35.17 | 32.03 | – | 0.32 | 0.29 |
| | 2 | – | 12.16 | 10.36 | – | 35.36 | 33.93 | – | 0.30 | 0.30 |
| | 3 | – | 11.93 | 11.54 | – | 32.40 | 35.69 | – | 0.25 | 0.32 |
| | 4 | – | 11.68 | 10.96 | – | 34.50 | 32.73 | – | 0.27 | 0.30 |
| | 5 | – | 11.89 | 10.86 | – | 32.53 | 32.73 | – | 0.25 | 0.29 |
| | Average | – | 11.82 | 10.90 | – | 33.99 | 33.42 | – | 0.28 | 0.30 |
| | StDev | – | 0.25 | 0.38 | – | 1.28 | 1.29 | – | 0.03 | 0.01 |
| | Cov (%) | – | 2.11 | 3.45 | – | 3.76 | 3.85 | – | 11.26 | 3.47 |

Table 3.3 - Failure modes observed with the adhesive S&P Resin 220 epoxy adhesive (ADH1), after one (T1) and two (T2) years of exposure to the environment studied (E1 to E6), including the reference (T0).

| Env. | Failure Modes - S&P Resin 220 Epoxy adhesive (ADH1) | | |
|---|---|---|---|
| | T0 | T1 | T2 |
| REF | N/A | – | – |
| E1 | – |  |  |
| E2 | – |  |  |
| E3 | – |  |  |
| E4 | – |  |  |
| E5 | – |  |  |
| E6 | – |  |  |

Table 3.4 - Failure modes observed with the adhesive Sikadur-30 (ADH2), after one (T1) and two (T2) years of exposure to the environment studied (E1 to E6), including the reference (T0).

| Env. | Failure Modes - Sikadur-30 (ADH2) | | |
| --- | --- | --- | --- |
| | T0 | T1 | T2 |
| REF | N/A | – | – |
| E1 | – |  |  |
| E2 | – |  |  |
| E3 | – |  |  |
| E4 | – |  |  |
| E5 | – |  |  |
| E6 | – |  |  |

## Part 4 – Bond between CFRP and Concrete

Table 4.1 - Total values of the initial stiffness ($K$), maximum pullout force ($F_{max}$) and corresponding loaded end slip ($s_{lmax}$) of pull-out tests of bond NSM-CFRP to concrete systems, after one (T1) and two (T2) years of exposure to the environment studied (E1 to E6), including the reference (T0).
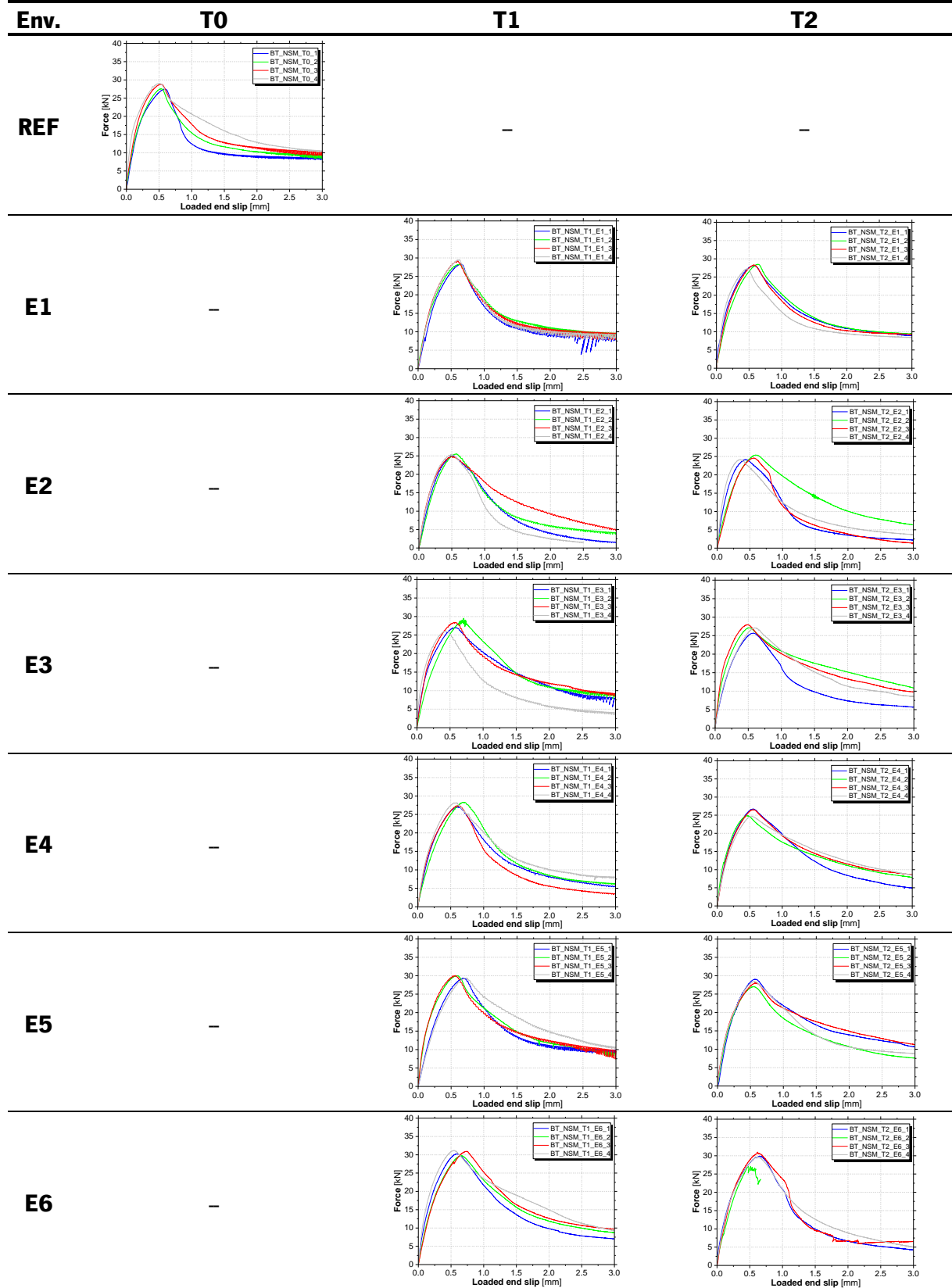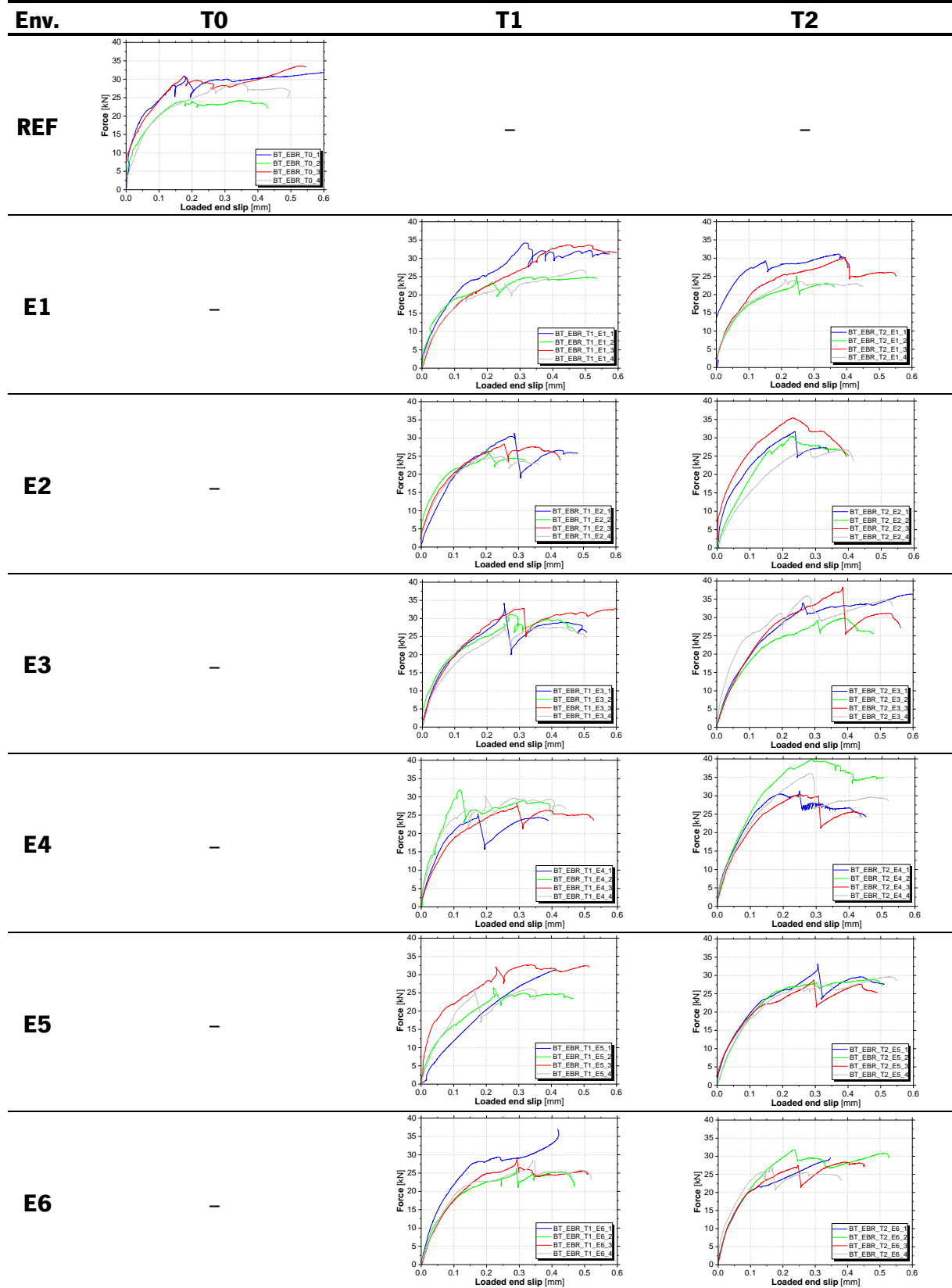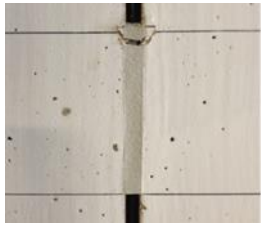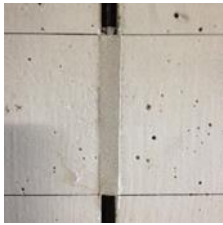
| Env. | Specimen Number | $K$ [kN/mm] | | | $F_{max}$ [kN] | | | $s_{lmax}$ [mm] | | | Failure mode | | |
|------|------|------|------|------|------|------|------|------|------|------|------|------|------|
| | | T0 | T1 | T2 | T0 | T1 | T2 | T0 | T1 | T2 | T0 | T1 | T2 |
| REF | 1 | 105.73 | – | – | 27.47 | – | – | 0.59 | – | – | F/A | – | – |
| | 2 | 113.74 | – | – | 27.55 | – | – | 0.54 | – | – | F/A + CC | – | – |
| | 3 | 120.93 | – | – | 28.81 | – | – | 0.53 | – | – | F/A | – | – |
| | 4 | 225.52 | – | – | 28.99 | – | – | 0.51 | – | – | F/A | – | – |
| | Average | 141.48 | – | – | 28.21 | – | – | 0.54 | – | – | – | – | – |
| | StDev | 48.8 | – | – | 0.70 | – | – | 0.03 | – | – | – | – | – |
| | CoV (%) | 34.50 | – | – | 2.48 | – | – | 5.69 | – | – | – | – | – |
| E1 | 1 | – | 84.52 | 81.01 | – | 28.30 | 28.07 | – | 0.65 | 0.57 | – | F/A + CC | F/A + CC |
| | 2 | – | 98.47 | 87.97 | – | 28.26 | 28.48 | – | 0.63 | 0.63 | – | F/A + CC | F/A |
| | 3 | – | 100.36 | 103.25 | – | 29.16 | 28.30 | – | 0.60 | 0.57 | – | F/A | F/A |
| | 4 | – | 98.01 | 147.03 | – | 29.50 | 27.27 | – | 0.60 | 0.47 | – | F/A | F/A |
| | Average | – | 95.34 | 104.81 | – | 28.81 | 28.03 | – | 0.62 | 0.56 | – | – | – |
| | StDev | – | 6.31 | 25.67 | – | 0.54 | 0.46 | – | 0.02 | 0.06 | – | – | – |
| | CoV (%) | – | 6.62 | 24.49 | – | 1.87 | 1.65 | – | 3.59 | 10.27 | – | – | – |
| E2 | 1 | – | 88.11 | 120.16 | – | 25.09 | 24.18 | – | 0.51 | 0.43 | – | A/C + CS | C + CS |
| | 2 | – | 75.89 | 77.31 | – | 25.53 | 25.41 | – | 0.57 | 0.61 | – | A/C + CS | F/A + CS |
| | 3 | – | 109.83 | 70.32 | – | 24.77 | 24.62 | – | 0.49 | 0.56 | – | A/C + CS | A + CS |
| | 4 | – | 101.97 | 176.78 | – | 25.36 | 24.18 | – | 0.49 | 0.35 | – | A/C + CS | A/C + CS |
| | Average | – | 93.95 | 111.14 | – | 25.19 | 24.60 | – | 0.52 | 0.49 | – | – | – |
| | StDev | – | 13.01 | 42.43 | – | 0.29 | 0.50 | – | 0.03 | 0.10 | – | – | – |
| | CoV (%) | – | 13.85 | 38.17 | – | 1.14 | 2.04 | – | 6.31 | 21.03 | – | – | – |
| E3 | 1 | – | 120.72 | 85.18 | – | 26.98 | 25.68 | – | 0.57 | 0.57 | – | F/A + CC | F/A + CS |
| | 2 | – | 76.90 | 138.47 | – | 29.54 | 27.11 | – | 0.71 | 0.51 | – | F/A | F/A + CC |
| | 3 | – | 117.12 | 165.28 | – | 28.40 | 27.94 | – | 0.55 | 0.48 | – | F/A + CC | F/A + CC |
| | 4 | – | 199.23 | 92.91 | – | 26.06 | 27.11 | – | 0.43 | 0.60 | – | F/A + CS | F/A + CC |
| | Average | – | 128.49 | 120.46 | – | 27.75 | 26.96 | – | 0.56 | 0.54 | – | – | – |
| | StDev | – | 44.31 | 32.93 | – | 1.33 | 0.81 | – | 0.10 | 0.05 | – | – | – |
| | CoV (%) | – | 34.49 | 27.34 | – | 4.79 | 3.02 | – | 17.39 | 8.60 | – | – | – |
| E4 | 1 | – | 89.80 | 106.57 | – | 27.00 | 26.70 | – | 0.61 | 0.54 | – | F/A + CS | F/A + CS |
| | 2 | – | 72.57 | 141.80 | – | 28.28 | 24.86 | – | 0.68 | 0.46 | – | F/A + CS | F/A + CC |
| | 3 | – | 104.10 | 102.39 | – | 27.39 | 26.50 | – | 0.63 | 0.55 | – | F/A + CS | F/A + CS |
| | 4 | – | 113.41 | 91.81 | – | 28.16 | 24.66 | – | 0.58 | 0.52 | – | F/A + CS | F/A + CC |
| | Average | – | 94.97 | 110.64 | – | 27.71 | 25.68 | – | 0.62 | 0.52 | – | – | – |
| | StDev | – | 15.42 | 18.77 | – | 0.53 | 0.93 | – | 0.04 | 0.03 | – | – | – |
| | CoV (%) | – | 16.24 | 16.97 | – | 1.92 | 3.60 | – | 5.81 | 6.34 | – | – | – |
| E5 | 1 | – | 78.62 | 99.98 | – | 29.29 | 29.04 | – | 0.68 | 0.58 | – | F/A + CC | F/A + CC |
| | 2 | – | 136.40 | 108.08 | – | 29.98 | 27.01 | – | 0.60 | 0.55 | – | F/A + CC | F/A + CS |
| | 3 | – | 160.80 | 113.30 | – | 30.04 | 27.98 | – | 0.56 | 0.58 | – | F/A + CC | F/A + CC |
| | 4 | – | 73.23 | 119.75 | – | 29.39 | 28.40 | – | 0.73 | 0.56 | – | F/A | F/A + CC |
| | Average | – | 112.26 | 110.28 | – | 29.68 | 28.11 | – | 0.64 | 0.57 | – | – | – |
| | StDev | – | 37.40 | 7.24 | – | 0.34 | 0.74 | – | 0.07 | 0.01 | – | – | – |
| | CoV (%) | – | 33.31 | 6.57 | – | 1.14 | 2.62 | – | 10.42 | 1.94 | – | – | – |
| E6 | 1 | – | 115.08 | 113.59 | – | 30.26 | 29.90 | – | 0.59 | 0.65 | – | F/A + CS | F/A + CS |
| | 2 | – | 89.30 | - | – | 29.77 | 27.11 | – | 0.66 | 0.47 | – | F/A + CC | - |
| | 3 | – | 83.99 | 101.28 | – | 30.96 | 30.99 | – | 0.75 | 0.65 | – | F/A + CC | F/A + CS |
| | 4 | – | 164.33 | 110.10 | – | 31.17 | 29.65 | – | 0.54 | 0.54 | – | F/A + CC | F/A + CS |
| | Average | – | 113.18 | 108.32 | – | 30.54 | 29.41 | – | 0.63 | 0.58 | – | – | – |
| | StDev | – | 31.79 | 5.18 | – | 0.56 | 1.42 | – | 0.08 | 0.08 | – | – | – |
| | CoV (%) | – | 28.09 | 4.78 | – | 1.83 | 4.83 | – | 12.45 | 13.39 | – | – | – |

Failure modes: F/A = debonding failure at CFRP-adhesive interface; A/C = debonding failure at adhesive-concrete interface; C = cohesive failure of concrete; A = cohesive failure of adhesive; CC = concrete cracking; CS = concrete splitting.

Table 4.2 - Mean values of the initial stiffness ($K$), maximum pullout force ($F_{max}$) and corresponding loaded end slip ($s_{max}$) of pull-out tests of bond EBR-CFRP to concrete systems, after one (T1) and two (T2) years of exposure to the environment studied (E1 to E6), including the reference (T0).

| Env. | Specimen Number | $K$ [kN/mm] | | | $F_{max}$ [kN] | | | $s_{max}$ [mm] | | | Failure mode | | |
|---|---|---|---|---|---|---|---|---|---|---|---|---|---|
| | | T0 | T1 | T2 | T0 | T1 | T2 | T0 | T1 | T2 | T0 | T1 | T2 |
| **REF** | 1 | - | – | – | 34.06 | – | – | 0.65 | – | – | C + F/A | – | – |
| | 2 | 335.45 | – | – | 25.47 | – | – | 0.43 | – | – | C | – | – |
| | 3 | - | – | – | 33.62 | – | – | 0.55 | – | – | C + F/A | – | – |
| | 4 | 250.13 | – | – | 28.92 | – | – | 0.50 | – | – | C | – | – |
| | Average | 292.79 | – | – | 30.52 | – | – | 0.53 | – | – | – | – | – |
| | StDev | 42.66 | – | – | 3.54 | – | – | 0.08 | – | – | – | – | – |
| | CoV (%) | 14.57 | – | – | 11.61 | – | – | 15.13 | – | – | – | – | – |
| **E1** | 1 | – | 232.29 | | – | 34.18 | 31.13 | – | 0.31 | 0.37 | – | C + F/A | C |
| | 2 | – | | 236.3 | – | 24.86 | 25.11 | – | 0.37 | 0.25 | – | C | C |
| | 3 | – | 245.87 | 325.74 | – | 33.69 | 30.26 | – | 0.45 | 0.39 | – | C + F/A | C |
| | 4 | – | 246.38 | 284.26 | – | 26.77 | 24.24 | – | 0.49 | 0.21 | – | C + F/A | C |
| | Average | – | 241.51 | 282.10 | – | 29.88 | 27.69 | – | 0.41 | 0.31 | – | – | – |
| | StDev | – | 6.53 | 36.55 | – | 4.12 | 3.04 | – | 0.07 | 0.08 | – | – | – |
| | CoV (%) | – | 2.70 | 12.95 | – | 13.79 | 10.99 | – | 16.60 | 25.88 | – | – | – |
| **E2** | 1 | – | 214.73 | 347.67 | – | 31.29 | 31.73 | – | 0.29 | 0.24 | – | C | C |
| | 2 | – | 367.14 | 236.48 | – | 26.94 | 30.37 | – | 0.20 | 0.23 | – | C | C + F/A |
| | 3 | – | 261.57 | 488.46 | – | 28.36 | 35.40 | – | 0.26 | 0.23 | – | C | C |
| | 4 | – | 259.1 | 174.04 | – | 24.86 | 26.73 | – | 0.25 | 0.28 | – | C | C |
| | Average | – | 275.64 | 311.66 | – | 27.86 | 31.06 | – | 0.25 | 0.24 | – | – | – |
| | StDev | – | 56.02 | 119.53 | – | 2.34 | 3.10 | – | 0.03 | 0.02 | – | – | – |
| | CoV (%) | – | 20.32 | 38.35 | – | 8.39 | 9.99 | – | 12.39 | 8.74 | – | – | – |
| **E3** | 1 | – | 346.87 | 288.71 | – | 34.17 | 36.43 | – | 0.25 | 0.59 | – | C | C |
| | 2 | – | 304.98 | 231.33 | – | 31.06 | 29.77 | – | 0.28 | 0.39 | – | C | C |
| | 3 | – | 268.27 | 245.78 | – | 33.24 | 38.32 | – | 0.62 | 0.39 | – | C + F/A | C |
| | 4 | – | 290.64 | 552.01 | – | 28.66 | 35.87 | – | 0.25 | 0.27 | – | C | C |
| | Average | – | 302.69 | 329.46 | – | 31.78 | 35.10 | – | 0.35 | 0.41 | – | – | – |
| | StDev | – | 28.67 | 130.21 | – | 2.13 | 3.21 | – | 0.16 | 0.12 | – | – | – |
| | CoV (%) | – | 9.47 | 39.52 | – | 6.69 | 9.14 | – | 44.73 | 28.07 | – | – | – |
| **E4** | 1 | – | 304.82 | 295.61 | – | 25.35 | 31.30 | – | 0.17 | 0.25 | – | C | C |
| | 2 | – | 501.36 | 347.72 | – | 31.87 | 39.81 | – | 0.12 | 0.28 | – | C | C |
| | 3 | – | 253.71 | 304.99 | – | 28.24 | 30.36 | – | 0.29 | 0.25 | – | C | C |
| | 4 | – | 362.4 | 273.72 | – | 30.22 | 36.11 | – | 0.19 | 0.28 | – | C | C |
| | Average | – | 355.57 | 305.51 | – | 28.92 | 34.40 | – | 0.19 | 0.27 | – | – | – |
| | StDev | – | 92.54 | 26.88 | – | 2.43 | 3.81 | – | 0.06 | 0.02 | – | – | – |
| | CoV (%) | – | 26.02 | 8.80 | – | 8.40 | 11.08 | – | 32.58 | 6.14 | – | – | – |
| **E5** | 1 | – | | 275.37 | – | 33.52 | 33.13 | – | 0.52 | 0.31 | – | C + F/A | C |
| | 2 | – | 225.82 | 236.83 | – | 26.54 | 28.93 | – | 0.22 | 0.48 | – | C | C |
| | 3 | – | | 239.23 | – | 32.68 | 28.72 | – | 0.34 | 0.30 | – | C + F/A | C |
| | 4 | – | 255.45 | 256.01 | – | 26.09 | 29.61 | – | 0.33 | 0.52 | – | C | C |
| | Average | – | 240.64 | 251.86 | – | 29.71 | 30.10 | – | 0.35 | 0.40 | – | – | – |
| | StDev | – | 14.82 | 15.45 | – | 3.41 | 1.78 | – | 0.11 | 0.10 | – | – | – |
| | CoV (%) | – | 6.16 | 6.14 | – | 11.48 | 5.92 | – | 29.84 | 24.99 | – | – | – |
| **E6** | 1 | – | 346.38 | 327 | – | 37.04 | 29.72 | – | 0.42 | 0.35 | – | C | C |
| | 2 | – | 274.11 | 359.9 | – | 26.26 | 31.79 | – | 0.29 | 0.23 | – | C | C |
| | 3 | – | 240.76 | 367.88 | – | 29.13 | 28.37 | – | 0.29 | 0.39 | – | C | C |
| | 4 | – | 242.92 | 440.37 | – | 28.39 | 27.04 | – | 0.34 | 0.17 | – | C | C |
| | Average | – | 276.04 | 373.79 | – | 30.21 | 29.23 | – | 0.34 | 0.28 | – | – | – |
| | StDev | – | 42.70 | 41.38 | – | 4.08 | 1.76 | – | 0.05 | 0.09 | – | – | – |
| | CoV (%) | – | 15.47 | 11.07 | – | 13.52 | 6.01 | – | 15.26 | 31.01 | – | – | – |

Failure modes (FM): C = cohesive failure of concrete; C + F/A = cohesive failure of concrete and debonding at laminate-adhesive interface.
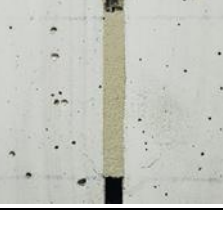
Table 4.3 - Total curves of force *vs.* loaded end slip on bond NSM-CFRP to concrete after one (T1) and two (T2) years of exposure to the environment studied (E1 to E6), including the reference (T0).

| Env. | T0 | T1 | T2 |
|------|-----|-----|-----|
| REF |  | – | – |
| E1 | – |  |  |
| E2 | – |  |  |
| E3 | – |  |  |
| E4 | – |  |  |
| E5 | – |  |  |
| E6 | – |  |  |

Table 4.4 - Total curves of force *vs.* loaded end slip on bond EBR-CFRP to concrete after one (T1) and two (T2) years of exposure to the environment studied (E1 to E6), including the reference (T0).

| Env. | T0 | T1 | T2 |
|------|-----|-----|-----|
| REF |  | – | – |
| E1 | – |  |  |
| E2 | – |  |  |
| E3 | – |  |  |
| E4 | – |  |  |
| E5 | – |  |  |
| E6 | – |  |  |

Table 4.5 - Failure modes observed on bond NSM-CFRP to concrete after one (T1) and two (T2) years of exposure to the environment studied (E1 to E6), including the reference (T0).

| Env. | Time | Specimen number | | | |
|---|---|---|---|---|---|
| | | 1 | 2 | 3 | 4 |
| REF | T0 |  | | | |
| E1 | T1 |  | | | |
| | T2 | | | | |
| E2 | T1 |  | | | |
| | T2 | | | | |
| E3 | T1 |  | | | |
| | T2 | | | | |
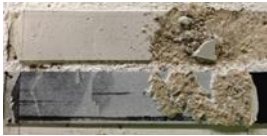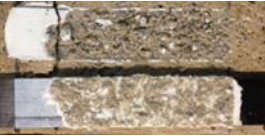
Table 4.6 - Failure modes observed on bond EBR-CFRP to concrete after one (T1) and two (T2) years of exposure to the environment studied (E1 to E6), including the reference (T0).

| Env. | Time | Specimen number | | | |
|------|------|-----------------|---|---|---|
| | | 1 | 2 | 3 | 4 |
| REF | T0 | | | | |
| E1 | T1 | | | | |
| | T2 | | | | |
| E2 | T1 | | | | |
| | T2 | | | | |
| E3 | T1 | | | | |
| | T2 | | | | |
| E4 | T1 | | | | |
| | T2 | | | | |
| E5 | T1 | | | | |
| | T2 | | | | |

## Part 5 – Dates of the tests

Table 5.1 - Dates of the tests performed on concrete, after one (T1) and two (T2) years of exposure to the environment studied (E1 to E6), including the reference (T0).

| Env. | Specim. Number | Date of the test | | | | | |
|------|------|------|------|------|------|------|------|
| | | Elastic modulus/Compressive strength | | | Pull-off | | |
| | | T0 (28 days) | T1 | T2 | T0 | T1 | T2 |
| REF | 1 | 08/12/2016 | – | – | 17/10/2018 | – | – |
| | 2 | 08/12/2016 | – | – | 17/10/2018 | – | – |
| | 3 | 08/12/2016 | – | – | 17/10/2018 | – | – |
| | 4 | 08/12/2016 | – | – | 17/10/2018 | – | – |
| E1 | 1 | – | 08/08/2019 | 31/07/2020 | – | 09/08/2019 | 05/09/2020 |
| | 2 | – | 08/08/2019 | 31/07/2020 | – | 09/08/2019 | 05/09/2020 |
| | 3 | – | 08/08/2019 | 31/07/2020 | – | 09/08/2019 | 05/09/2020 |
| | 4 | – | 08/08/2019 | 31/07/2020 | – | 09/08/2019 | 05/09/2020 |
| E2 | 1 | – | 09/08/2019 | 03/08/2020 | – | 09/08/2019 | 05/09/2020 |
| | 2 | – | 09/08/2019 | 03/08/2020 | – | 09/08/2019 | 05/09/2020 |
| | 3 | – | 09/08/2019 | 03/08/2020 | – | 09/08/2019 | 05/09/2020 |
| | 4 | – | 09/08/2019 | 03/08/2020 | – | 09/08/2019 | 05/09/2020 |
| E3 | 1 | – | 08/08/2019 | 31/07/2020 | – | 09/08/2019 | 05/09/2020 |
| | 2 | – | 08/08/2019 | 31/07/2020 | – | 09/08/2019 | 05/09/2020 |
| | 3 | – | 08/08/2019 | 31/07/2020 | – | 09/08/2019 | 05/09/2020 |
| | 4 | – | 08/08/2019 | 31/07/2020 | – | 09/08/2019 | 05/09/2020 |
| E4 | 1 | – | 08/08/2019 | 31/07/2020 | – | 09/08/2019 | 05/09/2020 |
| | 2 | – | 08/08/2019 | 31/07/2020 | – | 09/08/2019 | 05/09/2020 |
| | 3 | – | 08/08/2019 | 31/07/2020 | – | 09/08/2019 | 05/09/2020 |
| | 4 | – | 08/08/2019 | 31/07/2020 | – | 09/08/2019 | 05/09/2020 |
| E5 | 1 | – | 08/08/2019 | 31/07/2020 | – | 09/08/2019 | 05/09/2020 |
| | 2 | – | 08/08/2019 | 31/07/2020 | – | 09/08/2019 | 05/09/2020 |
| | 3 | – | 08/08/2019 | 31/07/2020 | – | 09/08/2019 | 05/09/2020 |
| | 4 | – | 08/08/2019 | 31/07/2020 | – | 09/08/2019 | 05/09/2020 |
| E6 | 1 | – | 16/01/2020 | 14/01/2021 | – | 09/08/2019 | 05/09/2020 |
| | 2 | – | 16/01/2020 | 14/01/2021 | – | 09/08/2019 | 05/09/2020 |
| | 3 | – | 16/01/2020 | 14/01/2021 | – | 09/08/2019 | 05/09/2020 |
| | 4 | – | 16/01/2020 | 14/01/2021 | – | 09/08/2019 | 05/09/2020 |

Table 5.2 - Dates of the tests performed on the CFRP laminates L10 and L50, after one (T1) and two (T2) years of exposure to the environment studied (E1 to E6), including the reference (T0).

| Env. | Specim. Number | Date of the test | | | | | |
| | | L10 | | | L50 | | |
| | | T0 | T1 | T2 | T0 | T1 | T2 |
|---|---|---|---|---|---|---|---|
| REF | 1 | 01/03/2017 | – | – | 06/11/2017 | – | – |
| | 2 | 01/03/2017 | – | – | 06/11/2017 | – | – |
| | 3 | 01/03/2017 | – | – | 06/11/2017 | – | – |
| | 4 | 01/03/2017 | – | – | 06/11/2017 | – | – |
| | 5 | 01/03/2017 | – | – | 06/11/2017 | – | – |
| | 6 | 01/03/2017 | – | – | 06/11/2017 | – | – |
| E1 | 1 | – | 06/08/2019 | 31/07/2020 | – | 07/08/2019 | 03/08/2020 |
| | 2 | – | 06/08/2019 | 31/07/2020 | – | 07/08/2019 | 03/08/2020 |
| | 3 | – | 06/08/2019 | 31/07/2020 | – | 07/08/2019 | 03/08/2020 |
| | 4 | – | 06/08/2019 | 31/07/2020 | – | 07/08/2019 | 03/08/2020 |
| | 5 | – | 06/08/2019 | 31/07/2020 | – | 07/08/2019 | 03/08/2020 |
| | 6 | – | 06/08/2019 | 31/07/2020 | – | 07/08/2019 | 03/08/2020 |
| E2 | 1 | – | 06/08/2019 | 03/08/2020 | – | 08/08/2019 | 03/08/2020 |
| | 2 | – | 06/08/2019 | 03/08/2020 | – | 08/08/2019 | 03/08/2020 |
| | 3 | – | 06/08/2019 | 03/08/2020 | – | 08/08/2019 | 03/08/2020 |
| | 4 | – | 06/08/2019 | 03/08/2020 | – | 08/08/2019 | 03/08/2020 |
| | 5 | – | 06/08/2019 | 03/08/2020 | – | 08/08/2019 | 03/08/2020 |
| | 6 | – | 06/08/2019 | 03/08/2020 | – | 08/08/2019 | 03/08/2020 |
| E3 | 1 | – | 06/08/2019 | 31/07/2020 | – | 07/08/2019 | 03/08/2020 |
| | 2 | – | 06/08/2019 | 31/07/2020 | – | 07/08/2019 | 03/08/2020 |
| | 3 | – | 06/08/2019 | 31/07/2020 | – | 07/08/2019 | 03/08/2020 |
| | 4 | – | 06/08/2019 | 31/07/2020 | – | 07/08/2019 | 03/08/2020 |
| | 5 | – | 06/08/2019 | 31/07/2020 | – | 07/08/2019 | 03/08/2020 |
| | 6 | – | 06/08/2019 | 31/07/2020 | – | 07/08/2019 | 03/08/2020 |
| E4 | 1 | – | 06/08/2019 | 31/07/2020 | – | 07/08/2019 | 03/08/2020 |
| | 2 | – | 06/08/2019 | 31/07/2020 | – | 07/08/2019 | 03/08/2020 |
| | 3 | – | 06/08/2019 | 31/07/2020 | – | 07/08/2019 | 03/08/2020 |
| | 4 | – | 06/08/2019 | 31/07/2020 | – | 07/08/2019 | 03/08/2020 |
| | 5 | – | 06/08/2019 | 31/07/2020 | – | 07/08/2019 | 03/08/2020 |
| | 6 | – | 06/08/2019 | 31/07/2020 | – | 07/08/2019 | 03/08/2020 |
| E5 | 1 | – | 06/08/2019 | 31/07/2020 | – | 07/08/2019 | 03/08/2020 |
| | 2 | – | 06/08/2019 | 31/07/2020 | – | 07/08/2019 | 03/08/2020 |
| | 3 | – | 06/08/2019 | 31/07/2020 | – | 07/08/2019 | 03/08/2020 |
| | 4 | – | 06/08/2019 | 31/07/2020 | – | 07/08/2019 | 03/08/2020 |
| | 5 | – | 06/08/2019 | 31/07/2020 | – | 07/08/2019 | 03/08/2020 |
| | 6 | – | 06/08/2019 | 31/07/2020 | – | 07/08/2019 | 03/08/2020 |
| E6 | 1 | – | 17/01/2020 | 14/01/2021 | – | 17/01/2020 | 14/01/2021 |
| | 2 | – | 17/01/2020 | 14/01/2021 | – | 17/01/2020 | 14/01/2021 |
| | 3 | – | 17/01/2020 | 14/01/2021 | – | 17/01/2020 | 14/01/2021 |
| | 4 | – | 17/01/2020 | 14/01/2021 | – | 17/01/2020 | 14/01/2021 |
| | 5 | – | 17/01/2020 | 14/01/2021 | – | 17/01/2020 | 14/01/2021 |
| | 6 | – | 17/01/2020 | 14/01/2021 | – | 17/01/2020 | 14/01/2021 |

Table 5.3 - Dates of the tensile tests performed on the epoxy adhesives *S&P Resin 220 epoxy adhesive* (ADH1) and *Sikadur-30* (ADH2), after one (T1) and two (T2) years of exposure to the environment studied (E1 to E6), including the reference (T0).

| Env. | Specim. Number | Date of the test | | | | | |
|---|---|---|---|---|---|---|---|
| | | *S&P Resin 220 epoxy adhesive* | | | *Sikadur-30* | | |
| | | T0 | T1 | T2 | T0 | T1 | T2 |
| REF | 1 | 14/06/2017 | – | – | 02/08/2017 | – | – |
| | 2 | 14/06/2017 | – | – | 02/08/2017 | – | – |
| | 3 | 14/06/2017 | – | – | 02/08/2017 | – | – |
| | 4 | 14/06/2017 | – | – | 02/08/2017 | – | – |
| | 5 | 14/06/2017 | – | – | 02/08/2017 | – | – |
| | 6 | 14/06/2017 | – | – | 02/08/2017 | – | – |
| E1 | 1 | – | 03/08/2019 | 05/08/2020 | – | 03/08/2019 | 05/08/2020 |
| | 2 | – | 02/08/2019 | 04/08/2020 | – | 02/08/2019 | 04/08/2020 |
| | 3 | – | 02/08/2019 | - | | 02/08/2019 | 05/08/2020 |
| | 4 | – | 02/08/2019 | 05/08/2020 | – | 02/08/2019 | 05/08/2020 |
| | 5 | – | 02/08/2019 | 05/08/2020 | – | 02/08/2019 | 05/08/2020 |
| E2 | 1 | – | 03/08/2019 | 05/08/2020 | – | 03/08/2019 | 05/08/2020 |
| | 2 | – | 03/08/2019 | 05/08/2020 | – | 03/08/2019 | 05/08/2020 |
| | 3 | – | 03/08/2019 | 05/08/2020 | – | 03/08/2019 | 05/08/2020 |
| | 4 | – | 03/08/2019 | 05/08/2020 | | 03/08/2019 | 05/08/2020 |
| | 5 | – | 03/08/2019 | 05/08/2020 | – | 03/08/2019 | 05/08/2020 |
| E3 | 1 | – | 03/08/2019 | 05/08/2020 | – | 03/08/2019 | 05/08/2020 |
| | 2 | – | 02/08/2019 | 04/08/2020 | – | 02/08/2019 | 04/08/2020 |
| | 3 | – | 02/08/2019 | 05/08/2020 | – | 02/08/2019 | 05/08/2020 |
| | 4 | – | 02/08/2019 | 05/08/2020 | | 02/08/2019 | 05/08/2020 |
| | 5 | – | 02/08/2019 | 05/08/2020 | – | 02/08/2019 | 05/08/2020 |
| E4 | 1 | – | 03/08/2019 | 05/08/2020 | – | 03/08/2019 | 05/08/2020 |
| | 2 | – | 03/08/2019 | 04/08/2020 | – | 02/08/2019 | 04/08/2020 |
| | 3 | – | 03/08/2019 | 05/08/2020 | – | - | 05/08/2020 |
| | 4 | – | 03/08/2019 | 05/08/2020 | | - | 05/08/2020 |
| | 5 | – | 03/08/2019 | 05/08/2020 | – | 02/08/2019 | 05/08/2020 |
| E5 | 1 | – | 03/08/2019 | 05/08/2020 | – | 03/08/2019 | 05/08/2020 |
| | 2 | – | 03/08/2019 | 04/08/2020 | – | 03/08/2019 | 04/08/2020 |
| | 3 | – | 03/08/2019 | 05/08/2020 | – | 03/08/2019 | 05/08/2020 |
| | 4 | – | 03/08/2019 | 05/08/2020 | | 03/08/2019 | 05/08/2020 |
| | 5 | – | 03/08/2019 | 05/08/2020 | – | 03/08/2019 | 05/08/2020 |
| E6 | 1 | – | 14/01/2020 | 08/01/2021 | – | 14/01/2020 | 08/01/2021 |
| | 2 | – | 14/01/2020 | 08/01/2021 | – | 14/01/2020 | 08/01/2021 |
| | 3 | – | 14/01/2020 | 08/01/2021 | – | 14/01/2020 | 08/01/2021 |
| | 4 | – | 14/01/2020 | 08/01/2021 | | 14/01/2020 | 08/01/2021 |
| | 5 | – | 14/01/2020 | 08/01/2021 | – | 14/01/2020 | 08/01/2021 |

Table 5.4 - Dates of the tests performed on bond NSM-CFRP and EBR-CFRP to concrete systems, after one (T1) and two (T2) years of exposure to the environment studied (E1 to E6), including the reference (T0).

| Env. | Specim. Number | Date of the test | | | | | |
|---|---|---|---|---|---|---|---|
| | | NSM | | | EBR | | |
| | | T0 | T1 | T2 | T0 | T1 | T2 |
| REF | 1 | 10/10/2017 | – | – | 12/10/2017 | – | – |
| | 2 | 10/10/2017 | – | – | 12/10/2017 | – | – |
| | 3 | 10/10/2017 | – | – | 13/10/2017 | – | – |
| | 4 | 10/10/2017 | – | – | 13/10/2017 | – | – |
| E1 | 1 | – | 23/07/2019 | 16/07/2020 | – | 30/07/2019 | 22/07/2020 |
| | 2 | – | 24/07/2019 | 15/07/2020 | – | 26/07/2019 | 21/07/2020 |
| | 3 | – | 23/07/2019 | 16/07/2020 | – | 26/07/2019 | 20/07/2020 |
| | 4 | – | 24/07/2019 | 15/07/2020 | – | 26/07/2019 | 20/07/2020 |
| E2 | 1 | – | 25/07/2019 | 17/07/2020 | – | 31/07/2019 | 23/07/2020 |
| | 2 | – | 25/07/2019 | 17/07/2020 | – | 31/07/2019 | 23/07/2020 |
| | 3 | – | 25/07/2019 | 17/07/2020 | – | 31/07/2019 | 23/07/2020 |
| | 4 | – | 25/07/2019 | 17/07/2020 | – | 31/07/2019 | 23/07/2020 |
| E3 | 1 | – | 23/07/2019 | 16/07/2020 | – | 29/07/2019 | 21/07/2020 |
| | 2 | – | 22/07/2019 | 15/07/2020 | – | 29/07/2019 | 21/07/2020 |
| | 3 | – | 24/07/2019 | 16/07/2020 | – | 30/07/2019 | 22/07/2020 |
| | 4 | – | 24/07/2019 | 16/07/2020 | – | 27/07/2019 | 21/07/2020 |
| E4 | 1 | – | 22/07/2019 | 16/07/2020 | – | 29/07/2019 | 20/07/2020 |
| | 2 | – | 23/07/2019 | 16/07/2020 | – | 27/07/2019 | 20/07/2020 |
| | 3 | – | 22/07/2019 | 16/07/2020 | – | 29/07/2019 | 21/07/2020 |
| | 4 | – | 22/07/2019 | 15/07/2020 | – | 30/07/2019 | 22/07/2020 |
| E5 | 1 | – | 23/07/2019 | 15/07/2020 | – | 26/07/2019 | 21/07/2020 |
| | 2 | – | 23/07/2019 | 16/07/2020 | – | 27/07/2019 | 21/07/2020 |
| | 3 | – | 24/07/2019 | 15/07/2020 | – | 27/07/2019 | 21/07/2020 |
| | 4 | – | 23/07/2019 | 16/07/2020 | – | 27/07/2019 | 22/07/2020 |
| E6 | 1 | – | 09/01/2020 | 05/01/2021 | – | 13/01/2020 | 07/01/2021 |
| | 2 | – | 09/01/2020 | 05/01/2021 | – | 10/01/2020 | 06/01/2021 |
| | 3 | – | 09/01/2020 | 05/01/2021 | – | 13/01/2020 | 06/01/2021 |
| | 4 | – | 09/01/2020 | 05/01/2021 | – | 13/01/2020 | 07/01/2021 |